BORNEO JOURNAL OF RESOURCE SCIENCE AND TECHNOLOGY

Volume 15 Number 1, June 2025
ISSN : 2229-9769
eISSN : 0128-2972

UNIMAS
UNIVERSITI MALAYSIA SARAWAK
PUBLISHER

BORNEO JOURNAL OF RESOURCE SCIENCE AND TECHNOLOGY

Borneo Journal of Resource Science and Technology (BJRST) publishes scientific articles in all fields of resource sciences. The journal welcomes the submission of manuscripts that meet the general criteria of significance and scientific excellence from but not limited to Borneo. Acceptance for publication is based on contributions to scientific knowledge, original data, ideas or interpretations and on their conciseness, scientific accuracy and clarity.

BJRST publishes scientific articles in all fields of resource sciences including land and forest resources, aquatic science, biodiversity and ecology, biotechnology and molecular biology, chemistry, microbiology, bioinformatics, plant science and zoology. It offers a forum for the discussion of local issues that are of global concern. It is a double-blind refereed online journal published bi-annually. Currently it is indexed by Scopus, MyCITE (Malaysian Citation Index),UDL edge Beta, DOAJ Directory of Open Access Journals, Index Copernicus, MyJurnal and Google Scholar.

When submitting the work, contributors are requested to make a declaration that the submitted work has not been published, or is being considered for publication elsewhere. Contributors have to declare that the submitted work is their own and that copyright has not been breached in seeking the publication of the work.

Views expressed by the author(s) in the article do(es) not necessarily reflect the views of the Editorial Committee.

Manuscripts can be submitted via https://publisher.unimas.my/ojs/index.php/BJRST

Correspondence on editorial matters should be addressed to:

Prof Dr Edmund Sim Ui Hang
Chief Editor
Borneo Journal of Resource Science and Technology
Faculty of Resource Science and Technology, Universiti
Malaysia Sarawak
94300 Kota Samarahan
Sarawak
Malaysia
uhsim@unimas.my

Contents

Borneo Journal of Resource Science and Technology (2025), 15(1): 1-22
DOI: https:doi.org/10.33736/bjrst.7458.2025

A Review of Sea Turtle Awareness Programmes in Malaysia

ANASTASIA TING JIA LEI* & RUHANA BINTI HASSAN

Faculty of Resource Science and Technology, Universiti Malaysia Sarawak, 94300 Kota Samarahan, Sarawak, Malaysia
*Corresponding authors: Tingana821@gmail.com
Received: 22 July 2024 Accepted: 10 April 2025 Published: 30 June 2025

ABSTRACT

Malaysia is blessed with important sea turtle nesting rookeries along its coasts. As the sea turtle population declines in the country, conservation efforts in the form of outreach are important to obtain support and civic engagement in this sector. To understand the sea turtle outreach efforts in Malaysia, the outreach programmes, programme types and strategies by Malaysian non-governmental organisations and government agencies are reviewed in this paper, by tracking their social media and websites between January 2023 and December 2024. The findings help conservation entities to identify respective outreach blind spots and take initiatives to improve wherever possible. Out of the 18 agencies analysed, 38.89% (7) conducted all four types of outreach programmes. Ecotourism and community outreach are the most commonly conducted programme types at 77.78% (14). Knowledge dissemination is employed by all organisations, while hands-on activities are used by 94.44% (17) organisations, and only 22.22% (4) of the organisations were found to employ knowledge application on top of the former two. This paper suggests that school and youth outreach programmes should be prioritised by more organisations, as pro-environmental attitudes are more easily shaped in younger participants. On top of that, all tracked organisations should continue in their efforts of employing multiple outreach strategies, ensuring the effectiveness of their programmes.

Keywords: Awareness, governmental agencies, Malaysia, non-governmental organisations, sea turtle

INTRODUCTION

Sea turtles inhabit the tropical and subtropical seas around the globe. There are two families of sea turtles: Cheloniidae, the hard-shelled family, comprises Green turtles (*Chelonia mydas*), Hawksbill turtles (*Eretmochelys imbricata*), Loggerhead turtles (*Caretta caretta*), Flatback turtles (*Natator depressa*), Olive Ridley turtles (*Lepidochelys olivacea*), and Kemp's Ridley turtles (*Lepidochelys kempii*); and Dermochelyidae, the leathery-shelled family, represented by Leatherback turtles (*Dermochelys coriacea*), the largest sea turtle species (Chan, 2006; Thomson *et al*., 2021). Out of the seven species, Malaysia is home for nesting and foraging to four: Green turtles, locally named "penyu agar/hijau"; Hawksbill turtles, "penyu karah/sisik"; Olive Ridleys or "penyu lipas"; and Leatherbacks or "penyu belimbing" (Zulkifli & Kamaludin, 2023). In addition to that, there have been sightings of Loggerheads in Malaysia, believed to have nested in Sarawak, and one reported to be stranded in ghost nets off the west coast of Peninsular Malaysia (Leh, 1985; Abdul Rahman *et al*., 2021). According to the International Union for Conservation of Nature and Natural Resources (IUCN) Red List, Green turtles are classified as endangered, Leatherbacks and Olive Ridleys as vulnerable, and Hawksbills as critically endangered on a global basis (IUCN-SSC Marine Turtle Specialist Group (MTSG), n.d.). On Malaysian beaches, Green turtles have the highest nesting number, reaching up to 15, 000 annual nests as recorded in Sabah Turtle Islands Park (Joseph *et al*., 2022), followed by Hawksbill turtles, with an annual average of 432 nests in Melaka, Malaysia (Salleh *et al*., 2018). Malaysia is one of the sea turtle nesting hotspots (Jolis *et al.*, 2015). As the total sea turtle population of all four species in Peninsular Malaysia declined from 2017 to 2021 (Fadli *et al.*, 2023), they have become legally protected and conserved by various government agencies and non-governmental organisations (NGO) within Malaysia, with the prominent examples of Department of Fisheries (DoF), Sarawak

Forestry Corporation (SFC), Sabah Wildlife Department (SWD), Perhentian Turtle Project (PTP), Reef Guardian, WWF-Malaysia, etc. In addition to conservation groundwork and research, each agency or organisation extends their focus to outreach programs to conjure collective efforts in sea turtle conservation.

Awareness programmes are one of the key approaches to educating the public on the plight of sea turtles and their conservation. The locals are indifferent towards the declining number of sea turtles as they lack knowledge of their importance to the marine ecosystem and the coastal communities, although turtle conservation awareness has been discovered to be higher among the younger generation than the older generation due to higher education levels and outreach efforts (Abd Mutalib *et al.*, 2013; Abdullah, & Halim, 2018). With the coastal migration of Green and Hawksbill sea turtles in Malaysia, particularly in Sabah and Sarawak as discovered by Pilcher *et al.* (2019), they are prone to fishery-based mortality such as shrimp fishing in nearshore Malaysian waters (Chan & Liew, 1996; Jaaman *et al.*, 2009; Project GloBAL, 2008). Outreach programs encouraging the widespread and consistent adoption of Turtle Excluder Devices (TEDs) among local fishermen are thus of utmost importance to ensure a decline in sea turtle bycatch mortalities (Tookes *et al*., 2023). Another example is turtle egg poaching and consumption, a practice deeply embedded in the local cultures, particularly in the older generations (Abd Mutalib *et al.*, 2013), calling for drastic measures to raise awareness and eradicate the illegal exploitations of sea turtles. Hassan *et al.* (2017) were able to inspire a decrease in the desire for turtle egg consumption through an awareness programme in Lundu, Sarawak, involving presentations and sea turtle interactive sessions. Other harmful behaviours of humans as described by Nahill (2021) may include disturbing in-water and nesting turtles, littering, obstructing nesting beaches and inconsiderate boating practices. Disturbance to sea turtles may include touching, blocking their paths or flashing white lights at nesting mothers; littering contributes to marine debris that may destroy marine habitats, cause entanglement and subsequently drowning events of sea turtles and other marine animals, and potentially fatal ingestion; coastal developments and the addition of man-made items (e.g., furniture or large debris) on nesting beaches can obstruct the paths of nesting mothers, cause light pollution and discourage nesting events; inconsiderate boating practices such as anchoring on coral reefs, speeding in nearshore waters and discharging fuels into the sea can damage the marine habitat and lead to boat strike events, in which sea turtles are struck, often to death, by the propellers of the boats. These anthropogenic pressures negatively impact the populations of sea turtles and other marine megafauna, that are key tourist attractions in the marine tourism industry (Read, 2008; Teh *et al*., 2018). It is therefore vital to raise awareness of the locals regarding the consequences of certain practices, increase their willingness to adopt alternative practices and advocate for more sustainable practices, developments and legislation.

From a historical aspect, turtle meat, tortoiseshells and eggs were widely consumed in Southeast Asia. For example, in Sarawak, Malaysia, the harvest of Green turtle eggs was a significant industry until the 1980s, and the extensive harvesting over the years led to the drastic decline of the nesting population (Chan, 2006). Hassan *et al.* (2022) reported an 82.6% decline in nesting turtles from the 1950s to the 2000s, reaching a plateau in the 2000s. Other research shows that the global abundance of certain species, namely Green and Olive Ridley turtles is increasing, but Leatherback turtles are decreasing (Mazaris *et al.*, 2017), highlighting the need for continuous conservation and protection. Although the trade of sea turtle products has been banned by the governments of Sabah and Sarawak under the Wildlife Conservation Enactment (1997) and Wildlife Protection Ordinance 1998 respectively (Jani *et al.*, 2020; Joseph *et al.*, 2022), and the trade of all turtle eggs have been banned in Terengganu under the Turtle Enactment 1951 (amendment 2021) (Yong, 2021), these illegal trades remained active in Malaysia, as they moved to underground markets (Gomez & Krishnasamy, 2019). For example, through the analysis of genetic samples, Pertiwi *et al.* (2020) found that 10% of the live and dead sea turtles illegally traded in Bali originated within Indonesia (Berau), and also outsourced from Malaysia (Terengganu and Sarawak). In other cases, there have been reports of poached green turtles (Joseph *et al*., 2019), and the harvest of hawksbill turtle shells in Semporna, Malaysia (Jeethvendra *et al.*, 2023). The reported

poaching of green and hawksbill turtles in the Coral Triangle suggests Malaysia is a potentially active trade source (World Wide Fund for Nature (WWF), 2015). With the conservation and exploitation of these creatures occurring at the same time, the efforts taken by conservationists can be said to be in vain. Successful public education on marine conservation has been demonstrated by local and international studies. For a local example, Ismail *et al.* (2021) discovered a 66.11% increase in excellent grades in sea turtle knowledge test scores after the conduction of Turtle Camp. Similarly, Virgili *et al*. (2024) proved that fishermen outreach is crucial in reducing sea turtle bycatch mortality, although the results of Thomas- Walters *et al*. (2020) showed that the decrease in sea turtle poaching was irrelevant to the awareness campaign conducted. Education and awareness must therefore be raised among the Malaysian communities to eradicate sea turtle exploitations and ensure sea turtle populations increase.

Despite being an important nesting rookery for sea turtles, Malaysia has witnessed a decline in Green and Hawksbill nesting populations (Chan, 2013), raising concerns regarding their conservation status and underlining the necessity of effective outreach programmes to promote awareness and engage the public in sea turtles conservation efforts. For context, the Malaysian population is approximately 34.1 million, with a median age of 30 years old (Department of Statistics Malaysia, n.d.). Malaysian primary school children are aged between 7 – 12, while secondary school children are aged between 13 – 17 years. In addition, Malaysia comprises diversity in ethnicity, culture, beliefs and religion, hence there are opportunities and challenges in awareness programmes and the conservation of sea turtles.

To understand the conservation awareness of sea turtles in Malaysia, this literature review provides an overview of the outreach programmes in the country, the programme types and strategies. Types of outreach programmes included in this review are school or youth outreach programmes, ecotourism, citizen science projects, funding/adoption programmes and fishermen or community outreach programmes. The objectives of this paper are to assess the types of awareness programmes aimed at sea turtle conservation in Malaysia implemented by governmental and non-governmental organisations and identify the key strategies employed in these programmes.

MATERIALS AND METHODS

This study used digital platforms to gather information about awareness programmes on sea turtles in Malaysia. Due to time constraints, virtual or verbal interviews were not included. A total of 18 marine conservation NGOs and government agencies within Malaysia with available virtual updates of awareness programmes were scrutinised. These organisations were compiled from the existing knowledge of the authors or searched on Google with keywords i.e., "sea turtle conservation in Malaysia", and were filtered according to the availability of sea turtle awareness programme updates within the assessed period. Websites were accessed by searching the names of each organisation on Google. The same was done for social media pages that were accessed by searching the corresponding agency names on the platforms or from the information provided on the website. Through the website and social media (Instagram and Facebook) of each conservation entity, the types of outreach programmes conducted, and the strategies employed were tabulated. For each website, the search for annual reports, volunteer and other outreach programmes was done by exploring the website navigation menu, usually displayed on a bar in the website header. Social media and blog posts of outreach activities conducted by each party were tracked from January 2023 until December 2024, and annual reports for the year 2023, if available by the date of analysis (18 December 2024), were examined.

Undated activities such as weekly talks or on-site facilities such as turtle information centres are presumed to be ongoing and thus included in the analysis. For organisations with more than one conservation focus (e.g., Corals, terrestrial wildlife, plants etc.), only outreach programmes designed to raise awareness about sea turtles or related to sea turtles (i.e., waste collection with the purpose of sea turtle conservation) were included in this review. Inactive organisations with inconsistent conduction of programmes and posts of outreach dated older than January 2023 were excluded from this review to omit inconsistent and outdated outreach efforts from this analysis.

The programmes conducted by each agency were then categorised into four main types of awareness programmes, namely school or youth outreach programmes, ecotourism, community outreach and citizen science or funding programmes, to visualise the corresponding outreach efforts. School or youth outreach encompasses all programmes aimed at youngsters below 18 years of age; ecotourism includes all sea-turtle-related tourism and volunteerism; community outreach involves fishermen and all members of the local community; and citizen science programmes refer to all projects involving the general public (citizen scientists), while funding programmes refer to adoption programmes and partnerships.

Citizen science and funding programmes are grouped together in this study as both involve the help of the public. The strategies employed by each agency were classified as "knowledge dissemination", "hands-on activities", or "knowledge application" according to the study by Ahmad-Kamil *et al.* (2024). Knowledge dissemination includes all forms of talks, video presentations, forums, seminars, and workshops; while hands-on activities refer to camps, volunteer activities, waste collection such as beach or underwater clean-ups, citizen science, Do-It-Yourself (DIY) or art activities, ecotourism and other practical activities; quizzes, art and DIY contests, including online posters and video competitions, are categorised as knowledge application.

RESULTS & DISCUSSION

In this study, there are 18 organisations involved in sea turtle conservation awareness (Table 1). Three out of 18 sampled organisations are federal and state parties, while the rest are NGOs. Given that governmental agencies such as DoF operate across a wider range in Malaysia (in this case Pahang, Melaka, Negeri Sembilan, Terengganu and Penang), while NGOs such as JTP, SEATRU and PTP concentrate on specific areas or islands with turtle conservation needs, it is no wonder that NGOs outnumber governmental agencies. In most cases, NGOs collaborate with governmental agencies for a comprehensive and inclusive approach to address challenges in conservation and outreach (Chaurasiya *et al.*, 2023). For example, WWF-Malaysia collaborated with the Department of Fisheries Melaka to conserve Hawksbill turtles in Melaka (See & Latip, 2023), or in the case of other marine conservation work, the collaboration between DoF and Reef Check Malaysia to conserve and restore the marine ecosystem (Reef Check Malaysia, 2023).

Table 1. A list of NGOs and Government Agencies sampled in this review. There are considerably more NGOs than government agencies

	NGOs	Government
List of organisations	World Wide Fund for Nature Malaysia (WWF-Malaysia)	Sarawak Forestry Corporation (SFC)
	Marine Research Foundation Asia (MRF)	Sabah Wildlife Department (SWD)
	Kudat Turtle Conservation Society (KTCS)	Department of Fisheries Malaysia (DoFM)
	Juara Turtle Project (JTP)	
	Marine Conservation and Research Organisation Malaysia (PULIHARA)	
	Sea Turtle Research Unit (SEATRU)	
	Perhentian Turtle Project (PTP)	
	MY Ocean Hope	
	Tengah Island Conservation (TIC)	
	Bubbles Turtle Conservation (BTC)	
	Tropical Research and Conservation Centre (TRACC)	
	Reef Guardian	
	Kapas Turtles	
	Turtle Conservation Society of Malaysia (TCS)	
	Scuba Junkie SEAS	
Total	15	3

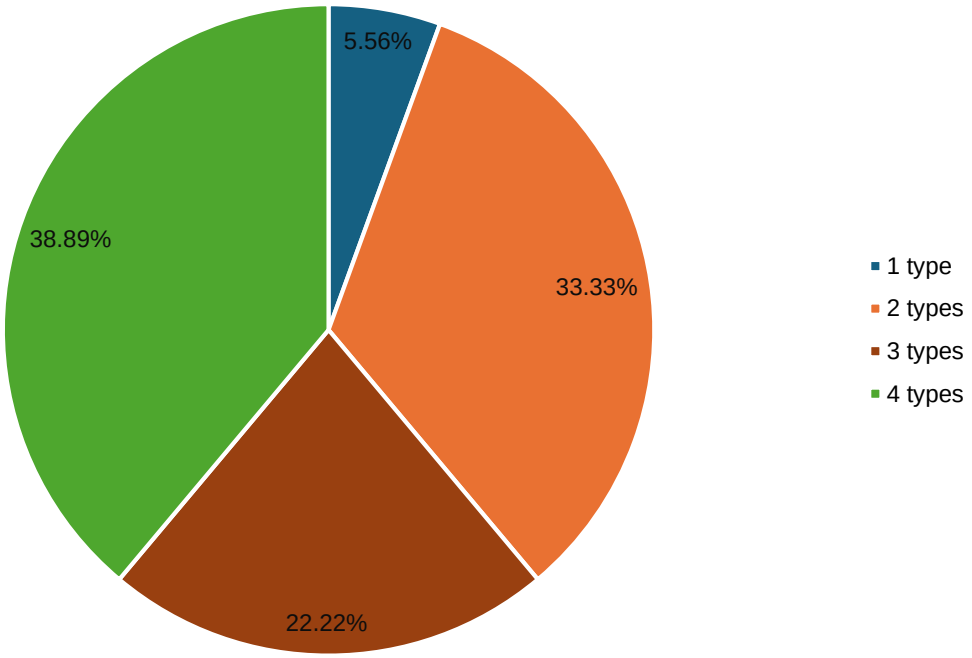

Figure 1. Pie chart of the percentage of organisations conducting one to four types of awareness programme(s). The majority conducted two to three types of awareness programmes

Government departments must work on more aspects of conservation than NGOs, encompassing but not limited to policy development, law enforcement and regulation and sustainability management all while taking into account the economic and social aspects of local communities, while NGOs focus more on conservation operations, advocacy for better policies, lobbying supports and raising awareness (Young & Dhanda, 2013; Carver & Sullivan, 2017; Chaurasiya *et al.*, 2023). With the collaborative goal of NGOs and government departments in wildlife conservation and protection, their efforts should be applauded regardless of their level of efforts.

Out of these organisations tracked, seven (38.89%) have an all-round focus in terms of the outreach programme types namely School/Youth Outreach, Ecotourism, Community Outreach and Citizen Science /Funding Programmes (Figure 1), whereas six (33.33%) agencies focused on two outreach programme types. A minority of four (22.22%) and one (5.56%) focused on three types and one type of outreach programmes respectively. Although the percentage of conservation entities conducting all four types of sea turtle outreach programmes is low, this is understandable as some organisations may be facing limited funding and manpower to conduct different types of programmes. For example, Poti *et al.* (2021) mentioned the discontinuation of SEATRU's outreach programme at Redang Primary School in 2014 due to a lack of funding. This could also be explained by the wide conservation scope of several organisations. For example, MRF Asia has various ongoing projects encompassing marine debris, sharks and rays etc.; TRACC Borneo focuses on coral restoration and WWF-Malaysia conserves terrestrial wildlife, forests, freshwater and marine ecosystems and others. Another plausible explanation may be the funders' goals prioritising other aspects of turtle conservation over awareness programmes, as most of the resources may be channelled towards conservation groundwork such as hatchery management or research instead of awareness programme conduction (Gruby *et al.*, 2023). Therefore, limited outreach programme implementation could be explained by funding and manpower constraints, a wide range of conservation focuses or the funders' priorities.

School Outreach Program

Figure 2 shows the number of organisations that conduct each type of outreach program. Ecotourism and community outreach were conducted by 77.78% of organisations, followed by citizen science/funding programmes (72.22%). School or youth outreach is the least conducted program type (66.67%). Despite this finding, school or youth outreach programmes serve as one of the most important channels to instil conservation and pro-environmental awareness in local communities and therefore should be prioritised by all organisations in their outreach plans. Boyd (2019) noted that environmental education and interventions during childhood can alter the lifelong beliefs and attitudes of youths and that children tend to share knowledge with their families, aiding in the spread of pro-environmental awareness (As the environment and its inhabitants are interlinked, sea turtle outreach can be classified under environmental education or intervention and pro-environmental behaviours refer to involvement in sea turtle conservation work in this review). This is supported by other studies stating that younger participants acquire new pro-environmental behaviours more easily than adults (Zelezny, 1999), are more responsive towards pro-environmental interventions (Liefländer & Bogner, 2014), and retain their childhood experiences until adulthood (Chawla, 2020). For example, Abd Mutalib *et al.* (2013) found that participants below 20 years of age obtained the highest score in the sea turtle survey in Setiu, Terengganu, whereas those aged between 50-59 obtained the lowest score, as some of them admitted that turtle egg consumption is a part of their cultural norms.

Meanwhile, Poti *et al*. (2021) reported a cease in sea turtle egg consumption in eight out of ten individuals who participated in sea turtle awareness programmes at Redang Primary School as children. The significance of environmental education in schools is emphasised as past research has indicated that environmental literacy (referring to knowledge, awareness, behaviour, attitude and involvement in environmental issues: Jannah *et al.*, 2013) possessed by local youths is moderate to low (Erdogan *et al.*, 2009). Although newer research found an increase in environmental awareness behaviours among the youths due to environmental education programs and the role of social media in raising environmental-related awareness, their level of participation in environmental-related issues remains low (Abdul Rahman, 2020; Nasir *et al.*, 2020; Norkhaidi *et al.*, 2021). With children being the future decision-makers of Malaysia, it is therefore of utmost importance to cultivate their awareness of sea turtle conservation since young to help them cope with these increasingly pressing conservation matters in the future.

Several past studies have shown that female students show a higher level of environmental awareness and responsibility than male students (Tikka *et al.*, 2000; Jannah *et al.*, 2013; Li *et al.*, 2022), while some studies like Larson *et al.* (2019) reported the opposite as males spend more outdoor times. Nevertheless, organisations targeting school outreach programmes should integrate outdoor or fieldwork experiences to provide more fun learning experiences and increase the engagement of both genders, effectively adding positive impacts to the long-term memories of students and improving their pro-environmental behaviours (Mann *et al.*, 2022). This is supported by Kuo *et al.* (2018) who discovered learning in nature increases classroom engagement significantly as compared to classroom learning.

In addition to that, Ives *et al.* (2018) suggest that establishing bonds with nature can instigate significant societal shifts towards greater respect and care for the environment, and childhood is a stage of opportunity to nurture these bonds. For a local example, Ismail *et al.* (2021) reported an increase in knowledge, positive perception and behaviour towards turtles through the implementation of Turtle Camp, involving school-based and outdoor programmes, in primary schools in Kemaman, Terengganu. Therefore, the implementation of outdoor programmes is favoured whenever possible, to allow youths to build positive connections with nature, and shape their conservation attitudes.

Ecotourism

A total of 14 (77.78%) agencies are involved in ecotourism. Ecotourism can increase conservation awareness among tourists of various ages and nationalities. It should involve education regarding the wildlife sighted, coupled with controlled and responsible interaction with wildlife such as turtle watching and hatchling

releases conducted by PULIHARA, DoF, BTC and so forth (Table 2). In addition to raising awareness, the revenue generated from sea turtle-related tourism can be channelled to fund relevant research and conservation programmes (Tisdell & Wilson, 2000). For example, the paid 3-day-2-night sea turtle volunteer programme by SFC and the marine park fees imposed by the Department of Marine Parks on the tourists are channelled towards the management of marine parks, and the protection and conservation of the marine environment (Ismail *et al.*, 2020). Ecotourism that includes environmental education and turtle sightings can cause a positive and significant increase in the desire and intentions of tourists to help sea turtles, demonstrating the importance of learning and wildlife interaction in the cultivation of pro-conservation sentiments and actions (Tisdell & Wilson, 2005). This is proven by Mendes *et al.* (2019), reporting that 89.1% of sampled tourists showed awareness and sensitivity regarding the conservation of sea turtles. However, the effectiveness of ecotourism in raising conservation awareness is greatly linked to the sustainability and responsibility of tourism operators, local industries and governments, as in some cases, these values are ignored for higher economic returns (Mihalic, 2016). For example, the development of touristy regions in terms of transportation, accommodation, agriculture etc. by the government and local industries, and the footprints of mass tourism (e.g., littering and noise pollution) may bring negative impacts to local biodiversities that are often overlooked to rake in economic benefits of tourism (Sahahiri *et al.*, 2023; Zhu *et al.*, 2023).

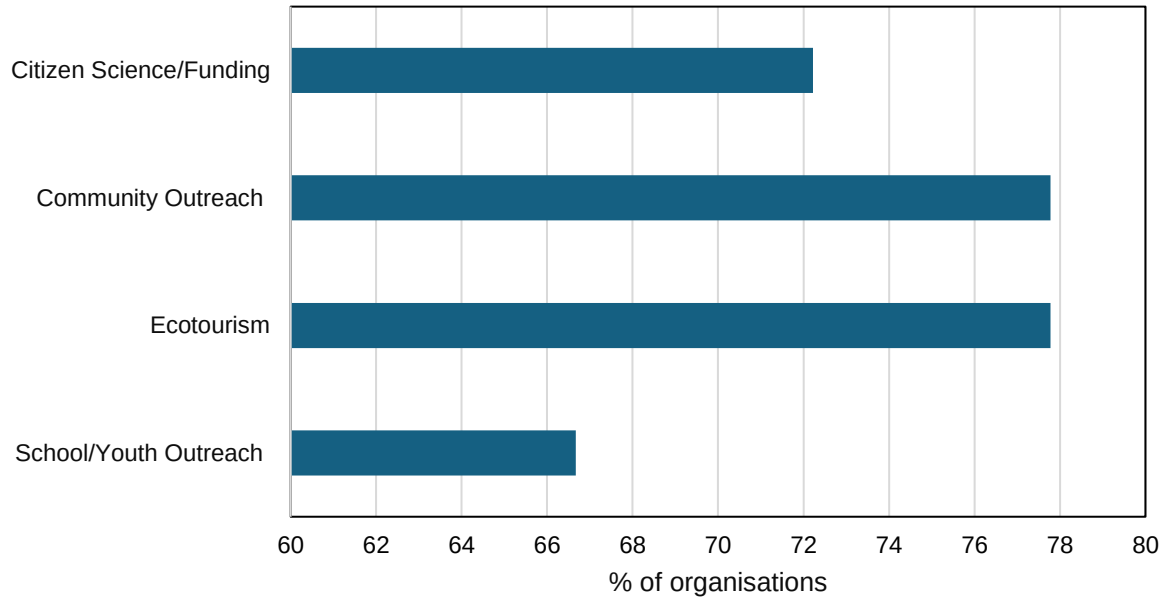

Figure 2. A bar chart of the percentage of organisations conducting each type of awareness programme. Community outreach and ecotourism are conducted by the same percentage of organisations

According to the Global Sustainable Tourism Council, private and governmental operators have the social responsibility to minimise environmental impacts while maximising environmental benefits (Marin-Pantelescu *et al.*, 2019). Given that most sea turtle conservation centres reviewed in this article (Table 2) operate in marine tourism hotspots on islands or along the coasts, outreach efforts extended towards the stakeholders, private or governmental tourism operators, are extremely crucial. Moreover, due to their strategic locations in the heart of tourism, ecotourism can be easily carried out by opening their conservation centres for tourist visits. The staff at these centres should be able to offer a clear overview of sea turtle species, ecology (natural habitat), biology (anatomy, behaviour, and reproduction), conservation measures and challenges faced (Dimopoulos *et al.*, 2009). This is in line with the programme structure proposed by Koeswiryono and Chandra (2021), stating that each tour should include (1) an explanation of displays of the protected turtle species, which in the case of Malaysia, are Green, Hawksbill, Leatherback, and Olive Ridley turtles, to impart knowledge on the distinguishing features of each species; (2) a tour of the hatchery, the hatchlings tank, and the adult turtle's exhibition pool, or (3)

in the case of most Malaysian conservation centres that lack the skills and fundings for rehabilitation, specimens of hatchling carcasses, turtle taxidermy and turtle carapace, coupled with explanations regarding the biology, care, threats and conservation measures. With the awareness raised, tourists and stakeholders can be more mindful of their footprints during their travels and sustainable tourism can be more easily attained with their cooperation.

Another aspect of ecotourism gradually gaining popularity in the sea turtle conservation sector over the years is the volunteer programme or volunteerism. Volunteering with conservation organisations allows tourists to work with the organisations for a short period. This is a clear example of a win-win situation, whereby volunteers get to experience sea turtle encounters and increase their skill sets, and conservation workers obtain practical help and funding while spreading awareness. Volunteerism may include a wide range of programme types. It can be as simple as a beach or underwater clean-up open for public participation on a touristy beach, or a programme that lasts for a short period (from days to weeks or months) and covers various types of activities, which, on top of conservation work, may include non-conservation-related miscellaneous work encompassing maintenance, gardening and mural or sign-making (Nahill, 2021).

With the knowledge and wildlife interaction experiences acquired during the volunteering period, tourists are more alert to anthropogenic impacts on sea turtles, may be more inclined towards eco-conscious choices and are properly equipped to educate their peers. Not to mention that volunteerism may bring greater profits to the local community businesses in sectors such as food, accommodation and other shopping places (McGehee & Andereck, 2009; Zahra & McGehee, 2013). Despite all the benefits it brings, some organisations reviewed in this paper may be unable to achieve its implementation due to various issues. One of the prominent issues may be insufficient funding, as this programme may require a significant monetary sum to construct appropriate accommodation facilities (for organisations in remote places) and employ adequate manpower (i.e. volunteer coordinators) to market and manage the programme and its participants (Liu, 2020).

Community Outreach

Similar to ecotourism, 14 (77.78%) out of 18 agencies in this study implemented community outreach programmes. This programme type is emphasised by most conservation entities as the coastal communities live interdependently with the marine ecosystem, and sea turtle egg poaching and consumption remain a common practice in many parts of Malaysia. The local communities should learn the importance of sea turtles as a keystone species in the marine ecosystem, which can then affect their livelihoods. With the shift of the era, conservation awareness and legal boundaries have largely reduced these unhealthy practices, though it is far from being completely eradicated.

To attract the attention of various age groups and mindsets that make up a community, community outreach requires creativity such as beautification projects in strategic locations (i.e. the beautifully decorated Turtle Alley with turtle-related information by Turtle Conservation Society) and practicality in terms of economy and social benefits. It is only natural for the communities reliant on sea turtles for consumptive uses in the past to shift to non-consumptive uses such as ecotourism and tourism businesses as discussed in the previous section (Wilson & Tisdell, 2003; Abdullah, & Halim, 2018; Brander *et al*., 2024), as they realise the economic benefits of live sea turtles to local businesses and the increase in job opportunities in the tourism and conservation sectors.

For instance, WWF reported that sea turtle-related tourism is estimated to generate money approximately three times the economy obtained from the trade of sea turtle products (eggs, tortoiseshells and meat) while increasing local jobs, funding monitoring programmes and reducing consumptive uses of sea turtles, and this should be part of the information imparted to the communities during outreach programmes to allow the locals to understand that sea turtles provide more benefits when alive than dead (Troëng & Drew, 2009). Therefore, engaging with the local communities and assisting their shift to non-consumptive income alternatives, for instance, the Kampung Mesra Penyu

Initiative by WWF-Malaysia and Mabul Community Market by Scuba Junkie Seas (Table 2), are crucial in promoting such transitions.

Turtle excluder devices or TEDs play a vital role in sea turtle conservation by mitigating fatal interactions between sea turtles and trawl fishing gear. TEDs are designed to fit within the neck of a trawl net, through which shrimp can freely pass through the bars to the back of the net, while larger animals such as turtles can escape through a flap in the mesh, reducing bycatch and drowning events (NOAA, 2021). Therefore, educating the fishermen on sustainable fishing with TEDs is an imperative step towards sea turtle conservation. Sankar and Raju (2003) documented the implementation of awareness camps in coastal districts to educate and promote sea turtle conservation, featuring demonstrations on TED fabrication, function, and assembly, successfully reducing the use of ray nets and cultivating fishermen's cooperation to protect sea turtle eggs during nesting seasons.

Nevertheless, only one organisation (MRF Asia) reviewed in this paper explicitly reported conducting an ongoing TED outreach project, which can be due to the challenges posed in persuading fishermen regarding the benefits of TEDs, as the lack of visible socio-economic benefits of TEDs towards fishermen may fuel their reluctance in adopting TEDs. As explained by Jenkins (2023), the proper, widespread and consistent use of TEDs may be harder to achieve, possibly due to its perceived complexity and incompatibility with the fishermen's needs. Despite these challenges, consistent outreach efforts in the form of workshops and continuous striving for TED structural improvements to minimise fishermen's inconvenience should be sustained for greater TED adoption and application success.

Table 2. Summary of names, websites, programmes conducted and the respective programme types and strategies employed by each conservation entity. The description of the programmes conducted (if provided) is included. Organisations were excluded if they lacked virtual updates of sea turtle-related awareness programmes in 2023 and 2024. The majority of organisations conduct more than one programme type and employ multiple strategies except for Sabah Wildlife Department (SWD)

Agency/ NGOs	Website	Turtle Awareness Programme	Summary of Programme Types	Summary of Strategies Employed
1. World Wide Fund for Nature Malaysia (WWF-Malaysia)	https://www.wwf.org.my/our_work/marine/protecting_endangered_marine_species/	• Turtle Camp for youths in Terengganu, Malaysia • Kampung Mesra Penyu Initiative at Kampung Padang Kemunting, Melaka to ensure a balance between improved community life quality and sea turtle conservation • Sea turtle mural in Tun Mustapha Park, Sabah • Protect Nature, Protect Our Future online fundraising programme for the conservation of Malayan tigers, Orangutans and sea turtles, with tax exemption receipts and gifts in return.	School/youth outreach, community outreach and funding programmes	Knowledge disseminati on and hands-on activities.
2. Marine Research Foundation Asia (MRF Asia)	https://www.mrf-asia.org/project/malaysia-turtle-excluder-devices-project-2007-present/	• Educational and practical workshops, including the use of short documentary videos to educate local fishermen and encourage the use of Turtle Excluder Devices (TEDs). This programme is expanded from Sabah to Peninsular Malaysia. • Educational booth at Turtle Islands Heritage Protected Areas (TIHPA) Conference 2023 • Sponsorships and partnerships with various other organisations, corporates, stakeholders and government departments. • Underwater clean-up with volunteers and other departments funded by KePKAS	Community outreach and funding programmes.	Knowledge disseminati on and hands-on activities.
3. Kudat Turtle Conservation Society (KTCS)	https://www.ktcsborneo.org/environmental-education-1	• Awareness talks in schools and villages, exhibitions. • Beach clean-ups with the Bavang Jamal Community • Rehabilitated turtle releases by Wildlife Rescue Unit Sabah • Sustainable Livelihood Project- includes capacity building, facilities improvement, business marketing etc. – to boost incomes of Kudat communities in support of their marine conservation efforts • Volunteer Programme • Citizen science – monitoring programme/ turtle egg protection programme - involving the local communities to provide training and skill enhancement. • Industrial training for students and staff of stakeholders	School outreach, community outreach, ecotourism and citizen science.	Knowledge disseminati on and hands-on activities.

*indicates Malaysian governmental agencies

Table 2. (continued)

Agency/ NGOs	Website	Turtle Awareness Programme	Summary of Programme Types	Summary of Strategies Employed
4. Juara Turtle Project (JTP)	https://www.juaraturtleproject.com/projects/environmental-program/	• Organise weekly visits to Juara Primary School in Kampung Juara of Tioman Island, Pahang to educate on different monthly topics and conduct activities ranging from presentations to games or outdoor activities such as snorkelling or beach clean-up. Bilingual and monthly rotation of topics and varying weekly activities keep the attention of the same audience group. • The volunteer programme allows tourists to be involved in turtle conservation work throughout the nesting season, increasing their knowledge and awareness. (Fees: RM1000-1500 per week) • Recycling Programme involving stakeholders and local communities • Juara Plastic Free Initiative – promoting sustainable alternatives to plastic among stakeholders (e.g., Use of metal straws instead of plastic straws)	School outreach, ecotourism, and community outreach.	Knowledge dissemination and hands-on activities.
5. Marine Conservation and Research Organisation Malaysia (PULIHARA), formerly known as Lang Tengah Turtle Watch (LTTW)	https://pulihara malaysia.org /what-we-do/	• Free educational talks for guests and school children coupled with specimen exhibition. • Volunteer Programme involving talks and hands-on conservation work (Fees starting at RM850 per week for locals and USD450 for foreigners) • School outreach programmes • Turtle Kids Club for children below 12 • Encourage the public to send in photos of sea turtles for Photo-ID • Turtle Adoption and Nest Adoption Programmes • Kelas Penyu aimed at children and locals at Pantai Chakar Hutan • Beach clean-ups with resort guests, school children and locals. • Turtle watching, hatchery visits, nest inspection and hatchling releases with the public • Informative talks provided at the Visitors' Hut at Tanjong Jara Resort, Dungun, Terengganu • Collaborated with Majlis Perbandaran Kemaman (MPK) to organise a beach clean-up at Pantai Chakar Hutan. • CSR Programmes • Educational booth at KDI Open Day • Partnership with Team Rakyat for only merchandise sales	Ecotourism, school outreach, community outreach and citizen science/funding programme.	Knowledge dissemination and hands-on activities.
6. Sea Turtle Research Unit (Seatru)	https://seatru.umt.edu.my/	• Allow day trips to the site for educational talks, site visits, nest checks and excavations. • Turtle Camps for school children comprise storytelling, games, group activities, quizzes, and on-site training in conservation work. • The TurtleTok contest encourages the public to produce videos related to sea turtles on social media to reach a wider audience. • 5D4N Volunteer Programme from RM680 • Sembang Ke Laut Podcast Project • Advertisement Board Partnership with businesses ranging from RM1000 (basic package) to RM 2000 (premium package).	Ecotourism, school outreach, community outreach and funding programme.	Knowledge dissemination and application, and hands-on activities
7. Perhentian Turtle Project (PTP) by Fuze Ecoteer	https://www.perhentianturtleproject.org/citizen-science	• Volunteer programme involving turtle conservation works (RM900 per week for locals) • Penyu Warrior Initiative – a citizen science encouraging the public to take photos of sea turtles and send them to the organisation for individual identification, complete with a set of guidelines • Turtle adoption programme and wish list – to fund necessary equipment for research and conservation work • Beach clean-ups • Collaboration with Mojo More Furniture – 10% of the proceeds from selling eco-friendly bookstands go to PTP.	Ecotourism, citizen science/funding programmes.	Knowledge dissemination and hands-on activities.
8. Sarawak Forestry Corporation (SFC)*	https://sarawakforestry.com /sea-turtle-conservation-program/	• 3D2N Volunteer Program at Pulau Talang-Talang (Fees: RM1000 for foreigners and RM450 for locals) • Adoption Programme - RM 100/year per nest or RM 200/year per turtle.	Ecotourism and funding programme.	Knowledge dissemination and hands-on activities.

*indicates Malaysian governmental agencies

Table 2. (continued)

Agency/ NGOs	Website	Turtle Awareness Programme	Summary of Programme Types	Summary of Strategies Employed
9. Department of Fisheries (DoF) *	https://marinepark.dof.gov.my/en/locations/tcic/	• Free ongoing exhibition of live sea turtles, specimens, photos and information boards in the Turtle Conservation and Information Center (TCIC) or Fish Ornamental Centre to educate the public. These centres are open in various locations such as Pantai Kerachut (Penang), Segari (Pahang), Port Dickson (Negeri Sembilan), Padang Kemunting (Melaka), Cherating (Pahang), Ma'Daerah (Terengganu) and Rantau Abang (Terengganu). • Regular organisation of beach clean-up programmes and hatchling releases that are open for public participation • Turtle specimens on display at Laman Agrofood Perikanan • Hatchling release programme • Sea Turtle Conservation Awareness Programme Kelantan 2024 at Kampung Kuala Rekang, Kandis, Kelantan	Community outreach and ecotourism.	Knowledge dissemination and hands-on activities
10. MY Ocean Hope	https://oceanhope.umt.edu.my/	• School tour • Beach clean-up • Workshop & seminars • Drawing contest	School outreach and community outreach.	Knowledge dissemination and application, and hands-on activities.
11. Tengah Island Conservation (TIC)	https://www.tengahislandconservation.org/community	• School outreach programmes that include lessons and activities related to sea turtle conservation. • Volunteer programme – hatchery maintenance, nest checks and excavations, nesting surveys, beach clean-ups and outreach programmes • Beach and underwater clean-ups • Fundraising campaigns that can be started by the public, sponsorships and donations from the public.	School outreach, community outreach, ecotourism and funding programmes.	Knowledge dissemination and hands-on activities.
12. Bubbles Turtle Conservation (BTC)	https://www.bubblesturtleconservation.com/	• On-site turtle talks in various languages to guests and school presentations • Hatchling releases and turtle watching with resort guests • Sea Turtle Conservation Experiential programme – patrols, hatchery maintenance, turtle talks, beach cleaning (RM1500 per pax per week) • Sponsorship programme for general sponsors, corporate sponsors, Sponsor-A-Nest etc. • Partnership with NEArt – joining NEArt membership with RM50 helps support BTC conservation works.	School outreach, ecotourism and funding programmes.	Knowledge dissemination and hands-on activities.
13. Tropical Research and Conservation Centre (TRACC)	https://tracc.org/life-at-tracc	• Volunteer programme with fees starting from EUR 1,300 – turtle photo ID, patrol and hatchling release (although they mainly focus on coral work) • Marine conservation seminars • Hatchling releases	Ecotourism and community outreach.	Knowledge dissemination and hands-on activities.
14. Reef Guardian	https://www.reefguardian.com.my/programmes/marine-conservation/sea-turtle-conservation	• Turtle-watching includes nesting mothers and hatchling release which are open to the Sugud Island Marine Conservation Areas (SIMCA) guests in Sabah. Briefings and Q&As will be conducted during these activities. • Organises school outreach programmes by inviting selected students to SIMCA to learn about marine conservation and providing training to Marine Science Undergraduate students. • Project AWARE – beach and underwater clean-ups involving tourists, government agencies and NGOs. • Infographics, posters, books, brochures and other exhibits are readily displayed at the office, together with the provision of video presentations and educational talks by staff. • Turtle adoption at RM200 per nest • Marine conservation talks at expeditions such as MIDE • Programme packages for educational field trips and visitation are open to students and the public.	School outreach, community outreach, ecotourism and citizen science/funding programmes.	Knowledge dissemination and hands-on activities.

*indicates Malaysian governmental agencies

Table 2. (continued)

Agency/ NGOs	Website	Turtle Awareness Programme	Summary of Programme Types	Summary of Strategies Employed
15. Kapas Turtles	https://kapasturtles.com/wp/	• Sign-making workshops, upcycling workshops, sharing sessions about Marine Protected Areas, video challenge • Karnival Kapas 2023 • On-site Sea Turtle Talks on every Saturday • Beach clean-ups – participants will be rewarded with snorkelling sessions, snacks and drinks • Volunteer programme - RM700 per person per week, for Malaysians. GBP 230 / EUR 260 per person per week for International volunteers (minimum period is 2 weeks) • #BringOurTurtlesBack Campaign – Sand sculpture contest 2023 to raise awareness and funds for sea turtle conservation in Terengganu, Malaysia. • Sea turtle nest adoption programme – each nest can be adopted with a minimum donation of RM400 • CSR and education programmes	Ecotourism and community outreach, funding programme.	Knowledge dissemination and application, and hands-on activities.
16. Turtle Conservation Society of Malaysia (TCS)	https://www.turtleconservationsociety.org.my/outreach/	• Turtles and firefly discovery trip- to share knowledge on sea turtles terrapins and fireflies. • Nature Discovery Trip – The 2D1N programme includes a Turtle and firefly discovery trip, a beach clean-up and trash analysis. 3D2N adds in a river cruise and mangrove planting session. • Turtle Alley – a themed lane decorated with turtle art on the walls and floor in Chinatown, Kuala Terengganu, Malaysia, complete with turtle-related stories and information. • Turtle Camp – educating teachers and students about turtles in schools. • Biodiversity talks – open to public participation to share knowledge about turtles and terrapins such as the pocket talk by Dr Pelf Nyok of TCS at Conservation Carnival NCTF 1.0 • Booth set-ups at events such as Dive Resort Travel Expo and Year End Bazaar • Distributed "Turtles of Malaysia" colouring books to children in rural Terengganu for free • Partnerships e.g. with Melvita and Watsons Malaysia, in which certain purchases will donate RM1 to TCS, or Royong, in which purchases give the consumers a chance to win a 3D2N stay at Shangri-La Rasa Sayang, Penang. • Awareness workshops involving soap and lotion-making, and turtle-related knowledge sharing. • CSR programmes with Bank Negara Malaysia, Ocean Network Express etc. • "18 Turtles – 18 Facts" Quiz Mania and trivia quizzes on Instagram	School outreach, community outreach, ecotourism, and citizen science/funding programmes.	Knowledge dissemination and application, and hands-on activities.
17. Sabah Wildlife Department (SWD) *	https://wildlife.sabah.gov.my/index.php	• Tour Programme of World Sea Turtle Day 2024 at six schools in Semporna in collaboration with WWF-Malaysia to raise awareness of the importance of protecting and conserving sea turtles and their habitats. • A meeting to initiate the Malaysia CITES Youth Network to include the younger generation in awareness campaigns focusing on turtle egg consumption.	School and youth outreach	Knowledge dissemination
18. Scuba Junkie SEAS	https://www.scubajunkieseas.org/	• Citizen science to help with Turtle ID database – photo submission from guests • Adopt A Turtle initiative – adopt a hatchling with RM100 • Volunteer programme starting at RM2,310 per week • Beach clean-ups • Sponsor a clean-up initiative • School outreach programmes • Conservation awareness talks for resort guests. • Work with the Mabul Community to develop the Mabul Community Market as an alternative to marine life exploitation. • Presentations and workshops available for the participation of local community • Partnership with Tee Mill Store to sell merchandise	School outreach, community outreach, ecotourism, funding programme	Knowledge dissemination, hands-on activities

*indicates Malaysian governmental agencies

Citizen Science/ Funding Programmes

A total of 13 (72.22%) conservation entities conducted citizen science projects or funding programmes. These programmes are similar in terms that both involve the general citizens in conservation and they can usually be performed without time or location constraints. Citizen science is a valuable tool for scientists to obtain information for research and conservation purposes while fostering civic involvement and raising awareness via explanations and practical involvement. Similarly, funding programmes provide explanations of the importance of sea turtle conservation and the uses of the raised funds to draw adopters and partners, simultaneously educating the potential funders. Citizen science projects are a cost-effective way of obtaining data from a wider geographical range, and over extended chronologies to increase the validity of the ongoing research while raising public awareness, and increasing scientific skill sets among citizen scientists (Lucrezi *et al.*, 2018).

Participation in these projects may be primarily directed at marine sports hobbyists such as divers and marine tourism operators as they may have access to valuable sea turtle-related information and photos (Martin *et al.*, 2016; Lucrezi *et al.*, 2018). Citizen scientists can contribute by adhering to structured protocols, sending in opportunistic data, or participating in crowdsourcing initiatives (Becken *et al.*, 2019). One example of a popular citizen science project is the photo-identification (photo-ID) project to understand the spatiotemporal distribution of sea turtles, which is implemented by several agencies in this review. This project, as described by various studies such as Long and Azmi (2017) and Hoh *et al.* (2022), is to encourage the public to send photos of sea turtles with a clear view of facial or flipper scutes for identification of individual turtles to relevant agencies, complete with metadata including the sighting location, the sighting date, the sighting time, and the camera model. From this process, the public learns about the individual uniqueness of sea turtle scutes (sea turtle biology), the importance of photo-ID (sea turtle research), and scientific processes and outcomes, thus increasing their knowledge and awareness regarding sea turtles. Protocols or guidelines provided through this project may allow the public to learn to behave appropriately around wildlife, ensuring that disturbances to sea turtles are minimised. However, citizen science projects may have limitations that may discourage some of the organisations from implementing them. The accuracy of the data collected by citizen scientists and volunteers is highly dependent on the completion and quality of the data. For example, the metadata of the photos, particularly the location, date and time of sighting, may be missing or the quality of the photos may be too blurred for individual identification (Long & Azmi, 2017). Another aspect to be considered is the increase in the size of the database, requiring longer processing time and manpower, even with the help of software due to possible inconsistencies in the photo quality (Long, 2016; Calmanovici *et al.*, 2018). On top of that, there is a chance that only those who are presently concerned about sea turtles and the environment are more inclined to participate in these programmes. Therefore, rewards and encouragements to the participants such as the opportunities to name newly identified turtles presently done by PULIHARA and the other NGOs should be provided to accentuate their sense of involvement and promote participation.

Outreach Education Framework

From Figure 3, 13 (72.22%) organisations employed two types of programme strategies (knowledge dissemination and hands-on activities), while 4 (22.22%) organisations used all three types of strategies. One (5.56%) organisation used only one programme strategy. As shown in Figure 4, all organisations employ knowledge dissemination as their outreach strategy, 94.44% (4) organisations employ hands-on activities, while only 22.22% (4) employ knowledge application on top of the other two strategies. From these findings, it can be deduced that 94.44% of organisations employ knowledge dissemination and hands-on activities as their outreach strategies, while only 22.22% include knowledge application. Only one organisation employed a single strategy (knowledge dissemination).

Effective environmental management and long-term conservation can be achieved by cultivating collective responsibilities through the main educational strategies known as “knowledge dissemination”, followed by “hands-on education” and “knowledge application” (Ahmad-Kamil *et al.*, 2024). Figure

5 describes the flow of implementing an effective environmental education programme, by integrating the General Teaching Model in Figure 6 (Hungerford *et al.*, 1988) into the outreach programme framework (Ahmad-Kamil *et al.*, 2024). The lessons to be disseminated in the awareness programmes are important factors determining the efficacy of the programmes and are therefore the core of outreach programmes conducted by all the organisations reviewed.

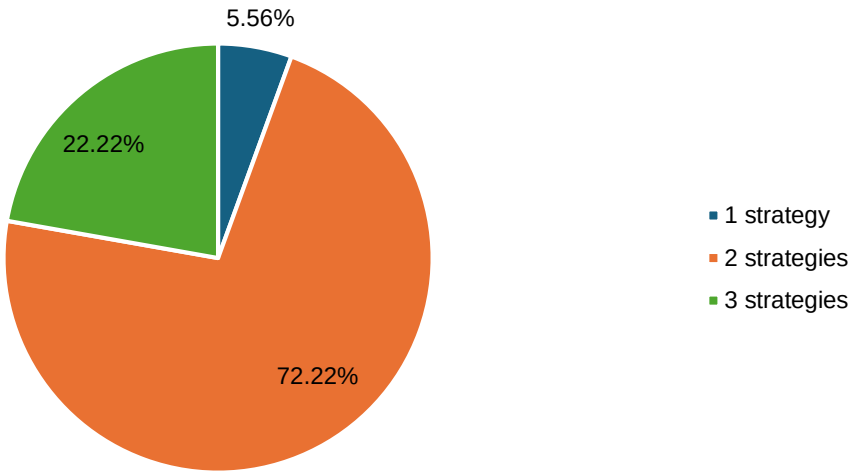

Figure 3. Pie chart showing the percentage of organisations adopting one, two or three strategies. 72.22% of organisations used 2 types of programme strategies in their outreach efforts

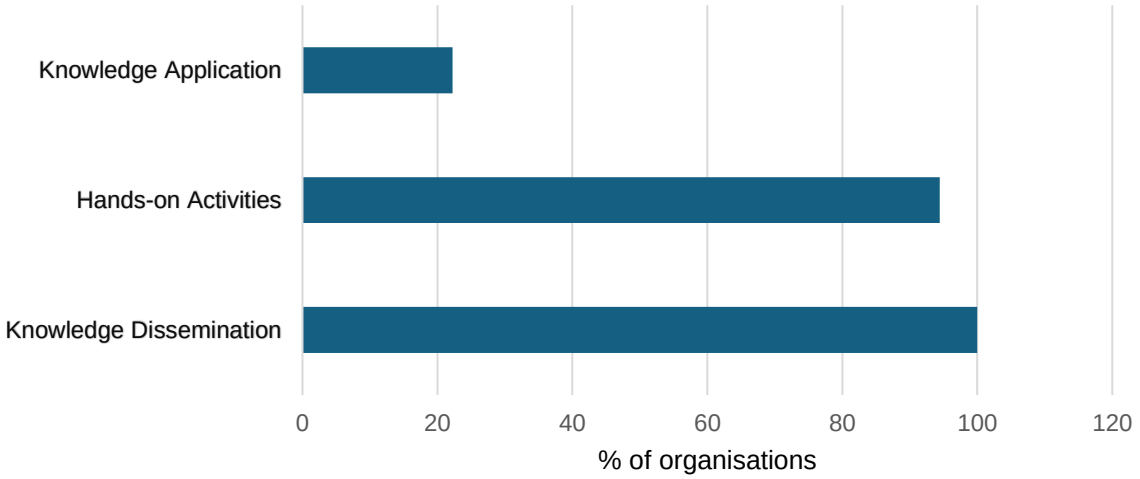

Figure 4. Bar chart of the percentage of organisations employing each programme strategy. Knowledge dissemination is employed by all organisations

This should include variables to construct positive behaviour toward the topic of interest, namely entry-level, ownership, and empowerment, which in the case of sea turtle awareness programmes, translate to basic sea turtle biology (specifically the morphological, reproductive, behavioural and nutritional characteristics and life cycle), threats and conservation measures, and the belief that personal action can make a difference to sea turtles along with a verbal commitment to sea turtle conservation, respectively (Dimopoulos *et al.*, 2009; Jiménez Acosta *et al.*, 2024). Poti *et al.* (2021) demonstrated the importance of long-term outreach efforts and debunking myths regarding the medicinal properties of sea turtle eggs, as it was discovered that most participants of the long-term awareness programme by SEATRU at Redang Primary School stopped sea turtle egg consumption due

to the knowledge obtained from the programme. Therefore, the lessons to be disseminated should be carefully planned out to ensure the conveyance of crucial information to reduce negative pressures on the sea turtle population.

Active learning activities in the form of hands-on activities and/or knowledge application after knowledge dissemination can aid in strengthening and broadening the knowledge and awareness of participants. For example, Frame *et al.* (2021) observed that a significant increase in wildlife conservation knowledge can be attributed to active-learning activities such as group problem-solving, games, group discussions, distinguishing unique flipper patterns between sea turtle species, beach clean-ups, and observing hatchlings emergence. Positive experience in hands-on activities can greatly pique the interests of students (Holstermann *et al.*, 2010). With the majority of organisations in this review employing hands-on activities, this may imply the greater convenience and usefulness of conducting hands-on activities such as waste collection on readily accessible beaches and volunteering activities to deal with manpower shortage than knowledge application. Schwichow *et al.* (2016) reported that both hands-on activities and knowledge dissemination are equally effective in increasing the scientific knowledge of school children, although they seem to do better in the aspects (hands-on or pen-and-paper) they were trained in.

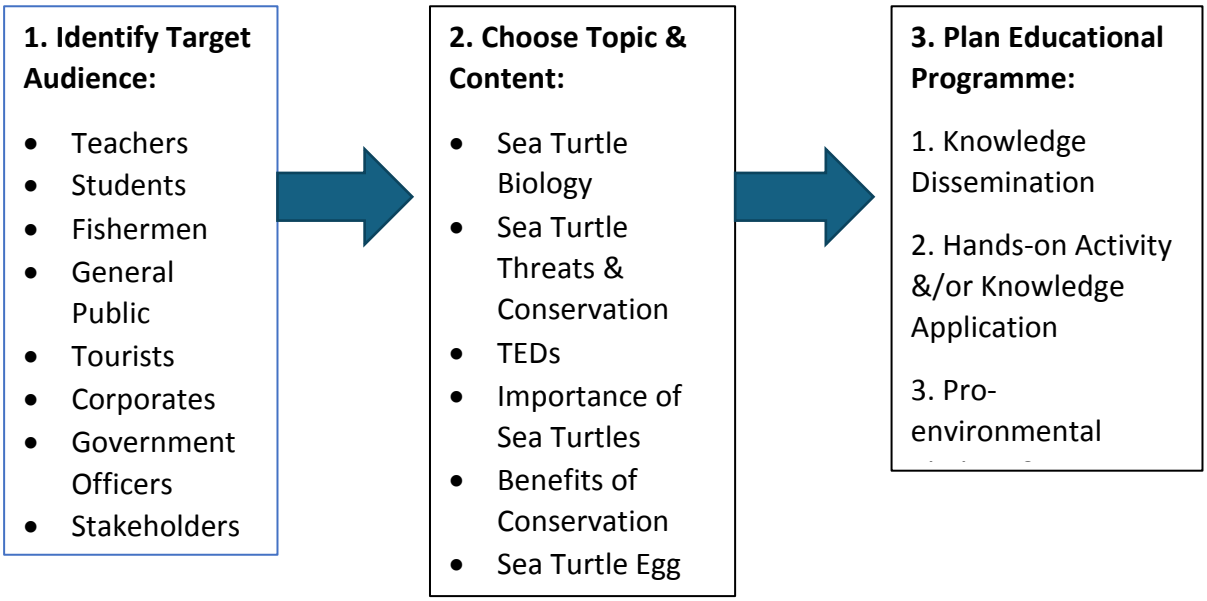

Figure 5. The framework for environmental education programmes, adapted from Ahmad-Kamil *et al.* (2024) and Gratwicke *et al.* (2016)

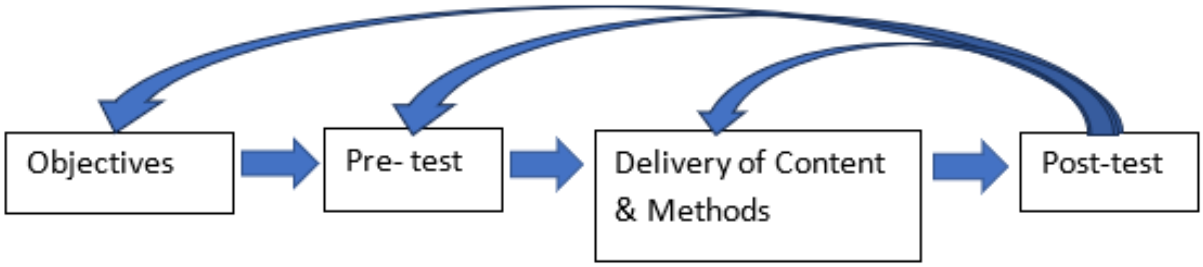

Figure 6. The General Teaching Model, adapted from Hungerford *et al.* (1988)

As sea turtle conservation encompasses both aspects, employing both strategies can maximise the effectiveness of awareness raising. As for knowledge application, Ta (2024) suggested that

low-effort contests offering various prizes can be effective in promoting conservation as evidenced by the success of the residential energy conservation contest in Vietnam. The launch of a sea turtle conservation campaign in Central Africa focusing on (1) knowledge dissemination in the form of public service announcements, awareness texts, posters, lectures etc. and (2) knowledge application in cooking contests to promote alternative food sources to sea turtles was effective in reducing turtle eggs consumption (Thomas- Walters *et al*., 2020). These studies by Schwichow *et al*. (2016) and Thomas- Walters *et al*. (2020) show that the employment of either hands-on activities or knowledge application on top of knowledge dissemination can contribute to awareness raising. Therefore, the strategy employment of the majority of the organisations in this study is adequate and should be maintained.

Recommendations

Broadening the scope of awareness programme types and consistency is crucial to altering the mindsets of local communities to protect Malaysia's sea turtle populations. To overcome the monetary and manpower challenges possibly faced by many organisations, this paper provides a few recommendations. Generating income by offering paid services such as guided tours, workshops and educational programmes is a great way to start. Transparency in terms of annual reports and updates can help to build trust with funding donors and stakeholders, paving the way for long-term funding. On the same note, using simple tools such as pre-and-post surveys to track and demonstrate the outcomes of each programme can help to secure funding from donors. Awareness can be raised with limited resources as well. An example would be expanding virtual efforts by conducting webinars or online sea turtle contests that can reach a broader audience with minimal costs in terms of logistics and manpower. Training volunteers, students or other community members in sea turtle knowledge and empowering them to conduct independent awareness programmes is another possible initiative. This has the potential to multiply the efforts of an organisation in the long term without the need for continuous output. To overcome the issue of the lack of trained personnel, establishing skill-based volunteering to attract professionals such as educators, content creators and graphic designers is a great way to fill in vacancies for programme hosts, programme development, event planning and so forth. By combining these approaches, organisations can overcome their challenges and sustainably extend their outreach efforts to foster greater impacts.

Limitations & Future Research

The following limitations in this study may be addressed in future research. Due to the time constraints of the authors, the scope and accuracy of this review may be limited as the documentation of outreach efforts is highly dependent on the transparency and activeness of each organisation in updating its annual reports, websites and social media. Some organisations such as WWF-Malaysia with more manpower and followers update their digital platforms more actively than others. Few organisations update their organisation activities via annual reports on time, while others fail to produce annual reports probably due to their lack of manpower and time. Other organisations may be inactive on digital platforms altogether and thus were not sampled. In addition, some social media posts of biodiversity programmes were excluded from this analysis due to the vague descriptions that may or may not include sea turtle-related activities. These issues may lead to biases in the dataset and limit the scope of this review. In future analyses, sufficient time should be allocated for a thorough analysis of the activities of each organisation to account for delays in virtual updates, and direct engagement with each organisation to minimise biases and gaps in the data collection. Moreover, in-depth analyses of the strategies employed in each programme conducted by the organisations and their impacts will be beneficial. In this study, limited literature on knowledge application in conservation awareness can be found and therefore would be a good topic to delve into as well.

CONCLUSION

As a sea turtle nesting hotspot, Malaysia is experiencing a decline in Green and Hawksbill nesting populations, highlighting the urgent need for effective awareness programmes to promote sea turtle conservation and civic engagement. The evidence presented in this paper indicates that school and youth outreach programmes must be prioritised by more sea turtle

conservation entities, as these initiatives are of utmost importance for shaping conservation attitudes in younger generations. Moreover, the majority of organisations were found to employ multiple outreach strategies, enhancing the effectiveness of their programmes. Efforts to secure sufficient funding and manpower or maximise the use of limited resources must be emphasised to enable organisations to further broaden their outreach focuses, raise more extensive awareness and counter sea turtle population declines. Future studies should include an analysis of the specific strategies adopted in each awareness programme conducted by each organisation and their effectiveness. Conducting virtual or verbal interviews with the personnel(s) from each organisation can refine these findings. These insights will help determine the most effective framework for sea turtle outreach programmes in Malaysia, and reduce anthropogenic pressures on sea turtle populations.

ACKNOWLEDGEMENTS

The authors would like to express their deepest appreciation to the Universiti Malaysia Sarawak for providing the opportunity to complete this paper. The authors would also like to acknowledge, with much appreciation, the crucial role of the UNIMAS PeTARY Library in providing all the necessary closed-access materials for this review.

REFERENCES

Abdul Rahman, H. (2020). Malaysian youth and environmental sustainability: A review. *Perspektif: Jurnal Sains Sosial dan Kemanusiaan*, 12(2): 43-54. DOI: 10.37134/perspektif.vol12.2.6.2020

Abdul Rahman, R., Wong, E.P., Joseph, J., Salleh, S.M., Khoo, S.N., Ismail, M.S., Rahim, M.A., Ramli, R., Ang, T.L., Lee, B.H., Chan, Z.S. & Long, S.L. (2021). First Record of a Stranded Loggerhead Turtle (*Caretta caretta*) in a Ghost Net off Penang, Malaysia. *Marine Turtle Newsletter*, 162: 22-24.

Abd Mutalib, A.H., Fadzly, N. & Foo, R. (2013). Striking a balance between tradition and conservation: General perceptions and awareness level of local citizens regarding turtle conservation efforts based on age factors and gender. *Ocean & Coastal Management*, 78: 56–63. DOI:10.1016/j.ocecoaman.2013.03.015

Ahmad-Kamil, E.I., Syed Zakaria, S.Z., Othman, M., Chen, F.L. & Deraman, M.Y. (2024). Enabling marine conservation through education: Insights from the Malaysian Nature Society. *Journal of Cleaner Production*, 435. DOI:10.1016/j.jclepro.2024.140554

Abdullah, N.A.A. & Halim, N.A. (2018). Local communities readiness and willingness in turtle-based ecotourism: Case study of turtle conservation area in Melaka Malaysia. *Journal of Tourism, Hospitality and Environment Management*, 3(11): 25-36.

Becken, S., Connolly, R.M., Chen, J. & Stantic, B. (2019). A hybrid is born: Integrating collective sensing, citizen science and professional monitoring of the environment. *Ecological Informatics*, 52: 35-45. DOI:10.1016/j.ecoinf.2019.05.001

Boyd, D. (2019). Utilising place-based learning through local contexts to develop agents of change in early childhood education for sustainability. *Education*, 47(8): 983–997. DOI:10.1080/03004279.2018.1551413

Brander, L., Eppink, F., Hof, C.M., Bishop, J., Riskas, K., Goñi, V.G., Teh, L. & Teh, L. (2024). Turtle Economic Value: The non-use value of marine turtles in the Asia-Pacific region. *Ecological Economics*, 219: 108148. DOI:10.1016/j.ecolecon.2024.108148

Calmanovici, B., Waayers, D., Reisser, J., Clifton, J. & Proietti, M. (2018). I3S Pattern as a mark-recapture tool to identify captured and free-swimming sea turtles: An assessment. *Marine Ecology Progress Series*, 589: 263–268. DOI:10.3354/meps12483

Carver, L. & Sullivan, S. (2017). How economic contexts shape calculations of yield in biodiversity offsetting. *Conservation Biology*, 31(5): 1053–1065. DOI:10.1111/cobi.12917

Chan, E.H. & Liew, H.C. (1996). Decline of the leatherback population in Terengganu, Malaysia, 1956-1995. *Chelonian Conservation and Biology*, 2(2): 196-203.

Chan, E.H. (2006). Marine turtles in Malaysia: On the verge of extinction? *Aquatic Ecosystem Health & Management*, 9(2): 175–184. DOI:10.1080/14634980600701559

Chan, E.H. (2013). A report on the first 16 years of a long-term marine turtle conservation project in Malaysia. *Asian Journal of Conservation Biology*, 2(2): 129–135.

Chaurasiya, P. & Gautam, D. (2023). Role of government and non-government organisations. *International Journal of Creative Research Thoughts*, 11(12): 9-14.

Chawla, L. (2020). Childhood nature connection and constructive hope: A review of research on connecting with nature and coping with environmental loss. *People and Nature*, 2(3): 619–642. DOI:10.1002/pan3.10128

Department of Statistics Malaysia. (2024). *The Population of Malaysia*. Retrieved December 22, 2024, from https://open.dosm.gov.my/dashboard/population

Dimopoulos, D. I., Paraskevopoulos, S. & Pantis, J. D. (2009). Planning educational activities and teaching strategies on constructing a conservation educational module. *International Journal of Environmental and Science Education*, 4(4): 351-364.

Erdogan, M., Kostova, Z. & Marcinkowski, T. (2009). Components of environmental literacy in elementary Science Education curriculum in Bulgaria and Turkey. *Eurasia Journal of Mathematics, Science and Technology Education*, 5(1): 15-26. DOI:10.12973/ejmste/75253

Fadli, S.N., Idris, N.H., Osman, M.J., Othman, N. & Ishak, M.H.I. (2023). Spatial distribution and the influence of surface temperature and green area on sea turtle nesting sites in Peninsular Malaysia. *IOP Conference Series: Earth and Environmental Science*, 1240(1): 012012. DOI:10.1088/1755-1315/1240/1/012012

Frame, J.R., Good, B., Slinger, P., Smith, M. P., Butler, B. & Marancik, D. (2021). Measuring of the effects of a sea turtle conservation education program on children's knowledge and attitudes in Grenada, West Indies. *Ocean & Coastal Management*, 211: 105752. DOI:10.1016/j.ocecoaman.2021.105752

Gomez, L. & Krishnasamy, K. (2019). *A rapid assessment on the trade in marine turtles in Indonesia, Malaysia and Viet Nam.* TRAFFIC. Petaling Jaya, Malaysia.

Gruby, R.L., Miller, D.C., Enrici, A. & Garrick, D. (2023). Conservation philanthropy: Growing the field of research and practice. *Conservation Science and Practice*, 5(5). DOI:10.1111/csp2.12977

Hassan, R. & Yahya, N.K. (2022). Green sea turtle (*Chelonia mydas*): A historical review with relevance to population size in Sarawak. *International Journal of Biology and Biomedical Engineering*, 16: 221–232. DOI:10.46300/91011.2022.16.28

Hassan, R., Yahya, N.K., Ong, L.M., Kheng, L.K., Abidin, Z.Z., Ayob, A. & Jainal, A.M. (2017). Public awareness program and development of education toolkit for green sea turtle conservation in Sarawak, Malaysia. *International Journal of Environmental and Science Education*, 12(3): 463-474. DOI: 10.12973/ijese.2016.1241p

Hoh, D., Fong, C.-L., Su, H., Chen, P., Tsai, C.-C., Tseng, K. & Liu, M. (2022). A dataset of sea turtle occurrences around the Taiwan coast. *Biodiversity Data Journal*, 10. DOI:10.3897/BDJ.10.e90196

Holstermann, N., Grube, D. & Bögeholz, S. (2010). Hands-on activities and their influence on students' interest. *Research in science education*, 40: 743-757. DOI:10.21203/rs.3.rs-5353475/v1

Hungerford, H.R. (1988). An environmental education approach to the training of elementary teachers: A teacher education programme. *UNESO-UNEP International Environmental Education Programme*, 27.

IUCN-SSC Marine Turtle Specialist Group (MTSG). (n.d.). *Marine Turtle Red List Assessment*. Retrieved May 14, 2024, from https://www.iucn-mtsg.org/statuses.

Ismail, N., Nyok, C.P. & Maryati, M. (2021). Turtle Awareness Program: A preliminary study on primary school students' knowledge on turtle conservation in Malaysia. *IOP Conference Series: Earth and Environmental Science*, 736(1): 012024. DOI:10.1088/1755-1315/736/1/012024

Ismail, Z., Abdul Mutalib, A., Ismail, F., Che Man, S. I., Ab Latiff, Z. & Zahali, Z. (2020). Effects of copper sulphate on the survival of free-living stage of *Schistocephalus coracidia*. *Journal of Sustainability Science and Management*, 15(6): 28–35. DOI:10.46754/jbsd.2020.09.001

Ives, C.D., Abson, D.J., von Wehrden, H., Dorninger, C., Klaniecki, K. & Fischer, J. (2018). Reconnecting with nature for sustainability. *Sustainability Science*, 13(5): 1389–1397. DOI:10.1007/s11625-018-0542-9

Jaaman, S.A., Lah-Anyi, Y.U. & Pierce, G.J. (2009). The magnitude and sustainability of marine mammal by-catch in fisheries in East Malaysia. *Journal of the Marine Biological Association of the United Kingdom*, 89(5): 907-920. DOI:10.1017/S002531540800249X

Jani, J.M., Jamalludin, M.A. & Long, S.H. (2020). To ban or not to ban? Reviewing an ongoing dilemma on sea turtle egg trade in Terengganu, Malaysia. *Frontiers in Marine Science*, 6: 1-18. DOI:10.3389/fmars.2019.00762

Jannah, M., Halim, L., Meerah, T.S.M. & Fairuz, M. (2013). Impact of environmental education kit on students' environmental literacy. *Asian Social Science*, 9(12). DOI:10.5539/ass.v9n12p1

Jeethvendra, K., Nishizawa, H., Alin, J., Muin, H. & Joseph, J. (2023). Illegal tortoiseshell harvest of hawksbill turtles (*Eretmochelys imbricata*) in Southeast Asia: Evidence from Baturua reef, Semporna, Sabah, Malaysia. *Journal of Sustainability Science and Management*, 18(7): 53–66. DOI:10.46754/jssm.2023.07.004

Jenkins, L.D. (2023). Turtles, TEDs, tuna, dolphins, and diffusion of innovations: Key drivers of adoption of bycatch reduction devices. *ICES Journal of Marine Science*, 80(3): 417–436. DOI:10.1093/icesjms/fsac210

Jiménez Acosta, D., Rodríguez Sandoval, M., Anaya Herrera, J. & Martinez Bula, L. (2024). Environmental education as a strategy that promotes the conservation of *Trachemys Callirostris* (Turtle) in students of the Santiago Apostle Educational Institution, Sucre, Colombia. *Migration Letters*, 21(S4): 291–301.

Jolis, G., Min, L.M., Mustafa, S.R.S., Sumamporuw, M., Rajan, S.G., Jumin, R. & Sharma, D.S. (2015). Sea turtle conservation in Malaysia: Issues, challenges and recommendations. Proceedings of the *Conference: Seminar and Workshop on Sea Turtle Conservation in Malaysia*, 1-3 September 2015, Kuala Terengganu, Malaysia. Marine Programme, WWF-Malaysia. pp. 1-6.

Joseph, J., Jolis, G., Jeethvendra, K., Jalimin, S.N., Nishizawa, H., Muin, H., Isnain, I. & Saleh, E. (2022). *Chapter 7: Research and conservation of marine turtles at nesting and foraging grounds*. In Yoshida, T. and Manjaji-Matsumoto, B.M (eds.) *The Marine Ecosystems of Sabah*. Kota Kinabalu, Malaysia, Penerbit Universiti Malaysia Sabah. pp. 95-123.

Joseph, J., Nishizawa, H., Alin, J.M., Othman, R., Jolis, G., Isnain, I. & Nais, J. (2019). Mass sea turtle slaughter at Pulau Tiga, Malaysia: Genetic studies indicate poaching locations and its potential effects. *Global Ecology and Conservation*, 17. DOI:10.1016/j.gecco.2019.e00586

Koeswiryono, D.P. & Chandra, I.M.K.A. (2021). Developing English module for turtle conservation guides. *Journal of English Language Teaching and Applied Linguistics*, 2(1): 1–8. DOI:10.21460/saga.2020.21.73

Kuo, M., Browning, M.H.E.M. & Penner, M.L. (2018). Do lessons in nature boost subsequent classroom engagement? Refueling students in flight. *Frontiers in Psychology*, 8: 2253. DOI:10.3389/fpsyg.2017.02253

Larson, L.R., Szczytko, R., Bowers, E.P., Stephens, L.E., Stevenson, K.T. & Floyd, M.F. (2019). Outdoor time, screen time, and connection to nature: Troubling trends among rural youth? *Environment and Behavior*, 51(8): 966-991.

Leh, C. (1985). Marine Turtles in Sarawak. *Marine Turtle Newsletter*, 35: 1-3.

Li, Y., Wang, B. & Saechang, O. (2022). Is female a more pro-environmental gender? Evidence from China. *International Journal of Environmental Research and Public Health*, 19(13): 8002. DOI:10.3390/ijerph19138002

Liefländer, A.K. & Bogner, F.X. (2014). The effects of children's age and sex on acquiring pro-environmental attitudes through environmental education. *The Journal of Environmental Education*, 45(2): 105–117. DOI:10.1080/00958964.2013.875511

Liu, T.-M. (2020). Applying Ostrom's common resource management principles to analyze institutional factors for the failure of the volunteer tourism program for green sea turtles conservation in Lanyu (Orchid Island), Taiwan. *Journal of Tourism and Cultural Change*, 18(6): 711–727. DOI:10.1080/14766825.2019.1634722

Long, R. (2016). Project success. *ITNOW*, 58(4): 4–7. DOI:10.1093/itnow/bww090

Long, S.L. & Azmi, N.A. (2017). Using photographic identification to monitor sea turtle populations at Perhentian Islands Marine Park in Malaysia. *Herpetological Conservation and Biology*, 12(2): 350-366.

Lucrezi, S., Milanese, M., Palma, M. & Cerrano, C. (2018). Stirring the strategic direction of scuba diving marine citizen science: A survey of active and potential participants. *PloS one*, 13(8): 1-28. DOI:10.1371/journal.pone.0202484

Mann, J., Gray, T., Truong, S., Brymer, E., Passy, R., Ho, S., Sahlberg, P., Ward, K., Bentsen, P., Curry, C. & Cowper, R. (2022). Getting out of the classroom and into nature: A systematic review of nature-specific outdoor learning on school Children's learning and development. *Frontiers in Public Health*, 10: 877058. DOI:10.3389/fpubh.2022.877058

Marin-Pantelescu, A., Tachiciu, L., Capusneanu, S. & Topor, D.I. (2019). Role of tour operators and travel agencies in promoting sustainable tourism. *Amfiteatru Economic*, 21(52): 654-669. DOI:10.24818/EA/2019/52/654

Martin, V., Smith, L., Bowling, A., Christidis, L., Lloyd, D. & Pecl, G. (2016). Citizens as scientists. *Science Communication*, 38(4): 495–522. DOI:10.1177/1075547016656191

Mazaris, A.D., Schofield, G., Gkazinou, C., Almpanidou, V. & Hays, G.C. (2017). Global sea turtle conservation successes. *Science Advances*, 3(9): 1-7. DOI:10.1126/sciadv.1600730

McGehee, N.G. & Andereck, K. (2009). Volunteer tourism and the "voluntoured": The case of Tijuana, Mexico. *Journal of Sustainable Tourism*, 17(1): 39-51. DOI:10.1080/09669580802159693

Mendes, S., Martins, J. & Mouga, T. (2019). Ecotourism based on the observation of sea turtles–A sustainable solution for the touristic promotion of São Tomé and Príncipe. *Cogent Social Sciences*, 5(1): 1-16. DOI:10.1080/23311886.2019.1696001

Mihalic, T. (2016). Sustainable-responsible tourism discourse – towards 'responsustable' tourism. *Journal of Cleaner Production*, 111: 461–470. DOI:10.1016/j.jclepro.2014.12.062

Nahill, B. (2021). Sea turtle ecotourism. *Sea Turtle Research and Conservation*, 95–104. DOI:10.1016/B978-0-12-821029-1.00010-6

National Oceanic and Atmospheric Administration (NOAA). (2021). *Turtle excluder devices*. Retrieved May 20, 2024, from https://www.fisheries.noaa.gov/southeast/bycatch/turtle-excluder-devices

Norkhaidi, S.B., Mahat, H. & Hashim, M. (2021). Environmentally-literate citizenry among malaysian youth to produce responsible environmental behaviour. *Akademika*, 91(1): 97–107. DOI:10.17576/akad-2021-9101-08

Pertiwi, N.P.D., Suhendro, M.D., Yusmalinda, N.L.A., Putra, I.N.G., Putri, I.G.R.M., Artiningsih, E.Y., Al-Malik, M.D., Cahyani, N.K.D. & Sembiring, A. (2020). Forensic genetic case study: Species identification and traceability of sea turtle caught in illegal trade in Bali, Indonesia. *Biodiversitas*, 21(9): 4276-4283. DOI:10.13057/biodiv/d210945

Pilcher, N.J., Bali, J., Buis, J., Chan, E.H., Devadasan, A., Isnain, I., Jamil, N.H., Joseph, J., Lau, M.M., Liew, H.C., Syed Abdul Kadir, S.A., Ruqaiyah, S., Tisen, O.B., Van der Merwe, J.P. & Williams, J. (2019). A review of sea turtle satellite tracking in Malaysia. *Indian Ocean Turtle Newsletter*, 29: 11-22.

Project GloBAL. (2008). Workshop Proceedings: Tackling fisheries bycatch: Managing and reducing sea turtle bycatch in gillnets. *Project GloBAL Technical Memorandum*, (1): 1-57. DOI:10.13140/RG.2.1.1414.7280

Poti, M., Long, S.L., Rusli, M.U., Mohd Jani, J., Hugé, J. & Dahdouh-Guebas, F. (2021). Changing trends and perceptions of sea turtle egg consumption in Redang Island, Malaysia. *Ecology and Society*, 26(4): 14. DOI: 10.5751/ES-12717-260414

Read, A.J. (2008). The looming crisis: Interactions between marine mammals and fisheries. *Journal of Mammalogy*, 89(3): 541-548. DOI: 10.1644/07-MAMM-S-315R1.1

Reef Check Malaysia. (2023). *Partnering for the Marine Ecosystem – Signing of a Memorandum of Understanding between Reef Check Malaysia and the Department of Fisheries*. Retrieved May 20, 2024, from https://www.reefcheck.org.my/press/ partnering-for-the-marine-ecosystem-signing-of-a-memorandum-of-understanding-between-reef-check-malaysia-and-the-department-of-fisheries

Sahahiri, R.M., Griffin, A.L. & Sun, Q. (2023). Investigating ecotourism opportunities measurements in a Complex Adaptive System: A systematic literature review. *Sustainability*, 15(3): 2678.

Salleh, S.M., Sah, S.A.M. & Chowdhury, A.J.K. (2018). Distribution, abundance, and clutch size of hawksbill turtle nests in Melaka, Malaysia. *Malaysian Applied Biology*, 47(3): 29-38.

Sankar, O.B. & Raju, M.A. (2003). Implementation of the Turtle Excluder Device in Andhra Pradesh. *Kachhapa*, (8): 2-5.

Schwichow, M., Zimmerman, C., Croker, S. & Härtig, H. (2016). What students learn from hands-on activities. *Journal of Research in Science Teaching*, 53(7): 980–1002. DOI:10.1002/tea.21320

See, K.W. & Latip, N.S.A. (2023). *Fusarium solani* Species Complex (FSSC) in Nests of Hawksbill Turtles (*Eretmochelys imbricata*) with High Hatching Success in Melaka, Malaysia. *Pertanika Journal of Science & Technology*, 31(5): 2601-2619. DOI:10.47836/pjst.31.5.29

Ta, C.L. (2024). Do conservation contests work? An analysis of a large-scale energy competitive rebate program. *Journal of Environmental Economics and Management*, 124: 102926. DOI:10.1016/j.jeem.2023.102926

Teh, L.S.L., Teh, L.C.L. & Jolis, G. (2018). An economic approach to marine megafauna conservation in the Coral Triangle: Marine turtles in Sabah, Malaysia. *Marine Policy*, 89: 1–10. DOI:10.1016/j.marpol.2017.12.004

Thomas-Walters, L., Vieira, S., Jiménez, V., Monteiro, D., Ferreira, B., Smith, R.J. & Veríssimo, D. (2020). Challenges in the impact evaluation of behaviour change interventions: The case of sea turtle meat and eggs in São Tomé. *People and Nature*, 2(4): 913–922. DOI:10.1002/pan3.10162

Thomson, R.C., Spinks, P.Q. & Shaffer, H.B. (2021). A global phylogeny of turtles reveals a burst of climate-associated diversification on continental margins. *Proceedings of the National Academy of Sciences*, 118(7). DOI:10.1073/pnas.2012215118

Tikka, P.M., Kuitunen, M.T. & Tynys, S.M. (2000). Effects of educational background on students' attitudes, activity levels, and knowledge concerning the environment. *The Journal of Environmental Education*, 31(3): 12–19. DOI:10.1080/00958960009598640

Tisdell, C. & Wilson, C. (2000). Economic, educational and conservation benefits of sea turtle based ecotourism : a study focused on Mon Repos. *Cooperative Research Centre for Sustainable Tourism*, 20.

Tisdell, C. & Wilson, C. (2005). Perceived impacts of ecotourism on environmental learning and conservation: Turtle watching as a case study. *Environment, Development and Sustainability*, 7(3): 291–302. DOI:10.1007/s10668-004-7619-6

Tookes, J.S., Yandle, T. & Fluech, B. (2023). The role of fisher engagement in the acceptance of turtle excluder devices in Georgia's shrimping industry. *ICES Journal of Marine Science*, 80(3): 407–416. DOI:10.1093/icesjms/fsac062

Troëng, S. & Drew, C. (2009). *Money Talks: Economic Aspects of Marine Turtle Use and Conservation by Sebastian Troëng and Carlos Drews*. Retrieved April 29, 2024, from https://wwf.panda.org/wwf_news/?153802/wwwpandaorglacmarineturtlespublications

Virgili, M., Petetta, A., Barone, G., Veli, D.L., Bargione, G. & Lucchetti, A. (2024). Engaging fishers in sea turtle conservation in the Mediterranean Sea. *Marine Policy*, 160: 105981. DOI:10.1016/j.marpol.2023.105981

Wilson, C. & Tisdell, C. (2003). Conservation and economic benefits of wildlife-based marine tourism: Sea turtles and whales as case studies. *Human Dimensions of Wildlife*, 8(1): 49–58. DOI:10.1080/10871200390180145

World Wide Fund for Nature (WWF). (2015). *Illegal Take and Trade of Marine Turtles in the Indian Ocean Region*. Retrieved May 25, 2024, from https://wwf.panda.org/wwf_news/?240870/Illegal-Take-and-Trade-of-Marine-Turtles-in-the-Indian-Ocean-Region

Yong, B. (2021). *Reconsider Ban on Turtle Egg Sale, Say Terengganu Traders*. Retrieved May 20, 2024, from https://www.macaranga.org/turtle-egg-sale-ban-terengganu-traders/

Young, S.T. & Dhanda, K.K. (2013). Role of governments and nongovernmental organizations. *Sustainability: Essentials for Business*, 214-241.

Zahra, A. & McGehee, N.G. (2013). Volunteer tourism: A host community capital perspective. *Annals of Tourism Research*, 42: 22-45. DOI:10.1016/j.annals.2013.01.008

Zelezny, L.C. (1999). Educational interventions that improve environmental behaviors: A meta-analysis. *The Journal of Environmental Education*, 31(1): 5–14. DOI:10.1080/00958969909598627

Zhu, Y., Chen, C., Zhang, G., Lin, Z., Meshram, S.G. & Alvandi, E. (2023). Investigation of West Lake ecotourism capabilities using SWOT and TOPSIS decision-making methods. *Sustainability*, 15(3): 2464. DOI:10.3390/su15032464

Zulkifli, N.S.H. & Kamaludin, M. (2023). Penilaian ekonomi nilai gunaan pasif bagi program pemuliharaan penyu laut di Terengganu, Malaysia. *Universiti Malaysia Terengganu Journal of Undergraduate Research*, 5(1): 11–21. DOI:10.46754/umtjur.v5i1.318

Borneo Journal of Resource Science and Technology (2025), 15(1): 23-31
DOI: https:doi.org/10.33736/bjrst.7355.2025

Influence of Monsoon Seasons on Seagrass Ecosystems on the Coast of Kota Kinabalu (Sabah, Malaysia)

MOHD AZAMUDDIN MOHD HASSAN[1], EJRIA SALEH[*1,2], ROHANA TAHIR[2] & JOHN MADIN[1]

[1]Borneo Marine Research Institute, Universiti Malaysia Sabah, Jalan UMS, 88400, Kota Kinabalu, Sabah, Malaysia; [2]Natural Disaster Research Centre, Faculty of Science and Technology, Jalan UMS, 88400, Kota Kinabalu, Sabah, Malaysia
*Corresponding author: ejsaleh@ums.edu.my
Received: 9 July 2024 Accepted: 26 February 2025 Published: 30 June 2025

ABSTRACT

Seagrass beds in Kampung Kebagu, Kota Kinabalu, Sabah, are notably affected by natural events and human activities. Seasonal monsoons particularly the Northeast Monsoon (NEM) and the Southwest Monsoon (SWM), intensify these effects, causing significant changes to the seagrass beds in a short period. This study aimed to determine seagrass coverage and leaf length during the NEM and SWM at Kampung Kebagu. The leaf length was focusing on the dominant species; *Enhalus acoroides* along the transect line. This study was conducted within a year from February 2023 until January 2024 to cover both monsoon periods. Seagrass coverage was estimated using 50 cm × 50 cm (0.25 m^2) quadrat with every 5 m interval along the transect line. Field measurements and data collection were done in February 2023, March 2023, May 2023, July 2023, September 2023, November 2023, and January 2024. The NEM was divided into two phases: February to March 2023 (T1) and November 2023 to January 2024 (T3). The SWM, identified as T2, spanned from May to September 2023. Further analysis of seagrass coverage and leaf length using Two-Way ANOVA was done to find significant effects of month between the parameters. There were significant different between seagrass coverage and months ($p < 0.05$). Seagrass coverage declined significantly to 38 ± 23% during the NEM but rebounded to 80 ± 11% in July 2023 during the SWM. The average leaf length of *E. acoroides* reached 29 ± 8 cm in May 2023 but was reduced to just 7 ± 2 cm by January 2024. Although this study was limited to a single year, it effectively captured fluctuations in seagrass coverage and leaf length across different seasonal monsoons. These results provide baseline data on how monsoon-related environmental changes affect seagrass ecosystems in this region.

Keywords: Kota Kinabalu, leaf length, northeast monsoon, seagrass coverage, southwest monsoon

INTRODUCTION

Seagrass is a unique marine angiosperm that can live up to a certain meter depth in the intertidal or subtidal zone. Malaysia is home to 17 different species of seagrass, which belong to three distinct families and these seagrass species are categorized into the genera *Enhalus, Halophila*, *Cymodocea, Halodule, Syringodium* and *Thalassia* (Kamal *et al*., 2023; Md-Nor, 2023).

Each genus contributes to the rich biodiversity of Malaysia's coastal and marine ecosystems. *Enhalus acoroides* is known as tape seagrass or tropical eelgrass and it is a large-sized seagrass found throughout the coastal waters of Southeast Asia and it can reach up to 1 meter or more in height (Bujang *et al*., 2018; Syed *et al*., 2019). The above-ground parts of the plant consist of long, strap-like leaves and flowers, while the below-ground parts include cord-like roots and thick rhizomes with black bristles. Seagrass provides numerous ecosystem services, and it may vary from biological importance such as being the nursery and feeding ground for marine species, and physical processes where seagrass assists in increasing the clarity of water by acting as a biological filter (Honda *et al*., 2013). Seagrass also provides habitat to marine life where coastal communities around the globe catch and collect their protein in seagrass areas thus becoming their livelihood (Green & Short, 2003).

The seasonal monsoon orients the climate in Malaysia; Northeast Monsoon (NEM) (November to March), the first inter-monsoon period (April), the Southwest Monsoon (SWM) (May to September), and the second inter-

monsoonal period (October) (Lolli *et al*., 2019). The extreme wave and storm events mainly occur during the peak of NEM. The changes of beach morphology in seagrass-dominated environments are influenced mainly by extreme wave events that lead to excessive erosion and deposition (Risandi *et al*., 2023). Coastal erosion may also occur when waves, longshore currents, and wind transport the sediment from shore and deposit it somewhere else (Prasad & Kumar, 2014). Monsoon rains can result in increased runoff from the land, carrying large amounts of sediment from rivers and streams into the coastal areas (Sadhwani *et al*., 2022). This soil erosion and sediment movement may result in sediment deposition in coastal regions, changing the dynamics and morphology of the shoreline and these processes affect the coastal ecosystems such as seagrass and mangrove ecosystems (Fitri *et al*., 2019; Figlus, 2022).

Patches of seagrass can be found near the coastal area and islands in Sabah. Record of seagrass species and its distribution in Kudat, Sabah were reported by Bujang *et al*. (2006) and Rajamani and Marsh (2015). Seagrass monitoring activities were also conducted on Pulau Gaya, Sabah (Short *et al*., 2014). There were two study sites (Kuari Bay & Police Beach) in Pulau Gaya that were reported to decline in seagrass total coverage due to excess sedimentation (Freeman *et al*., 2008). One of the remaining seagrass beds in the coastal area of Kota Kinabalu is located at Kampung Kebagu (Figure 1). However, it is prone to encounter seagrass beds degradation from both natural and anthropogenic activities. The natural cause primarily arises from seasonal monsoons, which bring changes in rainfall, wind, waves, and currents, thereby impacting seagrass coverage, leaf length and seabed sediment (Thomas, 2023; Yanalagaran *et al*., 2019; Govindasamy *et al*., 2013). During low tide, the seagrass is exposed to air and the nearby coastal communities glean on the seagrass bed for shellfish, sea cucumber, and small fish. This activity might affect the growth and coverage of the seagrass. Currently, no study on seagrass coverage and leaf length related to seasonal monsoons has been conducted in this area. More research is needed to understand the ecology and its response of seagrass on the seasonal variation. The objective of this study was to determine the seagrass coverage and leaf length between NEM and SWM at Kampung Kebagu. The findings of this study provide baseline data that will be important for the long-term monitoring of seagrass ecosystems in this area. This information is essential for documenting and understanding the changes and dynamics in seagrass beds in this area over time.

MATERIALS AND METHODS

Study Area

The study area is located in Kampung Kebagu, Kota Kinabalu (6º03'11.86" N, 116º06'35.62" E), Sabah. There were about 12 seagrass species identified in Sabah, and seven of the seagrass species are found in Kampung Kebagu (Thomas, 2023; Bujang *et al*., 2006; Phang, 2000). The study area is located about 2 km from the river mouth of the Sungai Menggatal (Figure 1). The river plays an important role as a source of terrestrial sediment. Thomas (2023) reported that the salinity, dissolved oxygen, and temperature near the seagrass meadow were about 25.74 ppt, 8 mg/L, and 34.7ºC, respectively. These environmental parameters are suitable for seagrass growth. The field trips for data collection and measurement were done during the NEM (February, March, November 2023 and January 2024) and SWM (May, July and September 2023). The tidal elevation was less than 0.5 m (Royal Malaysian Navy, 2023; Royal Malaysian Navy 2024).

Field Data Collection and Measurement

Seagrass coverage was estimated following the guidelines set by seagrass watch (McKenzie *et al*., 2009). Three transect lines were strategically established across the seagrass beds to ensure comprehensive data collection throughout the study area. These transects were positioned perpendicular to the shoreline to capture variations in seagrass coverage and leaf length of the dominant species at various distances from the coast. The layout of these transects lines illustrated in Figure 2, providing a clear visual representation of the study design. Each transect extended 50 meters from the shoreline on seagrass beds (Figure 3), with adjacent lines spaced 25 meters apart horizontally to facilitate effective assessment of seagrass coverage (%). To estimate the seagrass coverage, a 50 cm × 50 cm (0.25 m²) (Figure 4) quadrat was placed at 5-meter intervals along

each transect, starting from the zero-meter mark and continuing to the 50-meter endpoint.

The seagrass leaf length was measured using a 40-cm ruler (Figure 5). The ruler was placed from the base to the tip of the leaf of the dominant seagrass species along the transect lines. Measurements were taken within a quadrat placed at 5-meter intervals, starting from the 0-meter point and extending to the 50-meter endpoint. For each measurement, the leaf length was recorded from the sediment to the tip of the leaf for three different shoots, with three replicates taken to calculate the average value (McKenzie *et al*., 2009).

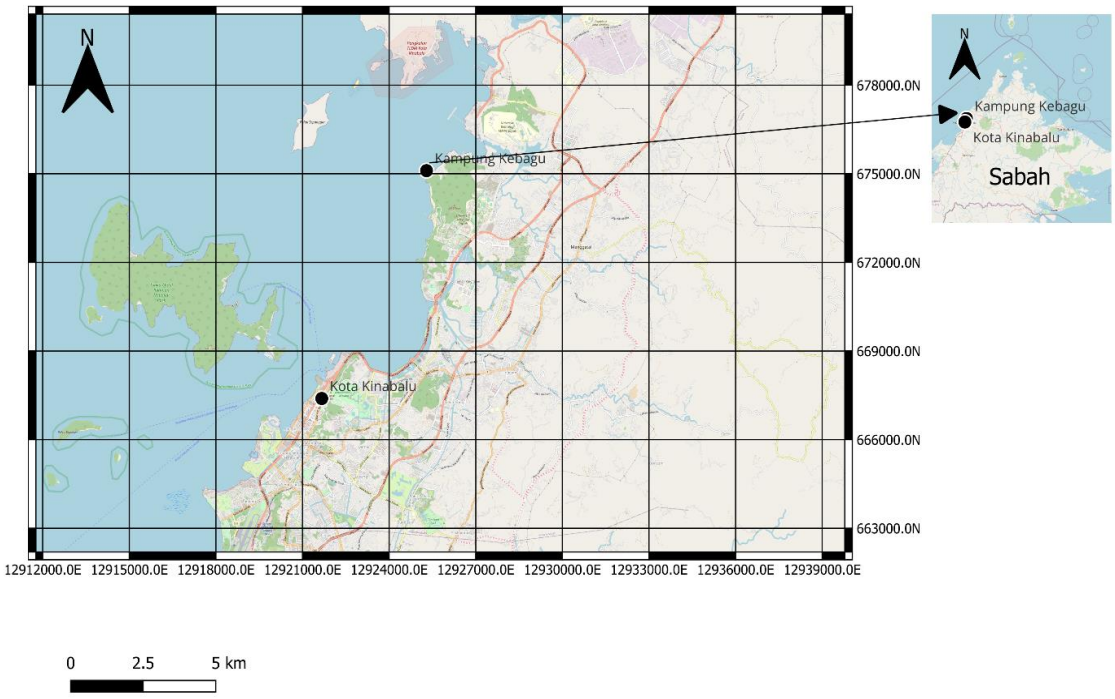

Figure 1. Location of the study area and sampling station

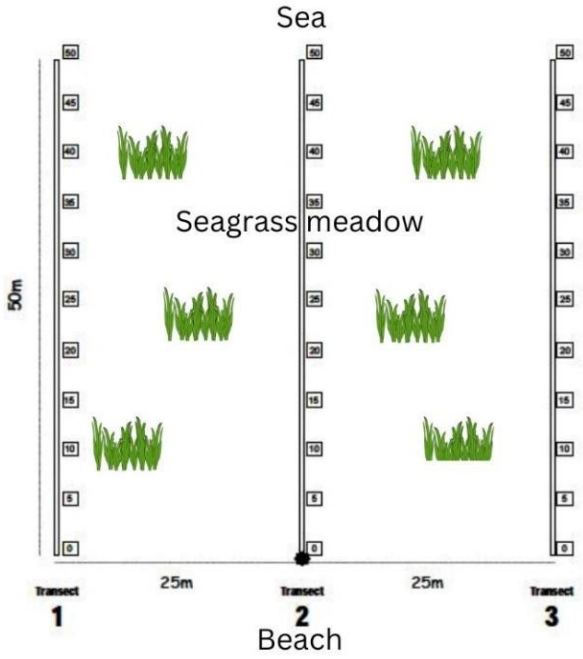

Figure 2. Illustration of the transect lines layout

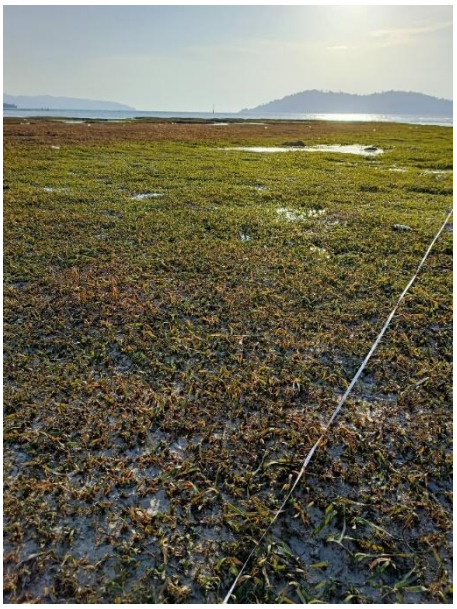

Figure 3. Transect lines on seagrass beds in Kampung Kebagu

Figure 4. Quadrat used for estimation of seagrass coverage

Figure 5. Measurement of leaf length using ruler

Data Analysis

The data collected and measured during the field trips were divided into three phases (T1, T2 and T3). The NEM, divided in two phases: February to March 2023 (T1) and November 2023 to January 2024 (T3). The SWM, marked as T2, occurred from May 2023 to September 2023. The mean and standard deviation for seagrass coverage and leaf length data were calculated using Microsoft Excel 2016. Two-Way ANOVA analysis was conducted to examine the effects of seasonal monsoon on the month and their interaction with both seagrass coverage and leaf length, with a significance level set at 0.05.

RESULTS AND DISCUSSION

Seagrass Coverage

The seagrass beds in Kampung Kebagu consist of mixed species within the beds (*Halophila ovalis*, *Enhalus acoroides*, *Oceana serulata, Halodule uninervis* and *Cymodocea rotundata)*. The seagrass beds were located about 100 m from the shoreline. No seagrass survived near the shoreline where the active longshore transport and resuspension of sediment occurred.

During the field trips, the most common seagrass species identified inside the quadrat was *E. acoroides*. This species was selected to serve as a reliable indicator of the seagrass ecosystem's health and dynamics during different seasonal monsoons. The pattern of seagrass coverage exhibited a notable rise starting from the initial phase of NEM in February-March 2023 (T1), culminating in its maximum extent in July 2023 during SWM (T2) (Figure 6). Following this peak, the seagrass coverage began to decrease from September 2023 until the onset of the second phase of NEM (T3).

During the NEM (T1) period, average seagrass coverage was approximately 38 ± 23% in February 2023 and increased to 53 ± 22% in March 2023 (Figure 6). Coverage continued to rise, reaching a peak of 80 ± 11% in July 2023 during the (SWM) (T2). However, the seagrass coverage was dropping to about 40 ± 15% by September 2023 (marked at the end of the SWM). The coverage declines persisted to 31 ± 14% and 31 ± 15% in November 2023 and January 2024 (T3), respectively. There were significant different between seagrass coverage and months ($p < 0.05$). These findings were aligned with the seagrass's study done by Saleh *et al*. (2020) in Pulau Gaya, Sabah where wave actions could reduce seagrass coverage to 41% during the NEM. However, the coverage has recovered up to 66% during the SWM period.

Leaf Length Variations

The pattern of seagrass leaf length exhibited a gradual decline from the early phase of the NEM (T1) to its later phase (T3) (Figure 7). During the T1 period, the average leaf length exhibited a steady increase, starting at approximately 20 ± 2 cm in February 2023 and growing to around 23 ± 5 cm in March 2023. This phase marked the initial stage of growth, with leaves gradually elongating. As the SWM (T2) phase commenced, the average leaf length continued to rise at approximately 29 ± 8 cm in May 2023. This growth trend stabilized during July 2023, indicating that the SWM provided optimal conditions for leaf development. However, with the onset of the second phase of NEM (T3), a gradual decline in leaf length became apparent. By September 2023 (as shown in Figure 6), the length had decreased to about 19 ± 4 cm, marking the start of a consistent reduction. This downward trend persisted, with leaf length shrinking further to approximately 12 ± 3 cm in November 2023 and reaching its lowest point of 7 ± 2 cm by January 2024.

This finding identified that the longest leaf length was measured in May 2023 during SWM (T2). This study aligned with study carried out in Indonesia at different monsoons. Rustam *et al*. (2013) reported the leaf length of *E. acoroides* were high during SWM. The growth rate of *E. acoroides* leaves can reach up to 5.6 cm/day and this period is characterized by optimal conditions for seagrass growth that, leading to increased productivity.

Analysis using Two-Way ANOVA showed that there was a statistically significant effect of month on leaf length where ($p < 0.05$). Seagrass was exposed in January 2024 (T3) as the low tide occurred in the morning. The burned and rotten seagrass leaves prone to become severely short during this period (Figure 8). The interaction between distance and month ($p < 0.05$)

suggested that these impacts are more pronounced closer to the shoreline as this part of the intertidal areas exposed to the sunlight compared to the seagrass beds located further offshore. This reflected exposure to daylight significantly reduced above-ground plant biomass due to desiccation and the scorching effect on leaves (Erftemeijer & Herman, 1994).

Overall, this study supports the idea that monsoonal disturbances have significant impact on the macroalgae community (Zainee & Rozaimi, 2020). Coverage and leaf lengths were varied across different seasonal monsoon where the observed seasonal and spatial variability underscores the sensitivity of seagrass ecosystems to environmental changes, particularly monsoonal influences. The peak productivity during SWM suggests that favourable light and nutrient conditions outweigh the potential stress from hydrodynamic forces like waves (Rustam *et al*., 2013). However, the decline during second phase of NEM (T3) associated with increased strong wind and heavy rainfall that leads to lower salinity and dissolved oxygen levels. Waves exposure and resuspended of sediment that led to turbidity peaks and finally negatively impacting seagrass (Peralta & Yusoff, 2014).

Seagrasses influence local hydrodynamics by minimizing sediment resuspension, enhancing light penetration, and supporting their growth. These variables may independently affect seagrass coverage and leaf length at different distances and across different monsoon. Bujang *et al*. (2006) mentioned one of the threats faced by intertidal seagrass in Sepangar Bay was waves driven by wind, sand movement, and erosion during the monsoon. Seagrass beds in Kampung Kebagu faced the same threats during the seasonal monsoon as the geographic location of this area in proximity with Sepangar Bay. This shown through the fluctuations of seagrass coverage and leaf length throughout the study.

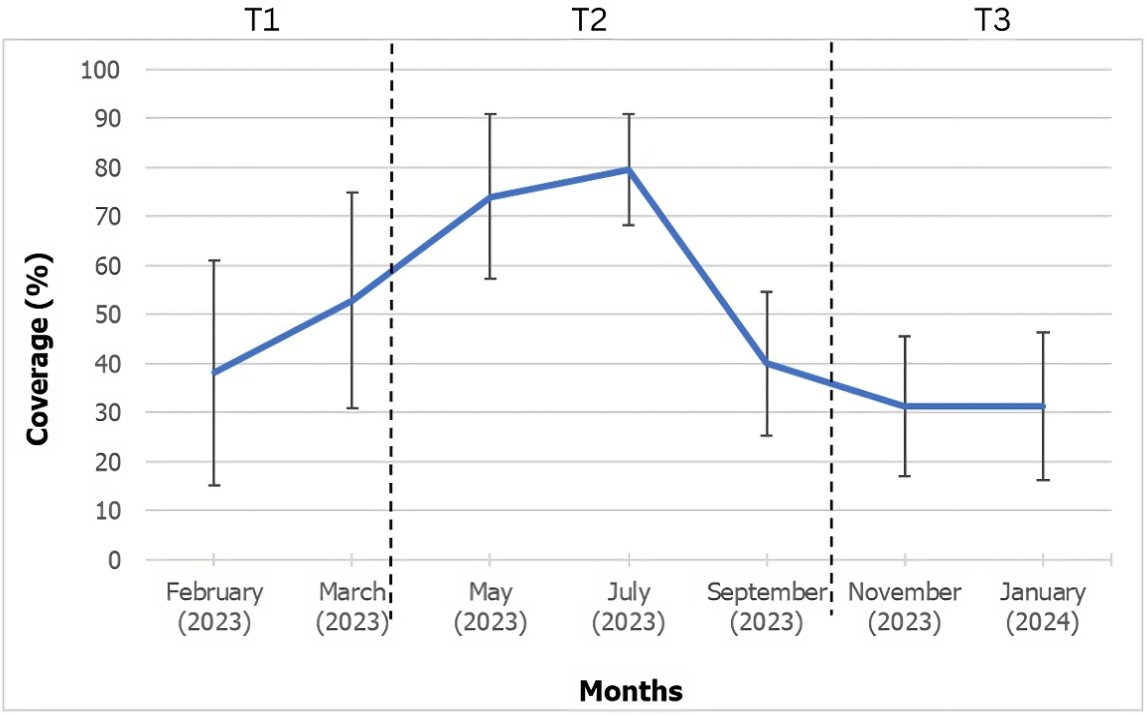

Figure 6. Changes in seagrass coverage (%) over three periods: First phase Northeast monsoon (T1), Southwest monsoon (T2), and Second phase Northeast monsoon (T3)

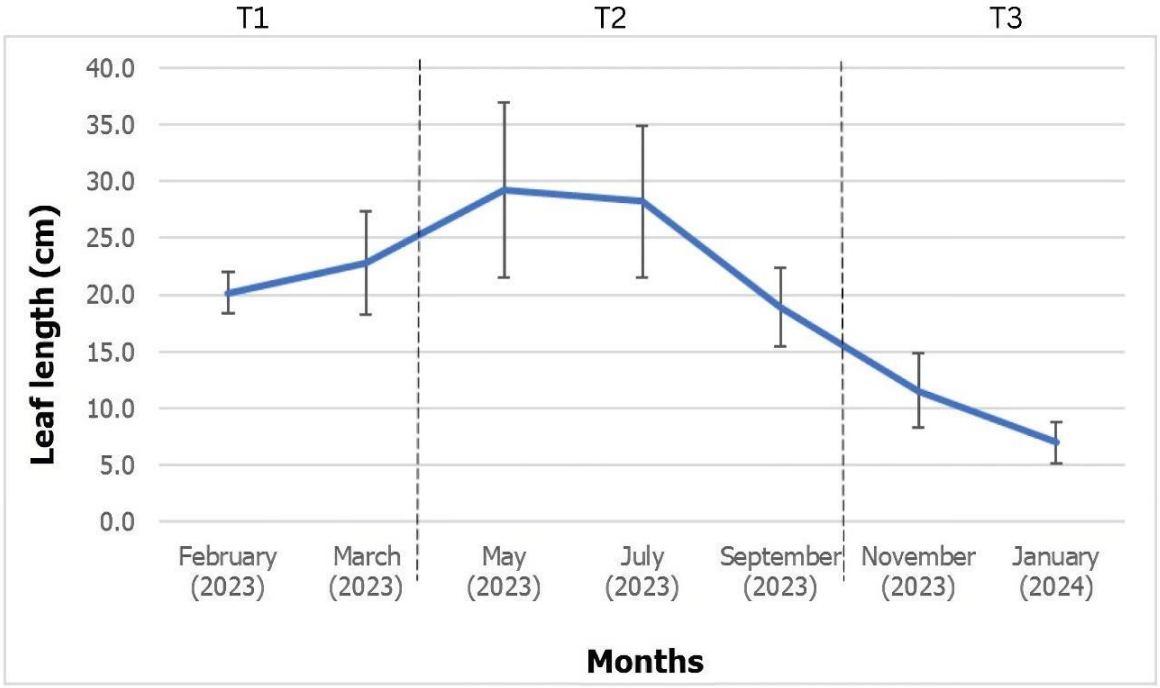

Figure 7. Changes in seagrass leaf length (cm) over three periods: First phase of Northeast monsoon (T1), Southwest monsoon (T2), and Second phase of Northeast monsoon (T3).

Figure 8. Exposure of seagrass to sunlight during low tide causes leaf burning

CONCLUSION

Monsoon seasons influence seagrass ecosystems. This study revealed distinct seasonal differences, with both seagrass coverage and leaf length peaking during the SWM and declining during the NEM. The findings reflect the significant impact of monsoonal dynamics on seagrass ecosystems in the coastal areas of Kota Kinabalu. The dominance of the seagrass species *E. acoroides* highlights its resilience and adaptability to changing environmental conditions, establishing its role as a crucial bioindicator for monitoring seagrass ecosystem health.

Although this study spanned only about a year, it clearly documented a fluctuation of

seagrass coverage and leaf length at different seasonal monsoon. During the NEM, the seagrass coverage down to 38 ± 23% but it was recovered to 80 ± 11% in July 2023 during SWM. The average length of *E. acoroides* leaves can be up to 29 ± 8 cm in May 2023 but mostly cut off to 7 ± 2 cm by January 2024.

These findings provide baseline data on the impacts of monsoon-related factors on the seagrass ecosystem at this site. It offers insights into the ecological responses of seagrass beds to seasonal monsoon variations in Sabah. This study emphasizes the importance of conservation measures, particularly during periods of environmental stress. Long-term monitoring and incorporating additional environmental parameter such as water quality, nutrient contain, wave velocity is recommended to improve better understanding on seagrass ecosystem resilience in the face of climate change and anthropogenic pressures.

ACKNOWLEDGEMENTS

This research was funded by the Universiti Malaysia Sabah under the research grant entitled: Baseline study on UMS marine ecosystem as an ecosystem approach to meet conservation and recreational objectives (DN20084) and Layang-Layang Coral Reef: Geomorphology and Variation of Marine Flora-Fauna (SDK0080-2019). The authors would like to thank the Borneo Marine Research Institute supporting staff (Mr. Jeffry Molius) and postgraduate students (Miss Shariffa Ishaziah Mohd Idris, Mr. Amir Syazwan Shawel, Miss Charissa Thalia, Mr. Muhammad Nor Afdall Nazahuddin and Miss Sarah Syazwani Shukhairi) for their technical support during field work.

REFERENCES

Bujang, J.S., Zakaria, M.H. & Arshad, A. (2006). Distribution and significance of seagrass ecosystems in Malaysia. *Aquatic Ecosystem Health & Management*, 9(2): 203-214. DOI: 10.1080/14634980600705576

Bujang, J. S., Zakaria, M. H., & Short, F. T. (2018). Seagrass in Malaysia: Issues and challenges ahead. *The wetland book II: Distribution, description, and conservation*, 1(3): 1875-1883. DOI 10.1007/978-94-007-6173-5_268-1

Erftemeijer, P.L. & Herman, P. M. (1994). Seasonal changes in environmental variables, biomass, production and nutrient contents in two contrasting tropical intertidal seagrass beds in South Sulawesi, Indonesia. *Oecologia*, 99: 45-59. DOI: 10.1007/BF00317082

Figlus, J. (2022). Modeling the movement of water and sediment in coastal environments. In *Coastal Flood Risk Reduction* (pp. 33-45). Elsevier. DOI:10.1016/B978-0-323-85251-7.00004-4

Fitri, A., Hashim, R., Abolfathi, S. & Abdul Maulud, K.N. (2019). Dynamics of sediment transport and erosion-deposition patterns in the locality of a detached low-crested breakwater on a cohesive coast. *Water*, 11(8): 1721. DOI:10.3390/w11081721

Freeman, A.S., Short, F.T., Isnain, I., Razak, F.A. & Coles, R.G. (2008). Seagrass on the edge: land-use practices threaten coastal seagrass communities in Sabah, Malaysia. *Biological Conservation*, 141(12): 2993-3005. DOI:10.1016/j.biocon.2008.09.018

Green, E.P., Short, F.T., Centre mondial de surveillance continue de la conservation de la nature, & Programme des Nations Unies pour l'environnement. (2003). *World atlas of seagrasses* (Vol. 298). Berkeley: University of California press.

Govindasamy, C., Arulpriya, M., Anantharaj, K., Ruban, P. & Srinivasan, R. (2013). Seasonal variations in seagrass biomass and productivity in Palk Bay, Bay of Bengal, India. *International Journal of Biodiversity and Conservation*, 5(7): 408-417. DOI: 10.5897/IJBC12.132

Honda, K., Nakamura, Y., Nakaoka, M., Uy, W.H. & Fortes, M.D. (2013). Habitat use by fishes in coral reefs, seagrass beds and mangrove habitats in the Philippines. *Plos one*, 8(8): e65735. DOI:10.1371/journal.pone.0065735

Kamal, A.H.M., Al-Asif, A., Idris, M.H., Bhuiyan, M.K.A. & Rahman, A.F.M. (2023). Trends in Seagrass Research and Conservation in Malaysian Waters. DOI: 10.11594/jtls.13.01.10.

Lolli, S., Khor, W.Y., Matjafri, M.Z. & Lim, H.S. (2019). Monsoon season quantitative assessment of biomass burning clear-sky aerosol radiative effect at surface by ground-based lidar observations in Pulau Pinang, Malaysia in 2014. *Remote Sensing*, 11(22): 2660. DOI:10.3390/rs11222660

McKenzie, L.J., Yoshida, R.L., Mellors, J.E. & Coles, R.G. (2009). Seagrass-watch. In Proceeding of a workshop for monitoring seagrass habitats in Indonesia. The Nature Conservancy, Coral Triangle Center, Sanur, Bali..

Peralta, H.M. & Yusoff, F. (2014). Seasonal environmental quality variations in a tropical seagrass ecosystem in the Straits of Malacca. *Malayan Nature Journal*, 59-74.

Phang, S.M. (2000). Seagrasses of Malaysia. Universiti Malaya, Botanical Monographs No. 2. Institute of Biological Sciences, Universiti Malaya, Kuala Lumpur

Prasad, D.H. & Kumar, N.D. (2014). Coastal erosion studies—a review. International Journal of Geosciences,341-345. DOI:10.4236/ijg.2014.53033

Rajamani, L. & Marsh, H. (2015). Mapping seagrass cost-effectively in the Coral Triangle: Sabah, Malaysia as a case study. *Pacific Conservation Biology*, 21(2): 113-121. DOI:10.1071/PC14908

Risandi, J., Rifai, H., Lukman, K.M., Sondak, C.F., Hernawan, U.E., Quevedo, J.M.D., Hidayat, R., Ambo-Rappe, R., Lanuru, M., McKenzie, L., Kohsaka, R. & Nadaoka, K. (2023). Hydrodynamics across seagrass meadows and its impacts on Indonesian coastal ecosystems: A review. *Frontiers in Earth Science*, 11. DOI 10.3389/feart.2023.1034827

Royal Malaysian Navy. (2023). Tide Tables 2023. National Hydrographic Centre Malaysia, Klang

Royal Malaysian Navy. (2024). Tide Tables 2024. National Hydrographic Centre Malaysia, Klang

Rustam, A., Bengen, D.G., Arifin, Z., Gaol, J.L. & Arhatin, R.E. (2013). Growth rate and productivity dynamics of *Enhalus acoroides* leaves at the seagrass ecosystem In Pari Islands based on In Situ and Alos Satellite Data. *International Journal of Remote Sensing and Earth Sciences)*, 10(1): 37-45.

Md-Nor, A., Wahid, M.E.A., Repin, I.M. & Piah, R.M., (2023). Malaysia Marine Ecological Gap Assessment Report. Department of Fisheries Malaysia, Ministry of Agriculture and Food Security. Putrajaya

Saleh, E., Tzuen-Kiat, Y. & Gallagher, J.B. (2020). Seagrass coverage and associated fauna at Gaya Island, Sabah, Malaysia: A pilot seagrass transplantation. *Borneo Journal of Marine Science and Aquaculture* , 4(1), 14-19.

Sadhwani, K., Eldho, T.I., Jha, M.K. & Karmakar, S. (2022). Effects of dynamic land use/land cover change on flow and sediment yield in a monsoon-dominated tropical watershed. *Water*, 14(22): 3666. DOI:10.3390/w14223666

Short, F.T., Coles, R., Fortes, M.D., Victor, S., Salik, M., Isnain, I., Andrew, J. & Seno, A. (2014). Monitoring in the Western Pacific region shows evidence of seagrass decline in line with global trends. *Marine Pollution Bulletin*, 83(2): 408-416. DOI:10.1016/j.marpolbul.2014.03.036

Syed, F., Zakaria, M. H., Bujang, J.S., Ramaiya, S.D. & Hayashizaki, K. (2019). Physicochemical properties of starches from seed and rhizome of Enhalus acoroides. *Philippine Journal of Natural. Sciences*, 24: 27-33.

Thomas, C. (2023). Status of seagrass meadow at Kampung Kibagu Beach, Kota Kinabalu, Sabah. (Undergraduate Thesis). Faculty of Science and Natural Resources, Universiti Malaysia Sabah

Yanalagaran, R., Ramli, N.I. & Ramadhansyah, P.J. (2019). Overview of Monsoon Induced Coastal Erosion Disaster in Peninsular Malaysia Based On Mass-Media Reports. In IOP Conference Series: *Earth and Environmental Science*, 244, (1): 012035. IOP Publishing. DOI:10.1088/1755-1315/244/1/012035

Zainee, N.F.A. & Rozaimi, M. (2020). Influence of monsoonal storm disturbance on the diversity of intertidal macroalgae along the eastern coast of Johor (Malaysia). *Regional Studies in Marine Science*, 40: 101481. DOI:10.1016/j.rsma.2020.101481

Borneo Journal of Resource Science and Technology (2025), 15(1): 32-54
DOI: https:doi.org/10.33736/bjrst.7238.2025

Antibiotic Resistance and Virulence Gene Profiles of *Vibrio parahaemolyticus*, *Vibrio cholerae*, and *Vibrio alginolyticus* Isolated from Commercial Shrimp Farm in Kuching, Sarawak

ELEXSON NILLIAN*, EASTERINA EMPINA EDWIN, DALENE LESEN, MANJU STEPHEN, MASTURA SANI

Faculty of Resource Science and Technology, Universiti Malaysia Sarawak, 94300, Kota Samarahan, Sarawak, Malaysia
*Corresponding author: nelexson@unimas.my
Received: 21 June 2024 Accepted: 2 May 2025 Published: 30 June 2025

ABSTRACT

In the management and treatment of *Vibrio* spp. infections in aquaculture, antibiotics have traditionally been used. Misuse of antibiotics, however, has led to the emergence of resistance strains. In this study, antibiotic susceptibility testing of 30 (n=30) *Vibrio* spp. isolates were performed by using 18 antibiotics, revealing resistance to at least two antibiotics. Antibiotics Ceftazidime, Meropenem, Gentamicin, Tetracycline, Nalidixic acid, Norfloxacin, Ciprofloxacin, and Chloramphenicol were 100% effective against all isolates of *V. parahaemolyticus*, *V. cholerae*, and *V. alginolyticus*. Meanwhile, 100% of *V. parahaemolyticus* and *V. alginolyticus* isolates were completely resistant to Penicillin G and Bacitracin, whereas 100% of *V. cholerae* isolates exhibited resistance to Penicillin G. The Multiple Antibiotic Resistance (MAR) indices of all isolates ranged from 0.11 to 0.33. The presence of isolates with MAR indices higher than 0.2 suggests potential contamination from sources with high antibiotic usage, such as wastewater or nearby agricultural and aquaculture activities. The findings highlight widespread antibiotic resistance among *Vibrio* spp., likely due to excessive antibiotics use in aquaculture settings. Additionally, virulence profile of each *Vibrio* spp. isolates was performed. While pathogenic potential is exhibited by some isolates, others lack key virulence genes associated with pathogenicity. All *V. parahaemolyticus* isolates showed the presence of *tlh*, *toxR*, and *toxS* genes, whille all *V. cholerae* isolates were positive with *toxS*, *toxR*, *rtxA*, and *rtxC* genes. None of the *V. alginolyticus* showed the presence of the nine tested virulence genes. However, given the high frequency of horizontal gene transfer among bacterial populations, continuous and comprehensive monitoring is crucial to prevent the spread of virulence genes between pathogenic and non-pathogenic strains. Therefore, continuous efforts to obtain more data on antibiotic resistance and bacterial virulence profiles in Sarawak is crucial for effective disease management and sustainable aquaculture practices.

Keywords: Antibiotic resistance, shrimp, virulence genes, *Vibrio alginolyticus*, *Vibrio cholerae*, *Vibrio parahaemolyticus*

INTRODUCTION

Controlling the population of *Vibrio* spp. presents significant challenges attributable to their pathogenicity and antibiotic resistance. These bacteria can cause diseases in both marine organisms and humans (Sampaio *et al*., 2022). Furthermore, the emergence of antibiotic-resistant strains of *Vibrio* spp. is increasingly worrisome, given the diminished efficacy of conventional treatments employing broad-spectrum antibiotics. Moreover, *Vibrio* spp. is acknowledged for possessing the highest growth rate among bacteria, and their adeptness at thriving in various environmental conditions, contributes to their resilience and persistence (Baker-Austin *et al*., 2020; Abioye *et al*., 2021).

In aquaculture, farmers commonly use antibiotics to treat bacterial infection, particularly vibriosis caused by *Vibrio* species. In shrimp farming, antibiotics such as oxytetracycline, tetracycline, quinolones, sulfonamides, enrofloxacin, norfloxacin, gentamicin, and trimethoprim are routinely used to reduce shrimp morbidity and mortality (Haifa-Haryani *et al*., 2022). In Malaysia, antibiotics are administered either via inclusion in feed additives or through immersion baths, serving as both prophylactic measures and therapeutic interventions for infected organisms (Ibrahim *et*

al., 2010; Amalina *et al*., 2019). However, excessive antibiotic use has led to reduced efficacy and the emergence of antimicrobial-resistant (AMR) strains. Furthermore, the spread of AMR bacteria may be facilitated across different geographic regions through the import and export of live aquatic animals and animal-derived products (Rodgers *et al*., 2011; Paria *et al*., 2021).

Beyond antibiotic resistance, identifying and monitoring virulence genes in *Vibrio* spp. helps assess their pathogenicity and improve disease management. *Vibrio* spp. infections have been documented as major contributors to instances of foodborne illness in Malaysia. *Vibrio parahaemolyticus*, in particular, is reported to be the cause of the highest seafood-associated gastroenteritis in various Asian countries (Elmahdi *et al*., 2016). Consumption of *Vibrio*-contaminated food products can result in gastroenteritis and may even lead to septicaemia and mortality in immunocompromised individuals (Abdullah Sani *et al*., 2013; Song *et al*., 2020). Additionally, the global occurrence of *V. parahaemolyticus* prompts efforts to understand their pathogenicity and their interactions with humans and aquatic animals (Wang *et al*., 2015). Although the majority of environmental isolates of *Vibrio* spp. are non-pathogenic, their genomes are highly dynamic, meaning that non-pathogenic strains can easily acquire virulence genes from pathogenic strains through horizontal gene transfer (Xu *et al*., 2017). Consequently, *Vibrio* spp. maintain an extensive reservoir of virulence genes, even in non-pathogenic strains (Zoqratt *et al*., 2018; Abdelaziz Gobarah *et al*., 2022).

Antibiotic resistance poses a substantial challenge to public health and economic stability. These issues underscore the urgent need for effective strategies to combat antibiotic resistance, as it is a growing threat with far-reaching implications. Efforts to mitigate these challenges require a multifaceted approach, including an improved understanding of *Vibrio* spp. biology, enhanced surveillance and monitoring, and the development of alternative treatment modalities to combat infections caused by these bacteria. The emergence of resistant strains not only compromises the efficacy of antibiotic treatment but also raises concerns about the potential for increased morbidity, mortality, and healthcare risks and costs (WHO, 2023). Moreover, antibiotic resistance transcends national borders, necessitating collaborative efforts across countries and sectors to address this pressing issue (Muteeb *et al*., 2023). As recognized by the WHO, antibiotic resistance poses a significant threat to global health security, emphasizing the critical importance of proactive measures to mitigate its impact (WHO, 2023).

Therefore, it is imperative to monitor and control the dissemination of AMR strains within a farm to limit their spread and aid in disease management. Consequently, this study expands on our previous findings on the prevalence of *Vibrio* spp. in a commercial shrimp farm (Lesen *et al*., 2024) by further examining the antibiotic resistance and virulence gene profiles of three *Vibrio* spp. isolated from the Telaga Air shrimp farm.

MATERIALS AND METHODS

Isolation and Enrichment of Bacteria

Samples were collected from Persatuan Nelayan Kawasan (PNK) Satang Biru, Lembaga Kemajuan Ikan Malaysia (LKIM), Telaga Air, Sarawak (0''N 110°11'51., 1°40'59, 1). Four sample types (water, sediment, shrimp, and effluent) were collected from two shrimp ponds. Overall, a total of 48 (n = 48) samples were collected from the shrimp farm over a single production cycle and the prevalence of *Vibrio* spp. were studied (Lesen *et al*., 2024). The sampling method was derived from the methodology outlined by Kaysner *et al*. (1990) with adaptations. During each sampling event, each sample type was collected from three distinct locations (sampling points) to constitute triplicates. Surface water and effluent samples, each amounting to at least 1 L, were collected in sterile polypropylene bottles at each sampling point. Shrimp were captured using a net and transferred to sterile plastic bags. Meanwhile, sediment was gathered using an ethanol-sterilized polyvinyl chloride (PVC) pipe and stored in sterile 50 mL microcentrifuge tubes. All samples were promptly transported to the laboratory in an ice box and processed within 24 hours of collection (Kaysner *et al*., 1990).

Before enrichment, the sediment and shrimp samples were homogenised using a sterilised conventional blender. One gram (for solid

samples) or 1 mL (for liquid samples) of each sample was thoroughly mixed with 9 mL of alkaline peptone water (APW) (Merck, Darmstadt, Germany) and pre-enriched through overnight incubation at 37 °C. Subsequently, the enriched cultures were spread and streaked on differential and selective media, Thiosulfate–citrate–bile salts–sucrose (TCBS) agar (Himedia, Mumbai, India) and CHROMAgar™ *Vibrio* (CHROMagar™, Paris, France), to acquire single colonies. On TCBS agar, *Vibrio parahaemolyticus* would appear as green colonies, while *V. cholerae* and *V. alginolyticus* would appear as yellow colonies. Meanwhile, on CHROMAgar™ *Vibrio*, *V. parahaemolyticus*, *V. cholerae*, and *V. alginolyticus* appear as mauve, blue, and milky white colonies, respectively.

Based on these morphologies, 10 pure isolates (n=10) of each *Vibrio* spp. were randomly selected and cultured in APW. The presumptive *V. parahaemolyticus* isolates were assigned codes TA01 – TA10, *V. cholerae* isolates as TA11 – TA20, and *V. alginolyticus* isolates as TA21 – TA30 (The source of each isolate is reported in Table 4, 5, and 6 in the Results section). Multiple rounds of culturing and streaking on selective media were conducted to ensure the isolation of pure cultures.

Confirmation of Isolates using Species-Specific Multiplex PCR

PCR was performed using species-specific primer sets to confirm the identity of each isolate. The DNA of each isolate was extracted by using cell-boiled method (Queipo-Ortuno, 2008). Multiplex PCR was conducted using three sets of primers that specifically targeted *V. parahaemolyticus*, *V. cholerae*, and *V. alginolyticus*, as designed by Kim *et al*. (2015). The primers used are shown in Table 1 below. Each 15 µL of the PCR mixture consisted of the following components: 7.5 µL exTEN 2X PCR Master Mix (1st BASE, Singapore), 0.6 µL of each primer with a concentration of 10 µM, 2.0 µL DNA template, and 1.9 µL sterile distilled water.

PCR amplification was performed using the T100™ Thermal Cycler (Bio-Rad, USA) following the specified conditions: initial denaturation at 94 °C for 5 minutes; 30 cycles comprising denaturation at 94 °C for 30 seconds, annealing at 60 °C for 30 seconds, and extension at 72 °C for 30 seconds; and a final extension step at 72 °C for 10 minutes (Kim *et al*., 2015). Subsequently, the PCR products were subjected to electrophoresis on a 1.5% (w/v) agarose gel at 80 V for one hour. The GeneRuler 100-bp and 1-kbp DNA ladders (Thermo Fisher Scientific, USA) were used as the molecular weight marker. A mixture of *V. parahaemolyticus* ATCC 27969, *V. cholerae* KCDC 13589, and *V. alginolyticus* ATCC 17749 served as the positive control, while sterile APW processed concurrently with the samples was utilised as the negative control to substitute the DNA template.

Antibiotic Susceptibility Test (AST)

Once the identity of each isolate was confirmed, the susceptibility of each isolate to different antibiotics was assessed using the disc diffusion assay, as outlined by the Clinical and Laboratory Standards Institute (Hudzicki, 2009; Clinical and Laboratory Standard Institute, 2015). The bacterial isolates were cultured in 10 mL Mueller-Hinton Broth (MHB) supplemented with 2% NaCl at 37 °C for 24 hours.

The following day, the overnight cultures were adjusted to a 0.5 McFarland standard. Using sterile cotton swabs, the cultures were spread onto Mueller-Hinton agar (MHA) plates supplemented with 2% NaCl and allowed to dry for five minutes. Then antibiotic discs were placed on the agar surface in triplicate using sterile forceps. The discs were positioned at approximately equal distances from each other to ensure accuracy. The antibiotics used in this susceptibility test included Ampicillin (AMP, 10 µg), Chloramphenicol (C, 30 µg), Penicillin G (P, 10 IU), Amoxicillin-clavulanic acid (AMC, 30 µg), Amikacin (AK, 30 µg), Erythromycin (E, 15 µg), Tetracycline (TE, 30 µg), Ceftazidime (CAZ, 30 µg), Ciprofloxacin (CIP, 5 µg), Cephalotin (KF, 30 µg), Norfloxacin (NOR, 10 µg), Gentamicin (CN, 10 µg), Rifampicin (RD, 5 µg), Imipenem (IPM, 10 µg), Kanamycin (K, 30 µg), Nalidixic acid (NA, 30 µg), Bacitracin (B, 10 IU), and Meropenem (MEM, 10 µg) (Oxoid, Hampshire, United Kingdom). These antibiotics are commonly employed to treat *Vibrio* spp. infections (Elmahdi *et al*., 2016). *Escherichia coli* ATCC® 25922 was used as control. All plates were then incubated at 37 °C for 24 hours.

Following incubation, the diameter of the antibiotic inhibition zone was measured, and the average was calculated based on triplicate measurements. The level of susceptibility was determined according to the guidelines in the Clinical and Laboratory Standards Institute's Document M-45 for *Vibrio* species (Clinical and Laboratory Standard Institute, 2015). From the susceptibility results, the Multiple Antibiotic Resistant (MAR) indices of the isolates were determined using the following formula Eq.(1):

$$\text{MAR index} = \frac{\text{Number of antibiotics the isolate}}{\text{Total number of antibiotic}} \quad \text{Eq. (1)}$$

Polymerase Chain Reactions (PCR) for Virulence Genes Detection

The DNA of each bacterial isolate was extracted using the boiled-cell method (Queipo-Ortuno, 2008). Multiplex and singleplex PCRs were conducted using nine primer sets targeting different virulence genes of *Vibrio* spp., as outlined in Table 2.

Table 1. Sequences, sources, and expected amplicon sizes of primer pairs used to target each *Vibrio* spp. in this study (Kim *et al*., 2015)

Target species	Primer name	Primer sequence (5'→ 3')	Product size (bp)
Vibrio parahaemolyticus	VP 1155272 F	AGCTT ATTGG CGGTT TCTGT CGG	297
	VP 1155272 R	CKCAA GACCA AGAAA AGCCG TC	
Vibrio cholerae	VC C634002 F	CAAGC TCCGC ATGTC CAGAA GC	154
	VC C634002 R	GGGGC GTGAC GCGAA TGATT	
Vibrio alginolyticus	VA 1198239 F	ACGGC ATTGG AAATT GCGAC TG	199
	VA 1198239 R	TACCC GTCTC ACGAG CCCAA G	

Table 2. List of primers targeting different virulence genes used in this study

Virulence gene	Primer name	Primer sequence (5'→ 3')	Product size (bp)	Annealing temperature (°C)	Reference
tdh	F-*tdh*	GTA AAG GTC TCT GAC TTT TGG AC	269	58	Bej *et al*. (1999)
	R-*tdh*	TGG AAT AGA ACC TTC ATC TTC ACC			
trh	F-*trh*	TTG GCT TCG ATA TTT TCA GTA TCT	500	58	Bej *et al*. (1999)
	R-*trh*	CAT AAC AAA CAT ATG CCC ATT TCC G			
tlh	tl-F	AAA GCG GAT TAT GCA GAA GCA CTG	450	58	Bej *et al*. (1999)
	tl-R	GCT ACT TTC TAG CAT TTT CTC TGC			
pirA	AP3-F	ATG AGT AAC AAT ATA AAA CAT GAA AC	333	53	Sirikharin *et al*. (2015)
	AP3-R	GTG GTA ATA GAT TGT ACA GAA			
V. cholerae-associated *toxS*	F-*toxS*	CCA CTG GCG GAC AAA ATA ACC	640	52	Sechi *et al*. (2004)
	R-*toxS*	AAC AGT ACC GTA GAA CCG TGA			
V. cholerae-associated *toxR*	F-*toxR*	TTT GTT TGG CGT GAG CAA GGT TTT	595	52	Sechi *et al*. (2004)
	R-*toxR*	GGT TAT TTT GTC CGC CAG TGG			
rtxA	*rtxA*-F	CTG AAT ATG AGT GGG TGA CTT ACG	417	55	Chow *et al*. (2001)
	rtxA-R	GTG TAT TGT TCG ATA TCC GCT ACG			
rtxC	*rtxC*-F	CGA CGA AGA TCA TTG ACG AC	263	55	Chow *et al*. (2001)
	rtxC-R	CAT CGT CGT TAT GTG GTT GC			
ctxB	ctx B_2	GAT ACA CAT AAT AGA ATT AAG GAT G	460	55	Chow *et al*. (2001)
	ctx B_3	GGT TGC TTC TCA TCA TGG AAC CAC			

The detection of *tdh*, *trh*, and *tlh* genes was carried out using a multiplex PCR method adapted from Bej *et al*. (1999), with minor adjustments. Each PCR reaction mixture (25 µL) comprised 12.5 µL of exTEN 2X PCR Master Mix (1st BASE), 1.25 µL of each 10 µM primer, 2.0 µL of DNA extract, and 3.0 µL of sterile distilled water. PCR conditions included initial denaturation at 94 °C for 5 min, followed by 30 cycles of denaturation at 94 °C for 1 min, annealing at 58 °C for 1 min, extension at 72 °C for 1 min, and a final extension at 72 °C for 10

min (Bej *et al*., 1999). A clinical isolate of *V. parahaemolyticus* (from laboratory stock), previously confirmed to possess the *tlh*, *tdh*, and *trh* genes, was used as the positive control.

The detection of the *pirA* gene was performed using a singleplex PCR under the following conditions: initial denaturation at 94 °C for 5 min, followed by 30 cycles of denaturation at 94 °C for 30 sec, annealing at 53 °C for 30 sec, extension at 72 °C for 40 sec, and a final extension at 72 °C for 7 min. The PCR mixture consisted of 7.5 µL of exTEN 2X PCR Master Mix (1st BASE, Singapore), 1.0 µL of each forward and reverse AP3 primer (10 µM concentration), 2.0 µL of DNA extract, and 5.5 µL of distilled water (Sirikharin *et al*., 2015). An environmental isolate of *V. parahaemolyticus* (from laboratory stock), previously confirmed to possess the *pirA* genes, was used as the positive control.

Meanwhile for the detection of *V. cholerae*-associated *toxR* and *toxS* genes, a multiplex PCR was performed following the method described by Sechi *et al*. (2004). The PCR mixture included 12.5 µL of exTEN 2X PCR Master Mix (1st BASE, Singapore), 1.0 µL of each 10 µM primer, 2.0 µL of DNA template, and 4.5 µL of sterile distilled water. PCR conditions were similar to those used for detecting *tdh*, *trh*, and *tlh* genes, with the annealing temperature adjusted to 52 °C and the final extension extended to 20 min (Sechi *et al*., 2004). A clinical isolate of *V. cholerae* that has been confirmed for the presence of *toxR* and *toxS* genes was used as the positive control.

Additionally, detection of *rtxA*, *rtxC*, and *ctxB* genes was conducted using a multiplex PCR mixture containing 12.5 µL of exTEN 2X PCR Master Mix (1st BASE, Singapore), 0.6 µl of each primer (10 µM concentration), 2.0 µL of DNA extract, and 6.9 µL of distilled water. The PCR protocol consisted of an initial denaturation at 95 °C for 5 min, followed by 25 cycles of denaturation at 95 °C for 1 min, annealing at 55 °C for 1 min, extension at 72 °C for 1 min, and a final extension at 72 °C for 10 min (Chow *et al*., 2001). A clinical isolate of *V. cholerae* that was confirmed for the presence of *rtxA*, *rtxC*, and *ctxB* genes was used as the positive control.

In all PCRs mentioned above, sterile distilled water (dH_2O) was used as the negative control. The reactions were conducted using the T100™ Thermal Cycler (Bio-Rad, USA). PCR products were visualised through agarose gel electrophoresis (AGE) with a 1.5% gel concentration. Electrophoresis was carried out at 80 V for 2 hours, and the gels were then stained with Ethidium bromide (EtBr) for one hour before visualisation using a safeVIEW-MINI2 Blue Light Transilluminator (Cleaver Scientific, Warwickshire, United Kingdom). The presence of bands was observed and recorded.

RESULTS

Isolation of *Vibrio* species

When plated on selective and differential media, such as TCBS and CHROMAgar™ *Vibrio*, different *Vibrio* spp. bacterial colonies appear with different coloured morphologies (Figure 1). *Vibrio parahaemolyticus* appeared as green colonies on TCBS agar, while *V. cholerae* and *V. alginolyticus* both appeared as yellow colonies (Figure 1a). Meanwhile, *V. parahaemolyticus*, *V. cholerae*, and *V. alginolyticus* appeared as mauve, blue, and milky white colonies, respectively, on CHROMAgar™ *Vibrio* (Figure 1b).

The anticipated sizes for the PCR products of *V. parahaemolyticus*, *V. alginolyticus*, and *V. cholerae using* the primer sets outlined in Table 1 are 297 bp, 199 bp, and 154 bp, respectively. Agarose gel electrophoresis (AGE) of the 30 isolates revealed bands that were consistent with the expected sizes. Based on PCR, it has been confirmed that each of the selected isolates were indeed their respective *Vibrio* species (Figure 2).

Antibiotic Susceptibility Test (AST) of *Vibrio* species

The antibiotic susceptibility test was performed using 18 antibiotics that are commonly used for controlling *Vibrio* spp. infections (Elmahdi *et al*., 2016). The responses of the isolates were categorised as susceptible (can be treated with the antibiotic), intermediate (may be treated with adjusted dosage), and resistant (cannot be treated with the antibiotic) based on guidelines from the Clinical and Laboratory Standards Institute (Clinical and Laboratory Standard Institute, 2015; CDC, 2019a). The test revealed varying responses of each isolate to the tested antibiotics.

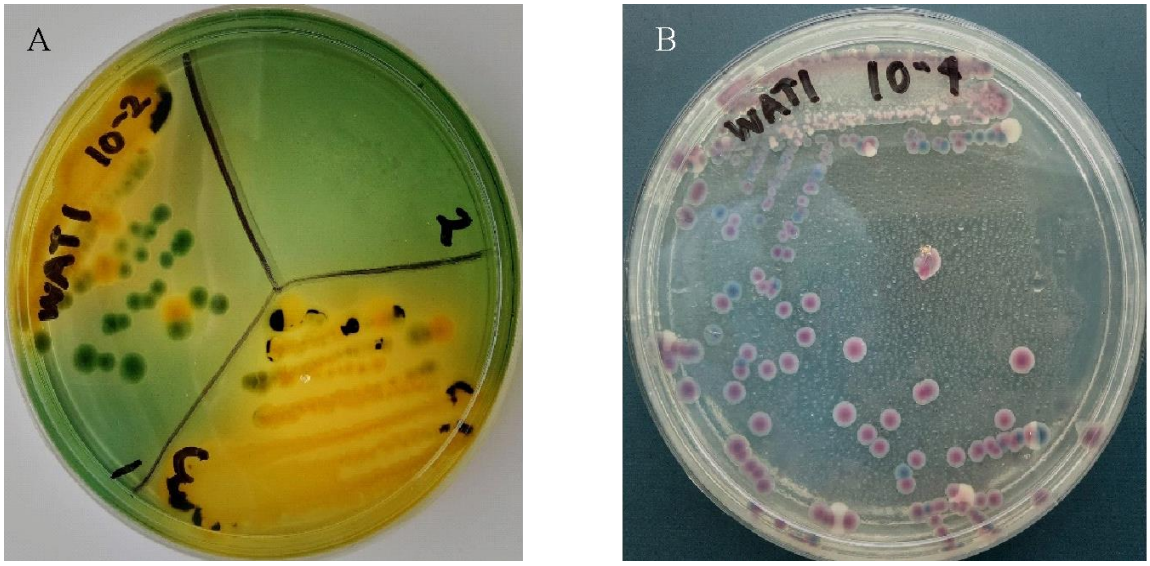

Figure 1. *Vibrio* spp. appearances on TCBS and CHROMAgar™ *Vibrio*. (a) *Vibrio parahaemolyticus* appears as green colonies, while V. cholerea and *V. alginolyticus* appear as yellow colonies on TCBS agar. (b) *Vibrio parahaemolyticus*, *V. cholerae*, and *V. alginolyticus* appear as mauve (purple), blue, and white colonies, respectively on CHROMAgar™ *Vibrio*

Analysis of Table 3 below indicates that Ceftazidime, Meropenem, Gentamicin, Tetracycline, Nalidixic acid, Norfloxacin, Ciprofloxacin, and Chloramphenicol were 100% effective against all isolates of *V. parahaemolyticus*, *V. cholerae*, and *V. alginolyticus*. Amoxicillin-clavulanate was effective against 100% of *V. parahaemolyticus* and *V. cholerae* isolates, while Erythromycin was 100% effective against all isolates of *V. parahaemolyticus* and *V. alginolyticus*. Conversely, it was observed that 100% of *V. parahaemolyticus* and *V. alginolyticus* isolates were completely resistant to Penicillin G and Bacitracin, whereas 100% of *V. cholerae* isolates exhibited resistance to Penicillin G.

Based on observations made during the measurement of the zone of inhibition after 24 hours of incubation, it was noted that a few isolates exhibited colony growth within the existing zone of inhibition, as depicted in Figure 3 below. Following several repeated tests using freshly subcultured pure isolates, consistent results were obtained. Therefore, these isolates were classified as resistant to the antibiotics, irrespective of the diameter of the inhibition zone. This growth within the zone of inhibition indicated the presence of resistant mutants (Hudzicki, 2009).

Multiple Antibiotic Resistance (MAR) Profiles

The antibiotic resistance profiles and MAR indices of *V. parahaemolyticus* isolates from the shrimp farm are detailed in Table 4 below. Eight distinctive antibiotic resistance patterns were observed among the *V. parahaemolyticus* isolates, with 2 isolates (*V. parahaemolyticus* TA01 and TA10) exhibiting the same resistance pattern of P-B, and another 2 isolates (*V. parahaemolyticus* TA02 and TA03) displaying an antibiotic resistance pattern of P-AK-KF-B. The remaining isolates exhibited varying patterns. Isolate TA01 and TA10 were respectively isolated from water and effluent samples, while isolate TA02 and TA03 were both isolated from water samples. The MAR indices of the *V. parahaemolyticus* isolates ranged from 0.11 to 0.39. Pattern P-B demonstrated the lowest MAR index (0.11), whereas pattern AMP-P-AK-KF-RD-IPM-B, belonging to isolate TA07 previously isolated from a shrimp sample, exhibited the highest MAR index (0.39).

In Table 5 below, the antibiotic resistance profiles and MAR (Multiple Antibiotic Resistance) indices of ten *V. cholerae* isolates from the shrimp farm are presented. Eight

distinctive antibiotic resistance patterns were observed, with 2 isolates (*V. cholerae* TA11 and TA12) exhibiting the same resistance pattern of P-KF-RD-IPM-B, while another 2 isolates (*V. cholerae* TA16 and TA18) displayed a resistance pattern of P-RD-B. The remaining isolates showed varying patterns from each other. The MAR indices of the *V. cholerae* isolates ranged from 0.11 to 0.33. Similar to the *V. parahaemolyticus* isolates, pattern P-B exhibited the lowest MAR index (0.11), while pattern AMP-P-E-KF-RD-B demonstrated the highest MAR index (0.33).

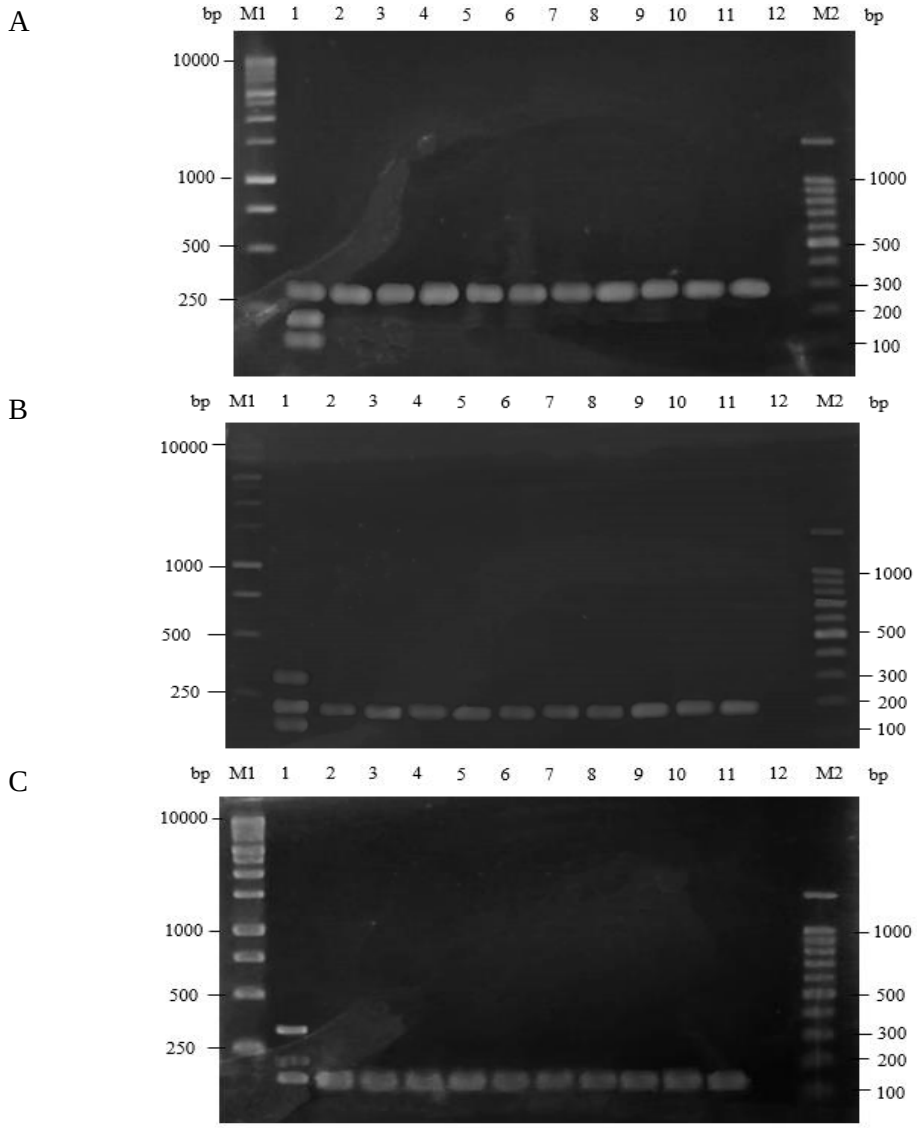

Figure 2. Gel electrophoresis of multiplex PCR for confirmation of (a) *Vibrio parahaemolyticus* isolates (297 bp; Lane 2 – 12: Isolate TA01 – TA10), (b) *Vibrio alginolyticus* isolates (199bp; Lane 2 – 12: Isolate TA11 – TA20), and (c) *Vibrio cholerae* (154 bp; Lane 2 – 12: Isolate TA21 – TA 30). Lane M1: 1 kbp DNA ladder; Lane M2: 100 bp DNA ladder; Lane 1: positive control (cocktail of *V. parahaemolyticus* ATCC 27969, *V. cholerae* KCDC 13589, and *V. alginolyticus* ATCC 17749); Lane 12: negative control

For *V. alginolyticus* isolates, eight different antibiotic resistance patterns were observed (Table 6). Among them, three isolates, namely TA24 and TA25 isolated from shrimps, and TA29 from effluent, exhibited the same patterns of P-RD-B. The MAR indices of the ten *V. alginolyticus* isolates ranged from 0.17 to 0.33. Isolate TA22, with the antibiotic resistance pattern of AMP-P-AMC-KF-IPM-B, exhibited the highest MAR index (0.33). Conversely, antibiotic resistance patterns P-RD-B, P-KF-B, and AMP-P-B displayed the lowest MAR index (0.17).

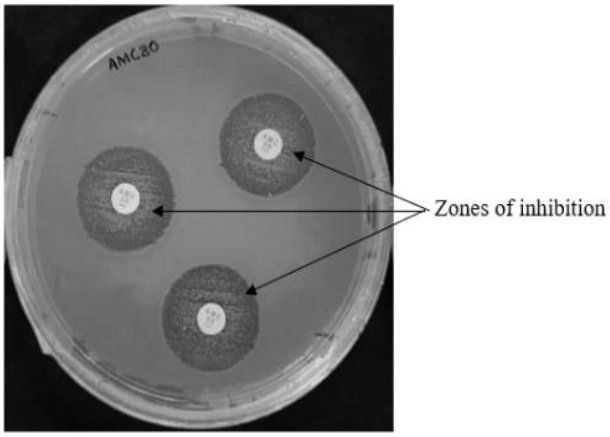

Figure 3. Colonies growth in zone of inhibition may indicate that the bacterium is resistant towards the antibiotic

Table 3. Antibiotic resistance profile of *Vibrio* spp. isolated from Telaga Air shrimp farm against 18 antibiotics

Antimicrobial Class	Antibiotic	Abbreviation	Number (%) of response of isolates to antibiotic								
			Vibrio parahaemolyticus (n=10)			*Vibrio cholera* (n=10)			*Vibrio alginolyticus* (n=10)		
			S	I	R	S	I	R	S	I	R
PenicillinS and β-lactam/ β-lactamase inhibitor combinations	Ampicillin	AMP10	2 (20)	5 (50)	3 (30)	6 (60)	2 (20)	2 (20)	6 (60)	1 (10)	3 (30)
	Amoxicillin-clavulanate	AMC30	10 (100)	-	-	10 (100)	-	-	9 (90)	-	1 (10)
	Penicillin G	P10	-	-	10 (100)	-	-	10 (100)	-	-	10 (100)
Cephalosporins/Cephems	Ceftazidime	CAZ30	9 (90)	1 (10)	-	10 (100)	-	-	10 (100)	-	-
	Cephalothin	KF30	-	3 (30)	7 (70)	2 (20)	1 (10)	7 (70)	4 (40)	-	6 (60)
Carbapenems	Imipenem	IPM10	8 (80)	-	2 (20)	6 (60)	-	4 (40)	2 (20)	5 (50)	3 (30)
	Meropenem	MEM10	10 (100)	-	-	10 (100)	-	-	10 (100)	-	-
Aminoglycosides	Amikacin	AK30	3 (30)	3 (30)	4 (40)	9 (90)	1 (10)	-	10 (100)	-	-
	Gentamicin	CN10	10 (100)	-	-	10 (100)	-	-	10 (100)	-	-
	Kanamycin	K30	3 (30)	6 (60)	1 (10)	7 (70)	3 (30)	-	8 (80)	2 (20)	-
Tetracyclines	Tetracycline	TE30	9 (90)	1 (10)	-	10 (100)	-	-	10 (100)	-	-
Quinolones	Nalidixic acid	NA30	10 (100)	-	-	10 (100)	-	-	10 (100)	-	-
	Norfloxacin	NOR10	10 (100)	-	-	10 (100)	-	-	10 (100)	-	-
Fluoroquinolones	Ciprofloxacin	CIP5	5 (50)	5 (50)	-	10 (100)	-	-	10 (100)	-	-
Phenicols	Chloramphenicol	C30	10 (100)	-	-	10 (100)	-	-	10 (100)	-	-
Macrolides	Erythromycin	E15	4 (40)	6 (60)	-	2 (20)	7 (70)	1 (10)	2 (20)	8 (80)	-
Ansamycins	Rifampicin	RD5	2 (20)	5 (50)	3 (30)	-	1 (10)	9 (90)	2 (20)	2 (20)	6 (60)
Polypeptides	Bacitracin	B10	-	-	10 (100)	2 (20)	-	8 (80)	-	-	10 (100)

Table 4. The antibiotic resistance profile patterns and multiple antibiotic resistance (MAR) indices of *V. parahaemolyticus* isolates

Isolate	Source	Antibiotic resistance profiles*	MAR index
TA01	Water	PB	0.11
TA02	Water	PAKKFB	0.22
TA03	Water	PAKKFB	0.22
TA04	Sediment	AMPPKFRDB	0.28
TA05	Sediment	PKFRDB	0.22
TA06	Sediment	AMPPAKKFKB	0.33
TA07	Shrimp	AMPPAKKFRDIPMB	0.39
TA08	Shrimp	PAKB	0.17
TA09	Effluent	PKFIPMB	0.22
TA10	Effluent	PB	0.11

*Antibiotics: Ampicillin (AMP); Penicillin G (P); Amoxicillin-clavulanate (AMC); Amikacin (AK); Erythromycin (E); Cephalothin (KF); Rifampicin (RD); Imipenem (IPM); Kanamycin (K); Bacitracin (B)

Table 5. The antibiotic resistance profile patterns and multiple antibiotic resistance (MAR) indices of *V. cholerae* isolates

Isolate	Source	Antibiotic resistance profiles*	MAR index
TA11	Water	PKFRDIPMB	0.28
TA12	Water	PKFRDIPMB	0.28
TA13	Water	AMPPEKFRDB	0.33
TA14	Sediment	AMPPKFRDB	0.28
TA15	Sediment	PKFRDIPM	0.22
TA16	Sediment	PRDB	0.17
TA17	Shrimp	PKFRD	0.17
TA18	Shrimp	PRDB	0.17
TA19	Effluent	PKFRDIPMB	0.28
TA20	Effluent	PB	0.11

*Antibiotics: Ampicillin (AMP); Penicillin G (P); Amoxicillin-clavulanate (AMC); Amikacin (AK); Erythromycin (E); Cephalothin (KF); Rifampicin (RD); Imipenem (IPM); Kanamycin (K); Bacitracin (B)

Table 6. The antibiotic resistance profile patterns and multiple antibiotic resistance (MAR) indices of *V. alginolyticus* isolates

Isolate	Source	Antibiotic resistance profiles*	MAR index
TA21	Shrimp	AMPPKFRDB	0.28
TA22	Shrimp	AMPPAMCKFIPMB	0.33
TA23	Shrimp	PKFIPMB	0.22
TA24	Shrimp	PRDB	0.17
TA25	Shrimp	PRDB	0.17
TA26	Effluent	PKFRDB	0.22
TA27	Effluent	PKFB	0.17
TA28	Effluent	PKFRDIPMB	0.28
TA29	Effluent	PRDB	0.17
TA30	Effluent	AMPPB	0.17

*Antibiotics: Ampicillin (AMP); Penicillin G (P); Amoxicillin-clavulanate (AMC); Amikacin (AK); Erythromycin (E); Cephalothin (KF); Rifampicin (RD); Imipenem (IPM); Kanamycin (K); Bacitracin (B)

Detection of Virulence Genes in *Vibrio* species

Virulence genes detection was performed on all 30 *Vibrio* spp. isolates by using primer sets that target the specific virulence gene sequences. Table 7 below summarised the results of the PCR where presence of specific bands was observed and recorded. PCR was conducted on ten *V. parahaemolyticus* isolates to detect all virulence genes listed in Table 1.

Based on the PCR results, the presence of *tlh*, *toxS*, and *toxR* genes was observed in all ten *V. parahaemolyticus* isolates (Table 7). In Figure 4 below, a band with a size of 450 bp was detected in all *V. parahaemolyticus* isolates, consistent with the expected size of the *tlh* gene. However, no bands corresponding to the expected sizes of *trh* and *tdh* genes were identified. In Figure 5, two bands were observed in each isolate, with sizes of 640 bp and 596 bp, matching the

anticipated sizes of *toxS* and *toxR*, respectively. Meanwhile, the detection of the *pirA* gene, which contributes to some strains of *V. parahaemolyticus* the ability to cause Acute Hepatopancreatic Necrosis Disease (AHPND), yielded negative results for all *V. parahaemolyticus* isolates (Figure 6).

Meanwhile, in the *V. cholerae* isolates, four virulence genes were positively detected in all ten isolates. As depicted in Figure 7 below, two bands with sizes of 640 bp and 595 bp, corresponding to the expected sizes of the *toxS* and *toxR* genes, respectively, were observed for each isolate. Moreover, in Figure 8, two positive bands corresponding to the *rtxA* (417 bp) and *rtxC* (263 bp) genes were observed for each *V. cholerae* isolate, while *ctxB* (460 bp) was not detected in any of the isolates.

No positive detection of the nine targeted virulence genes was observed in all *V. alginolyticus* isolates. As depicted in Figure 9, no bands were detected for all ten isolates in the detection of the *toxR* and *toxS* genes (similar results were observed with the other virulence genes). This indicates that none of the isolated *V. alginolyticus* harbour the targeted virulence genes.

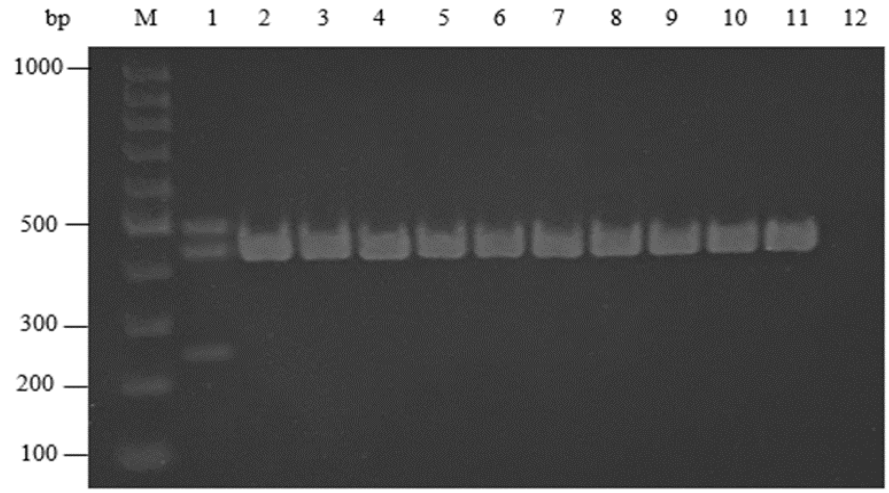

Figure 4. PCR result for the detection of *tdh* (269 bp), *trh* (500 bp), and *tlh* (450 bp) virulence genes in *V. parahaemolyticus* isolates viewed in 1.5% agarose gel. Lane M: 100 bp DNA ladder; lane 1: positive control; lane 2 – 11: *V. parahaemolyticus* TA01 – TA10; lane 12: negative control (sterile dH_2O).

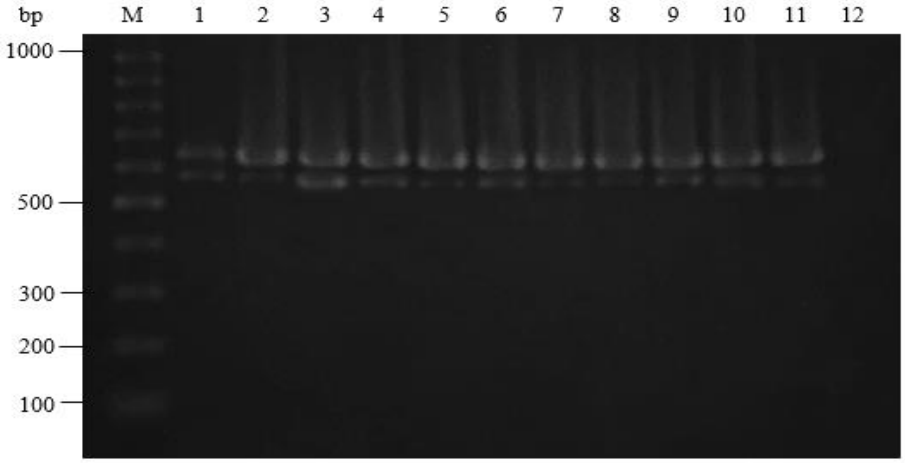

Figure 5. PCR result for the detection of *toxR* (596 bp) and *toxS* (640 bp) virulence genes in *V. parahaemolyticus* isolates viewed in 1.5% agarose gel. Lane M: 100 bp DNA ladder; lane 1: positive control; lane 2 – 11: *V. parahaemolyticus* TA01 – TA10; lane 12: negative control (sterile dH_2O).

Table 7. Detection of virulence genes in *Vibrio* spp. isolates using PCR

Vibrio spp.	Isolate	Virulence gene								
		tdh	*trh*	*tlh*	*toxS*	*toxR*	*toxA*	*rtxA*	*rtxC*	*ctxB*
Vibrio parahaemolyticus	TA01	-	-	+	+	+	-	-	-	-
	TA02	-	-	+	+	+	-	-	-	-
	TA03	-	-	+	+	+	-	-	-	-
	TA04	-	-	+	+	+	-	-	-	-
	TA05	-	-	+	+	+	-	-	-	-
	TA06	-	-	+	+	+	-	-	-	-
	TA07	-	-	+	+	+	-	-	-	-
	TA08	-	-	+	+	+	-	-	-	-
	TA09	-	-	+	+	+	-	-	-	-
	TA10	-	-	+	+	+	-	-	-	-
Vibrio cholera	TA11	-	-	-	+	+	-	+	+	-
	TA12	-	-	-	+	+	-	+	+	-
	TA13	-	-	-	+	+	-	+	+	-
	TA14	-	-	-	+	+	-	+	+	-
	TA15	-	-	-	+	+	-	+	+	-
	TA16	-	-	-	+	+	-	+	+	-
	TA17	-	-	-	+	+	-	+	+	-
	TA18	-	-	-	+	+	-	+	+	-
	TA19	-	-	-	+	+	-	+	+	-
	TA20	-	-	-	+	+	-	+	+	-
Vibrio alginolyticus	TA21	-	-	-	-	-	-	-	-	-
	TA22	-	-	-	-	-	-	-	-	-
	TA23	-	-	-	-	-	-	-	-	-
	TA24	-	-	-	-	-	-	-	-	-
	TA25	-	-	-	-	-	-	-	-	-
	TA26	-	-	-	-	-	-	-	-	-
	TA27	-	-	-	-	-	-	-	-	-
	TA28	-	-	-	-	-	-	-	-	-
	TA29	-	-	-	-	-	-	-	-	-
	TA30	-	-	-	-	-	-	-	-	-

(+): positive detection; (-): no detection

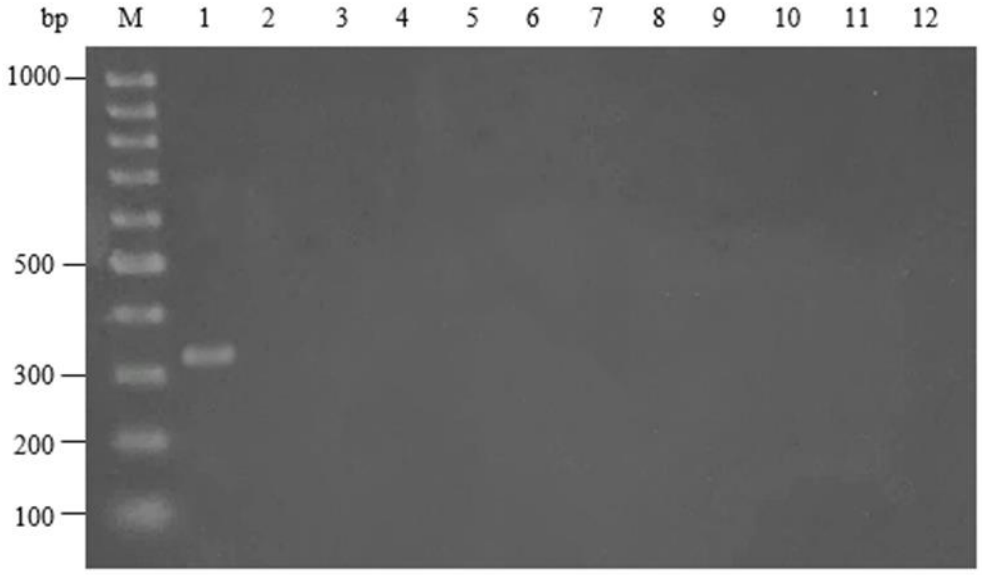

Figure 6: PCR result for the detection of pirA (333 bp) virulence genes in *V. parahaemolyticus* isolates viewed in 1.5% agarose gel. Lane M: 100 bp DNA ladder; lane 1: positive control; lane 2 – 11: *V. parahaemolyticus* TA01 – TA10; lane 12: negative control (sterile dH_2O)

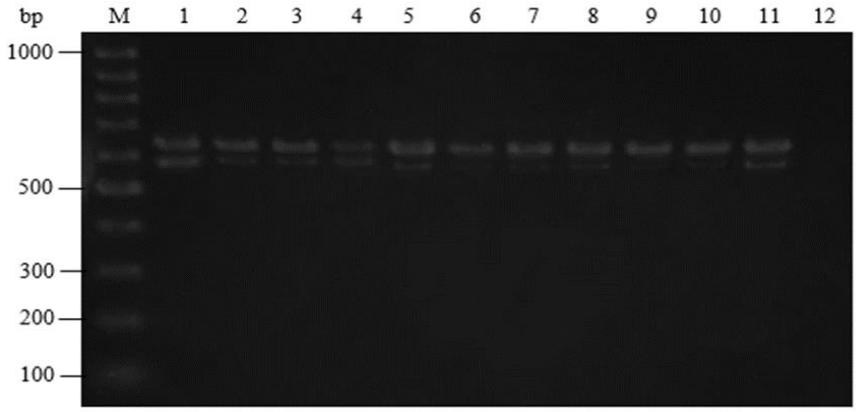

Figure 7. PCR result for the detection of *toxR* (595 bp) and *toxS* (640 bp) virulence genes in *V. cholerae* isolates viewed in 1.5% agarose gel. Lane M: 100 bp DNA ladder; lane 1: positive control; lane 2 – 11: *V. cholerae* TA11 – TA20; lane 12: negative control (sterile dH_2O)

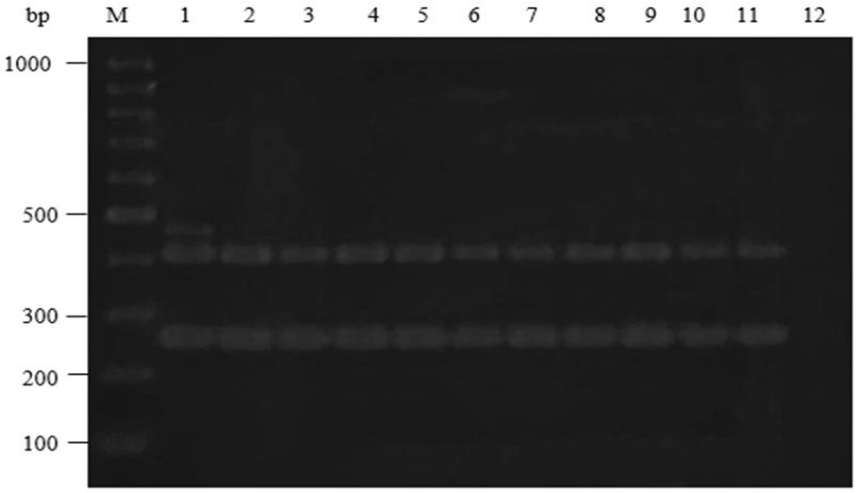

Figure 8. PCR result for the detection of *rtxA* (417 bp), *rtxC* (263 bp) and *ctxB* (460 bp) virulence genes in *V. cholerae* isolates viewed in 1.5% agarose gel. Lane M: 100 bp DNA ladder; lane 1: positive control; lane 2 – 11: *V. cholerae* TA11 – TA20; lane 12: negative control (sterile dH_2O)

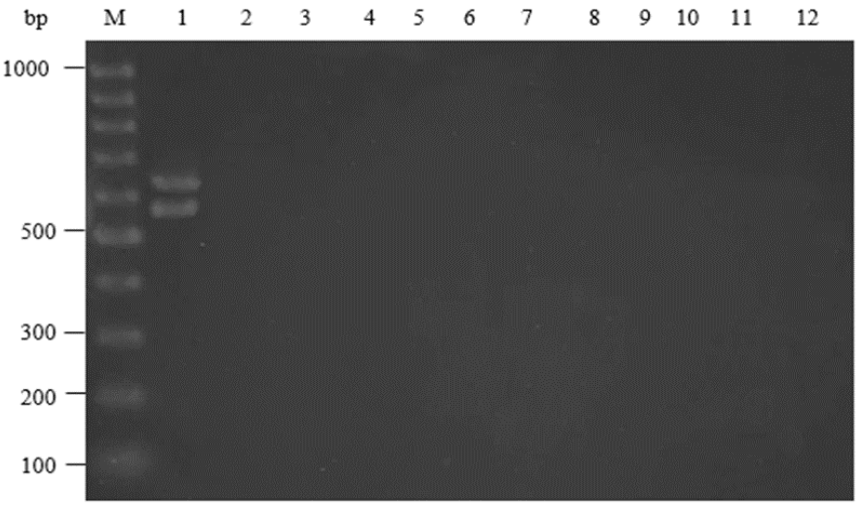

Figure 9. PCR result for the detection of *toxR* (595 bp) and *toxS* (640 bp) virulence genes in *V. alginolyticus* isolates viewed in 1.5% agarose gel. Lane M: 100 bp DNA ladder; lane 1: positive control; lane 2 – 11: *V. alginolyticus* TA21 – TA30; lane 12: negative control (sterile dH_2O)

DISCUSSION

The antibiotic susceptibility test revealed that all 30 *Vibrio* spp. isolates exhibited multiple resistance to at least two antibiotics. These findings parallel those of an antibiotic resistance study conducted in cultured shrimp farms in the Philippines, where *Vibrio* spp. isolated from ponds employing antibiotics displayed resistance to multiple antibiotics (Tendencia & De la Peña, 2001; Elmahdi *et al*., 2016). The MAR indices of the *Vibrio* spp. isolated from Telaga Air shrimp farm ranged from 0.11 to 0.39, with the majority (60%) of the total isolates having MAR indices exceeding 0.2. Our findings align with those of Devadas *et al*. (2015), who reported that 63.8% of zoonotic bacteria, including *V. parahaemolyticus*, isolated from shrimp aquaculture environments in Selangor, exhibited MAR indices greater than 0.2. Our finding suggests that these isolates likely originated from environments with considerable antibiotic pressure, consistent with aquaculture systems where prophylactic or therapeutic antibiotic usage is prevalent. Despite the farm manager's assertion that antibiotic treatment was not administered in the Telaga Air shrimp farm, the presence of isolates with MAR indices exceeding 0.2 suggests they may have originated from a contaminated source with extensive antibiotic use. This suggests the existence of residual antibiotics originating from wastewater or nearby agricultural and aquaculture activities (Hanna *et al*., 2023). Additionally, certain antibiotics demonstrate stability and can persist in the environment long after their use has ceased, leading to contamination by the accumulated residual antibiotics (Larsson, 2014; Lundborg & Tamhankar, 2017).

The implications of MAR > 0.2 in aquaculture are significant. It not only suggests ongoing antibiotic pressure in the farming environment but also indicates potential public health risks through the food chain and the surrounding ecosystem. Resistant *Vibrio* strains may transfer resistance genes to other environmental or pathogenic bacteria via horizontal gene transfer. Moreover, the presence of high MAR index values in isolates from water, sediment, and shrimp samples underscores the widespread nature of this resistance across various environmental compartments within the shrimp farm. From the standpoint of AMR dissemination, aquaculture alarmingly plays a significant role in the emergence, persistence, and transmission of resistance factors within the aquatic environment. The environment, as a whole, serves as a vast reservoir of antibiotic resistance genes (ARGs), with the aquatic environment, in particular, serving as a crucial reservoir of mobile genetic elements (MGEs) carrying these ARGs. Hence, the aquatic environment serves as a common ground for the transmission of antimicrobial resistance between bacteria (Salgueiro *et al*., 2024). Moreover, the boundaries between species in aquatic environments are narrow due to the genomic plasticity of *Vibrio* species. Horizontal gene transfer between them, even between the environmental and clinical strains, are frequent events (Liang *et al*., 2022).

Overall, shrimp-derived isolates, particularly from *V. parahaemolyticus* and *V. alginolyticus*, tend to exhibit higher MAR indices compared to those from water, sediment, or effluent, suggesting greater antibiotic selective pressure in host-associated environments. This pattern may suggest increased selective pressure for antibiotic resistance in host-associated bacteria, possibly due to antibiotic use in aquaculture or accumulation of residues in shrimp tissues (Luu *et al*., 2021). This notion is further supported by a study by Sharma *et al*. (2021), which found that farm-raised shrimp—fed artificially formulated diets and raised in a shared aquatic microbiota—tend to harbour a higher prevalence of ARGs in their guts compared to wild-caught shrimp. Evidently, chitin, the predominant structural component of shrimp and other crustacean exoskeletons, has been identified as a potential intermediary surface facilitating the proliferation and dissemination of AMR through biofilm attachment, as highlighted by Meibom *et al*. (2005). Future investigations employing molecular typing and resistance gene profiling would provide deeper insights into the relationships and mechanisms underpinning these resistance patterns.

Numerous studies have highlighted the high resistance of *V. parahaemolyticus*, *V. cholerae*, and *V. alginolyticus* to ampicillin (Oh *et al*., 2011; Elmahdi *et al*., 2016; Abioye *et al*., 2023). Al-Othrubi *et al*. (2014) reported that over 50%

of *V. parahaemolyticus* isolated from cockles and shrimp samples from various Malaysian markets displayed high resistance to ampicillin. Similarly, Amalina *et al*. (2019) found that the majority of *Vibrio* spp. isolated from cultured groupers in farms across Peninsular Malaysia exhibited high resistance to ampicillin. However, in this investigation, only 30% of *V. parahaemolyticus* and *V. alginolyticus* isolates, and 20% of *V. cholerae* isolates, exhibited resistance to ampicillin, with the remaining isolates displaying susceptibility or intermediate resistance to the antibiotic. Notably, *V. parahaemolyticus* exhibited a higher proportion of isolates with intermediate resistance (50%) compared to the other two *Vibrio* spp., indicating that the dosage of the ampicillin antibiotics needs to be adjusted to treat infection caused by some of the *V. parahaemolyticus* strains (CDC, 2019b). Overall, only a small percentage of isolates from the Telaga Air shrimp farm displayed resistance to ampicillin.

In this investigation, antibiotics belonging to specific classes remained highly effective at controlling all *Vibrio* spp. isolates, including phenicols (Chloramphenicol), tetracyclines (Tetracycline), cephalosporins (Ceftazidime), fluoroquinolones (Ciprofloxacin), quinolones (Norfloxacin and Nalidixic acid), aminoglycosides (Gentamicin), and carbapenems (Meropenem). These antibiotics operate through diverse mechanisms to combat bacterial infections. Phenicol, tetracycline, and aminoglycoside antibiotics hinder protein synthesis, with phenicols targeting the 50s ribosomal subunit, and tetracyclines and aminoglycosides affecting the 30s ribosomal subunit (Kapoor *et al*., 2017). Notably, tetracycline is often recommended for treating severe *Vibrio* spp. infections due to its capacity to impede the synthesis of pathogenic extracellular enzymes, particularly proteases and lipases (Elmahdi *et al*., 2016). Meanwhile, cephalosporins and carbapenems inhibit cell wall synthesis or function, thereby disrupting bacterial growth and multiplication (Kapoor *et al*., 2017). Additionally, fluoroquinolones and quinolones hinder DNA replication and synthesis, and impede cell division by interfering with the function of DNA gyrase and topoisomerases (Hooper & Jacoby, 2016; Correia *et al*., 2017).

In contrast, both Penicillin G and Bacitracin were found to be completely ineffective against the *Vibrio* spp. isolates in this study. Resistance of *Vibrio* spp. to these antibiotics has been documented in several previous studies. For instance, Amalina *et al*. (2019) reported that 82% of *Vibrio* spp. isolated from cultured grouper in Peninsular Malaysia exhibited resistance to Penicillin G, while over 50% of the isolates were also resistant to Bacitracin. Furthermore, Sahilah *et al*. (2014) found that 98% of *V. parahaemolyticus* isolated from cockles along the east coast of Peninsular Malaysia showed resistance to Bacitracin. These variations in resistance patterns, including those observed in the present study, suggest that geographical differences may play a significant role in shaping antibiotic resistance profiles among *Vibrio* species (Amalina *et al*., 2019). Besides, these antibiotics have been used for a long time in the industry in Malaysia, thus supporting the claim that continuous exposure to antibiotics will cause bacteria to develop resistance to them (Kathleen *et al*., 2016; Amalina *et al*., 2019)

Bacteria, especially pathogenic strains, often undergo natural genetic changes over time, leading to their development of antimicrobial resistance. However, rapid emergence and dissemination of these multidrug-resistant (MDR) strains are exacerbated by human activities, particularly through the excessive use and misuse of antimicrobials in humans, animals, and plants (WHO, 2023). The spread of resistance genes among bacteria in aquatic environments can occur swiftly through horizontal gene transfer. Several studies have documented the discovery of resistance genes in clinical isolates of *Vibrio* spp. that were previously identified in environmental isolates, suggesting genetic exchange between clinical and environmental strains (Elmahdi *et al*., 2016).

The isolates in this study underwent screening to detect the presence of virulence genes alongside assessing their susceptibility to antibiotics. The detection of the *tlh* gene in all *V. parahaemolyticus* isolates, contrasted with its absence in the *V. cholerae* and *V. alginolyticus* isolates, suggests high conservation of this gene in *V. parahaemolyticus*, often utilised as a signature molecular marker for the species (Gutierrez West *et al*., 2013). Nevertheless, several studies have indicated the presence of the

tlh gene in other *Vibrio* spp. apart from *V. parahaemolyticus*. As reported by Wang *et al*. (2007), the *tlh* gene is widespread in various *Vibrio* spp., including *V. alginolyticus*, *V. harveyi*, *V. vulnificus*, and *V. anguillarum* (Yáñez *et al*., 2015). Consequently, the *tlh* gene may not be as exclusive to *V. parahaemolyticus* as previously assumed, potentially diminishing its precision as a species-specific marker.

Most pathogenic strains of *V. parahaemolyticus* typically possess the *tdh* and/or *trh* genes alongside the *tlh* genes (Yáñez *et al*., 2015). In clinical isolates, the *tdh* gene was detected in the majority (95%) of cases, highlighting thermostable direct hemolysin (TDH) as one of the main virulence factors produced by *V. parahaemolyticus* (Liu, 2003; Wang *et al*., 2015). The absence of both *tdh* and *trh* genes, which encode TDH and its homolog, TDH-related hemolysin (TRH), respectively, in all isolates may suggest that these isolates are non-pathogenic or have low pathogenicity in humans, as these two genes are commonly utilised as indicators of *V. parahaemolyticus* pathogenicity (Bej *et al*., 1999; Gutierrez West *et al*., 2013). Our findings are consistent with numerous studies indicating that the majority of environmental strains of *V. parahaemolyticus* are non-pathogenic, with the *tdh* and/or *trh* genes detected only infrequently in these strains (Caburlotto *et al*., 2009). However, the incidence of pathogenic *Vibrio* spp. continues to rise annually, resulting in an increase in infection cases (Elmahdi *et al*., 2016). There are also evidences suggesting that pathogenic *V. parahaemolyticus* acquired *tdh* genes through horizontal gene transfer (Okuda *et al*., 2001).

While the precise roles of the *tlh* gene in *V. parahaemolyticus* pathogenicity remain unclear, it encodes for phospholipase A2 and thermolabile hemolysin, both of which have been reported to induce lysis of human erythrocytes (Shinoda *et al*., 1991; Wang *et al*., 2015). Furthermore, its expression has been demonstrated to be upregulated in environments resembling those of the human intestines, suggesting its involvement in the adaptation, survival, and virulence of *V. parahaemolyticus* within the host gastrointestinal tract (Gotoh *et al*., 2010; Yáñez *et al*., 2015). This notion is further supported by findings indicating that HeLa, Chang liver, and RAW264.7 cells treated with purified TLH protein exhibit severe cytotoxicity, which is dose and time-dependent, thereby suggesting that TLH shares similar biological functions with the TDH and TRH toxins (Wang *et al*., 2012; Wang *et al*., 2015). Therefore, despite the unclear roles of TLH proteins in *V. parahaemolyticus* pathogenicity, it is premature to rule out these *V. parahaemolyticus* isolates as non-pathogenic simply because the *tdh* and *trh* genes were not detected. Moreover, some studies report that 10% of clinical isolates of *V. parahaemolyticus* lack the *tdh* and *trh* genes but still exhibit high cytotoxicity to gastrointestinal cells, suggesting that there are other virulence factors that contributed to their pathogenicity (Raghunath, 2014).

One of the diseases causing significant losses in shrimp farms is Acute Hepatopancreatic Necrosis Disease (AHPND). This disease is induced by specific strains of *V. parahaemolyticus* (VP_{AHPND}) carrying the plasmid (pVA1) containing *pirA* and *pirB* genes, encoding binary toxins PirA and PirB (Sirikharin *et al*., 2015; Dhar *et al*., 2019; Hossain *et al*., 2020). The presence of both toxin subunits is necessary for the manifestation of AHPND pathologies, and these toxins induce hepatopancreatic necrosis in infected shrimp, leading to rapid progression and 100% mortality in severely infected ponds (Sirikharin *et al*., 2015; Hossain *et al*., 2020). For *pirA* gene detection, the AP3 detection method has been widely used in previous studies and is recommended for confirming AHPND-positive strains (Hossain *et al*., 2020). Compared to other VP_{AHPND} detection methods (AP1 and AP2), the primer sets employed in the AP3 method have shown the highest sensitivity and specificity (Sirikharin *et al*., 2015; Hossain *et al*., 2020). In this study, none of the *Vibrio* spp. isolates, particularly the *V. parahaemolyticus* isolates, exhibited the presence of the *pirA* gene, indicating that these isolates are not AHPND-causing strains. However, continuous monitoring is essential as there have been reported cases where the acquisition of *pirA* and *pirB* genes through horizontal gene transfer has transformed non-AHPND strains into VP_{AHPND} strains (Dhar *et al*., 2019).

In all *V. cholerae* isolates, two out of three virulence genes typically associated with pathogenicity were detected: the *rtxA* and *rtxC* genes belonging to the repeat in toxin (RTX)

family. This family encompasses gene clusters including *rtxA*, encoding a putative cytotoxin, *rtxC*, encoding an acyltransferase, and *rtxB* and *rtxD*, involved in producing proteins responsible for toxin transportation (Chow *et al*., 2001). Chow *et al*. (2001) demonstrated a concurrent relationship between positive detection of *rtxA* and *rtxC* genes and positive results in HEp-2 cytotoxicity assays in clinical and environmental *V. cholerae* isolates, and vice versa. This finding demonstrated the integrity between the genotypic and phenotypic expressions of these genes across strains. Supporting this association, strains with deleted RTX gene clusters showed negative results in PCR detection and cytotoxicity assays (Chow *et al*., 2001). Therefore, the presence of both *rtxA* and *rtxC* in *V. cholerae* isolates from the Telaga Air shrimp farm indicates their pathogenic potential.

Additionally, the *ctxB* gene is a fundamental component that encodes the cholera toxin (CT), responsible for cholera syndrome characterised by acute diarrheal diseases (Chow *et al*., 2001; Takahashi *et al*., 2021). CT is regarded as the primary virulence factor in *V. cholerae* and is frequently associated with strains of significant pandemic potential (Chow *et al*., 2001). All *V. cholerae* isolates in this study lacked the *ctxB* gene. According to Chow *et al*. (2001), non-epidemic *V. cholerae* non-O1 serogroup strains that are positive for *rtxA* and *rtxC* but negative for *ctxB* only caused sporadic, milder cases of diarrhoea. However, these strains should not be underestimated as RTX cytotoxins can still induce necrosis and inflammation in the gastrointestinal tract (Chow *et al*., 2001; Kim *et al*., 2012).

The primers used for targeting the *toxR* and *toxS* genes used in this study (Table 1) were originally used for targeting *V. cholerae*-associated *toxR* and *toxS* genes. However, subsequent studies revealed that the *toxR* gene is also present in other *Vibrio* spp., including *V. parahaemolyticus*, *V. alginolyticus*, *V. mimicus*, *V. fluvialis*, and *V. vulnificus*, with homologous sequences observed in the internal portion of the nucleotide sequences of the *toxR* genes of at least three different *Vibrio* species (Okuda *et al*., 2001; Wang *et al*., 2015). As such, *toxR* and its integral membrane binding partner, *toxS* genes were also detected in all *V. parahaemolyticus* isolates in addition to all *V. cholerae* isolates in this study. Unlike the *tdh*, *trh*, and *tlh* gene in *V. parahaemolyticus* and *rtxA*, *rtxC*, and *ctxB* genes in *V. cholerae*, *toxR* and *toxS* are not directly related to the expression of virulence factors. Instead, they encode integral membrane proteins, ToxR and ToxS, that activate the transcription of virulence genes in the *Vibronaceaea* family (Pfau and Taylor, 1998; Lembke *et al*., 2020). The *toxR* gene was initially discovered as a regulatory gene for the *ctx* gene encoding CT in *V. cholerae*. The presence of these genes in *V. parahaemolyticus* isolates suggests that they may have acquired these exogenous genes through horizontal gene transfer (Sechi *et al*., 2000). Indeed, a study by Lin *et al*. (1993) showed that *V. parahaemolyticus*-associated ToxR protein is highly similar to the ToxR protein produced by *V. cholerae*.

It was later discovered that *toxR* gene plays a multifaceted role and is not only responsible to regulate the expression of virulence genes, but also in coordinating the regulation of multiple genes that can affect the survival and adaptability of *Vibrio* spp. in various environmental conditions (Okuda *et al*., 2001). For example, *toxR* was initially known to promote the expression of *tdh* gene with the presence of *toxS* gene in *V. parahaemolyticus* (Lin *et al*., 1993; Zhang *et al*., 2018). However, since *tdh* gene was not detected in the *V. parahaemolyticus* isolates in this study, the detection of both *toxR* and *toxS* genes in all isolates suggests that these genes play other roles that contribute to the adaptability and survival of the isolates. Similarly, the absence of *ctxB* gene in the *V. cholerae* isolates suggested that the *toxR* and *toxS* gene that were detected in them plays role other than the expression of the *ctx* virulence genes.

Contrary to the initial belief that the primary roles of the *toxR* and *toxS* genes are to stimulate the expression of virulence genes in the *Vibronaceae* family, a study by Okuda *et al*. (2001) demonstrated that the original function of these genes was to modulate the expression of outer membrane proteins (OMP)-encoding genes for bacterial adaptation in various environmental conditions. ToxR-modulated expression of OMPs was shown to contribute to the ability of *Vibrio* spp. to survive in the gastrointestinal tract by facilitating colonisation, stimulating the expression of virulence factors, and conferring bile resistance (Okuda *et al*.,

2001; Lembke *et al*., 2020). These findings lend support to the results obtained in this study, suggesting that the presence of *toxR* and *toxS* genes in the isolates may play a more significant role in the adaptability of the *Vibrio* spp. rather than in the expression of their virulence genes, especially considering the absence of associated virulence genes.

Moreover, several studies have indicated the involvement of the *toxR* gene in the regulation of biofilm formation. The expression of ToxR protein has been reported to be influenced by cell density and is implicated in the quorum sensing (QS) mechanism of *V. cholerae*, *V. parahaemolyticus*, *V. alginolyticus*, and *V. anguillarum*, which can coordinate biofilm formation in response to environmental cues (Chen *et al*., 2018; Zhang *et al*., 2018; Zhang *et al*., 2021). A study conducted by Chen *et al*. (2018) suggested that ToxR plays a pivotal role in biofilm formation in *V. parahaemolyticus*. The reduced biofilm formation observed in a *toxR* mutant strain compared to the wild-type *V. parahaemolyticus* indicates the involvement of ToxR in promoting biofilm production. In addition, the restoration of biofilm formation in the complemented mutant strain further supports the role of ToxR in this process (Chen *et al*., 2018). Therefore, ToxR likely regulates genes or pathways that contribute to the formation of mature biofilms, thereby enhancing the adaptability and pathogenicity of *V. parahaemolyticus* (Gao *et al*., 2022).

In all *V. alginolyticus* isolates, none of the tested virulence genes were detected. Despite the *toxR* gene being commonly reported in many studies as the second most frequently detected virulence gene in *V. alginolyticus* after the *ompK* gene, no positive detections were observed in any *V. alginolyticus* isolates from the Telaga Air shrimp farm (Abd Wahid *et al*., 2022). Additionally, the *tlh* genes associated with *V. parahaemolyticus*, which were reportedly found in all seven *V. alginolyticus* strains from shrimp hatcheries in Southern China as reported by Xue *et al*. (2022), were not detected in all *V. alginolyticus* isolates in this study (Abd Wahid *et al*., 2022). The absence of other virulence genes originally from various *Vibrio* spp. in all isolates suggests a low frequency of gene transfer events between *V. alginolyticus* and other *Vibrio* spp. in the shrimp farm or few strains are retaining these genes through horizontal gene transfer mechanisms (Xue *et al*., 2022).

While this study primarily focused on the phenotypic and genotypic characterization of antibiotic resistance and the presence of selected virulence genes in *Vibrio* spp. isolates, the potential relationship between these two factors is of significant interest. Although no formal analysis was conducted to examine correlations between multidrug resistance and the presence of virulence genes in this study, the literature suggests that the relationship between antibiotic resistance and virulence traits can be complex. Previous studies have shown that antibiotic resistance and virulence genes can be independently acquired and maintained in bacterial populations (Beceiro *et al*., 2013). However, there are instances where both traits may be co-selected or linked under certain environmental conditions or selective pressures. Factors such as bacterial species, the mechanisms of resistance and virulence, regulatory networks, ecosystems and environmental factors, such as antibiotic use in aquaculture, may influence the presence and expression of both resistance and virulence traits (Cepas & Soto, 2020).

Several studies have reported conflicting findings regarding the relationship between antimicrobial resistance and virulence. For example, strains of uropathogenic *E. coli* (UPEC) that exhibited resistance to quinolones were found to possess fewer virulence factors or showed decreased expression of virulence genes associated with the development of cystitis and pyelonephritis in the urinary tract (Vila *et al*., 2002). Similarly, an inverse relationship between antibiotic resistance and virulence was observed in Non-O1, Non-O139 *V. cholerae* isolates, reportedly due to a fitness trade-off (Abioye *et al*., 2023). In contrast, increased virulence linked to the development of swarming motility in *Pseudomonas aeruginosa* has been associated with increased resistance to polymyxin B, ciprofloxacin, and gentamicin (Beceiro *et al*., 2013). However, another study reported no correlation between biofilm formation, virulence factors, and antibiotic resistance in *P. aeruginosa*, thereby contradicting the previous findings (Gajdács *et al*., 2021). These discrepancies highlight the complex and multifactorial nature of the relationship between antibiotic resistance and

virulence in bacteria, which can vary depending on the species, genetic background, and environmental conditions. Further investigation, including more extensive analyses of the genomic and environmental factors influencing these traits, is essential to fully understand the interplay between antibiotic resistance and virulence of the *Vibrio* isolates in this study.

In order to curtail the dissemination of MAR bacterial strains and prevent the transfer of virulence genes among bacteria within shrimp farms, employing prudent practices is imperative. Farmers must prioritise the cultivation and provision of specific pathogen-free (SPF) shrimp stocks, a measure proven to enhance shrimp production across numerous countries (Nillian *et al*., 2022). However, effective disease control necessitates strict management protocols encompassing physical barriers, meticulous water treatment control, carrier exclusion strategies, and vigilant feed management systems (Nillian *et al*., 2022). Furthermore, regular monitoring of *Vibrio* spp. prevalence and antibiotic resistance patterns within farms assumes paramount importance, serving as a pivotal precursor to informed management decisions.

CONCLUSION

This study has provided valuable insights into the antibiotic resistance profiles and virulence gene profiles of *Vibrio* spp. isolates obtained from the Telaga Air shrimp farm in Kuching, Sarawak. The primary objectives of the study were to assess the antibiotic resistance patterns and the presence of virulence genes in *Vibrio* spp. isolates, and to evaluate their potential public health risk. The findings indicate widespread antibiotic resistance among *Vibrio* spp. isolates, likely attributed to the extensive use of antibiotics or the presence of their residuals in aquaculture settings. Additionally, the presence of isolates with MAR indices higher than 0.2 suggests potential contamination from sources with high antibiotic usage, such as wastewater or nearby agricultural and aquaculture activities. The study also identified significant diversity in the virulence gene profiles among *Vibrio* spp. isolates. While some isolates exhibited key virulence genes associated with pathogenicity, others lacked these genes, indicating variability in their pathogenic potential. These findings highlight the importance of continuous testing and monitoring to mitigate the risks of antibiotic resistance and pathogenic *Vibrio* spp. in shrimp farming environments.

However, despite the findings obtained in this study, the surveillance data is only limited to the strains isolated from the Telaga Air shrimp farm, and hence, do not represent the comprehensive epidemiology in Sarawak. Moreover, given the high occurrence of horizontal gene transfer within bacterial populations, ongoing and a more comprehensive monitoring is essential to ensure that limited spread of virulence genes occurs between pathogenic and non-pathogenic strains. Additionally, monitoring antibiotic usage and bacterial resistance patterns is crucial for effective disease management and sustainable aquaculture practices.

ACKNOWLEDGEMENT

The project was funded by Matching Research (International) INT/F07/UB/86419/2024) and Fundamental Research Grant Scheme (FRGS/1/2019/STG05/UNIMAS/03/2), Universiti Malaysia Sarawak. This work forms part of collaboration with Lembaga Kemajuan Ikan Malaysia (LKIM).

CONFLICT OF INTEREST

All authors declare that they have no conflicts of interest in preparing this article.

REFERENCES

Abd Wahid, M.E., Mohamad, M., Mohamed, N.N. & Afiqah-Aleng, N. (2022). Vibriosis in green mussels. *In Aquaculture Pathophysiology*, 515-529. DOI:10.1016/b978-0-323-95434-1.00069-3

Abdelaziz Gobarah, D.E., Helmy, S.M., Mahfouz, N.B., Fahmy, H.A., & Abou Zeid, M.A.E.H.M. (2022). Virulence genes and antibiotic resistance profile of *Vibrio* species isolated from fish in Egypt. *Veterinary Research Forum*, 13(3): 315-321. DOI:10.30466/vrf.2021.520767.3117

Abdullah Sani, N., Ariyawansa, S., Babji, A.S. & Hashim, J.K. (2013). The risk assessment of *Vibrio parahaemolyticus* in cooked black tiger shrimps (*Penaeus monodon*) in Malaysia. *Food Control*, 31(2): 546-552. DOI:10.1016/j.foodcont.2012.10.018

Abioye, O.E., Nontongana, N., Osunla, C.A. & Okoh, A.I. (2023). Antibiotic resistance and virulence genes profiling of *Vibrio cholerae* and *Vibrio mimicus* isolates from some seafood collected at the aquatic environment and wet markets in Eastern Cape Province, South Africa. *PLoS ONE*, 18(8): e0290356. DOI:10.1371/journal.pone.0290356

Abioye, O.E., Osunla, A.C. & Okoh, A.I. (2021). Molecular detection and distribution of six medically important *Vibrio* spp. in selected freshwater and brackish water resources in Eastern Cape Province, South Africa. *Frontiers in Microbiology*, 12: 617703. DOI:10.3389/fmicb.2021.617703

Al-Othrubi, S.M., Kqueen, C.Y., Mirhosseini, H., Hadi, Y.A. & Radu, S. (2014). Antibiotic resistance of *Vibrio parahaemolyticus* isolated from cockles and shrimp sea food marketed in Selangor, Malaysia. *Clinical Microbiology: Open Access*, 03(03): 148-154. DOI:10.4172/2327-5073.1000148

Amalina, N.Z., Santha, S., Zulperi, D., Amal, M.N., Yusof, M.T., Zamri-Saad, M. & Ina-Salwany, M.Y. (2019). Prevalence, antimicrobial susceptibility and plasmid profiling of *Vibrio* spp. isolated from cultured groupers in Peninsular Malaysia. *BMC Microbiology*, 19(1): 251. DOI:10.1186/s12866-019-1624-2

Baker-Austin, C., Trinanes, J. & Martinez-Urtaza, J. (2020). The new tools revolutionizing *Vibrio* science. *Environmental Microbiology*, 22(10): 4096-4100. DOI:10.1111/1462-2920.15083

Beceiro, A., Tomás, M. & Bou, G. (2013). Antimicrobial resistance and virulence: a successful or deleterious association in the bacterial world?. *Clinical Microbiology Reviews*, 26(2): 185–230. DOI:10.1128/CMR.00059-12

Bej, A.K., Patterson, D.P., Brasher, C.W., Vickery, M.C.L., Jones, D.D. & Kaysner, C.A. (1999). Detection of total and hemolysin-producing *Vibrio parahaemolyticus* in shellfish using multiplex PCR amplification of *tl*, *tdh* and *trh*. *Journal of Microbiological Methods*, 36: 215-225.

Caburlotto, G., Gennari, M., Ghidini, V., Tafi, M. & Lleo, M.M. (2009). Presence of T3SS2 and other virulence-related genes in *tdh*-negative *Vibrio parahaemolyticus* environmental strains isolated from marine samples in the area of the Venetian Lagoon, Italy. *FEMS Microbiology Ecology*, 70(3): 506-514. DOI:10.1111/j.1574-6941.2009.00764.x

CDC. (2019a). *Glossary of terms related to antibiotic resistance*. Retrieved from https://www.cdc.gov/narms/resources/glossary.html#:~:text=Results%20of%20antimicrobial%20susceptibility%20testing,cannot%20be%20treated%20with%20drug

CDC. (2019b). *Vibrio species causing vibriosis.* Retrieved from https://www.cdc.gov/*Vibrio*/index.html

Cepas, V. & Soto, S.M. (2020). Relationship between virulence and resistance among gram-negative bacteria. *Antibiotics*, 9(10): 719. DOI:10.3390/antibiotics9100719

Chen, L., Qiu, Y., Tang, H., Hu, L.F., Yang, W.H., Zhu, X.J., Huang, X.X., Wang, T. & Zhang, Y.Q. (2018). ToxR is required for biofilm formation and motility of *Vibrio parahaemolyticus*. *Biomedical and Environmental Sciences*, 31(11): 848-850. DOI:10.3967/bes2018.112

Chow, K.H., Ng, T.K., Yuen, K.Y. & Yam, W.C. (2001). Detection of RTX toxin gene in *Vibrio cholerae* by PCR. *Journal of Clinical Microbiology*, 39(7): 2594-2597. DOI:10.1128/jcm.39.7.2594-2597.2001

Clinical and Laboratory Standard Institute. (2015). *Methods for antimicrobial dilution and disk susceptibility testing of infrequently isolated or fastidious bacteria*. *3rd ed. CLSI guideline M45*. Wayne, PA: CLSI.

Correia, S., Poeta, P., Hébraud, M., Capelo, J.L. & Igrejas, G. (2017). Mechanisms of quinolone action and resistance: Where do we stand? *Journal of Medical Microbiology*, 66(5): 551-559. DOI:10.1099/jmm.0.000475

Dhar, A., Piamsomboon, P., Aranguren Caro, L., Kanrar, S., Adami, R. & Juan, Y. (2019). First report of acute hepatopancreatic necrosis disease (AHPND) occurring in the USA. *Diseases of Aquatic Organisms*, 132(3): 241-247. DOI:10.3354/dao03330

Elmahdi, S., DaSilva, L.V. & Parveen, S. (2016). Antibiotic resistance of *Vibrio parahaemolyticus* and *Vibrio vulnificus* in various countries: A Review. *Food Microbiology*, 57: 128-134. DOI:10.1016/j.fm.2016.02.008

Gajdács, M., Baráth, Z., Kárpáti, K., Szabó, D., Usai, D., Zanetti, S. & Donadu, M.G. (2021). No Correlation between Biofilm Formation, Virulence Factors, and Antibiotic Resistance in *Pseudomonas aeruginosa*: Results from a Laboratory-Based In Vitro Study. *Antibiotics (Basel, Switzerland)*, 10(9): 1134. DOI:10.3390/antibiotics10091134

Gao, L., Ouyang, M., Li, Y., Zhang, H., Zheng, X.-F., Li, H.-X., Rao, S.-Q., Yang, Z.-Q., & Gao, S. (2022). Isolation and characterisation of a lytic vibriophage OY1 and its biocontrol effects against *Vibrio* spp. *Frontiers in Microbiology*, 13. DOI:10.3389/fmicb.2022.830692

Gotoh, K., Kodama, T., Hiyoshi, H., Izutsu, K., Park, K.-S., Dryselius, R., Akeda, Y., Honda, T., & Iida, T. (2010). Bile acid-induced virulence gene expression of *Vibrio parahaemolyticus* reveals a novel therapeutic potential for bile acid sequestrants. *PLoS ONE*, 5(10). DOI:10.1371/journal.pone.0013365

Gutierrez West, C.K., Klein, S.L. & Lovell, C.R. (2013). High frequency of virulence factor genes *tdh*, *trh*, and *tlh* in *Vibrio parahaemolyticus* strains isolated from a pristine estuary. *Applied and Environmental Microbiology*, 79(7): 2247-2252. DOI:10.1128/aem.03792-12

Haifa-Haryani, W.O., Amatul-Samahah, Md.A., Azzam-Sayuti, M., Chin, Y.K., Zamri-Saad, M., Natrah, I., Amal, M.N., Satyantini, W.H. & Ina-Salwany, M.Y. (2022). Prevalence, antibiotics resistance and plasmid profiling of *Vibrio* spp. isolated from cultured shrimp in Peninsular Malaysia. *Microorganisms*, 10(9): 1851. DOI:10.3390/microorganisms10091851

Hanna, N., Tamhankar, A.J. & Stålsby Lundborg, C. (2023). Antibiotic concentrations and antibiotic resistance in aquatic environments of the WHO Western Pacific and South-East Asia regions: A systematic review and probabilistic environmental hazard assessment. *The Lancet Planetary Health*, 7(1): e45-e54. DOI:10.1016/s2542-5196(22)00254-6

Hooper, D.C. & Jacoby, G.A. (2016). Topoisomerase inhibitors: Fluoroquinolone mechanisms of action and resistance. *Cold Spring Harbor Perspectives in Medicine*, 6(9): a025320. DOI:10.1101/cshperspect.a025320

Hossain, Md.M., Uddin, Md.I., Islam, H., Fardoush, J., Rupom, Md.A., Hossain, Md.M., Farjana, N., Afroz, R., Hasan-Uj-Jaman, Roy, H.S., Shehab, Md.A. & Rahman, Md.A. (2020). Diagnosis, genetic variations, virulence, and toxicity of AHPND-positive *Vibrio parahaemolyticus* in *Penaeus monodon*. *Aquaculture International*, 28(6): 2531-2546. DOI:10.1007/s10499-020-00607-z

Hudzicki, J. (2009). *Kirby-Bauer disk diffusion susceptibility test protocol*. Retrieved from https://asm.org/getattachment/2594ce26-bd44-47f6-8287-0657aa9185ad/Kirby-Bauer-Disk-Diffusion-Susceptibility-Test-Protocol-pdf.pdf

Ibrahim, A.B., Khan, M.A., Ayob, M.Y. & Norrakiah, A.S. (2010). Pesticide and antibiotic residues in freshwater aquaculture fish: Chemical risk assessment from farm to table. *Asian Journal of Agro-Industry*, 3(3): 328-334.

Kapoor, G., Saigal, S. & Elongavan, A. (2017). Action and resistance mechanisms of antibiotics: A guide for clinicians. *Journal of Anaesthesiology Clinical Pharmacology*, 33(3): 300. DOI:10.4103/joacp.joacp_349_15

Kathleen, M.M., Samuel, L., Felecia, C., Reagan, E. L., Kasing, A., Lesley, M. & Toh, S.C. (2016). Antibiotic Resistance of Diverse Bacteria from Aquaculture in Borneo. *International Journal of Microbiology*, *2016*: 2164761. DOI:10.1155/2016/2164761

Kaysner, C.A., Abeyta, C., Stott, R.F., Krane, M.H. & Wekell, M.M. (1990). Enumeration of *Vibrio* species, including *V. cholerae*, from samples of an oyster growing area, Grays Harbor, Washington. *Journal of Food Protection*, 53(4): 300-302. DOI:10.4315/0362-028x-53.4.300.

Kim, H.-J., Ryu, J.-O., Lee, S.-Y., Kim, E.-S. & Kim, H.-Y. (2015). Multiplex PCR for detection of the *Vibrio* genus and five pathogenic *Vibrio* species with primer sets designed using comparative genomics. *BMC Microbiology*, 15(1): 239. DOI:10.1186/s12866-015-0577-3

Kim, Y.R., Lee, S.E., Kang, I.-C., Nam, K.I., Choy, H.E. & Rhee, J.H. (2012). A bacterial RTX toxin causes programmed necrotic cell death through calcium-mediated mitochondrial dysfunction. *The Journal of Infectious Diseases*, 207(9): 1406-1415. DOI:10.1093/infdis/jis746

Larsson, D.G. (2014). Antibiotics in the environment. *Upsala Journal of Medical Sciences*, 119(2): 108-112. DOI:10.3109/03009734.2014.896438

Lembke, M., Höfler, T., Walter, A., Tutz, S., Fengler, V., Schild, S. & Reidl, J. (2020). Host stimuli and operator binding sites controlling protein interactions between virulence master regulator ToxR and ToxS in *Vibrio cholerae*. *Molecular Microbiology*, 114(2): 262-278. DOI:10.1111/mmi.14510

Lesen, D., Nillian, E., Awang Baki, D.N. & Robin, T. (2024). Prevalence of *Vibrio parahaemolyticus*, *Vibrio cholerae*, and *Vibrio alginolyticus* in a white-leg shrimp (*Litopenaeus vannamei*) farm in Sarawak. *Pertanika Journal of Science and Technology*, 32(5): 2233–2257. DOI:10.47836/pjst.32.5.17

Liang, J., Liu, J., Wang, X., Sun, H., Zhang, Y., Ju, F., Thompson, F. & Zhang, X.H. (2022). Genomic Analysis Reveals Adaptation of *Vibrio campbellii* to the Hadal Ocean. *Applied and Environmental Microbiology*, 88(16): e0057522. DOI:10.1128/aem.00575-22

Lin, Z., Kumagai, K., Baba, K., Mekalanos, J.J. & Nishibuchi, M. (1993). *Vibrio parahaemolyticus* has a homolog of the *Vibrio cholerae* toxRS operon that mediates environmentally induced regulation of the thermostable direct hemolysin gene. *Journal of Bacteriology*, 175(12): 3844-3855. DOI:10.1128/jb.175.12.3844-3855.1993

Liu, H. (2003). Analysis of collective food poisoning events in Shanghai from 1990 to 2000. *Chinese Journal of Natural Medicines*, 5: 17-20.

Lundborg, C.S. & Tamhankar, A.J. (2017). Antibiotic residues in the environment of South East Asia. *BMJ*, 2017(358): j2440. DOI:10.1136/bmj.j2440

Luu, Q.H., Nguyen, T.B., Nguyen, T.L., Do, T.T., Dao, T.H. & Padungtod, P. (2021). Antibiotics use in fish and shrimp farms in Vietnam. *Aquaculture Reports*, 20: 100711. DOI:10.1016/j.aqrep.2021.100711

Meibom, K.L., Blokesch, M., Dolganov, N.A., Wu, C.Y. & Schoolnik, G.K. (2005). Chitin induces natural competence in *Vibrio cholerae*. *Science (New York, N.Y.)*, 310(5755): 1824–1827. DOI:10.1126/science.1120096

Muteeb, G., Rehman, M.T., Shahwan, M. & Aatif, M. (2023). Origin of antibiotics and antibiotic resistance, and their impacts on drug development:A narrative review. *Pharmaceuticals (Basel, Switzerland)*, 16(11): 1615. DOI: 10.3390/ph16111615

Nillian, E., Zakaria, N.D., Lesen, D., Yusoff, N.H., Ismail, N.S., Tung, T.S. & Bilung, L. (2022). Comparison distribution of *Vibrio* species in stocking to harvesting process of shrimp at commercialize shrimp farm. *International Journal of Biology and Biomedical Engineering*, 16: 168-174. DOI:10.46300/91011.2022.16.22

Oh, E.-G., Son, K.-T., Yu, H., Lee, T.-S., Lee, H.-J., Shin, S., Kwon, J.-Y., Park, K., & Kim, J. (2011). Antimicrobial resistance of *Vibrio parahaemolyticus* and *Vibrio alginolyticus* strains isolated from farmed fish in Korea from 2005 through 2007. *Journal of Food Protection*, 74(3): 380-386. DOI:10.4315/0362-028x.jfp-10-307

Okuda, J., Nakai, T., Chang, P.S., Oh, T., Nishino, T., Koitabashi, T. & Nishibuchi, M. (2001). The *toxR* gene of *Vibrio* (*listonella*) *anguillarum* controls expression of the major outer membrane proteins but not virulence in a natural host model. *Infection and Immunity*, 69(10): 6091-6101. DOI:10.1128/iai.69.10.6091-6101.2001

Paria, P., Behera, B.K., Mohapatra, P.K. & Parida, P.K. (2021). Virulence factor genes and comparative pathogenicity study of TDH, TRH and TLH positive *Vibrio parahaemolyticus* strains isolated from whiteleg shrimp, *Litopenaeus vannamei* (Boone, 1931) in India. *Infection, Genetics and Evolution*, 95: 105083. DOI:10.1016/j.meegid.2021.105083

Pfau, J.D. & Taylor, R.K. (1998). Mutations in *toxR* and *toxS* that separate transcriptional activation from DNA binding at the cholera toxin gene promoter. *Journal of Bacteriology*, 180(17): 4724-4733. DOI:10.1128/jb.180.17.4724-4733.1998

Queipo-Ortuño Maria Isabel, De Dios Colmenero, J., Macias, M., Bravo, M.J. & Morata, P. (2008). Preparation of bacterial DNA template by boiling and effect of immunoglobulin G as an inhibitor in real-time PCR for serum samples from patients with brucellosis. *Clinical and Vaccine Immunology*, 15(2): 293-296. DOI:10.1128/cvi.00270-07

Raghunath P. (2015). Roles of thermostable direct hemolysin (TDH) and TDH-related hemolysin (TRH) in *Vibrio parahaemolyticus*. *Frontiers in Microbiology*, 5: 805. DOI:10.3389/fmicb.2014.00805

Rodgers, C.J., Mohan, C.V. & Peeler, E.J. (2011). The spread of pathogens through trade in aquatic animals and their products. *Revue Scientifique et Technique de l'OIE*, 30(1): 241-256. DOI:10.20506/rst.30.1.2034

Sahilah, A.M., Laila, R.A., Sallehuddin, H. Mohd., Osman, H., Aminah, A. & Ahmad Azuhairi, A. (2014). Antibiotic resistance and molecular typing among cockle (*Anadara granosa*) strains of *Vibrio parahaemolyticus* by polymerase chain reaction (PCR)-based analysis. *World Journal of Microbiology and Biotechnology*, 30(2): 649–659. DOI:10.1007/s11274-013-1494-y

Salgueiro, H.S., Ferreira, A. C., Duarte, A.S. & Botelho, A. (2024). Source attribution of antibiotic resistance genes in estuarine aquaculture: A machine learning approach. *Antibiotics*, 13(1): 107. DOI:10.3390/antibiotics13010107

Sampaio, A., Silva, V., Poeta, P. & Aonofriesei, F. (2022). Vibrio spp.: Life strategies, ecology, and risks in a changing environment. Diversity, 14(2): 97. DOI:10.3390/d14020097

Sechi, L.A., Duprè, I., Deriu, A., Fadda, G. & Zanetti, S. (2000). Distribution of *Vibrio cholerae* virulence genes among different *Vibrio* species isolated in Sardinia, Italy. *Journal of Applied Microbiology*, 88: 475-481.

Sharma, L., Nagpal, R., Jackson, C.R., Patel, D. & Singh, P. (2021). Antibiotic-resistant bacteria and gut microbiome communities associated with wild-caught shrimp from the United States versus imported farm-raised retail shrimp. *Scientific Reports*, 11(1): 3356. DOI:10.1038/s41598-021-82823-y

Shinoda, S., Matsuoka, H., Tsuchie, T., Miyoshi, S.-I., Yamamoto, S., Taniguchi, H. & Mizuguchi, Y. (1991). Purification and characterisation of a lecithin-dependent haemolysin from *Escherichia coli* transformed by a *Vibrio parahaemolyticus* gene. *Journal of General Microbiology*, 137(12): 2705-2711. DOI:10.1099/00221287-137-12-2705

Sirikharin, R., Taengchaiyaphum, S., Sanguanrut, P., Chi, T.D., Mavichak, R., Proespraiwong, P., Nuangsaeng, B., Thitamadee, S., Flegel, T.W. & Sritunyalucksana, K. (2015). Characterization and PCR detection of binary, Pir-like toxins from *Vibrio parahaemolyticus* isolates that cause acute hepatopancreatic necrosis disease (AHPND) in shrimp. *PLoS ONE*, 10(5). DOI:10.1371/journal.pone.0126987

Song, X., Zang, J., Yu, W., Shi, X. & Wu, Y. (2020). Occurrence and identification of pathogenic *Vibrio* contaminants in common seafood available in a Chinese traditional market in Qingdao, Shandong Province. *Frontiers in Microbiology*, 11: 1488. DOI:10.3389/fmicb.2020.01488

Takahashi, E., Ochi, S., Mizuno, T., Morita, D., Morita, M., Ohnishi, M., Koley, H., Dutta, M., Chowdhury, G., Mukhopadhyay, A.K., Dutta, S., Miyoshi, S.-I. & Okamoto, K. (2021). Virulence of cholera toxin gene-positive *Vibrio cholerae* Non-O1/non-o139 strains isolated from environmental water in Kolkata, India. *Frontiers in Microbiology*, 12: 726273. DOI:10.3389/fmicb.2021.726273

Tendencia, E.A. & de la Peña, L.D. (2001). Antibiotic resistance of bacteria from shrimp ponds. *Aquaculture*, 195(3-4): 193-204. DOI:10.1016/s0044-8486(00)00570-6

Vila, J., Simon, K., Ruiz, J., Horcajada, J.P., Velasco, M., Barranco, M., Moreno, A. & Mensa, J. (2002). Are quinolone-resistant uropathogenic *Escherichia coli* less virulent? *The Journal of Infectious Diseases*, 186(7): 1039–1042. DOI:10.1086/342955

Wang, R.Z., Fang, S., Wu, D.L., Wu, D., Lian, J., Fan, J., Zhang, Y., Wang, S. and Lin, W. (2012). Screening of a ScFv antibody that can neutralize effectively the cytotoxicity of *Vibrio parahaemolyticus* TLH. *Applied and Environmental Microbiology*, 78: 4967-4975. DOI:10.1128/AEM.00435-12

Wang, R., Zhong, Y., Gu, X., Yuan, J., Saeed, A.F. & Wang, S. (2015). The pathogenesis, detection, and prevention of *Vibrio parahaemolyticus*. *Frontiers in Microbiology*, 6: 144. DOI:10.3389/fmicb.2015.00144

Wang, S.X., Zhang, X.H., Zhong, Y.B., Sun, B.G. & Chen, J.X. (2007). Genes encoding the *Vibrio harveyi* haemolysin (VHH)/thermolabile haemolysin (TLH) are widespread in vibrios. *Acta Microbiologica Sinica*, 47(2007): 874-881.

WHO. (2023). *Antimicrobial resistance*. Retrieved from https://www.who.int/news-room/fact-sheets/detail/antimicrobial-resistance

Xu, Y., Wang, C., Zhang, G., Tian, J., Liu, Y., Shen, X. & Feng, J. (2017). ISCR2 is associated with the dissemination of multiple resistance genes among *Vibrio* spp. and *Pseudoalteromonas* spp. isolated from farmed fish. *Archives of Microbiology*, 199(6): 891-896. DOI:10.1007/s00203-017-1365-2

Xue, M., Huang, X., Xue, J., He, R., Liang, G., Liang, H., Liu, J. & Wen, C. (2022). Comparative genomic analysis of seven *Vibrio alginolyticus* strains isolated from shrimp larviculture water with emphasis on chitin utilisation. *Frontiers in Microbiology*, 13: 925747. DOI:10.3389/fmicb.2022.925747

Yáñez, R., Bastías, R., Higuera, G., Salgado, O., Katharios, P., Romero, J., Espejo, R. & García, K. (2015). Amplification of TLH gene in other *Vibrionaceae* specie by specie-specific multiplex PCR of *Vibrio parahaemolyticus*. *Electronic Journal of Biotechnology*, 18(6): 459-463. DOI:10.1016/j.ejbt.2015.09.007

Zhang, Y., Hu, L., Osei-Adjei, G., Zhang, Y., Yang, W., Yin, Z., Lu, R., Sheng, X., Yang, R., Huang, X. & Zhou, D. (2018). Autoregulation of *toxR* and its regulatory actions on major virulence gene loci in *Vibrio parahaemolyticus*. *Frontiers in Cellular and Infection Microbiology*, 8: 291. DOI:10.3389/fcimb.2018.00291

Zhang, Y., Qiu, Y., Xue, X., Zhang, M., Sun, J., Li, X., Hu, L., Yin, Z., Yang, W., Lu, R. & Zhou, D. (2021). Transcriptional regulation of the virulence genes and the biofilm formation associated operons in *Vibrio parahaemolyticus*. *Gut Pathogens*, 13(1): 15. DOI:10.1186/s13099-021-00410-y

Zoqratt, M.Z.H.M., Eng, W.W.H., Thai, B.T., Austin, C.M. & Gan, H.M. (2018). Microbiome analysis of Pacific white shrimp gut and rearing water from Malaysia and Vietnam: Implications for aquaculture research and management. *PeerJ*, 6: e5826. DOI:10.7717/peerj.5826

Borneo Journal of Resource Science and Technology (2025), 15(1): 55-69
DOI: https:doi.org/10.33736/bjrst.7828.2025

Antifungal, Anti-Biofilm, and Anti-Phospholipase Effects of *Pseudomonas aeruginosa* Bacteriocins on Clinical Yeast Pathogens

ALI NABEEL AL-MIZEL *, HAMZIA ALI AJAH, RAGHAD ABDULLATIF ABUDLRAZAQ

Department of Biology, College of Science, Mustansiriyah University, Baghdad, Iraq
*Corresponding author: alinabeel@uomustansiriyah.edu.iq
Received: 13 September 2024 Accepted: 21 February 2025 Published: 30 June 2025

ABSTRACT

Yeast infections pose a significant challenge around the world, especially with the rising of antifungal drug resistance. This study investigates the antifungal, anti-biofilm and anti-phospholipase activity of bacteriocins produced by the bacterium *Pseudomonas aeruginosa* against 12 yeast isolates which were selected from 57 according to their high resistance to commonly used antifungal drugs, high biofilm production and phospholipase production. Additionally, this study tested the viability of the yeast cells tested after exposure to the bacteriocin. Forty *P. aeruginosa* isolates were tested and the most potent bacteriocin producing isolate was selected. The partially purified pyocins had high antifungal activity with a range of 40.57 µg ml^{-1} to 81.15 µg ml^{-1} minimum inhibitory concentration (MIC) against multiple clinical and drug resistant *Candida* and *Cryptococcus* isolates and surpassed the conventionally used antifungal drugs. It also possessed strong anti-biofilm activity, though its anti-phospholipase activity is varied and isolate dependent, and the viability of the yeast cells was significantly reduced. The high antimicrobial activity of the bacteriocin shows its potential as a therapeutic agent against yeast infections, especially those with high antifungal resistance and biofilm production. These findings can be beneficial to improve patients' outcome as more novel antifungal therapeutic drugs are needed.

Keywords: Bacteriocin, Biofilm, *Candida*, *Cryptococcus*, Phospholipase

INTRODUCTION

The increased resistance of microbes to antimicrobial drugs is rising and with it the deaths related to antimicrobial resistance (Oneill, 2014). Fungal infections represent a public health concern worldwide especially those that are caused by yeasts which result in substantial increase in morbidity and mortality rates (Van de Veerdonk *et al*., 2015; Pal, 2018; Lima *et al*., 2022; Kakar *et al*., 2022), these yeasts can be transported through different door handles, elevators and restaurant tables and staff due to poor personal hygiene, especially *Candida* (Abid *et al*., 2023). Studies have shown that co-infections with pathogenic yeasts can lead to worst outcomes in COVID-19 patients by causing COVID-19 related Candidiasis (Garcia-Vidal *et al*., 2021; Arastehfar *et al*., 2020).

Candida albicans has also been shown to be a causative agent of urinary tract infections (Haghighipour *et al*., 2019; Al-Baqer *et al*., 2021), vaginal infections (Perinelli *et al*., 2018; Hussein *et al*., 2019), oral thrushes (Beute *et al*., 2022; Karajacob *et al*., 2023) and accidental implantation of the yeast during surgery and injections (Wang *et al*., 2019).

Cryptococcus as well as causes a variety of infections especially in immunocompromised patients, by affecting the skin, bones and central nervous system and causing meningitis (Vechi *et al*., 2019; Hayashida *et al*., 2017). The increased use and misuse of antifungal drugs has been related to increased antifungal resistance especially of *C. albicans* and the emergence of resistance in non albicans species as well (Gow *et al*., 2022; M El-Ganiny *et al*., 2021).

One major factor that contributes to the pathogenicity of yeasts is their ability to form biofilms, it serves as a barrier that protects them from antifungal drugs which increases their persistence and makes them hard to manage, the ability to form these biofilms is associated with increased mortality rates especially in patients with candidemia (Vitális *et al*., 2020; Hamady & Marei, 2021; Zhu *et al*., 2022). Another major virulence factor is the extracellular

phospholipases which cause the degradation of phospholipids of the cell membrane of target cells, which disrupts cellular activities and could lead to cell death or changes to the cell membrane that facilitate adherence. *C. albicans* isolates with high phospholipase production were shown to have higher rate of deaths *in vivo* in mice and higher rates of adherence to oral epithelial cells compared to *C. albicans* isolates with lower phospholipase production (Ellepola *et al*., 2014). Phospholipase is an enzyme produced by *Cryptococcus* that hydrolyses phospholipids in the lungs and cellular membranes by breaking down the ester bonds. Phospholipases have shown to enhance the adhesion to lung epithelial cells, it is also required for interstitial tissue growth and efficient transfer from the lung to the brain (Montoya *et al*., 2021).

The requirement for alternative and novel drugs is increasing as the antifungal resistance has been on the rise. Bacteriocins are antimicrobial peptides that have gotten the attention for antimicrobial therapy against bacteria and fungi as seen in the bacteriocin of *Pediococcus pentosaceus* (Taher, 2017). Especially those bacteriocins produced by *P. aeruginosa* show great antibacterial activity (Ling *et al*., 2010; Oluyombo *et al*., 2019; Behrens *et al*., 2020; Paškevičius *et al*., 2022). On the other hand, the antimicrobial activity of these bacteriocins against yeasts, especially those that have high resistance to conventional antifungals is still relatively unexplored.

This study investigated the antimicrobial activity of the cell free supernatant (CFS) of *P. aeruginosa* that contains the pyocins against 4 selected test microbial isolates (two *Staphylococcus aureus* isolates, one *P. aeruginosa*, and one *C. albicans*) which were selected for screening purposes according to previous studies and displayed susceptibility to the pyocins (Mohamed *et al*., 2021; Alqahtani *et al*., 2022). The antifungal drugs resistance, biofilm and phospholipase producing capability of the yeast isolates were investigated and the strongest ones overall were selected. This study also determines the antifungal, anti-biofilm and anti-phospholipase activity of the partially purified bacteriocin of the selected *P. aeruginosa* against multiple species of yeast isolates of *Candida* and *Cryptococcus*, in addition the viability of these yeast isolates was tested after exposure to the bacteriocins. This study may fill a gap in the literature by finding the potential use of *P. aeruginosa* bacteriocins as antifungal, anti-biofilm and anti-phospholipase agents especially against antifungal resistant yeasts, which would improve patients' well-being.

MATERIALS AND METHODS

Source and Identification of Bacterial and Yeast Isolates

A total of 40 *P. aeruginosa* isolates were specifically selected and collected from clinical samples (oral, vaginal and skin) from Al-Baladi Teaching Hospital and Medical City hospitals. The initial identification of the isolates involved microscopic examination and biochemical testing. Microscopic examination involved observation of colony morphology, pigmentation, size and shape; Gram staining to identify characteristic features of *P. aeruginosa*. Biochemical tests involved the use of oxidase and catalase tests, differential media like MacConkey agar (HiMedia Laboratories, Mumbai) and Triple Sugar iron (TSI) slants (HiMedia Laboratories, Mumbai). Pseudomonas Cetrimide Agar (Oxoid, Basingstoke) specialized media was subsequently used to confirm the identity of isolates.

In addition, three different bacterial test isolates (two *S. aureus* isolates, and one *P. aeruginosa*) were employed for screening purposes. They were selected based on previous studies that investigated the antimicrobial effect of *P. aeruginosa* pyocins (Mohamed *et al*., 2021; Alqahtani *et al*., 2022). These isolates were obtained from Microbiology laboratory, at Mustansiriyah University, College of Science, Department of Biology.

A total of 57 yeast isolates were specifically selected from different clinical samples (Oral, Vaginal, sputum, and urine) from Al-Baladi Teaching Hospital and Medical City hospitals. They included different species of *Candida* and *Cryptococcus*. All yeast isolates were identified using microscopic and macroscopic techniques and the specialized media Candida Chromogenic Differential Agar (HiMedia Laboratories, Mumbai) was used for confirmation.

Moreover, all isolates, both bacterial and yeast were further identified using the VITEK 2 Compact System using the manufacturer's procedures (bioMérieux inc, Durhan, NC 27112, USA).

Preparation of Isolates

After identification, all isolates were prepared by culturing them on brain heart infusion (BHI) broth (Neogen, USA) at 37 °C for 24 hours to ensure they were in optimal physiological conditions for the subsequent experimental procedures. BHI broth provides a nutrient-rich environment that promotes a healthy growth and ensures reliable results in the following experimental procedures.

Selection of Yeast Isolates

Of the 57 yeast isolates, 12 of them were selected based on their high resistance to commonly used antifungal drugs and their significant biofilm and phospholipase production. The following techniques were followed to select the 12 yeast isolates:

Antifungal Susceptibility Test of Yeast Isolates

The antifungal susceptibility tests were performed using commercially available discs (HiMedia, Mumbai) for 5 antifungal agents: Amphotericin B (100 µg/Disc), Clotrimazole (10 µg/Disc), Fluconazole (25 µg/Disc), Ketoconazole (10 µg/Disc), and Nystatin (100 µg/Disc). The disc diffusion method was employed, and the results were recorded based on the zone diameters provided in the HiMedia product data sheet. Interpretation of results was conducted in accordance with available breakpoints from HiMedia, EUCAST, and CLSI where applicable. However, it is important to note that CLSI and EUCAST guidelines primarily provide breakpoints for Amphotericin B and Fluconazole, while breakpoints for Clotrimazole, Ketoconazole, and Nystatin were not available for disk diffusion testing. Consequently, the interpretation of results for these agents relied on HiMedia product data.

As a result, the absolute interpretation of susceptibility was less critical in this case than identifying isolates with the strongest resistance profiles. The primary goal of this method was to identify and select the yeast isolates exhibiting the highest resistance to these antifungal agents. These isolates, exhibiting the strongest resistance profiles, were then selected for further testing with *P. aeruginosa* pyocins.

All yeast isolates were diluted in normal saline to a 0.5 McFarland standard (approximately 1×10^6 cell ml^{-1}) and inoculated on Mueller-Hinton Agar supplemented with 2% glucose, in accordance with the Clinical and Laboratory Standards Institute (CLSI), as it enhances fungal growth and ensures consistency. Then the 5 antifungal discs were added to the cultured Petri dishes using sterile forceps and were gently pressed. Then the Petri dishes were cultured for 24 - 48 hours at 35 °C. Finally, the results were measured and recorded. The identification of the resistance of these isolates to the commercially used antifungal drugs also helps to explore the potential inhibitory effects of pyocins compared to the conventionally used antifungal drugs.

Biofilm Production

Biofilm production was assessed using the described technique (Ball *et al*., 2022) with slight alteration. Each yeast isolate was inoculated into 2 mL of BHI broth with 0.25% Glucose then incubated at 37°C for 24 hours. Then all cultures were adjusted to 0.5 McFarland standard and inoculated in a freshly made BHI Broth. After that sterile 96-well microtiter plates were inoculated with 200 µL of the adjusted culture and incubated at 37°C for 24 hours. Next wells were rinsed with PBS 3 times then the microplates were flipped to dry. Then 200 µL of 0.1% Crystal Violet Stain (BDH, England) was added to each well and incubated for 15 minutes. After incubation the wells were rinsed again 3 times with PBS. Then 200 µL of ethanol:acetone of a ratio of 80:20 were added to each well and read at 450 nm using an ELISA Reader. The optical density was recorded for each well.

Each isolate was inoculated on 3 wells and the mean of each of them was calculated. Three wells of sterile BHIB without any microorganisms were also used as a negative control. The threshold for biofilm detection was determined by calculation the mean OD of the negative control and adding two times the standard deviation. This ensures that any OD value above the cutoff accounts for background

noise. Despite the calculated cutoff this study followed commonly used thresholds for classification: Isolates with (OD > 0.320) were considered strong biofilm producers, isolates with (OD value between 0.120 - 0.320) were considered moderate biofilm producers, and isolates with (OD value < 0.120) were considered non/weak biofilm producers. The classifications for biofilm production were selected based on a previously established method (Al-Dabbagh Ali *et al*., 2023). The identification of these strong biofilm-producing isolates lays the groundwork for exploring the potential inhibitory effects of pyocins on biofilm formation.

Phospholipase production

Phospholipase activity was assessed using Egg Yolk Agar (EYA) following the method described by (Fule *et al*., 2015). The EYA was inoculated with 10 µL of the McFarland (1×10^6 CFU mL^{-1}) adjusted yeast isolates and incubated at 37°C for 72 hours. Then the results were determined by measuring the diameter of the colonies and the precipitation zones around them and calculating the PZ (Phospholipase Activity) Value using the following formula, Eq.(1):

$$PZ\ value = \frac{Colony\ Diameter\ (mm)}{Colony\ Diameter\ (mm) + Precipitation\ Diameter\ (mm)} \quad \text{Eq. (1)}$$

Phospholipase activity was categorised into 5 categories (Al-Dabbagh Ali *et al*., 2023) based on the PZ values as follows: 1.00 (Negative), 0.90-0.99 (Weak), 0.80-0.89 (Poor), 0.70-0.79 (Moderate), and <0.70 (Intense). The identification of these strong phospholipase-producing isolates lays the groundwork for exploring the potential effects of pyocins on phospholipase formation.

Screening for Strongest Pyocinogenic *P. aeruginosa* Isolates

The goal of this stage was to screen for the capability of *P. aeruginosa* isolates to produce bacteriocins, and select the strongest one. All 40 isolates of *P. aeruginosa* were screened for their bacteriocins production using a slightly modified version of the original method described by (Morse *et al*., 1976). First the isolates were cultured overnight on nutrient broth. The following day, the isolates were diluted at a 1:50 ratio in fresh nutrient broth medium and incubated for 3 hours in shaker incubator at 80 rpm. Then 2 µg ml^{-1} Mitomycin C was introduced on nutrient broth to induce bacteriocin production. Then it was incubated in shaker incubator at 80 rpm. After about 3 hours the culture was centrifuged at 6700 × g for 20 minutes and the cell free supernatant (CFS) was acquired.

Then CFS was tested against three bacterial and one yeast isolates for screening purposes (two *S. aureus* isolates, one *P. aeruginosa*, and one *C. albicans*) due to lack or no access to standard strains. These three bacterial isolates were selected according to previous studies of antimicrobial activity of *P. aeruginosa* pyocins against these species therefore they were chosen as positive control (Mohamed *et al*., 2021; Alqahtani *et al*., 2022), on the other hand *C. albicans* was used to determine the effectiveness of pyocin against yeast isolates. Agar well diffusion method was used, wells were made and filled with 200 µL of the crude CFS to ensure adequate diffusion and a measurable inhibition zone on Mueller Hinton Agar after it was inoculated with 0.5 McFarland compared yeast suspension. The petri dishes were then incubated at 35 °C for 24 hours (35 °C ± 2 °C as per EUCAST and CLSI guidelines). The inhibition zones were recorded in mm. The isolate of *P. aeruginosa* with the strongest inhibition rate against all test isolates was selected and determined as the strongest bacteriocin producer isolate.

Production of the Partially Purified Bacteriocin

After the screening was done and the strongest bacteriocin producer isolate was selected, this method aims to partially purify the R and S type pyocins. The same method described by (Morse *et al*., 1976) was used for bacteriocin production; however, in this step, the bacteriocin containing CFS was subjected to partial purification. Two successive rounds of ammonium sulphate precipitation were conducted. The first round aimed for 60% saturation, at which point the precipitate was discarded, as R and S pyocins do not precipitated at this level; the second round increased the saturation from 60% to 90%, resulting in the precipitation of R and S pyocins, which are retained at this range. The pyocin precipitate was then collected and dissolved in 25 mL phosphate buffer (PH 7.4). Then 20 ml of the suspension was dialysed overnight against

phosphate buffer using dialysis membranes with a molecular weight cutoff (MWCO) ranging from 8-14 kDa which ensures that S and R type bacteriocins are retained.

Then Bradford technique (Kielkopf *et al*., 2020) was utilised to determine the bacteriocins suspensions protein concentrations. Where a standard curve was plotted using different known concentrations of bovine serum albumin (BSA). BSA was diluted with phosphate buffer, each BSA dilution was then added into cuvettes, Coomassie brilliant blue G-250 (CBB) dye (Cepham Life Sciences, USA) was then added, then the mixture was incubated for 5 minutes before measuring the optical density at 595 nm using a spectrophotometer, then a standard curve was formed.

After that the same procedure was used to measure the bacteriocin concentration, where CBB dye was added to the pyocin suspensions, incubated for 5 minutes, then measuring the optical density at 595 nm using the spectrophotometer where the OD was used to determine the protein concentration of the bacteriocin suspensions by comparing it with the BSA curve.

Determination of Partially Purified Bacteriocins MIC and sub-MIC

The antifungal activity of the partially purified bacteriocins against 10 *Candida* and 2 *Cryptococcus* isolates was measured using the resazurin microtiter plate assay method in a 96 wells microplate (Sarker *et al*., 2007). Each column contained a different isolate. Rows 1-7 contained 50 µL sabouraud dextrose broth (SDB), 100 µL of the serially two fold diluted partially purified bacteriocin, and 50 µL of 0.5 McFarland standard diluted yeast suspension in SDB at a ratio of 1:100. Row 8 served as the control, containing 150 µL of SDB and 50 µL of a 0.5 McFarland standard suspension diluted in SDB at a 1:100 ratios. The Microtiter plate was then incubated at 37°C. After incubation 30 µL of 0.02% resazurin dye (Solarbio, China) was added to each well. The wells would turn red if there is any microbial activity in said wells, otherwise the wells remain blue. The lowest concentration of partially purified bacteriocin added to wells in each column with a blue color was determined as the minimum inhibitory concentration. The sub-MIC values were determined as the concentrations of pyocins in the wells immediately following the MIC wells in the dilution series.

Anti-biofilm and Anti-phospholipase Activity of Pyocin

The effect of pyocin on biofilm formation was studied using a 96 wells microtiter plate, all experiments were done in triplets and 3 times for 24, 48 and 72 hours at 37 °C, for the control and pyocin treatment. Yeast isolates were first incubated overnight on SDB. A turbidity similar to that of McFarland solution (10^6) was then prepared from the yeast culture in normal saline. A volume of 100 µL of the sub-MIC (final concentration) for each isolate was added into the wells. Followed by 80 µL of freshly made SDB and 20 µL of the prepared yeast suspension was then added. The control contained 180 µL SDB and 20 µL of the prepared yeast suspension. After incubation, the medium was discarded from the microtitper plate and was washed two times using PBS and left to dry for 15 minutes, then 200 µL of crystal violet was added to the wells and incubated for 20 minutes. The plate was washed 3 times with PBS and left to dry at room temperature. Finally 200 µL of a mixture of ethanol:acetone (80:20 v/v) was added to the wells and incubated for 10 minutes before reading the optical density at 450 nm using an ELISA Reader (Adeyemo *et al*., 2022). The results were obtained 3 times for 3 consecutive days and the effect of pyocin on biofilm formation was calculated using the following formula, Eq. (2):

$$\%\ \text{Inhibition of Biofilm formation} = \frac{\text{OD of Control} - \text{OD of treatment}}{\text{OD of Control}} \times 100\% \quad \text{Eq. (2)}$$

As for the effect of pyocin on phospholipase production, all experiments were done in triplets for both treatment and control. Yeast isolates were first incubated overnight on SDB. A turbidity similar to that of McFarland solution (10^6) was then prepared from the yeast culture in normal saline. A volume of 20 µL of the prepared yeast suspension was then added to 80 µL of freshly prepared SDB and mixed with 100 µL of sub- MIC (final concentration) pyocin and was incubated at 37 °C for 24 hours. Control contained 180 µL of SDB and 20 µL of the prepared yeast suspension. Then a needle was used to inoculate the yeasts onto the surface of EYA, and incubated at 37 °C for 24 hours. Finally, the colony size and precipitation zone

for control and treatment were measured and the PZ value was calculated. The phospholipase activity was divided into 5 categories according to the PZ values as follows: 1.00 PZ value is negative phospholipase activity, 0.90-0.99 PZ value is weak phospholipase activity, 0.80-0.89 PZ value is poor phospholipase activity, 0.70-0.79 PZ value moderate phospholipase activity, and <0.70 PZ value is intense phospholipase activity (Al-Dabbagh *et al*., 2023).

Effect of the Pyocin on the Viability of Yeast Cells

The effect of pyocin on the yeast isolates viability was tested using (Bahuguna *et al*., 2017) with slight alterations. All experiments were done in triplets. Yeast isolates were first incubated overnight on SDB. A turbidity similar to that of McFarland solution (10^6 CFU mL^{-1}) was then prepared from the yeast culture in normal saline. A volume of 200 µL of the prepared yeast suspension was then added to 800 µL of freshly made SDB in plain tubes, after that 1 mL of sub-MIC (final concentration of the pyocin) was added to the plain tube. Control contained 1.8 mL SDB and 200 µL of the prepared yeast suspension. Isolates were then incubated at 37 °C for 24 hours to test cell viability at various times. Ninety-six-well microtiter plates were used, wells were filled with 50 µL of the treatment and control separately, and 50 µL MTT (3-(4,5-dimethylthiazol-2-yl)-2,5-diphenyltetrazolium bromide) dye (Solarbio, China) was added to reach a 0.5 mg mL^{-1} final concentration, then they were incubated for 3 hours. After that the solution was discarded and wells were filled with 150 µL DMSO solvent and was measured at 590 nm using an ELISA reader. Finally, viability inhibition percentages were then calculated using the following formula, Eq.(3):

$$\text{Viability inhibition } \% = \frac{\text{OD Control} - \text{OD Treatment}}{\text{OD Control}} \times 100\% \quad \text{Eq. (3)}$$

RESULTS AND DISCUSSION

Identification of Isolates

A total of 40 *P. aeruginosa* isolates were successfully identified, they appeared with flat and colorless colonies on MacConkey agar and fluorescent green to yellow green on Pseudomonas Cetrimide Agar. They were identified using VITEK 2 compact system (bioMérieux inc, Durhan, NC 27112, USA).

Candida isolates exhibited different colors on *Candida* Chromogenic Differential Agar indicating each different species. *C. albicans* appeared light green, *C. glabrata* appeared cream to white, *C. dubliniensis* appeared pale green, *C. krusei* appeared purple, *C. tropicalis* appeared blue to purple, *C. kefyr* appeared cream to white, *C. utilis* appeared pink, and *C. parapsilosis* appeared white to cream. *Cryptococcus* isolates were also confirmed microscopically through their distinctive capsule formation. All isolates were identified by VITEK 2 compact system (bioMérieux inc, Durhan, NC 27112, USA).

Selection of the Yeast Isolates

Antifungal Susceptibility Test

The antifungal susceptibility test revealed that most the 57 had high antifungal resistance, though the 12 with the highest resistance were selected for further studies. The yeast isolates exhibited a varying susceptibility to Clotrimazole. For instance, *C. kefyr* (isolate 5) demonstrated high resistance to it, while the other isolates exhibited either full or intermediate susceptibility to it. All 12 isolates were resistant to the other antifungal agents tested. Figure 1 shows the results of the antifungal susceptibility test for the selected yeast isolates.

Biofilm and Phospholipase Production

The negative control had a mean OD of 0.042 with a standard deviation of 0.001, resulting in a cutoff value of 0.0446. All isolates exhibited OD values above the cutoff which confirms biofilm production. Since Isolates with (OD > 0.320) were considered strong biofilm producers, isolates with (OD value between 0.120 - 0.320) were considered moderate biofilm producers, and isolates with (OD value < 0.120) were considered non/weak biofilm producers. Table 1 summarises the biofilm production level of the 12 selected isolates

The screening measurements of ODs at 450 nm revealed a diverse spectrum of biofilm production among the tested isolates. Notably, 12 isolates emerged as the strongest biofilm

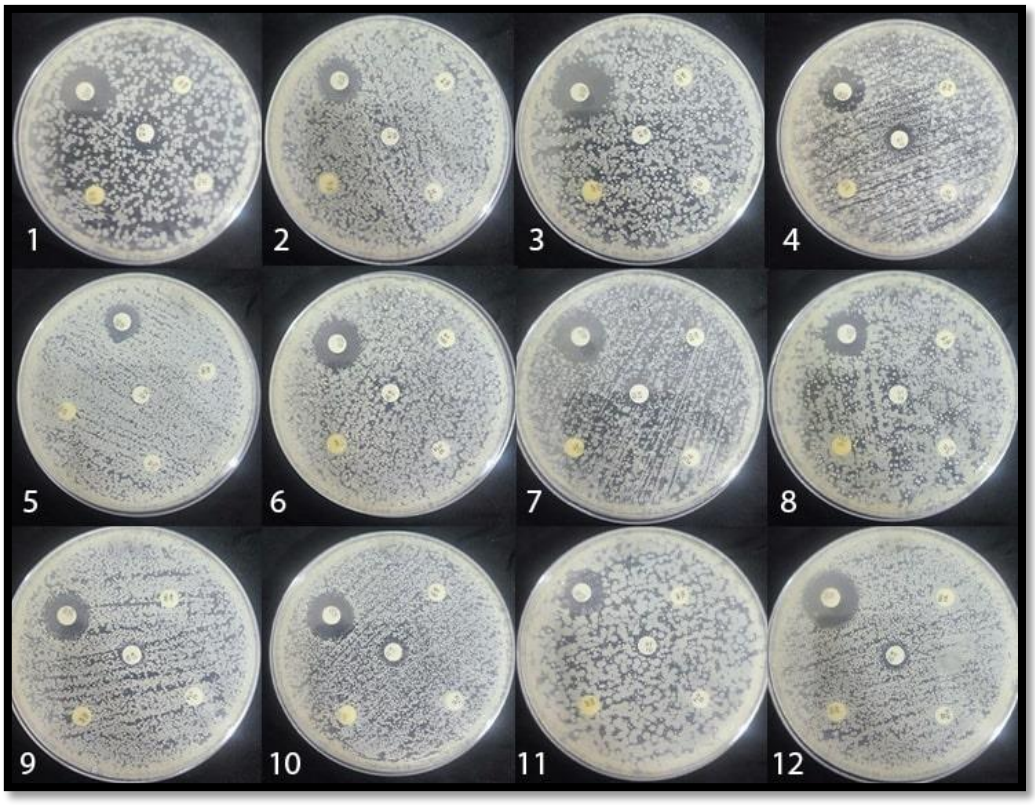

Figure 1. Antifungal susceptibility test against the 12 selected yeast isolates. As shown in the figure all 12 selected isolates showed high resistance to the 4 used antifungal drugs, except for Clotrimazole. The numbers represent the isolates as follows: 1) *C. krusei*, 2) *C. tropicalis*, 3) *C. dubliniensis*, 4) *C. guilliermondii*, 5) *C. kefyr*, 6) *C. parapsilosis*, 7) *C. albicans*, 8) *C. albicans*, 9) *C. glabrata*, 10) *C. utilis*, 11) *C. neoformans*, 12) *C. laurentii*

Table 1. Biofilm producing capability indicated by optical density (OD) of the selected yeast isolates over the course of 24 hours at 37 °C

	Isolate Species	OD mean	Production Level
n.		Cutoff value: 0.0446	
1	*C. krusei*	0.277	Moderate
2	*C. tropicalis*	0.583	Strong
3	*C. dubliniensis*	0.249	Moderate
4	*C. guilliermondii*	0.302	Moderate
5	*C. kefyr*	0.131	Moderate
6	*C. parapsilosis*	0.148	Moderate
7	*C. albicans*	0.400	Strong
8	*C. albicans*	0.342	Strong
9	*C. glabrata*	0.270	Moderate
10	*C. utilis*	0.326	Strong
11	*C. neoformans*	0.178	Moderate
12	*C. laurentii*	0.810	Strong

producers, representing various species within the *Candida* and *Cryptococcus* genera.

Among the identified isolates, *C. tropicalis*, *C. albicans*, *C. utilis*, and *C. laurentii* exhibited particularly strong biofilm production, as evidenced by their elevated optical density readings. While isolates such as *C. krusei*, *C. dubliniensis*, and *C. parapsilosis* demonstrated moderate biofilm production, indicating a lower propensity for biofilm formation. While their biofilm-forming abilities may be less pronounced, these isolates still represent valuable subjects for further investigation, due to their high antifungal resistance and intense phospholipase activity.

Table 2. Phospholipase activity of the yeast isolates according to the measured PZ values

n	Isolate Species	PZ mean	Phospholipase activity
1	*Candida krusei*	0.375	Intense
2	*C. tropicalis*	0.250	Intense
3	*C. dubliniensis*	0.230	Intense
4	*C. guilliermondii*	0.444	Intense
5	*C. kefyr*	0.500	Intense
6	*C. parapsilosis*	0.192	Intense
7	*C. albicans*	0.538	Intense
8	*C. albicans*	0.375	Intense
9	*C. glabrata*	0.187	Intense
10	*C. utilis*	0.238	Intense
11	*C. neoformans*	0.227	Intense
12	*C. laurentii*	0.214	Intense

Utilising PZ values as a measure for phospholipase activity, 12 isolates with high degrees of enzymatic activity, spanning multiple species within the *Candida* and *Cryptococcus* genera were selected. All the 12 isolates selected exhibited intense phospholipase activity as shown in Table 2.

Among the identified isolates, *C. albicans*, *C. glabrata*, and *C. kefyr* demonstrated particularly high PZ values, which is indicative of their high phospholipase production. Isolates such as *C. parapsilosis*, *C. dubliniensis*, and *C. neoformans* exhibited slightly lower PZ values, though still within the range of intense phospholipase activity.

Screening for Strongest Pyocinogenic *P. aeruginosa*

The agar well diffusion method results revealed that (10) 25% out of the 40 *P. aeruginosa* isolates were pyocinogenic and had antimicrobial activity against the test isolates. Among these, isolates 2 and 5 of *P. aeruginosa* demonstrated the strongest antimicrobial activity. However, isolate 5 was preferred due to its superior antimicrobial activity against the test yeast isolate *C. albicans*, which aligned with the study's primary objective. Table 3 presents the antimicrobial activity against the four test isolates.

Production of the Partially Purified Pyocin

Determination of bacteriocin suspension concentration is important to find its MIC. The crude extract which was obtained after centrifugation (6700 × g) of the Mitomycin C induced *P. aeruginosa* culture had a concentration of 1.75 mg mL^{-1}. After the precipitate was dissolved in 25 mL phosphate buffer the concentration was 2.96 mg mL^{-1} and 2.59 mg mL^{-1} after being dialysed. Table 4 presents the Purification profile of Bacteriocin from *P. aeruginosa*. These concentrations were measured using Bradford technique (Kielkopf *et al*., 2020).

Determination of Partially Purified Bacteriocins MIC and sub-MIC by Microtiter Plate Assay Method

The MIC values of the bacteriocin are presented in Table 5 against all tested the yeast isolates. The degree of susceptibility is varied among the yeast isolates, ranging from 40.57 µg mL^{-1} to 81.15 µg mL^{-1}.

The results shed light on the potential of *P. aeruginosa* bacteriocin as an alternative for antifungal drugs against yeasts, especially against clinical antifungal resistant ones. Varying levels of yeast susceptibility and MIC of the partially purified bacteriocin have been revealed indicating its effectiveness against the yeast isolates. Potent antifungal activity has been observed against the yeast isolates with MIC ranging from 40.57 µg mL^{-1} to 81.15 µg mL^{-1} across different isolates. With 50% of the isolates of the *Candida* isolates showed susceptibility to 40.57 µg ml^{-1} MIC and the other 50% of *Candida* isolates showed susceptibility 81.15 µg mL^{-1} MIC. Both the *Cryptococcus* isolates on the other hand showed 40.57 µg mL^{-1} MIC indicating the possibility of having higher susceptibility to the partially purified bacteriocin. Notably the two *C. albicans* isolates had different MICs which could be explained if

the two isolates are of different strains and utilizing a type of resistance against the bacteriocins. The ability of the bacteriocin to inhibit the growth of the drug resistance yeast holds great value especially due to its ability to surpass the antifungal activity of the drugs used in this study. It is important to point out that further studies should be made to test its effectiveness *in vivo*, its possible clinical applications and its safety.

Table 3. Antimicrobial activity of *P. aeruginosa* isolates 2 and 5 which exhibited the highest antimicrobial potential against the selected test isolates (two *S. aureus* isolates, one *P. aeruginosa*, and one *C. albicans*). All zones were measured and noted in mm units

	Test isolate species			
P. aeruginosa Isolate number	*S. aureus 1*	*S. aureus 2*	*P. aeruginosa*	*C. albicans*
2	19	13	19	18
5	13	19	0	25

Table 4. Purification profile of Bacteriocin from *P. aeruginosa*

Purification Step	Volume (mL)	Activity (AU/mL)	Protein concentration (mg/mL)	Specific Activity (AU/mg)	Total Activity (AU)	Purification (folds)	Yield (%)
Crude extract	200	125	1.75	71.4	25000	1.00	100%
Ammonium sulphate precipitation	25	130	2.96	43.9	3250	0.61	13%
Dialysis	20	135	2.59	52.1	2700	0.72	10.8%

Table 5. MIC (μg ml^{-1}) of the *P. aeruginosa* bacteriocin against the 12 pathogenic yeast isolates

n.	Species	MIC (μg ml^{-1})
1	*C. krusei*	81.15
2	*C. tropicalis*	81.15
3	*C. dubliniensis*	40.57
4	*C. guilliermondii*	81.15
5	*C. kefyr*	81.15
6	*C. parapsilosis*	40.57
7	*C. albicans*	81.15
8	*C. albicans*	40.57
9	*C. glabrata*	40.57
10	*C. utilis*	40.57
11	*C. neoformans*	40.57
12	*C. laurentii*	40.57

Anti-biofilm and Anti-phospholipase Activity of Pyocin

Results for the biofilm inhibition percentage were calculated. The means, standard error and inhibition percentage (24, 48 and 72 hours) of the control and pyocin treated ODs were calculated and presented in Table 6, P values were calculated for the 24, 48 and 72 hours. They were all significantly lower than 0.05. Treatment with the pyocin showed high inhibition of biofilm for all isolates, reaching a maximum of 82% at 72 hours for isolate number 1 which is *C. krusei*, and a minimum of 14% at 24 hours also for the same *C. krusei* isolate. At sub-MIC concentrations, pyocin does not kill the yeast cells but induces significant stress that impairs their ability to form biofilms. The stress response triggered by pyocin likely disrupts the early stages of biofilm formation, including cell adhesion and the production of the extracellular matrix. This leads to a reduction in biofilm formation without completely inhibiting cell growth. The progressive inhibition observed over time suggests that pyocin acts as a stress factor that prevents the initiation of biofilm

formation. The experiment conducted aimed to assess the impact of a treatment compared to a control group on optical density at 450 nm and inhibition percentage over three time intervals: 24, 48, and 72 hours. Each row represents a distinct condition, presented as Control and Treatment, while each column corresponds to a specific time point.

Analyzing the data, it's evident that the control group exhibited increasing optical densities overtime and treatment group exhibited consistent optical densities indicating high inhibition rates over time. For instance, in the first row, the control group demonstrated optical densities of 0.282 ± 0.011, 0.511 ± 0.027, and Treatment group demonstrated optical densities of 1.343 ± 0.292 at 24, 48, and 72 hours, respectively. The inhibition percentages for these time points were 14.87%, 57.86%, and 82.22%, indicating a progressive increase in inhibition over time.

Comparatively, the treatment group displayed lower optical densities at all time points (0.240 ± 0.005, 0.215 ± 0.033, and 0.238 ± 0.010, respectively), suggesting the potential inhibitory effect induced by the treatment. These differences between the control and treatment groups were statistically significant, as indicated by the p values ($p<0.05$) for all time points.

Furthermore, considering the trends across all rows, it's notable that the Treatment consistently led to decreased optical densities and inhibition percentages compared to the control group, emphasizing its inhibitory effect. The results of the phospholipase experiment suggest a nuanced response among different isolates to the treatment, with an overall non-significant difference observed between the control and treatment groups ($p = 0.899$). This indicates that the treatment did not have a uniform effect across all isolates collectively. However, individual isolate responses highlight a diverse range of reactions to the treatment, suggesting an isolate-specific effect. P values for each isolate have been calculated and presented in Table **7** to show the significance of the effect.

For instance, while isolate 2 (*C. tropicalis*) exhibited an increase in phospholipase activity under treatment conditions compared to the control group, isolates 3, 6, 7, 8, 10, 11 and 12 displayed a notable decrease in phospholipase activity. In contrast, Isolates 1, 4, 5 and 9 showed no significant change. Isolate 7 and 8 which are both *C. albicans* in particular, demonstrated complete inhibition of phospholipase activity under treatment conditions. These observations indicate that the treatment possesses an isolate-specific effect, such as genetic makeup or stress response mechanisms which influences phospholipase production. Isolates with minimal changes in phospholipase activity between control and treatment groups may indicate a lack of response to the treatment or negligible impact on phospholipase production.

Overall, the varied responses among isolates underscore the importance of considering isolate-specific effects when assessing the efficacy of treatments targeting phospholipase activity. Further investigation into the underlying mechanisms driving these differential responses is important to explain the treatment's isolate-specific effects comprehensively.

Effect of the Pyocin on the Viability of Yeast Cells

The MTT assay was utilized to assess cell viability as an indicator with optical density (OD) measured at 630 nm. The extremely low P value obtained (<0.05) indicates a statistically significant difference between the control and treatment groups, suggesting a notable impact of the treatment on cell viability.

Examining the individual results presented in Table 8, it's evident that the treatment exerted a substantial effect on cell viability compared to the control condition. Across all isolates, the treatment led to a decrease in optical density which is indicative of reduced cell viability. For example, in isolate 1 (*C. krusei*), the control group exhibited an OD of 0.624 ± 0.144, while the treatment group showed a significantly lower OD of 0.303 ± 0.020, indicating a substantial decrease in cell viability corresponding to an inhibition percentage of 51.44%.

This trend is consistent across all isolates, with the treatment group consistently demonstrating lower OD values compared to the control group. Notably, isolate 10 (*C. utilis*) displayed a particularly high inhibition percentage (83.98%), indicating a potent effect of the treatment on reducing cell viability.

Table 6. The effect of pyocin on the biofilm activity of the yeast isolates recorded 3 times over the course of 3 consecutive days (24, 48 and 72 hours)

Isolate			Optical Density at 450 nm			Inhibition %		
			24 hours ± SE	48 hours ± SE	72 hours ± SE	24 H	48 H	72 H
1	*C. krusei*	Control	0.282 ± 0.011	0.511 ± 0.027	1.343 ± 0.292	14.87	57.86	82.22
		Treatment	0.240 ± 0.005	0.215 ± 0.033	0.238 ± 0.010			
2	*C. tropicalis*	Control	0.262 ± 0.005	0.452 ± 0.024	1.085 ± 0.090	15.12	68.95	81.39
		Treatment	0.222 ± 0.006	0.140 ± 0.019	0.202 ± 0.031			
3	*C. dubliniensis*	Control	0.345 ± 0.081	0.492 ± 0.019	0.780 ± 0.172	29.12	57.24	70.31
		Treatment	0.245 ± 0.012	0.210 ± 0.022	0.231 ± 0.018			
4	*C. guilliermondii*	Control	0.339 ± 0.034	0.395 ± 0.019	0.912 ± 0.166	52.40	63.32	61.23
		Treatment	0.161 ± 0.002	0.145 ± 0.008	0.353 ± 0.026			
5	*C. kefyr*	Control	0.236 ± 0.022	0.412 ± 0.034	0.740 ± 0.116	39.49	51.09	67.47
		Treatment	0.143 ± 0.002	0.201 ± 0.034	0.240 ± 0.003			
6	*C. parapsilosis*	Control	0.253 ± 0.002	0.494 ± 0.035	0.728 ± 0.056	16.84	43.93	63.56
		Treatment	0.210 ± 0.009	0.277 ± 0.003	0.265 ± 0.047			
7	*C. albicans*	Control	0.317 ± 0.077	0.470 ± 0.011	0.719 ± 0.085	53.04	60.19	68.33
		Treatment	0.149 ± 0.011	0.187 ± 0.022	0.227 ± 0.042			
8	*C. albicans*	Control	0.349 ± 0.056	0.485 ± 0.033	0.894 ± 0.131	49.85	69.82	79.72
		Treatment	0.175 ± 0.013	0.146 ± 0.012	0.181 ± 0.017			
9	*C. glabrata*	Control	0.228 ± 0.032	0.487 ± 0.028	0.748 ± 0.070	25.36	61.01	69.16
		Treatment	0.170 ± 0.023	0.190 ± 0.032	0.230 ± 0.007			
10	*C. utilis*	Control	0.437 ± 0.043	0.447 ± 0.030	0.730 ± 0.024	60.33	56.03	57.75
		Treatment	0.173 ± 0.014	0.196 ± 0.028	0.308 ± 0.027			
11	*Cryptococcus neoformans*	Control	0.343 ± 0.050	0.435 ± 0.060	0.654 ± 0.107	42.09	58.03	62.02
		Treatment	0.199 ± 0.019	0.182 ± 0.021	0.248 ± 0.036			
12	*C. laurentii*	Control	0.491 ± 0.007	0.435 ± 0.026	0.968 ± 0.133	55.32	53.98	54.87
		Treatment	0.219 ± 0.019	0.200 ± 0.013	0.437 ± 0.025			
		p Value	p<0.05	p<0.05	p<0.05			

Table 7. The effect of pyocin on the phospholipase activity of the yeast isolates. SE stands for Standard Error

Isolate			Pz value ± SE	P value
1	*C. krusei*	Control	0.430 ± 0.009	0.188
		Treatment	0.480 ± 0.035	
2	*C. tropicalis*	Control	0.571 ± 0.051	0.012
		Treatment	0.385 ± 0.036	
3	*C. dubliniensis*	Control	0.282 ± 0.085	0.017
		Treatment	0.475 ± 0.070	
4	*C. guilliermondii*	Control	0.392 ± 0.032	0.578
		Treatment	0.437 ± 0.036	
5	*C. kefyr*	Control	0.386 ± 0.017	0.651
		Treatment	0.433 ± 0.097	
6	*C. parapsilosis*	Control	0.320 ± 0.064	0.141
		Treatment	0.434 ± 0.019	
7	*C. albicans*	Control	0.504 ± 0.119	0.051
		Treatment	1.000 ± 0.000	
8	*C. albicans*	Control	0.431 ± 0.056	0.016
		Treatment	1.000 ± 0.000	
9	*C. glabrata*	Control	0.397 ± 0.028	0.696
		Treatment	0.408 ± 0.018	
10	*C. utilis*	Control	0.238 ± 2E-17	0.021
		Treatment	0.392 ± 0.022	
11	*Cryptococcus neoformans*	Control	0.310 ± 0.082	0.0002
		Treatment	0.641 ± 0.088	
12	*C. laurentii*	Control	0.214 ± 0.023	0.0007
		Treatment	0.507 ± 0.007	

Overall, these findings underscore the efficacy of the treatment in reducing cell viability, as evidenced by the significant differences observed between the control and treatment groups across all isolates. This reduction is consistent across all isolates, with varying levels of inhibition. Notably, in some cases, the decrease in viability is linked to the stress induced by pyocin at sub-MIC concentrations, which likely interferes with metabolic processes and cell wall integrity, ultimately affecting the cell's ability to proliferate and perform other metabolic processes.

Table 8: Effect of pyocins on the optical density (O. D) the viability of the yeast isolates over 24 hours. SE stands for Standard Error

Isolate			O. D ± SE	Inhibition %
1	*C. krusei*	Control	0.624 ± 0.144	51.44
		Treatment	0.303 ± 0.020	
2	*C. tropicalis*	Control	0.863 ± 0.208	69.78
		Treatment	0.261 ± 0.020	
3	*C. dubliniensis*	Control	0.643 ± 0.034	57.40
		Treatment	0.274 ± 0.010	
4	*C. guilliermondii*	Control	0.937 ± 0.012	70.43
		Treatment	0.277 ± 0.009	
5	*C. kefyr*	Control	0.832 ± 0.130	68.49
		Treatment	0.262 ± 0.019	
6	*C. parapsilosis*	Control	0.708 ± 0.022	65.88
		Treatment	0.241 ± 0.018	
7	*C. albicans*	Control	0.848 ± 0.054	74.76
		Treatment	0.214 ± 0.016	
8	*C. albicans*	Control	0.624 ± 0.003	76.61
		Treatment	0.146 ± 0.015	
9	*C. glabrata*	Control	0.802 ± 0.025	80.68
		Treatment	0.155 ± 0.020	
10	*C. utilis*	Control	0.899 ± 0.081	83.98
		Treatment	0.144 ± 0.007	
11	*Cryptococcus neoformans*	Control	1.155 ± 0.072	77.06
		Treatment	0.265 ± 0.024	
12	*C. laurentii*	Control	0.991 ± 0.075	79.05
		Treatment	0.207 ± 0.020	
		p Value	$p<0.05$	

CONCLUSION

This study highlights the potential of *P. aeruginosa* bacteriocins as an alternative for treating clinical yeast infections. The high antifungal activity of the bacteriocin and inhibiting the growth of yeasts especially those that are resistant to conventional antifungal drugs shows its value as being possibly an alternative therapeutic option where other antifungals are ineffective with MICs ranging between 40.57 - 81.15 µg ml^{-1} against *Candida* and *Cryptococcus* isolates. This observed efficacy of the pyocins against a diverse range of *Candida* and *Cryptococcus* species underscores their potential as a valuable therapeutic option. This may represent a significant step forward in the field of antimicrobial therapy against yeasts especially in the light of the rising challenge of antifungal resistance.

Additionally, the pyocins were highly effective in inhibiting biofilm formation and treatment with the pyocin showed high inhibition of biofilm for all isolates, reaching a maximum of 82% at 72 hours against *C. krusei*.

Finally, the effect of pyocin on phospholipase production showed varying results which can indicate specie-specific response indicated by the two *C. albicans* isolates having a complete cessation of phospholipase production. It also indicates a stress induced virulence which led some of the isolates to display an increase in phospholipase production. A significant reduction in the viability of yeast across all isolates was observed, confirming the efficacy of

pyocins as a valuable treatment option. These findings highlight the promise of pyocins as a broad spectrum antimicrobial agent and their potential role in addressing the rising issue of antifungal resistance.

ACKNOWLEDGMENTS

The authors would like to thank Mustansiriyah University in Iraq (www.uomustansiriyah.edu.iq) for their support in the current work.

REFERENCES

Abid, S.A., Aziz, S.N., Saeed, N.A.-H.A.H., Mizil, S.N., Al-Kadmy, I.M.S., Hussein, N.H., Al-Saryi, N., Ibrahim, S.A. & Hussein, J.D. (2023). Investigation of virulence factors in microbial organisms that associated with public health risk isolates from different environmental regions. *Al-Mustansiriyah Journal of Science*, 33: 5. DOI: 10.23851/mjs.v33i5.1303

Adeyemo, R. O., Famuyide, I. M., Dzoyem, J. P., & Lyndy Joy, M. (2022). Anti-biofilm, antibacterial, and anti-quorum sensing activities of selected South African plants traditionally used to treat diarrhoea. *Evidence-Based Complementary and Alternative Medicine: eCAM*, 2022, 1307801. DOI:10.1155/2022/1307801

Al-Baqer, T. M., Al-Gharrawi, S. A. R., & Saeed, N. A. A. (2021). Causative microorganisms and antibiotics susceptibilities in children with urinary tract infection. *Al-Mustansiriyah Journal of Science*, 32(1): 5–9. DOI:10.23851/mjs.v32i1.948

Ali Hameed Al-Dabbagh, A., Ali Ajah, H. & Abdul Sattar Salman, J. (2023). Detection of virulence factors from *Candida* spp. Isolated from oral and vaginal candidiasis in Iraqi patients. *Archives of Razi Institute*, 78(1): 465–474. DOI:10.22092/ARI.2022.359464.2420

Alqahtani, A., Kopel, J. & Hamood, A. (2022). The in vivo and in vitro assessment of pyocins in treating *Pseudomonas aeruginosa* infections. *Antibiotics (Basel, Switzerland)*, 11(10): 1366. DOI:10.3390/antibiotics11101366

Arastehfar, A., Carvalho, A., Nguyen, M.H., Hedayati, M.T., Netea, M.G., Perlin, D.S. & Hoenigl, M. (2020). COVID-19-Associated Candidiasis (CAC): An underestimated complication in the absence of immunological predispositions? *Journal of Fungi*, 6: 211. DOI: 10.3390/jof6040211

Bahuguna, A., Khan, I., Bajpai, V.K. & Kang, S.C. (2017). MTT assay to evaluate the cytotoxic potential of a drug. *Bangladesh Journal of Pharmacology*, 12(2): 8. DOI:10.3329/bjp.v12i2.30892

Ball, A.L., Augenstein, E.D., Wienclaw, T.M., Richmond, B.C., Freestone, C.A., Lewis, J.M., Thompson, J.S., Pickett, B.E. & Berges, B.K. (2022). Characterization of *Staphylococcus aureus* biofilms via crystal violet binding and biochemical composition assays of isolates from hospitals, raw meat, and biofilm-associated gene mutants. *Microbial Pathogenesis*, 167: 105554. DOI: 10.1016/j.micpath.2022.105554

Behrens, H.M., Lowe, E.D., Gault, J., Housden, N.G., Kaminska, R., Weber, T.M., Thompson, C.M. A., Mislin, G.L.A., Schalk, I.J., Walker, D., Robinson, C.V. & Kleanthous, C. (2020). Pyocin S5 import into *Pseudomonas aeruginosa* reveals a generic mode of bacteriocin transport. *mBio*, 11(2): 10-1128. DOI: 10.1128/mBio.03230-19

Beute, J.E., Kim, A.Y., Park, J.J., Yang, A., Torres-Shafer, K., Mullins, D.W. & Sundstrom, P. (2022). The IL-20RB receptor and the IL-20 signaling pathway in regulating host defense in oral mucosal candidiasis. *Frontiers in Cellular and Infection Microbiology*, 12: 979701. DOI: 10.3389/fcimb.2022.979701

Ellepola, A.N.B., Joseph, B.K. & Khan, Z.U. (2014). The postantifungal effect and phospholipase production of oral *Candida albicans* from smokers, diabetics, asthmatics, denture wearers and healthy individuals following brief exposure to subtherapeutic concentrations of chlorhexidine gluconate. *Mycoses*, 57(9): 553–559. DOI:10.1111/myc.12194

Fule, S.R., Das, D. & Fule, R.P. (2015). Detection of phospholipase activity of *Candida albicans* and non albicans isolated from women of reproductive age with vulvovaginal candidiasis in rural area. *Indian Journal of Medical Microbiology*, 33(1): 92–95. DOI:10.4103/0255-0857.148392

Garcia-Vidal, C., Sanjuan, G., Moreno-García, E., Puerta-Alcalde, P., Garcia-Pouton, N., Chumbita, M., Fernandez-Pittol, M., Pitart, C., Inciarte, A., Bodro, M., Morata, L., Ambrosioni, J., Grafia, I., Meira, F., Macaya, I., Cardozo, C., Casals, C., Tellez, A., Castro, P., Marco, F., García, F., Mensa, J., Martínez, J.A., Soriano, A. & COVID-19 Researchers Group. (2021). Incidence of co-infections and superinfections in hospitalized patients with COVID-19: A retrospective cohort study. Clinical Microbiology and Infection: The Official Publication of the European Society of

Clinical Microbiology and Infectious Diseases, 27: 83–88. DOI: 10.1016/j.cmi.2020.07.041

Gow, N.A.R., Johnson, C., Berman, J., Coste, A.T., Cuomo, C.A., Perlin, D.S., Bicanic, T., Harrison, T.S., Wiederhold, N., Bromley, M., Chiller, T. & Edgar, K. (2022). The importance of antimicrobial resistance in medical mycology. *Nature Communications*, 13: 5352. DOI: 10.1038/s41467-022-32249-5

Haghighipour, S., Pourahmad, M., Noorbakhsh, M. & Mohammadi, R. (2019). *Candida* urinary tract infection among ICU patients in Isfahan, Iran. *Archives of Clinical Infectious Diseases*, 14. DOI: 10.5812/archcid.86472

Hamady, A. & Marei, Y. (2021). Detection of als1 and hwp1 genes involved in biofilm formation in *Candida albicans* isolated from catheter-associated candiduria. *Microbes and Infectious Diseases*, 2(3): 558–566. DOI: 10.21608/mid.2021.76052.1153

Hayashida, M.Z., Seque, C.A., Pasin, V.P., Enokihara, M.M.S.E. & Porro, A.M. (2017). Disseminated cryptococcosis with skin lesions: Report of a case series. *Anais Brasileiros de Dermatologia*, 92: 69–72. DOI: 10.1590/abd1806-4841.20176343

Hussein, M., Yassin, A. & El-Gelany, F. (2019). Characterization, virulence factors, and antifungal susceptibility of vulvovaginal *Candida* isolated from women at Qena, Egypt. *Egyptian Journal of Microbiology*, 54: 13–24. DOI: 10.21608/ejm.2019.10543.1091

Kakar, A., Sastré-Velásquez, L.E., Hess, M., Galgóczy, L., Papp, C., Holzknecht, J., Romanelli, A., Váradi, G., Malanovic, N. & Marx, F. (2022). The membrane activity of the amphibian temporin B peptide analog TB_KKG6K sheds light on the mechanism that kills *Candida albicans*. *mSphere*, 7: e0029022. DOI: 10.1128/msphere.00290-22

Karajacob, A.S., Azizan, N.B., Al-Maleki, A.R.M., Goh, J.P.E., Loke, M.F., Khor, H.M., Ho, G.F., Ponnampalavanar, S. & Tay, S.T. (2023). *Candida* species and oral mycobiota of patients clinically diagnosed with oral thrush. *PloS One*, 18: e0284043. DOI: 10.1371/journal.pone.0284043

Kielkopf, C.L., Bauer, W. & Urbatsch, I.L. (2020). Bradford assay for determining protein concentration. *Cold Spring Harbor Protocols*, 2020: 102269. DOI: 10.1101/pdb.prot102269

Lima, T., Gunnarsson, S.B., Coelho, E., Evtuguin, D. V., Correia, A., Coimbra, M.A., Cedervall, T. & Vilanova, M. (2022). β-glucan-functionalized nanoparticles down-modulate the proinflammatory response of mononuclear phagocytes challenged with *Candida albicans*. *Nanomaterials (Basel, Switzerland)*, 12: 2475. DOI: 10.3390/nano12142475

Ling, H., Saeidi, N., Rasouliha, B.H. & Chang, M.W. (2010). A predicted S-type pyocin shows a bactericidal activity against clinical *Pseudomonas aeruginosa* isolates through membrane damage. *FEBS Letters*, 584: 3354–3358. DOI: 10.1016/j.febslet.2010.06.021

El-Ganiny, M.A., Yossef, E.N. & Kamel, A.H. (2021). Prevalence and antifungal drug resistance of nosocomial *Candida* species isolated from two university hospitals in Egypt. *Current Medical Mycology*, 7(1): 31–37. DOI: 10.18502/cmm.7.1.6181

Mohamed, A.A., Elshawadfy, A.M., Amin, G. & Askora, A. (2021). Characterization of R-pyocin activity against Gram-positive pathogens for the first time with special focus on *Staphylococcus aureus. Journal of Applied Microbiology*, 131(6): 2780–2792. DOI:10.1111/jam.15134

Montoya, M.C., Magwene, P.M. & Perfect, J.R. (2021). Associations between Cryptococcus genotypes, phenotypes, and clinical parameters of human disease: A review. *Journal of Fungi (Basel, Switzerland)*, 7(4): 260. DOI:10.3390/jof7040260

Morse, S.A., Vaughan, P., Johnson, D. & Iglewski, B. H. (1976). Inhibition of *Neisseria gonorrhoeae* by a bacteriocin from *Pseudomonas aeruginosa*. *Antimicrobial Agents and Chemotherapy*, 10(2): 354–362. DOI: 10.1128/AAC.10.2.354

Oluyombo, O., Penfold, C.N. & Diggle, S.P. (2019). Competition in biofilms between cystic fibrosis isolates of *Pseudomonas aeruginosa* is shaped by R-pyocins. *mBio*, 10(1): e01828-18. DOI: 10.1128/mBio.01828-18

O'Neill, J. (2014). Antimicrobial resistance: Tackling a crisis for the health and wealth of nations (The Review on Antimicrobial Resistance). United Kingdom: The Review on Antimicrobial Resistance. Available at: https://amr-review.org/

Pal, M. (2018). Morbidity and mortality due to fungal infections. *Journal of Applied Microbiology and Biochemistry*, 1(1): 1-3. DOI: 10.21767/2576-1412.100002.

Paškevičius, Š., Dapkutė, V., Misiūnas, A., Balzaris, M., Thommes, P., Sattar, A., Gleba, Y. & Ražanskienė, A. (2022). Chimeric bacteriocin S5-PmnH engineered by domain swapping efficiently controls *Pseudomonas aeruginosa* infection in murine keratitis and lung models. *Scientific Reports*, 12: 5865. DOI: 10.1038/s41598-022-09865-8

Perinelli, D., Campana, R., Skouras, A., Bonacucina, G., Cespi, M., Mastrotto, F., Baffone, W. & Casettari, L. (2018). Chitosan loaded into a hydrogel delivery system as a strategy to treat vaginal co-infection. *Pharmaceutics*, 10(1): 23. DOI: 10.3390/pharmaceutics10010023.

Sarker, S.D., Nahar, L. & Kumarasamy, Y. (2007). Microtitre plate-based antibacterial assay incorporating resazurin as an indicator of cell growth, and its application in the in vitro antibacterial screening of phytochemicals. *Methods*, 42(4): 321-324. DOI: 10.1016/j.ymeth.2007.01.006

Taher, N.A. (2017). Antimicrobial effect of bacteriocin produced by *Pediococcus pentosaceus* on some clinical isolates. *Al-Mustansiriyah Journal of Science*, 27: 26–30. DOI: 10.23851/mjs.v27i5.163

Van de Veerdonk, F.L., Joosten, L.A.B. & Netea, M.G. (2015). The interplay between inflammasome activation and antifungal host defense. *Immunological Reviews*, 265: 172–180. DOI: 10.1111/imr.12280

Vechi, H.T., Theodoro, R.C., de Oliveira, A.L., da Silva Gomes, R.M., de Almeida Soares, R.D., Freire, M.G. & Baumgardt Bay, M. (2019). Invasive fungal infection by *Cryptococcus neoformans var. grubii* with bone marrow and meningeal involvement in a HIV-infected patient: A case report. *BMC Infectious Diseases*, 19: 220. DOI: 10.1186/s12879-019-3831-8

Vitális, E., Nagy, F., Tóth, Z., Forgács, L., Bozó, A., Kardos, G., Majoros, L. & Kovács, R. (2020). *Candida* biofilm production is associated with higher mortality in patients with candidaemia. *Mycoses*, 63(4): 352-360. DOI: 10.1111/myc.13049

Wang, J., Zhang, Z., Zhang, M., Yang, B., Wang, T., Sun, X., Chen, X., Zhang, M.Y., Guo, Z.Y. & Jiang, X. (2019). A rare primary *Candida parapsilosis* infection of the knee joint in a patient without predisposing factors: A case report. *Medicine*, 98(6): e14327. DOI: 10.1097/MD.0000000000014327

Zhu, B., Li, Z., Yin, H., Hu, J., Xue, Y., Zhang, G., Zheng, X., Chen, W., & Hu, X. (2022). Synergistic antibiofilm effects of pseudolaric acid A combined with fluconazole against *Candida albicans* via inhibition of adhesion and yeast-to-hypha transition. *Microbiology Spectrum*, 10(2): e01478-21. DOI: 10.1128/spectrum.01478-21.

Borneo Journal of Resource Science and Technology (2025), 15(1): 70-80
DOI: https:doi.org/10.33736/bjrst.7752.2025

Optimization of Lactic Acid Fermentation Conditions for the Production of Antibacterial Peptides Targeting *Pantoea* spp. for Rice Leaf Blight Control

SITI NORAZURA JAMAL*[1,2], DHILIA UDIE LAMASUDIN[2], BELAL J. MUHIALDIN[3], NOOR BAITY SAIDI[2], KOK SONG LAI[4] & MOHD TERMIZI YUSOF[5]

[1]Faculty of Applied Sciences, Universiti Teknologi MARA, Kuala Pilah Campus, Pekan Parit Tinggi, 72000 Kuala Pilah, Negeri Sembilan, Malaysia; [2]Department of Cell and Molecular Biology, Faculty of Biotechnology and Biomolecular Sciences, Universiti Putra Malaysia, 43400, Serdang, Selangor, Malaysia; [3]Department of Food Science and Nutrition, University of Minnesota, 1334 Eckles Ave, Saint Paul, MN 55108, USA; [4]Health Sciences Division, Abu Dhabi Women's College, Higher Colleges of Technology, 41012, Abu Dhabi, UAE; [5]Department of Microbiology Faculty of Biotechnology and Biomolecular Sciences, Universiti Putra Malaysia, 43400, Serdang, Selangor, Malaysia
*Corresponding authors: norazura6775@uitm.edu.my
Received: 3 September 2024 Accepted: 21 November 2024 Published: 30 June 2025

ABSTRACT

This study aimed to optimize the production of antibacterial peptides from *Bactronophorus thoracites* via lactic acid fermentation, specifically focusing on *Pantoea* species to manage rice leaf blight. The main goal was to investigate sustainable and environmentally friendly approaches to address this agricultural disease using bioactive compounds derived from marine sources. The fermentation process was refined using Response Surface Methodology (RSM), producing highly reliable results confirmed by the analysis of variance (ANOVA) and strong determination coefficients (R^2 = 0.9952 for *Pantoea ananatis* and R^2 = 0.9967 for *Pantoea stewartii*). The optimized parameters included a 4-day fermentation duration, a 3% (w/v) glucose concentration, and a 0.92% (w/v) solid-to-water ratio. These conditions closely matched predictive models and were further validated by a residual standard error (RSE) of less than 5%. The study identified the minimum inhibitory concentration (MIC) of the bioactive peptides, determining that 125 µg/ml was effective against the target bacteria. The hydrolysates produced in this study show promise as a natural method to control rice leaf blight and may have broader applications in agricultural disease management. This research highlights the potential of optimized lactic acid fermentation to produce effective antimicrobial agents, contributing to sustainable agriculture and offering new biotechnological strategies for plant disease control.

Keywords: Antimicrobial peptides, bioactive molecules, lactic acid fermentation, *Pantoea* spp., rice disease control

INTRODUCTION

Rice leaf blight, mainly attributed to different strains of *Pantoea* spp., represents a major agricultural challenge affecting rice production worldwide. First reported in Venezuela in 2002 (González *et al*., 2015), the disease has since been identified in several Asian countries, manifesting as water-soaked lesions on rice leaves and resulting in dramatic yield losses, sometimes up to 70% (Azizi & Zulperi, *et al*., 2019; Toh *et al*., 2019). The emergence of different Pantoea species, including *P. stewartii* and *P. ananatis*, in regions like Malaysia has heightened the need for effective and sustainable control measures (Azizi & Ismail, *et al*., 2019; Azizi & Zulperi, *et al*., 2019; Toh *et al*., 2019). Conventional strategies, particularly the use of agrochemicals, have faced criticism due to their environmental impacts and the increasing resistance of pathogens to these chemicals (Khan *et al*., 2012; Naqvi, 2019; Abdallah *et al*., 2020; Sopialena *et al*., 2021). This situation has redirected attention towards the investigation of new antimicrobial agents, particularly antimicrobial peptides (AMPs), which not only play a crucial role in innate immune defense against a wide range of pathogens but also show promising potential in managing plant diseases, such as defensins and cyclotides, which inhibit fungal pathogens like Fusarium and Magnaporthe species in crops like wheat and rice (De Zoysa, 2013; Tassanakajon *et al*., 2015; Yuan *et al*., 2022).

In this context, molluscs, particularly bivalves like *Bactronophorus thoracites*, are recognized for their rich protein content and essential amino acids, making them a viable source for AMP production (Lee *et al*., 2019; Jamal *et al*., 2022). Lactic acid fermentation has emerged as an innovative technique for

converting high molecular weight proteins into bioactive peptides with reduced molecular weights, offering several advantages over other hydrolysis methods. Compared to enzymatic hydrolysis, lactic acid fermentation is more cost-effective as it utilizes naturally occurring lactic acid bacteria (LAB) rather than expensive enzymes, and unlike chemical hydrolysis, it avoids harsh chemicals and extreme conditions, preserving the structural integrity and bioactivity of the peptides.

Additionally, lactic acid fermentation enhances bioactivity by producing synergistic bioactive compounds like organic acids and bacteriocins, selectively hydrolyzes proteins to release targeted bioactive peptides, and improves safety by reducing anti-nutritional factors and producing antimicrobial compounds that extend shelf life. Its natural, sustainable process is versatile and easily integrated into food systems, making it a superior method for producing functional peptides from diverse raw materials. This process is facilitated by LAB strains, which secrete proteolytic enzymes to break down protein substrates, liberating peptides and generating various bioactive compounds (Muhialdin *et al*., 2020; Jamal *et al*., 2022). The effectiveness of this hydrolysis depends on factors such as the LAB strain used, the type of protein involved, and the duration of fermentation (Muhialdin *et al*., 2020; Jamal *et al*., 2022).

Considering the varying specificities and abilities of different LAB strains, especially *Lactobacillus casei*, it is crucial to examine the factors affecting the lactic acid fermentation of *Bactronophorus thoracites*. Traditionally, the pH-stat method has been used to assess the impact of reaction parameters (Arulrajah *et al*., 2020). Additionally, RSM has proven effective in optimizing parameters that affect the hydrolysis of various protein types (Harun *et al*., 2017; Amin & Cheng, 2019; Arulrajah *et al*., 2020).

This study aims to bridge a crucial gap by exploring the optimal conditions for lactic acid fermentation in producing bioactive peptides from *B. thoracites*. By highlighting the sustainable and eco-friendly aspects of this method, the research seeks to leverage the antimicrobial properties of these peptides, especially against *Pantoea* spp., as a promising solution for managing rice leaf blight. This effort not only advances agricultural sustainability but also paves the way for new biotechnological research, investigating the potential of marine-derived bioactive compounds in plant disease management.

MATERIALS & METHODS

Sampling

In December 2020, *Bactronophorus thoracites* specimens were obtained from a mangrove forest near Kelanang Beach in Banting, Selangor, Malaysia, at the coordinates 2° 48'44.5" N and 101° 22'08.5" E. The shipworms were carefully packaged in plastic bags and kept refrigerated during transport to the Plant Molecular Biology Laboratory (PMB Lab) at the Faculty of Biotechnology and Biomolecular Science, Universiti Putra Malaysia (UPM), in Serdang, Selangor, Malaysia.

Preparation of Crude Extract

The collected shipworms were thoroughly cleaned and homogenized at 4 °C using a Waring laboratory blender. The resulting homogenate was mixed with 20 ml of chilled, deionized water, also maintained at 4 °C, and divided into small polyethylene bags (10 cm by 15 cm). The samples were initially frozen overnight at −80 °C in a Thermo Scientific freezer. Once frozen, they underwent freeze-drying in a Labconco FreeZone freeze dryer until a stable weight was achieved. After freeze-drying, the samples were ground into a fine powder using a Waring laboratory-grade blender and passed through a 200 μm mesh sieve. The finely milled powder was collected in screw-capped bottles and stored at −20 °C for future use.

Lactic Acid Fermentation

Optimisation of lactic acid fermentation conditions was carried out using RSM and Central Composite Design (CCD) in Design-Expert® software, following the protocol of Muhialdin *et al*. (2020) with slight modifications. The fermentation process took place in a 100 ml conical flask, which was kept in a shaking water bath at 37 °C with continuous agitation at 100 rpm. The fermentation began by adding 2% (v/v) starter culture, and the mixture was incubated for periods of 2, 4, 6, and 8 days

at 37 °C. Cell count analysis was conducted at each fermentation stage using the spread plate method. Approximately 0.1 ml of each fermented sample was plated on fresh MRS agar and incubated at 37 °C for 48 hours. The colonies were counted, and results were expressed as colony-forming units per milliliter (CFU/ml). To stop the fermentation process, the mixture was heated to 100 °C for 30 minutes with intermittent stirring, rapidly cooled in an ice bath, and centrifuged at 14,000 × g for 20 minutes. The resulting *Bactronophorus thoracites* Fermented Protein (BTFP) was collected, and inhibition percentages were recorded before freeze-drying. The BTFP was then stored at −20 °C for further analysis.

Experimental Design, Modeling, and Statistical Analysis

The experiments were designed, and data were analyzed using Design-Expert® software, version 13.0. A Central Composite Design (CCD) approach was applied to assess the effects of three variables across five levels, focusing on their influence on antimicrobial activity against *P. ananatis* and *P. stewartii*. The variables and their respective levels are detailed in Table 1, with the experimental design provided in Table 2. A total of 20 experiments were conducted, including three replicates at the central point. Randomization was employed to minimize potential bias from unforeseen factors. The data were modeled using a second-order polynomial equation or its simplified form, as illustrated in Eq.(1):

$$\boldsymbol{Y = z_0 + \sum z_1\ A + \sum z_{12}\ AB + \sum z_{123}\ AA} \quad \text{Eq.(1)}$$

In this equation, "Y" represents the response variable, specifically the antibacterial effect against *P. ananatis* and *P. stewartii*. The term "z□" denotes the model's intercept, while "z□" corresponds to the coefficient linked to variable A. The coefficients "z□□" and "z□□□" reflect the interaction effects between variables AB and AA, respectively. This equation accounts for the quadratic, linear, and interaction effects of the process variables on the antibacterial activity. The significance of each variable's coefficient was assessed using the Student's t-test. The relevance, accuracy, and impact of the process variables on the results were also evaluated through Analysis of Variance (ANOVA).

Antimicrobial Activity

The antimicrobial effectiveness of BTFP from each experimental trial was evaluated against *P. ananatis* and *P. stewartii*, with a non-hydrolyzed sample serving as a control. The procedure involved mixing 500 µL of Luria Broth (LB) containing 10^6 CFU/ml with 500 µL of the BTFP sample. The mixture was then incubated at 30°C for 24 hours. After incubation, the absorbance was measured at 600 nm using a spectrophotometer, following the method described by Mohamad Asri *et al*. (2020). This absorbance reading was essential for determining antimicrobial activity. The level of antimicrobial efficacy was calculated using a specific formula, as shown in Eq.(2), based on the absorbance values obtained. The sample showing the highest antimicrobial activity was then freeze-dried (Labconco FreeZone, USA) and further characterized.

$$Inhibition\% = \frac{(24\ h\ control - 0\ h\ control) - (24\ h\ sample - 0\ h\ sample)}{0\ h\ control} \quad \text{Eq.(2)}$$

Validation of optimum condition

Design-Expert® software was employed to predict the optimal conditions for maximizing antimicrobial activity. To validate the model's accuracy, BTFP was hydrolyzed under various randomly selected conditions. The resulting hydrolysates were freeze-dried and evaluated for antimicrobial activity. Predicted outcomes were then compared with actual experimental results using a t-test and residual standard error (RSE), as outlined in Eq. (3). Following the methodologies of Arulrajah *et al*. (2021) and Zakaria *et al*. (2021), predictions were deemed accurate if the RSE value remained below 5%.

$$RSE\ (\%) = \left|\frac{Actual\ value - Predicted\ value}{Predicted\ value}\right| \times 100\% \quad \text{Eq.(3)}$$

Effective Inhibition Concentration

The antibacterial effectiveness of BTFP was evaluated following modified methods from Jamal *et al*. (2022). Bacterial cultures were mixed with LB, and varying concentrations of BTFP were introduced to identify the minimum concentration necessary to inhibit bacterial growth. The cultures were incubated at 30 °C for 24 hours, after which inhibition of growth was assessed. The lowest concentration of BTFP that

successfully prevented visible bacterial growth was recorded as the MIC. To determine the Minimum Bactericidal Concentration (MBC), samples were plated on agar and incubated at 37 °C for 24 hours. The concentration at which no bacterial growth was observed was recorded as the MBC. The procedure was repeated three times to ensure accuracy and consistency.

Data Analysis

The data are reported as the mean of three replicates, with standard deviations calculated within a 95% confidence interval.

Table 1. The four independent variables and their coded levels of independent variables for the lactic acid fermentation optimization

Symbol	Independent variable	Coded level				
		-1.68	-1	0	+1	+1.68
A	Fermentation day	0.6	2	4	6	7.4
B	Glucose concentration (%)	1.3	2	3	4	4.7
C	S/W ratio (% w/v)	0.85	0.88	0.92	0.96	0.99

Table 2. Central Composite Design (CCD) design for optimizing lactic acid fermentation conditions under different levels of process variables

Run	Independent variables			Code level		
	A (day)	B (% v/v)	C (% w/v)	A	B	C
1	0.6	3	0.92	-1.68	0	0
2	2	2	0.88	-1	-1	-1
3	2	2	0.96	-1	-1	1
4	2	4	0.88	-1	1	-1
5	2	4	0.96	-1	1	1
6	4	1.32	0.92	0	-1.68	0
7	4	3	0.85	0	0	-1.68
8	4	3	0.92	0	0	0
9	4	3	0.92	0	0	0
10	4	3	0.92	0	0	0
11	4	3	0.92	0	0	0
12	4	3	0.92	0	0	0
13	4	3	0.92	0	0	0
14	4	3	0.99	0	0	1.68
15	4	4.68	0.92	0	1.68	0
16	6	2	0.88	1	-1	-1
17	6	2	0.96	1	-1	1
18	6	4	0.88	1	1	-1
19	6	4	0.96	1	1	1
20	7.4	3	0.92	1.68	0	0

Note: A = Fermentation Day; B = Glucose concentration (% v/v); C = Substrate/water ratio (% w/v)

RESULTS & DISCUSSION

Model Fitting and Variance Analysis (ANOVA)

A three-level factorial design was employed to evaluate the impact of fermentation time, glucose concentration, and solid-to-water (S/W) ratio on the antimicrobial activity of BTFP produced through lactic acid fermentation. Table 3 outlines the experimental design, along with both the actual and predicted values for each variable. Statistical analysis was performed using ANOVA to assess the significance of the variables. The results demonstrated that all independent variables significantly influenced their respective responses in the fermentation process. Specifically, the F-values for BTFP's antimicrobial inhibition against *Pantoea*

ananatis (Y1) and *Pantoea stewartii* (Y2) were 230.89 and 339.64, respectively.

The statistical data revealed that the probability of the observed effects occurring by random chance was just 0.01%, confirming the robustness of the findings. Furthermore, the p-values for each response were extremely low ($p< 0.05$), reinforcing the relevance of the models. The actual inhibition percentages ranged from 3.105% to 63.759% for Y1 and from 0.550% to 57.132% for Y2, reflecting the real data obtained from the experimental design matrix and the predicted responses calculated using CCD, as shown in Table 3.

Table 4 presents the quadratic polynomial models. Equations 4 and 5 describe the empirical relationships between the independent and dependent variables for each response. The coefficient of determination R^2 for Y1 (0.9952) and Y2 (0.9967) revealed a strong alignment between the experimental data and the quadratic polynomial models, as confirmed by ANOVA. Although R^2 tends to increase with the inclusion of additional variables, regardless of their statistical significance, it remains a valuable indicator of model fit. Moreover, the predicted R^2 (pred R^2) values of 0.9733 for Y1 and 0.9881 for Y2 indicated that the regression model had high predictive accuracy in estimating the response values, consistent with the findings of Che Sulaiman *et al*. (2017).

According to Zainol *et al*. (2021) and Zakaria *et al*. (2021), an R^2 value exceeding 0.9 denotes a strong fit and correlation between experimental results and the regression model. Therefore, the model developed in this study successfully captured nearly 99% of the variability in the response variables. Additionally, the adjusted R^2 (Adj. R^2) serves as a critical metric in evaluating the model's suitability, reflecting the explanatory power of the regression models when multiple variables are considered. The adjusted R^2 values for antimicrobial inhibition were 0.9909 (Y1) and 0.9938 (Y2), affirming the models' capability to predict the optimal conditions for maximizing antimicrobial inhibition by the protein hydrolysates.

Table 3. CCD, predicted, and response values of two dependent variables under different lactic acid fermentation conditions

Run	Independent variables			Code level			Response variable (%)			
							Y_1		Y_2	
	A	B	C	A	B	C	Act.	Pred.	Act.	Pred.
1	0.6	3	0.92	-1.68	0	0	3.105	5.189	3.117	4.252
2	2	2	0.88	-1	-1	-1	5.600	5.600	0.550	0.272
3	2	2	0.96	-1	-1	1	8.298	7.140	8.870	8.621
4	2	4	0.88	-1	1	-1	13.947	12.309	11.365	10.325
5	2	4	0.96	-1	1	1	19.370	19.240	16.788	16.748
6	4	1.32	0.92	0	-1.68	0	21.210	20.343	13.690	13.099
7	4	3	0.85	0	0	-1.68	14.811	14.514	13.668	14.017
8	4	3	0.92	0	0	0	59.675	61.509	53.359	55.377
9	4	3	0.92	0	0	0	63.759	61.509	52.759	55.377
10	4	3	0.92	0	0	0	60.861	61.509	55.924	55.377
11	4	3	0.92	0	0	0	60.276	61.509	56.107	55.377
12	4	3	0.92	0	0	0	63.683	61.509	57.132	55.377
13	4	3	0.92	0	0	0	60.624	61.509	56.893	55.377
14	4	3	0.99	0	0	1.68	23.240	22.528	23.526	22.650
15	4	4.68	0.92	0	1.68	0	23.417	23.274	17.104	17.169
16	6	2	0.88	1	-1	-1	18.252	19.095	13.645	14.057
17	6	2	0.96	1	-1	1	19.343	21.694	16.487	17.900
18	6	4	0.88	1	1	-1	8.608	10.481	10.149	10.770
19	6	4	0.96	1	1	1	17.757	18.471	12.037	12.688
20	7.4	3	0.92	1.68	0	0	18.983	15.890	14.091	12.430

Note: A = Fermentation Day (Day); B = Glucose concentration (% v/v); C = Substrate/water ratio (% w/v); Y_1 = *P. ananatis*; Y_2 = *P. stewartii*; Act. = Actual; Pred = Prediction

Table 4. The quadratic polynomial equations for the two responses based on the coded factors of lactic acid fermentation

Response	Equation	R^2	Adj. R^2	Pred. R^2	Regression (p-value)	Lack-of-fit
Y_1	61.51 + 3.18A + 0.87B + 2.38C + 3.83AB - 0.2649AC + 1.35BC + 18.02A^2 - 14.04B^2 - 15.2C^2	0.9952	0.9909	0.9733	< 0.0001	0.2554
Y_2	55.38 + 2.43A + 1.21B + 2.57C + 3.33AB- 1.13AC- 0.4814BC - 16.63A^2 - 14.23B^2 - 13.1C^2	0.9967	0.9938	0.9881	< 0.0001	0.7338

Note: A = Fermentation Day (Day); B = Glucose concentration (% v/v); C = Substrate/water ratio (% w/v); Y_1 = *P. ananatis*; Y_2 = *P. stewartii*; Adj. = Adjusted; Pred = Prediction

Response Surface Analysis and the Impact of Fermentation Variables

This research explored how three key fermentation factors—fermentation duration, glucose concentration, and the solid-to-water (S/W) ratio—influenced the antimicrobial properties of BTFP during lactic acid fermentation, using *Lactobacillus casei* as the starter culture. Three-dimensional response surface plots were generated to visually represent the interactions between these variables and their effect on antimicrobial activity against *Pantoea ananatis* (Y1) and *Pantoea stewartii* (Y2). These plots, shown in Figures 1 and 2, were instrumental in identifying the optimal conditions for maximizing antimicrobial effectiveness. The construction of these plots was based on the significant interaction effects revealed by ANOVA.

Figure 1(a) and 2(a) illustrate the combined effects of fermentation time and glucose concentration, with the S/W ratio held constant at 0.92%. The data showed that antimicrobial activity against Y1 and Y2 increased with higher glucose levels, up to 3%, and fermentation durations of up to 4 days. However, reducing either the glucose concentration or the fermentation time led to a decline in antimicrobial efficacy. This finding is consistent with the results of Sánchez-Clemente *et al*. (2020), who observed that adding a carbon source like glucose enhances the growth of lactic acid bacteria (LAB) and boosts their antimicrobial properties. Additionally, moderate glucose levels can accelerate fermentation, leading to increased carbon dioxide production.

Figure 1(b) and 2(b) highlight the effects of fermentation duration and the S/W ratio, while maintaining glucose concentration at 3%. Extending the fermentation period to 4 days and keeping the S/W ratio at 0.92% improved antimicrobial performance against Y1 and Y2. However, further increases in these variables resulted in decreased antimicrobial activity. This pattern aligns with the findings of Muhialdin *et al*. (2020), who reported that antimicrobial activity peaked after 48 hours of fermentation but declined after 60-72 hours. Similarly, Rodríguez *et al*. (2017) observed a reduction in *Limosilactobacillus fermentum* viability after 24 hours of fermentation, which may explain the drop in antimicrobial effectiveness during extended fermentation periods. Prolonged fermentation could decrease the viability of *L.casei*, impairing its ability to hydrolyze BTCP and thereby reduce antimicrobial activity. This reduction in antimicrobial activity over time can be attributed to the extended fermentation period often leads to the accumulation of organic acids, particularly lactic acid, which lowers the pH of the environment. A significantly reduced pH can negatively impact the survival of *L. casei* and its metabolic activity (Muhialdin *et al*.; 2020).

Figure 1(c) and 2(c) show the combined influence of glucose concentration and S/W ratio during a 4-day fermentation period. Optimal antimicrobial activity against Y1 and Y2 was achieved with a 0.92% S/W ratio and a glucose concentration of 3%. Arulrajah *et al*. (2021)

noted that substrates with higher moisture content are more readily fermented by certain *Lactobacillus* species, likely due to their need for ample water availability. The optimal S/W ratio identified in this study indicates that *L. casei* requires sufficient water to effectively break down BTCP into smaller peptides during fermentation. Overall, the antimicrobial activity of BTFP against Y1 and Y2 increased to a peak, then declined, in response to varying fermentation durations, glucose concentrations, and S/W ratios.

Validation of Predicted Optimal Conditions

To assess the accuracy and reliability of the results, five independent validation tests were performed, as outlined in Table 5. This step was crucial for verifying the effectiveness and robustness of the final models established in this study. The comparison between the actual experimental results and the predicted outcomes was conducted by calculating the residual standard error (RSE) percentages, which were then evaluated against the estimates provided by Eq. (3). The models were deemed precise if the RSE percentages were below 5%, reflecting a close alignment between observed and predicted values. Table 5 illustrates that all RSE percentages were within this 5% threshold, confirming the precision and dependability of the models used.

Effective Inhibition Concentration of BTFP

The findings from this study reveal that BTFP demonstrates considerable antimicrobial efficacy. As shown in Table 6, BTFP achieved notable antimicrobial activity, with MICs of 125 µg/ml against both *P. ananatis* and *P. stewartii*. This performance is particularly significant when compared to other antimicrobial peptides (AMPs) tested against these pathogens, which typically exhibit MIC values ranging between 200–500 µg/ml (Arulrajah *et al*., 2020; Muhialdin *et al*., 2021). The lower MIC of BTFP highlights its superior potency and efficiency in inhibiting these bacterial strains, positioning it as a highly effective alternative for combating these plant pathogens.

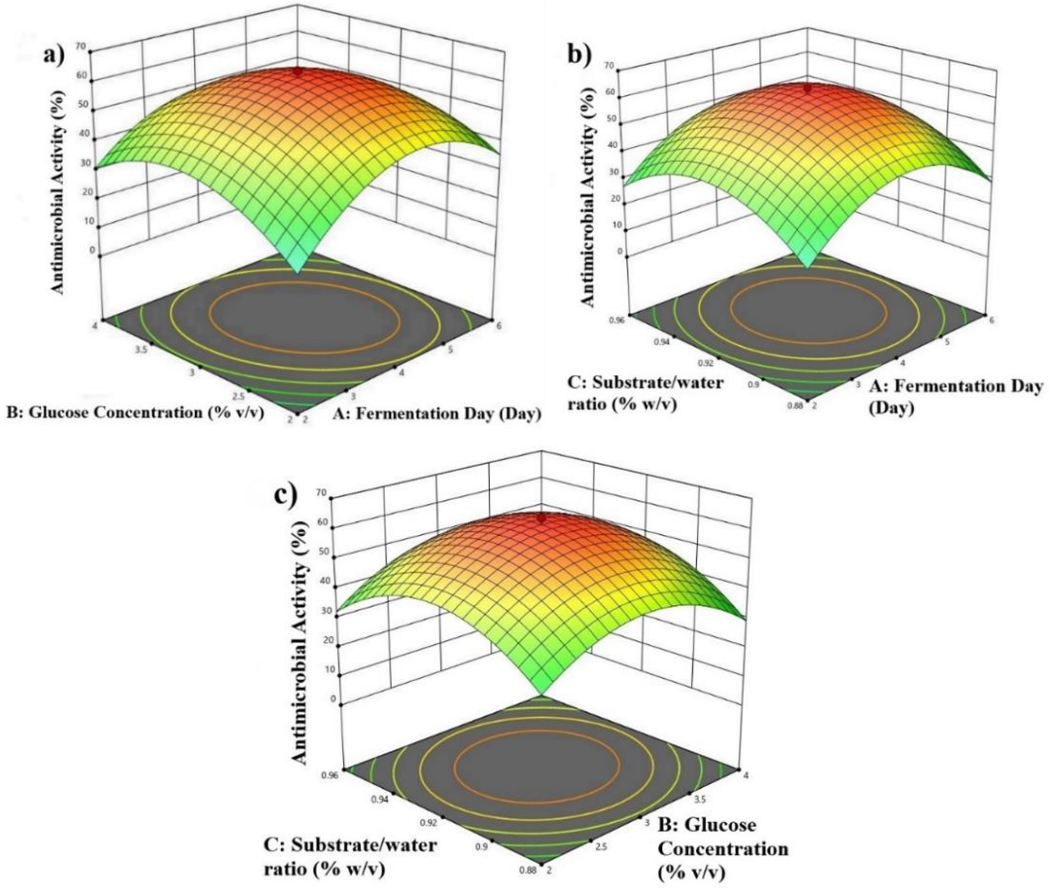

Figure 1. The 3D contour plots showing the influence of variable parameters on the antimicrobial activity of BTFP against Y_1 (*P. ananatis*). (a) Day vs glucose concentration, (b) Day vs S/W ratio, and (c) Glucose concentration vs S/W ratio

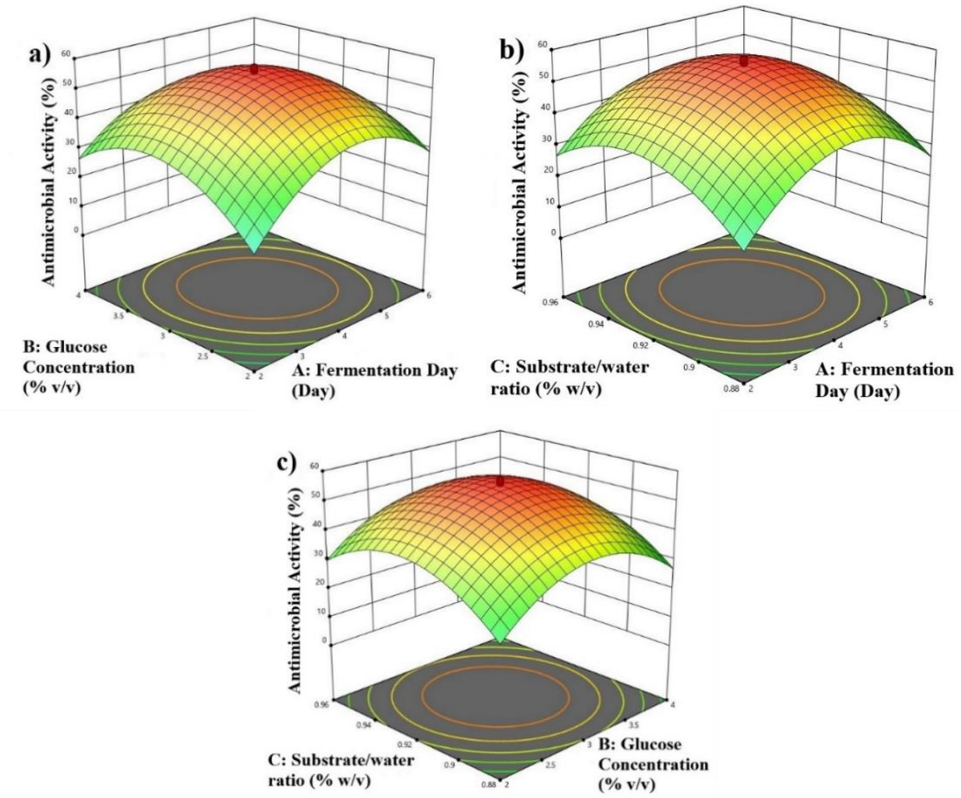

Figure 2. The 3D contour plots showing the influence of variable parameters on the antimicrobial activity of BTFP against Y_2 (*P. stewartii*). (a) Day vs glucose concentration, (b) Day vs S/W ratio, and (c) Glucose concentration vs S/W ratio

Table 5. Actual and predicted responses for the model verification of lactic acid fermentation

	Variables			Y_1			Y_2		
				Inhibition (%)		RSE (%)	Inhibition (%)		RSE (%)
	A	B	C	Actual	Predicted		Actual	Predicted	
1	2.5	2.1	0.91	31.85	33.054	-3.643	26.77	27.554	2.845
2	3.5	2.5	0.93	52.42	54.624	-4.035	51.331	49.105	4.533
3	4.5	3.5	0.94	56.289	55.387	1.629	48.217	49.325	2.246
4	5.0	3.9	0.95	41.522	40.532	2.443	33.646	34.301	1.910
5	5.5	3.8	0.95	36.221	37.369	-3.072	30.028	31.343	4.196

Note: A = Fermentation Day; B = Glucose concentration (% v/v); C = Substrate/water ratio (% w/v). Response variables for antimicrobial activity (%): Y_1 = *P. ananatis*; Y_2 = *P. stewartii*. Data are expressed as the mean ± S.D. of triplicate samples

Furthermore, the MBCs for these bacterial strains were found to be 500 µg/ml. These levels of antimicrobial efficacy exceed those reported in previous research; for instance, a study on a peptide derived from the mollusc *Babylonia spirata* found MICs of 1000 µg/ml against *Staphylococcus aureus* and *Aspergillus fumigatus* (Kuppusamy & Ulagesan, 2016). The potent bactericidal properties of BTFP, characterized by MBC and MIC values of ≤ 500 µg/ml, align with earlier studies highlighting the concentration-dependent nature of AMP effects (Buda De Cesare *et al*., 2020; Sanchez Armengol *et al*., 2021). Research indicates that AMPs can interfere with various intracellular processes, such as inhibiting transcription, disrupting translation, , and hindering macromolecule synthesis, thereby contributing to their antimicrobial efficacy (Erdem Büyükkiraz & Kesmen, 2022; Naiel *et al*., 2023; Seyfi *et al*., 2020).

Table 6. The effects of BTFP on antimicrobial activity, MIC, MBC, and bactericidal and bacteriostatic

Sample	Microorganisms	Antimicrobial activity (%)	MIC (µg/ml)	MBC (µg/ml)	Bactericidal/ Bacteriostatic (MBC/MIC)
BTFP	*P. ananatis*	70.136 ± 0.273%	125	500	Bactericidal
	P. stewartii	70.024 ± 0.244%	125	500	Bactericidal
Control	*P. ananatis*	n.a	n.a	n.a	n.a
	P. stewartii	n.a	n.a	n.a	n.a

Note: MIC = Minimum inhibitory concentration; MBC = Minimum Bactericidal concentration; n.a = No activity; Control = *B. thoracites* crude extract; Bactericidal = MBC/MIC ≤ 4; Bacteriostatic = MBC/MIC > 4. Antimicrobial activity was measured in percentage (%) and the values were expressed as mean ± standard error (SEM).

CONCLUSION

This study effectively employed Response Surface Methodology (RSM) to refine the lactic acid fermentation process for proteins from *B. thoracites*. The ANOVA results, which showed high coefficients of determination (R^2) of 0.9952 for *P. ananatis* and 0.9967 for *P. stewartii*, affirm the validity and reliability of our methodology. The quadratic models successfully mapped the relationships between the adjusted variables and their effects on antimicrobial activity. The identified optimal fermentation parameters—4 days, a glucose concentration of 3% (w/v), and a solid-to-water (S/W) ratio of 0.92% (w/v)—aligned with our predictions and were confirmed by a residual standard error (RSE) of less than 5%. Moreover, the minimum concentrations necessary to achieve inhibitory or bactericidal effects were 125 µg/ml, consistent with previous findings that BTFP's antimicrobial efficacy is dependent on concentration. Overall, the hydrolysates generated in this study exhibit significant potential as natural agents against rice leaf blight, suggesting their practical use in managing this agricultural issue. This underscores the effectiveness of our optimised fermentation process in producing potent antimicrobial agents.

REFERENCES

Abdallah, Y., Liu, M., Ogunyemi, S.O., Ahmed, T., Fouad, H., Abdelazez, A., Yan, C., Yang, Y., Chen, J. & Li, B. (2020). Bioinspired Green Synthesis of Chitosan and Zinc Oxide Nanoparticles with Strong Antibacterial Activity against Rice Pathogen *Xanthomonas oryzae* pv. oryzae. *Molecules*, 25(20): 4795. DOI:10.3390/molecules25204795

Amin, A.M. & Cheng, S.K. (2019). Optimization of enzymatic hydrolysis condition of angelwing clam (*Pholas orientalis*) meat using alcalase® to obtain maximum degree of hydrolysis. *Malaysian Applied Biology*, 48(3): 55–62. https://jms.mabjournal.com/index.php/mab/article/view/1839

Arulrajah, B., Muhialdin, B.J., Zarei, M., Hasan, H. & Saari, N. (2020). Lacto-fermented Kenaf (*Hibiscus cannabinus* L.) seed protein as a source of bioactive peptides and their applications as natural preservatives. *Food Control*, 110: 106969. DOI:10.1016/j.foodcont.2019.106969

Arulrajah, B., Muhialdin, B.J., Qoms, M.S., Zarei, M., Hussin, A.S.M., Hasan, H. & Saari, N. (2021). Production of cationic antifungal peptides from kenaf seed protein as natural bio preservatives to prolong the shelf-life of tomato puree. *International Journal of Food Microbiology*, 359: 109418. DOI:10.1016/j.ijfoodmicro.2021.109418

Azizi, M.M.F., Ismail, S.I., Hata, E.M., Zulperi, D., Ina-Salwany, M.Y. & Abdullah, M.A.F. (2019). First Report of *Pantoea stewartii* subsp. indologenes Causing Leaf Blight on Rice in Malaysia. *Plant Disease*, 103(6): 1407–1407. DOI:10.1094/PDIS-08-18-1403-PDN

Azizi, M.M.F., Zulperi, D., Rahman, M.A.A., Abdul-Basir, B., Othman, N.A., Ismail, S.I., Hata, E.M., Ina-Salwany, M.Y. & Abdullah, M.A.F. (2019). First Report of *Pantoea ananatis* Causing Leaf Blight Disease of Rice in Peninsular Malaysia. *Plant Disease*, 103(8): 2122. DOI:10.1094/PDIS-01-19-0191-PDN

Buda De Cesare, G., Cristy, S.A., Garsin, D.A. & Lorenz, M.C. (2020). Antimicrobial Peptides: a New Frontier in Antifungal Therapy. *MBio*, 11(6): 1–21. DOI:10.1128/mBio.02123-20

Che Sulaiman, I.S., Basri, M., Fard Masoumi, H.R., Chee, W.J., Ashari, S.E. & Ismail, M. (2017). Effects of temperature, time, and solvent ratio on the extraction of phenolic compounds and the anti-radical activity of Clinacanthus nutans Lindau leaves by response surface methodology. *Chemistry Central Journal*, 11(1): 54. DOI:10.1186/s13065-017-0285-1

De Zoysa, M. (2013). Antimicrobial Peptides in Marine Mollusks and their Potential Applications. In *Marine Proteins and Peptides*, John Wiley & Sons, Ltd. pp. 695–707. DOI:10.1002/9781118375082.ch35

Erdem Büyükkiraz, M. & Kesmen, Z. (2022). Antimicrobial peptides (AMPs): A promising class of antimicrobial compounds. *Journal of Applied Microbiology*, 132(3): 1573–1596. DOI:10.1111/jam.15314

González, A.D., Franco, M.A., Contreras, N., Galindo-Castro, I., Jayaro, Y. & Graterol, E. (2015). First Report of *Pantoea agglomerans* Causing Rice Leaf Blight in Venezuela. *Plant Disease*, 99(4): 552–552. DOI:10.1094/PDIS-07-14-0736-PDN

Harun, Z., Amin, A.M., Sarbon, N.M. & Zainol, M.K.M. (2017). Optimisation of enzymatic protein hydrolysis of mud crab (*Scylla* sp.) to obtain maximum angiotensin-converting enzyme inhibitory (ACEI) activity using response surface methodology. *Malaysian Applied Biology*, 46(3): 33–40. http://mabjournal.com/index.php?option=com_content&view=article&id=674&catid=59:current-view&Itemid=56

Jamal, S.N., Donny, D.A. & Lamasudin, D.U. (2022). The Influence of Enzymatic Hydrolysis on Antimicrobial Activity Against Rice Pathogens from *Bactronophorus thoracites* (Shipworm) Protein Hydrolysate. *Malay. J. Biochem. Mol. Biol.*, 25(3): 47–57. DOI:10.22452/mjbmb.vol25no3.1

Jamal, S.N., Muhialdin, B.J., Saidi, N.B., Song, L.K., Yusof, M.T. & Lamasudin, D.U. (2022). The effect of lactic acid fermentation of *Bactronophorus thoracites* on antimicrobial activity against rice pathogens. *Malaysian Journal of Microbiology*, 18(6): 592–601. DOI:10.21161/mjm.221499

Khan, J.A., Siddiq, R., Arshad, H.M.I., Anwar, H.S., Saleem, K. & Jamil, F.F. (2012). Chemical control of bacterial leaf blight of rice caused by *Xanthomonas oryzae* pv. oryzae. *Pakistan Journal of Phytopayjology*, 24(2): 97–100. DOI:10.7324/JOP.2012.97

Kuppusamy, A. & Ulagesan, S. (2016). Antimicrobial Activity of Protein Hydrolysate from Marine Molluscs *Babylonia spirata* (Linnaeus, 1758). *Journal of Applied Pharmaceutical Science*, 6(7): 73–77. DOI:10.7324/JAPS.2016.60711

Lee, S.Y., Mohamed, R. & Lamasudin, D.U. (2019). Morphology and molecular phylogenetic placement of a coastal shipworm (*Bactronophorus thoracites* (Gould, 1862), Teredinidae) from Peninsular Malaysia. *Regional Studies in Marine Science*, 29: 100694. DOI:10.1016/j.rsma.2019.100694

Mohamad Asri, N., Muhialdin, B.J., Zarei, M. & Saari, N. (2020). Low molecular weight peptides generated from palm kernel cake via solid state lacto-fermentation extend the shelf life of bread. *LWT*, 134: 110206. DOI:10.1016/j.lwt.2020.110206

Muhialdin, B.J., Abdul Rani, N.F. & Meor Hussin, A.S. (2020). Identification of antioxidant and antibacterial activities for the bioactive peptides generated from bitter beans (*Parkia speciosa*) via boiling and fermentation processes. *LWT*, 131: 109776. DOI:10.1016/j.lwt.2020.109776

Muhialdin, B.J., Kadum, H. & Meor Hussin, A.S. (2021). Metabolomics profiling of fermented cantaloupe juice and the potential application to extend the shelf life of fresh cantaloupe juice for six months at 8 °C. *Food Control*, 120: 107555. DOI:10.1016/j.foodcont.2020.107555

Naiel, M.A.E., Ghazanfar, S., Negm, S.S., Shukry, M. & Abdel-Latif, H.M.R. (2023). Applications of antimicrobial peptides (AMPs) as an alternative to antibiotic use in aquaculture – A mini-review. *Annals of Animal Science*, 23(3): 691–701. DOI:10.2478/aoas-2022-0090

Naqvi, S.A.H. (2019). Bacterial Leaf Blight of Rice: An Overview of Epidemiology and Management with Special Reference to-Indian-Sub-Continent. *Pakistan Journal of Agricultural Research*, 32(2): 359–380. DOI:10.17582/journal.pjar/2019/32.2.359.380

Rodríguez de Olmos, A., Correa Deza, M.A. & Garro, M.S. (2017). Selected lactobacilli and bifidobacteria development in solid state fermentation using soybean paste. *Argentine Journal of Microbiology*, 49(1): 62–69. DOI:10.1016/j.ram.2016.08.007

Sánchez-Clemente, R., Guijo, M.I., Nogales, J. & Blasco, R. (2020). Carbon Source Influence on Extracellular pH Changes along Bacterial Cell-Growth. *Genes*, 11(11): 1292. DOI:10.3390/genes11111292

Sanchez Armengol, E., Harmanci, M. & Laffleur, F. (2021). Current strategies to determine antifungal and antimicrobial activity of natural compounds. *Microbiological Research*, 252: 126867. DOI:10.1016/j.micres.2021.126867

Seyfi, R., Kahaki, F.A., Ebrahimi, T., Montazersaheb, S., Eyvazi, S., Babaeipour, V. & Tarhriz, V. (2020). Antimicrobial Peptides (AMPs): Roles, Functions and Mechanism of Action. *International Journal of Peptide Research and Therapeutics*, 26(3): 1451–1463. DOI:10.1007/s10989-019-09946-9

Sopialena, Suyadi, Jannah, R. & Tantiani, D. (2021). Control of bacterial leaf blight disease in several varieties of rice plants (*Oryza sativa* L.) by using bacteria of *Paenibacilus polymyxa* Mace. *IOP Conference Series: Earth and Environmental Science*, 800(1): 12026. DOI:10.1088/1755-1315/800/1/012026

Tassanakajon, A., Somboonwiwat, K. & Amparyup, P. (2015). Sequence diversity and evolution of antimicrobial peptides in invertebrates. *Developmental & Comparative Immunology*, 48(2): 324–341. DOI:10.1016/j.dci.2014.05.020

Toh, W.K., Loh, P.C. & Wong, H.L. (2019). First Report of Leaf Blight of Rice Caused by *Pantoea ananatis* and *Pantoea dispersa* in Malaysia. *Plant Disease*, 103(7): 1764–1764. DOI:10.1094/PDIS-12-18-2299-PDN

Yuan, C., Zheng, X., Liu, K., Yuan, W., Zhang, Y., Mao, F. & Bao, Y. (2022). Functional Characterization, Antimicrobial Effects, and Potential Antibacterial Mechanisms of NpHM4, a Derived Peptide of *Nautilus pompilius* Hemocyanin. *Marine Drugs*, 20(7): 459. DOI:10.3390/md20070459

Zainol, M.K., Abdul Sukor, F.W., Fisal, A., Tuan Zainazor, T.C., Abdul Wahab, M.R. & Zamri, A.I. (2021). Optimization of enzymatic protein hydrolysis conditions of Asiatic hard clam (Meretrix meretrix). *Food Research*, 5(4): 153–162. DOI:10.26656/fr.2017.5(4).701

Zakaria, F., Tan, J.-K., Mohd Faudzi, S.M., Abdul Rahman, M.B. & Ashari, S.E. (2021). Ultrasound-assisted extraction conditions optimisation using response surface methodology from Mitragyna speciosa (Korth.) Havil leaves. *Ultrasonics Sonochemistry*, 81: 105851. DOI:10.1016/j.ultsonch.2021.105851

Borneo Journal of Resource Science and Technology (2025), 15(1): 81-96
DOI: https:doi.org/10.33736/bjrst.6088.2025

Pharmacological Properties and Health Benefits of *Aquilaria* Leaf Extract: A Review of its Antioxidant, Antidiabetic, Antimicrobial, Anti-Inflammatory, and Gastrointestinal Regulation Effect

NADIA NABILA MOHD KODEEM[1], BALKIS A TALIP*[1], KHAIRUNNISA ABDHUL MUTHALIB[1], MOHAMAD IKHWAN JAMALUDIN[2], ABD FATHUL HAKIM ZULKIFLI[3], NORHAYATI MUHAMMAD[1], HATIJAH BASRI[1], NUR HAFIZAH MALIK[1] & HAZIAN SALLEH[4]

[1]Department of Technology and Natural Resources, Faculty of Applied Sciences and Technology, Universiti Tun Hussein Onn Malaysia, Pagoh Higher Education Hub, KM1 Jalan Panchor, 84600, Panchor, Johor, Malaysia; [2]BioInspired Device and Tissue Engineering Research Group, School of Biomedical Engineering and Health Sciences, Faculty of Engineering, Universiti Teknologi Malaysia, Skudai 81300, Johor, Malaysia; [3]Centre of Automotive and Powertrain Technology, Faculty of Engineering Technology, Universiti Tun Hussein Onn Malaysia, Pagoh Higher Education Hub, KM1 Jalan Panchor, 84600, Panchor, Johor, Malaysia; [4] Synergy One Holding Sdn Bhd., Blok 3A, MTDC-UTM Technology Centre, Technology Park, 81300, Skudai, Johor.
*Corresponding email: balkis@uthm.edu.my
Received: 18 September 2023 Accepted: 10 February 2025 Published: 30 June 2025

ABSTRACT

Aquilaria or Karas tree belongs to the *Thymelaeaceae* family, a famous agarwood producer. This plant is widely distributed in the Indomalesia region, including Malaysia. Recently, these plants have attracted the attention of researchers. Infected wood resin from *Aquilaria* plants, also known as agarwood, is widely used for perfume production, religious and medicinal purposes. Due to the long development time of the plants and the need to inoculate them to initiate agarwood resin production, farmers have sought an alternative source of income by marketing the leaves of the *Aquilaria* tree. *Aquilaria* leaves are also known to have antioxidant, antidiabetic, antimicrobial, and anti-inflammatory properties and are commonly used to regulate the gastrointestinal tract. In contrast to the abundant benefits of the *Aquilaria* leaves, there were lacking reports on the cytotoxicity of the leaves and their extract. Therefore, this review investigates and points out the pharmacological properties of Aquilaria leaves, their human health benefits, and toxicity of the leaves based on the in-vitro and in-vivo studies as it is crucial for safety consumption and downstream applications, including food and beverages, pharmaceutical and cosmeceutical industry.

Keywords: *Aquilaria* leaves, pharmacological properties, toxicity effect

INTRODUCTION

Aquilaria spp., also commonly acknowledged as agarwood, karas, or oudh (Maharani *et al*., 2016; Surjanto *et al*., 2019), is a member of the Thymelaeaceae that is extensively dispersed in Southern Asia and is readily available in Malaysia (Kenzo *et al*., 2019; Razak *et al*., 2019; Surjanto *et al*., 2019). *Aquilaria* trees are massive, rapid-growing, and can reach heights of 30 meters and diameters of 2.5 meters (Razak *et al*., 2019; Zainurin *et al*., 2020).

This genus contains 21 species, 13 of which are agarwood producers. *Aquilaria malaccensis*, *Aquilaria rostrata*, *Aquilaria microcarpa*, *Aquilaria beccariana*, and *Aquilaria hirta* are the most common species in Malaysia. On the other hand, the species of *Aquilaria subintegra* and *Aquilaria sinensis* are native to southern Thailand and China, respectively. In addition, *Aquilaria crassna* is widely distributed in Cambodia, Laos, Vietnam, and northern Thailand (Lee & Mohamed, 2016; Adhikari *et al*., 2021).

Historically, each part of the Aquilaria tree has been beneficial for its use in food and beverages and its medicinal and cosmetic applications (Zakaria *et al*., 2020). Agarwood or a dark resinous stem part cannot be produced by *Aquilaria* trees, whether wild or cultivated, unless they have been externally injured by physical damage, insect feeding, or microbial

infection (Zhang *et al*., 2012). Agarwood resin is one of the costliest natural products in the world (Zakaria *et al*., 2020).

However, the difficulty of resin formation leads to unlawful deforestation and a reduction of the *Aquilaria* plant population (Desa *et al*., 2021). In addition, agarwood production has been inconsistent and rampant illegal logging, which poses a threat to agarwood propagation is leading to an increase in the planting of agarwood trees to compensate for insufficient supply (Desa *et al*., 2021; Lee & Mohamed, 2016). Besides the agarwood resin, the hydrosol from the agarwood essential oil hydro distillation is the secondary product, which consists of the water-soluble compound. Globally, it has been diluted for human consumption (Kahar *et al*., 2021).

Due to the plant's long growing season and the need for induction to produce dark resinous stem or agarwood, farmers have sought profitable alternatives (Adam *et al*., 2017). While *Aquilaria* leaves are usually considered waste during pruning, they can be used as income substitutes while awaiting agarwood formation (Wangiyana *et al*., 2022). According to Zakaria *et al.* (2020), *Aquilaria* leaves have a tremendous potential for therapeutic use. In ancient times, *Aquilaria* leaves were traditionally used to treat trauma, hypertension, constipation, diabetes, headaches and digestive ailments (Zhou *et al.*, 2008; Kakino *et al*., 2010[a]; Prakhanon *et al*., 2011).

Rashid *et al*. (2020) reported that dried *Aquilaria* leaves contain crude fibre, protein and carbohydrates suitable for usage in the food and beverages industries. These include tea in bags or with other foods such as ice cream, cookies, or coffee (Adam *et al*., 2017). According to Hsiao *et al.* (2021), *Aquilaria* leaves are used to make a nourishing herbal tea, and consumption steadily rises over time (Adam *et al*., 2017). In Malaysia, *Aquilaria* leaves are used as an ingredient in tea and coffee. The cultivation area in Malaysia has become a tourist attraction that allows visitors to admire the landscape while drinking tea made from *Aquilaria* leaves, such as in Hoga Gaharu Tea Valley, Gopeng, Perak. *Aquilaria* leaf extract is also an active ingredient in coffee formulation to enhance the health benefits of coffee products such as HOGA coffee and Black Gaharu, which have several flavours, including mocha latte, matcha, and classic black.

Furthermore, *Aquilaria* leaves have also been utilised to manufacture tea in Indonesia, which is one of the potential herbal product advancements (Wangiyana *et al*., 2022). Research and development of *Aquilaria* leaf tea in Indonesia has thoroughly addressed the finished product selection of raw materials, processing, safety, and marketing. To date, there are seven brands of *Aquilaria* leaf teas in Indonesia (Wangiyana *et al*., 2022).

The consumption of *Aquilaria* can bring health benefits to humans. *Aquilaria* leaves are highly abundant and available, allowing their use for commercial purposes and capable of becoming new prospects for product development. The excellent pharmacological properties of *Aquilaria* leaves can be utilised as an ingredient for downstream applications, including in the food and beverage, pharmaceutical and cosmeceutical industries.

On the other hand, consuming plant leaves-based products and herbs might have side effects and toxicity concerns towards human health. This issue leads to the in-vitro and in-vivo toxicity tests, which can help determine the toxicity level of the product. In this case, many toxicity studies of *Aquilaria* leaves and their extract have been conducted by the researcher. However, the study of the cytotoxicity of *Aquilaria* leaves is too scattered. Therefore, in this review, the pharmacological effects and toxicity of the *Aquilaria* leaves are discussed and organised.

Materials and Methods

This review article searched all literature using six databases: Google Scholar, Elsevier, PubMed, Web of Science, local books, and thesis dissertation. The keywords used for identification of the sources were "*Aquilaria* leaves", or "agarwood leaves", "antioxidant activity of *Aquilaria* leaves", "antidiabetic properties of *Aquilaria* leaves", or "antibacterial properties of *Aquilaria* leaves" or "anti-inflammatory properties of *Aquilaria* leaves" or "laxative properties of *Aquilaria* leaves" or "cytotoxicity of *Aquilaria* leaves". All articles or books regarding *Aquilaria* leaves were taken from 2008 until 2023.

This article delves deeper into the pharmacological properties and cytotoxicity of *Aquilaria* leaves and their extract. Moreover, in order to improve the sensitivity of searched data, the top 250 from searched databases, ordered by relevance, including journal articles, proceedings, books, and dissertations, were included in the study. Non-English periodicals were omitted, and the review focused solely on English content to ensure clear interpretation.

Pharmacological properties of *Aquilaria* leaves

Natural bioactive substances found in plants are known as phytochemicals and are divided into two categories according to function in plant metabolism: primary and secondary metabolites. Amino acids, chlorophyll, proteins, and carbohydrates are primary metabolites, while alkaloids, phenolic compounds, and terpenoids are secondary metabolites (Krishnaiah *et al*., 2009).

While the bioactivity of *Aquilaria* has been highly appreciated and has recently piqued the curiosity of researchers in recent years, it has not yet been adequately explored (Hsiao *et al.*, 2021). Various phytochemical compounds are found in *Aquilaria* leaves, and all of these compounds are related to pharmacological properties (Ridwanti *et al*., 2020). Studies have shown that flavonoid and 2-(2-phenylethyl) chromone are the predominant constituents in *Aquilaria* leaves (Wang *et al*., 2018).

Aquilaria leaves consist of many chemical constituents, including chromones, phenolic acids, steroids, fatty acids, benzophenones, xanthonoids, flavonoids, terpenoids, and alkanes that provide various benefits towards human health (Adam *et al*., 2017; Razak *et al*., 2019). Mangiferin, genkwanin, genkwanin-5-O-β-primeveroside, iriflophenone 2-O-α-L-rhamnopyranoside, iriflophenone 3-C-β-D-glucoside, and iriflophenone 3,5-C-β-D-diglucopyranoside have been recognised as potent phenolic compounds in the *Aquilaria* leaves (Hashim *et al*, 2016; Ibrahim, 2016). This review focuses on the potential of antioxidant, antidiabetic, antibacterial, anti-inflammatory and laxative effects in *Aquilaria* leaves.

Antioxidant Properties

The production of reactive oxygen species (ROS), which are necessary for tissue homeostasis and cell communication, occurs due to regular physiological activities. Unfortunately, too many radical species negatively affect cells and promote various diseases, including damage to DNA, lipids, and proteins (Su *et al*., 2019). Antioxidants can break down ROS and neutralise metabolically active products to protect cells from oxidative damage associated with illnesses such as ageing, cancer, and diabetes (Wil et *al.*, 2014). The antioxidant and phenolic compounds, which comprise phenolic acids, tannins, and flavonoids, are plentiful in plants, especially in the leaves (Batubara *et al*., 2018; Surjanto *et al*., 2019). According to Batubara *et al*. (2018), *Aquilaria* leaves have high antioxidant activity.

The study by Surjanto *et al*., (2019) reported in North Sumatera, Indonesia, showed that *A. malaccensis* leaves collected in the Sigiring-giring village contain terpenoids and saponins. The leaves of *A. malaccensis* from S. Kalangan II have tannins and saponins. The 50 % inhibition concentration (IC50) of 2,2-diphenyl-1-picrylhydrazyl (DPPH) assay showed that the leaf extract from S. Kalangan II was higher than that from Sigiring-giring village (Surjanto *et al*., 2019). The secondary metabolites component is influenced by extrinsic factors, which include humidity, temperature, precipitation and solar radiation, which are usually related to the geographical location, climate and soil composition (Xu *et al*., 2022; Ciocan *et al*., 2023)

In addition, Hendra *et al*. (2016) examined the antioxidant activity of *A. malaccensis* leaves regarding the effects of different stages of leaf maturity with different solvents as extraction mediums on antioxidant activity. The free radical scavenging inhibition (IC50) indicates that the old, matured leaves with methanol extraction had the highest antioxidant compared to young leaves, which are 19.62 ± 1.49 μg/ml and 68.52 ± 2.12 μg/ml, respectively. The growth-differentiation balance theory proposes that longer-growing plant parts have more defensive resources, enhancing antioxidant activity in old leaf extract due to more secondary metabolites (Hendra *et al*., 2016). Moreover, the development process of the leaf leads to an

increase in photosynthesis capability and antioxidant activity (Nadeem & Zeb, 2018).

In contrast, a study by Wongwad *et al*. (2019) reported that the DPPH scavenging assay revealed that extracts from young leaves demonstrate significantly higher antioxidant activity compared to those from mature leaves. The IC50 values for young leaf extracts ranged from 13.3 to 26.5 μg/mL, whereas for mature leaf extracts, the IC50 values were between 37.5 and 71.4 μg/mL. This finding aligns with recent studies by Kuntorini *et al*. (2022), which discovered that ethanol extracts from green fruits and young leaves have more antioxidant activity than older leaves. The younger leaves had a higher flavonoid content, which contributed to their increased antioxidant activity.

Regarding their phytochemical properties, Huda *et al*. (2009) reported that *A. malaccensis* leaves contain antioxidants. In this regard, phytochemical screening shows the presence of alkaloids, steroids, saponins, and flavonoids in *A. malaccensis* leaf extract. As a result, all crude extract of *A. malaccensis* has a high potential as an antioxidant source, especially methanol crude (Huda *et al*., 2009).

Based on the DPPH assay and 2,2'-azino-bis (3-ethylbenzthiazoline-6-sulphonic acid) (ABTS) radical assay, flavonoids isolated from ethanolic extract of *A. sinensis* leaves have potential antioxidant activity (Duan *et al*., 2015). In addition, Yang *et al.* (2018) isolated flavonoids from wild *A. sinensis* leaves using sophisticated high-speed counter-current chromatography and a multilayer spiral separation column. The four isolated flavonoids showed nitrite scavenging behaviours, namely apigenin-7,4′-diethyl ether, genkwanin, quercetin, and kaempferol. Figure 1 shows quercetin is the most effective nitrite scavenging, while kaempferol exhibited the least nitrite scavenging properties (Yang *et al*., 2018). Hence, *Aquilaria* leaves can be incorporated into food and beverage products or utilised in pharmaceutical and cosmetic products as they can reduce free radicals and disease occurrence.

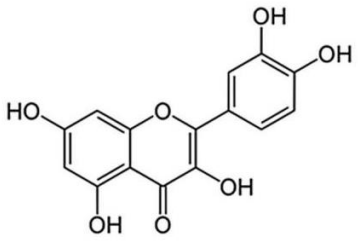

Quercetin

Figure 1. Quercetin chemical compound

Anti-diabetic Properties

Diabetes is a growing non-communicable disease affecting up to 693 million adults (Saeedi *et al*., 2019), increasing the risk of mortality, blindness, and kidney failure (Cole & Florez, 2020). According to the American Diabetes Association (2021), there are four types of diabetes: Type I, Type II, specialised types, and gestational diabetes mellitus. In 2019, over 463 million adults had type 2 diabetes due to obesity, inactivity, and unhealthy dietary habits (Tsunoda *et al*., 2022). Diabetes can be treated by decreasing glucose absorption in the intestine, using α-glucosidase inhibitors to slow glucose uptake (He *et al*., 2014; Ezzat *et al*., 2017; Tsunoda *et al*., 2022).

Acarbose, the first microorganism-derived drug approved in Europe and the United States, has been found to lower HbA1c and lipid profile better than metformin (He *et al*., 2014; Tsunoda *et al*., 2022). However, prolonged use can lead to gastrointestinal problems (He *et al*., 2014). Lifestyle changes and pharmacological treatment using drugs can help minimise diabetes-related mortality and morbidity (Marín-Peñalver *et al*., 2016; Blaslov *et al*., 2018), but they may also result in autoimmune assaults, β-cell dysfunction, and insulin resistance in people with diabetes mellitus (Manukumar *et al*., 2017).

Formulations from herbal sources are favoured because they are cost-effective and can prevent secondary complications while posing a minimal risk of complication (Manukumar *et al.*, 2017). Yin *et al*. (2014) and Elbashir *et al*. (2018) discovered that several medicinal plants have significant potential as natural antidiabetic medicines due to their high antioxidant and antidiabetic potential. Thitikornpong *et al*. (2019) reported that the *A. crassna* leaves and isolated mangiferin have a higher α-glucosidase inhibitory effect than acarbose, which is 0.1840 ± 0.0032, 0.5714 ± 0.0044, and 17.3947 ± 0.0189 mg/mL respectively. In this light, mangiferin, as shown in Figure 2, is a vital compound attributed to the antidiabetic properties of *Aquilaria* leaves.

Zulkiflie *et al*. (2013) reported the potential of local *Aquilaria spp.* leaves can be used as antidiabetic drugs. Methanolic extract of *A. malaccensis* and *A. hirta* inhibited α-amylase and α-glucosidase enzymes more effectively than acarbose. The inhibition percentages for α-glucosidase for *A. malaccensis* and *A. hirta* at 1000 µg/ml are higher than acarbose, about 35.14% and 36.42%, respectively. The inhibition percentages for α-amylase for *A. malaccensis* and *A. hirta* at 1000 µg/ml are higher than acarbose, about 23.04% and 18.23%, respectively. The phenolic compounds responsible for the α-glucosidase inhibitory properties of the 70% aqueous ethanolic extract of the leaves of A. sinensis are mangiferin, iriflophenone 3,5-C-β-D-glucopyranoside, iriflophenone 3-C-β-D-glucoside and iriflophenone 2-O-α-L-rhamnopyranoside in which the mangiferin has the highest potency of α-glucosidase inhibitor (Feng *et al.*, 2011).

In addition, iriflophenone 3-C-glucoside (IPG), a compound isolated from *A. sinensis*, was shown in in vitro and in vivo experiments to have a high potential to lower fasting blood glucose levels in mice with streptozotocin (STZ)-induced diabetes and to increase glucose uptake in adipocytes. In this research, IPG was isolated from the leaf extract of *A. sinensis* leaf extract using column chromatography before it was induced in fasting STZ mice. IPG can reduce blood glucose levels by 46.4% and increase glucose uptake by 53% in rats (Pranakhon *et al.*, 2015).

Air-dried *A. malaccensis* leaves extracted with methanol showed the highest α-glucosidase enzyme inhibitory activity, whereas ethanol, chloroform, water, and hexane extract showed shallow values. Methanol appears to be the most effective solvent for *Aquilaria* leaf extraction compared to water and chloroform. Air-dried samples exhibited better α-glucosidase inhibition activity than oven-dried samples. This might be because the oven's high drying temperature destroys some compounds involved in the antidiabetic activity (Ahmad *et al*., 2019).

Both the aqueous and methanol extracts of *A. malaccensis* leaves efficiently reduced normal glucose levels of male ICR mice with streptozotocin diabetes at 50 mg /kg body weight (Fayyadh *et al*., 2020). Furthermore, Said *et al.* (2016) stated that the ethanol and ethyl acetate extract of *A. malaccensis* leaves increased glucose transporter 4 (GLUT4) in the skeletal muscle of diabetic Wistar rats when induced by 0.01 g/kg body weight of *A. malaccensis* leaf extract (Said *et al.*, 2016). Therefore, this shows that *Aquilaria* leaves can be used as green sources of diabetic medication treatment with lower side effects on human health. Table 1 illustrates the antidiabetic activity of *Aquilaria* leaves.

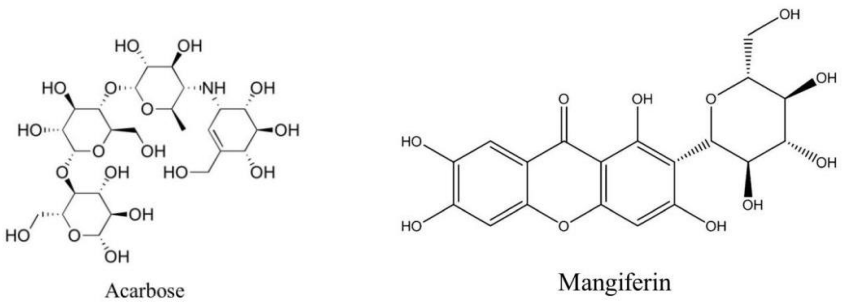

Figure 2. Chemical structure of the acarbose, a drug for Type II diabetes mellitus and mangiferin, an antidiabetic bioactive compound found in *Aquilaria* leaves

Table 1. Antidiabetic activity of the *Aquilaria* leaves

Species	Experiment	Sample tested	Results	References
Aquilaria crassna	α-glucosidase inhibition (IC50)	Leaves extract	0.1840 ± 0.0032 mg/mL	Thitikornpong *et al*. (2019)
		Isolated mangiferin	0.5714 ± 0.0044 mg/mL	
Aquilaria hirta	α-glucosidase inhibition (IC50)	Methanol extract	452.82 µg/mL	Zulkiflie *et al.* (2013)
	α-amylase inhibition (IC50)	Methanol extract	301.99 µg/mL	Zulkiflie *et al.* (2013)
Aquilaria malaccensis	α-glucosidase inhibition (IC50)	Air dried (leaves) ethanolic extract	396.12 ± 6.42 µg/mL	Ahmad *et al.* (2019)
		Air dried (leaves) methanolic extract	196.31 ± 4.11 µg/mL	
		Oven-dried (leaves) ethanolic extract	295.37 ± 5.42 µg/mL	
		Oven-dried (leaves) methanolic extract	598.22 ± 418 µg/mL	
	α-glucosidase inhibition (IC50)	Methanol extract	375.50 µg/mL	Zulkiflie *et al.* (2013)
	α-amylase inhibition (IC50)	Methanol extract	397.23 µg/mL	Zulkiflie *et al,* (2013)
	Glucose uptake in skeletal muscle on rats	Ethanol fraction	Increase the level of GLUT4 by 24.5%	Said *et al*. (2016)
		Ethyl acetate fraction	Increase level of GLUT4 by 20.6%	
Aquilaria sinensis	α-glucosidase inhibition (IC50)	Mangiferin	126.5 ± 14.5 µg/mL	Feng *et al*. (2011)
		Iriflophenone 2-O-a-L-rhamnopyranoside	143.7 ± 10.6 µg/mL	
		Iriflophenone 3-C-b-D-glucoside	165.1 ±11.3 µg/mL	
		Iriflophenone	138.3 ±7.3 µg/mL	
	Test of glucose uptake on rats	Iriflophenone 3-C-β-glucoside	Increase glucose uptake 53% and reduce blood glucose by 46%	Pranakhon *et al*. (2015)

Antibacterial Properties

There are many types of antibiotics widely used in the world. Antibiotics interfere with bacterial cells, including attacking cell walls, inhibiting protein biosynthesis, inhibiting the DNA replication process, and inhibiting folic acid metabolism (Kapoor *et al*., 2017). *Aquilaria* leaves have been reported to have antibacterial properties against various microorganisms. Microorganisms were treated with or exposed to *Aquilaria* leaf extract to observe the effect on the cell. Kammonwannasit *et al.* (2013) reported that cells of the *Staphylococcus epidermidis* treated with extracts swelled and the cell wall ruptured.

The ethanol extract of *A. macrocarpa Baill* also had a minimum inhibitory concentration (MIC) of 1.0 mg/ml against *Staphylococcus aureus* and *Bacillus cereus*, 1.25 mg/mL against *Staphylococcus epidermidis, Pseudomonas aeruginosa, Bacillus subtilis,* and *Escherichia coli*, and 10 mg/mL against *Salmonella typhi* and *Proteus mirabilis* (Sari *et al.*, 2019).

According to Jihadi (2020), an ethanolic leaf extract of *A. malaccensis* proved efficient against multidrug-resistant Gram-negative bacteria. The minimal inhibitory concentrations for *Acinetobacter baumannii* and *Klebsella pneumonia* (ATCC 10031) were 32 mg/mL and 64 mg/mL for *Escherichia coli* and *Klebsella pneumonia* (ATCC 700603), respectively. Furthermore, Sari *et al*. (2019) discovered that the ethanolic extract of *A. malaccensis* had a MIC of 1.25 mg/ml against *Staphylococcus aureus, Bacillus cereus, Staphylococcus epidermidis, Pseudomonas aeruginosa, Bacillus subtilis, Escherichia coli, Salmonella typhi*, and *Proteus mirabilis.*

Furthermore, significant antibacterial activity against *Salmonella enterica and Staphylococcus aureus* has been determined in oven-dried leaves of *A. malaccensis* hexane extract at 150 and 300 mg/ml, respectively (Ahmad *et al.*, 2019). The chloroform extract from *A. malaccensis* also inhibited the culture of gram-positive and gram-

negative bacteria, including *Shigella boydii* and *Escherichia coli* (Begum, 2016).

Freeze-dried aqueous extract of A. crassna leaves also showed inhibition against *Staphylococcus epidermidi*s at a 6 mg/ml concentration. The bacterial cells were swollen and disrupted by the extract, and bacterial biofilm development was suppressed. The bacterial cell wall broke down after 24 hours of treatment with the extract (Kamonwannasit *et al.,* 2013).

Dash *et al.* (2008) performed antimicrobial determination of an aqueous extract of *A. malaccensis* leaves at a concentration of 50 mg/ml and showed zonation inhibition in *Shigella flexneri* and *Pseudomonas aeruginosa* at 18 mm and 15 mm, respectively. In addition, the methanolic extract of *A. malaccensis* at a concentration of 50 mg/ml showed inhibition of *Shigella flexneri, Pseudomonas aeruginosa*, and *Bacillus subtilis* with 15 mm, 14 mm and 15 mm, respectively (Dash *et al.,* 2008). Thus, the antibacterial properties of *Aquilaria* leaves can be used to develop pharmaceutical and cosmetic products such as anti-acne products and wound treatment. The antibacterial activity of *Aquilaria* leaf is shown in Table 2.

Table 2. Antimicrobial activity of the *Aquilaria* leaves

Species	Extraction	Assay	Microogranism	Result	Reference
Aquilaria microcarpa	Ethanolic extract	Disc diffusion method	*Escherichia coli*	6.11 ± 0.02 mm	Sari *et al.* (2019)
			Staphylococcus aureus	6.12 ± 0.02 mm	
			Bacillus cereus	6.07 ± 0.02 mm	
	Ethanolic extract	MIC	*Escherichia coli*	1.25 mg/mL	
			Staphylococcus aureus, Bacillus cereus	1.25 mg/mL	
Aquilaria crassna	Aqueous extract	MIC	*Staphylococcus epidermidis*	6.00 mg/mL	Kammonwannasit *et al.* (2013)
		Determination of minimum bactericidal concentration	*Staphylococcus epidermidis*	12 mg/mL	
Aquilaria malaccensis	Ethanolic extract	Disc diffusion method	*Escherichia coli*	6.39 ± 0.02 mm	Sari *et al.* (2019)
			Staphylococcus aureus	6.73 ± 0.02 mm	
			Bacillus cereus	6.81 ± 0.02 mm	
	Ethanolic extract	MIC	*Escherichia coli, Staphyococcus aureus, Bacillus cereus*	1.25 mg/ml	
	Aqueous extract	Disc diffusion method	*Escherichia coli, Staphyococcus aureus*	6.67 mm	Hendra *et al.* (2016)
	Methanolic extract			6.83 mm	
Aquilaria agallocha	Methanolic extract	Agar cup plate method	*Bacillus subtillis*	19.00 mm	Dash *et al.* (2008)

Anti-inflammatory Properties

Inflammation occurs in response to the invasion of foreign organisms, such as pathogenic microorganisms and dust particles, that begin to disrupt the process of tissue repair and restoration of normal body homeostasis to protect the body (Arulselvan *et al.*, 2016; Azab *et al*., 2016; Eissa *et al.,* 2020). Inflammation is classified into two groups: acute inflammation, which is a simple process that can continue for a few minutes or up to a few days, and whose main characteristic is the leakage of plasma proteins or fluid and the movement of leukocytes to extravascular areas, and chronic inflammation, an essential response of the body's immune system (Arulselvan *et al.*, 2016). Several studies have reported that inflammation causes chronic and degenerative diseases (Arulselvan *et al.*, 2016; Eissa *et al*., 2020).

In the meantime, synthetic anti-inflammatory drugs can have intolerable side effects on human health, such as organ damage, developmental disorders, and gastrointestinal bleeding (Eissa *et al*., 2020; Wojcieszyska *et al*., 2022). Thus, herbal drinks are recognised globally as a traditional medicine capable of reducing inflammation. Researchers are interested in developing efficient and safe bio-based alternative chemicals for treating and preventing inflammation to avoid the adverse effects of synthetic drugs (Eissa *et al*., 2020). Polyphenolic compounds can be anti-inflammatory agents by lowering the release of inflammatory mediators and stabilising cell membranes (Adam *et al*., 2017).

Aquilarinoside A, iriflophenone, 7-b–D-glucoside of 5-O-methyl apigenin, 5-O-xylosylglycoside of 7-O-methyl apigenin, luteolin, genkwanin, hydroxygenkwanin, aquisiflavoside, iriflophenone 3,5-C-β-D-diglucoside, iriflophenone 3-C-β-D-glucoside, mangiferin, and genkwanin 5-O-β-primevoside have been attributed anti-inflammatory properties in *Aquilaria* leaves (Eissa *et al*., 2020). Qi *et al.* (2009) found that hydroxygenkwanin and luteolin (Figure 3) were compounds with IC50 of 0.80 ± 0.13 µmol/L and 2.03 ± 0.24 µmol/L respectively, that had the highest inhibitory activity against neutrophil respiratory burst.

Eissa *et al.* (2018) showed that the in-vitro study of leaf extract of *A. malaccensis* inhibited protein (albumin) denaturation in a dose-dependent manner in the studied concentration range of 400-16000 g/mL. In addition, the aqueous extract of *A. crassna* was reported to have potent inhibition of interleukin-1α (IL-1α) and interleukin-8 (IL-8), while 70% of the ethanol extract displayed inhibition of IL-1α only (Wongwad *et al.*, 2019). Besides, a single oral administration with *A. sinensis* leaf extract at a dose of 848 mg/kg can minimise the inflammation generated by xylene or carrageenan injection into the paw of mice (Zhou *et al.*, 2008, as referenced in Chiangsaen *et al.*, 2016).

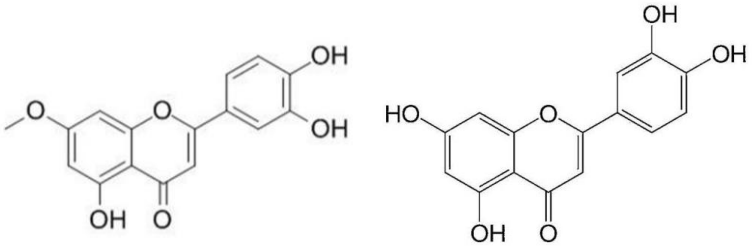

Figure 3. Chemical compounds found in *A. malaccensis* leaf that have a significant anti-inflammatory effect

Gastrointestinal Regulation (Laxative Effect)

Constipation could lead to intestinal obstruction in the human gastrointestinal tract due to the difficulty and pain in the movement of stiff stools. This issue should be treated promptly, as severe constipation might require surgery (Forootan *et al.,* 2018). There are two significant causes of constipation. First, the main reason is the slow movement of stool or constipation of the bowel outlet. The second reason is inadequate water intake, metabolic disorders, medication use, neurological disorders, myopathic disorders, and structural abnormalities (Jani & Marsicano, 2018).

Jani and Marsicano (2018) reported that patients suffering from constipation should increase their fibre and water intake, exercise healthily, and regularly perform toilet training. Apart from this practice, patients are also advised to take medications with laxative effects, such as lubiprostone, linaclotide, magnesium oxide, and sennoside (Figure 4) (Kakino *et al.,* 2010[a]; Kakino *et al.,* 2010[b]; Forootan *et al*., 2018). When the laxative agent is ingested, the laxative helps retain fluid or water in the stool to soften the consistency, increase secretion in the bowel, lubricate the stool movement and decrease the surface tension (Portalatin & Winstead, 2012; Bashir & Sizar, 2019)

However, ingestion of linaclotide affects visceral afferent neurons and reduces nociception, whereas ingestion of lubiprostone causes mild to moderate nausea and diarrhoea (Wilson & Schey, 2015). Furthermore, medications commonly used for constipation treatment, such as magnesium oxide or sennoside, the primary component of senna, lead to severe diarrhoea (Kakino *et al.*, 2010[a]). This could be due to genkwanin 5-O-β-primeveroside (Figure 4) and mangiferin, which exhibit laxative properties (Kakino *et al*., 2010[b]). Hence, this shows that the *Aquilaria* leaves can be used to develop medication for constipation and bowel movement problems as the leaves can exhibit laxative properties. Several studies have reported that *Aquilaria* leaves have a laxative effect on constipation (Table 3) (Hara *et al*., 2008; Kakino *et al*., 2010[a]; Kakino *et al*., 2010[b]; Ito *et al*., 2012).

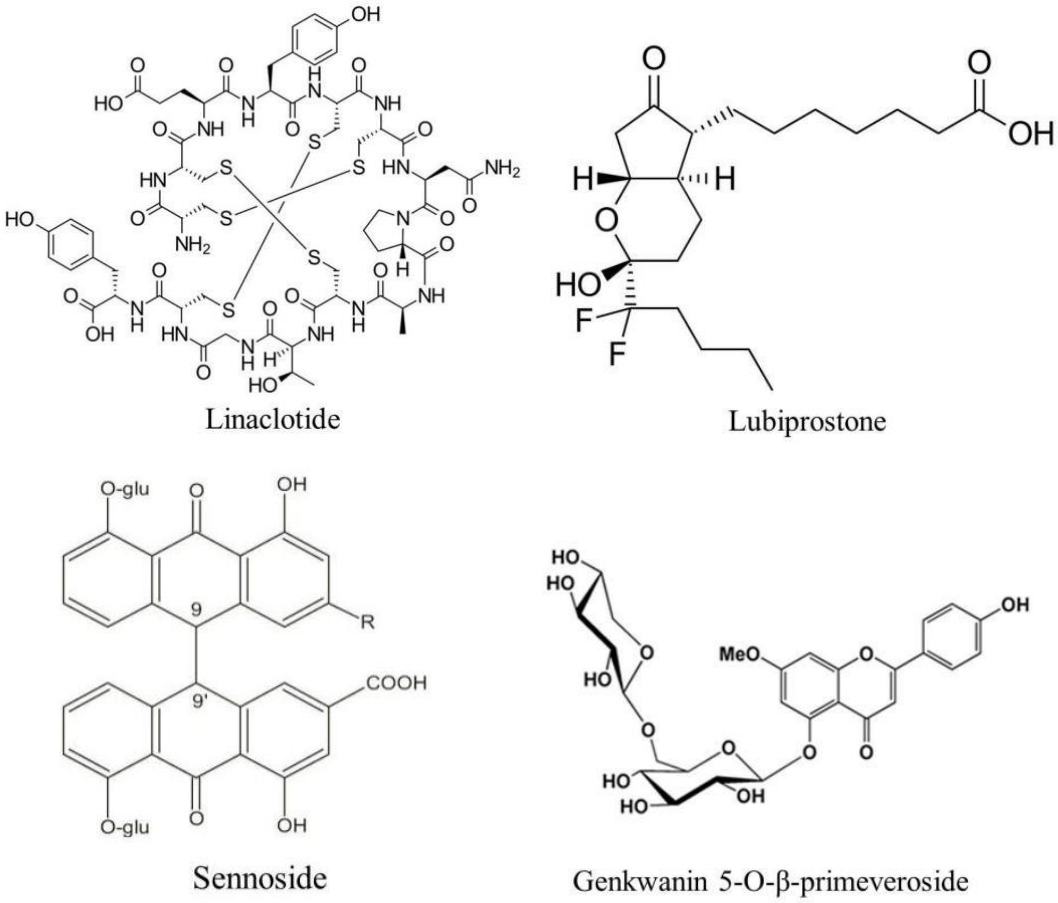

Figure 4. The chemical compound of the drugs for gastrointestinal disease, linaclotide lubiprostone, sennoside, and genkwanin 5-O-β-primeveroside

Table 3. Laxative effect of *Aquilaria* leaves

Species	Test conducted	Sample tested	Results	References
A. sinensis	In vivo test on rat / mice	Ethanol extract	Restored the stool frequency and weight to about 91 to 99 %	Kakino *et al*., (2010[b])
		Acetone–methanol extract	Reduced the diarrhea frequency in mice	Hara *et al.*, (2008)
A. crassna		Ethanol extract	Restored the stool frequency and weight to about 111 to 116 %	Kakino *et al*., (2010[b])
		Ethanol extract	Several compounds isolated from the extract are capable of increasing the stool frequency	Ito *et al*., (2012)

Table 4. Toxicity of *Aquilaria* leaves

Aquilaria species	Sample	Testing subject	Leaves toxicity	Dosage of toxicity	Reference
A. malaccensis	Methanolic extract	Human cells	Cytotoxic activity on peripheral blood mononuclear cells and results in DNA fragmentation	IC50 = 24.5 mg /mL LD50 = 4537 mg/kg	Adam *et al*. (2018)
	Aqueous extract	Rats	Shows toxicity towards liver and kidney of rats	2000 mg/kg	Razak *et al*. (2018)
A. sinensis	Extract	Mice	No symptom of toxicity on mice sperm and bone marrow after oral fed	Not detected	Li *et al.* (2015)
	Extract	*Salmonella* cell	No signs of toxicity with salmonella reversion test	Not detected	Li *et al.* (2015)
A. crassna	Ethanolic extract	Mice	No signs of toxicity	Higher than 2000 mg/kg	Ghan *et al.* (2016)
	Aqueous extract		No sign of abnormalities or death	Higher than 15,000 mg/kg	Kamonwannasit *et al*. (2013)
	Hydro distilled essential oils		No signs of toxicity	LD50 = 2000 mg/kg	Dahham *et al.* (2016).
A. subintegra	Chloroform extract	Brine shrimp	Low to moderate toxicity	LC50=531.18 ± 49.53 µg/mL	Bahrani *et al.* (2014)
		Human cells	No cytotoxic activity	Not detected	Bahrani *et al.* (2014)

Cytotoxicity of *Aquilaria* leaves

Natural product demand has sparked scientific curiosity about their biological impacts. As a result, additional research is required to evaluate their harmful effects and to define acceptable intake thresholds for safe use. This is because some extremely toxic active compounds found in plant extracts or natural goods might harm people (Adam *et al*., 2018).

Inoculation of *Aquilaria* trees using fungi is safe to handle and does not significantly impact the environment (Kahar *et al.*, 2021). Inoculation can be done by physical or mechanical methods, chemistry, and microorganisms (Tan *et al.*, 2019). Chemical induction can have questionable effects on the result of agarwood trees directly or indirectly to humans. However, Tan *et al*. (2019) concluded that the induction mechanism of *Aquilaria* trees only affects the stem part, which leads to the formation of agarwood, while the effect on the leaves and roots is small.

Adam *et al.* (2018) stated that the methanolic extract of *A. malaccensis* had a cytotoxic effect and can be classified as mildly hazardous Class III. *A. malaccensis* leaves methanol extract also causes DNA fragmentation with a comet-like appearance in human peripheral blood mononuclear cells (PBMCs), indicating that it is genotoxic (Adam *et al.*, 2018). Furthermore, *A. malaccensis* was found to be toxic to the liver and kidneys of rats in a sub-acute toxicity study at a concentration of 2000 mg/kg aqueous extract (Razak *et al*., 2018).

According to Bahrani *et al.* (2014), the chloroform extract from *A. subintegra* leaf extract displayed minimal toxicity in the brine shrimp fatality experiment at a concentration of LC50 = 531.18 ± 49.53 g/mL. *A. sinensis (Lour.) Gilg*. leaves had an acute oral LD50 of more than 21.5 g/kg in mice. Each dosing group's micronucleus rate, sperm shape abnormalities, and frequency of reverse mutations were not substantially different from the negative control (Li *et al*., 2015).

Next, the suggested oral LD50 in female mice of crude ethanol extract of *A. crassna* (CE), young leaves containing a mixture of α-tocopherol (α-TOH) and CE/α-TOH is estimated to be more than 2000 mg/kg (Ghan *et al*., 2016). After administering a high dose of 15,000 mg/kg

aqueous extract of *A. crassna* leaves, the mice showed no aberrant toxicity or death (Kamonwannasit *et al.,* 2013). Furthermore, the LD50 of *A. crassna* hydro distilled essential oils in female Swiss mice was more significant than 2000 mg/kg (Dahham *et al.,* 2016). The cytoxicity of *Aquilaria* leaves is shown in Table 4.

CONCLUSION

Aquilaria leaf extract has potent antioxidants and antidiabetic, antibacterial, anti-inflammatory, and laxative effects. The leaves of the species *A. malaccensis, A. sinensis* and *A. crassna* have been shown to have antioxidant properties that inhibit free radical scavenging activity. These leaves have antioxidants which capable of inhibiting free radical scavenging activity. The content of antioxidant-active leaves is influenced by the locations of the cultivated plant, the maturity of the leaves, the type of species, and the method of leaf extraction.

In addition, several bioactive compounds in the *Aquilaria* leaves, including mangiferin, iriflophenone 3,5-C-β-D-glucopyranoside, iriflophenone 3-C-β-D-glucoside, and iriflophenone 2-O-α-L-rhamnopyranoside have potential as an antidiabetic agent. Mangiferin in the leaf extract of *A. sinensis* and *A. malaccensis* has shown the ability to increase glucose transport and decrease blood glucose. In addition, most *Aquilaria* leaves have antibacterial properties against gram-positive and gram-negative bacteria.

Furthermore, *Aquilaria* leaves contain hydroxygenkwanin and luteolin, which have anti-inflammatory properties, while genkwanin 5-O-β-primeveroside has a beneficial laxative effect. Although the extract from *Aquilaria* leaves is generally safe, the extract from the leaves of the species *A. malaccensis* is slightly harmful to the DNA of humans and rats. Therefore, it should be taken only in small amounts.

In conclusion, *Aquilaria* leaves have great potential and are suitable for use in the food and beverages, pharmaceutical and cosmeceutical industries, as they can also benefit human health. *Aquilaria* leaves can be incorporated into food and beverage products and utilised as functional food. Besides, it can be used for medication for diabetics and constipation, as well as a good source of antioxidants. In addition, *Aquilaria* leaves also have good antibacterial and anti-inflammatory properties, which can be used to develop pharmaceutical and cosmetic products. However, further study on the in-vivo cytotoxicity is essential for the safety of the consumer.

CONFLICT OF INTEREST

Authors declare no conflict of interest.

FUNDING

This research was supported by Ministry of Higher Education (MOHE) through Prototype Development Research Grant Scheme (PRGS), PRGS/1/2024/SKK01/UTHM/02/1 for a study framework and Universiti Tun Hussien Onn Malaysia (UTHM) through a Research Enhancement Graduate Grant, RE-GG (vot Q057) for a graduate research assistant.

ACKNOWLEDGMENTS

This research was supported by Ministry of Higher Education (MOHE) through Prototype Development Research Grant Scheme (PRGS), PRGS/1/2024/SKK01/UTHM/02/1 and Universiti Tun Hussien Onn Malaysia (UTHM) through a Research Enhancement Graduate Grant, RE-GG (vot Q057). This research was also conducted in collaboration with Synergy One Holding Sdn. Bhd. as an industry partner.

REFERENCES

Adam, A.Z., Lee, S.Y. & Mohamed, R. (2017). Pharmacological properties of agarwood tea derived from *Aquilaria (Thymelaeaceae)* leaves: An emerging contemporary herbal drink. *Journal of Herbal Medicine*, 10: 37-44. DOI:10.1016/j.hermed.2017.06.002

Adam, A.Z., Tajuddin, S.N., Sudmoon, R., Chaveerach, A., Abdullah, U.H., Mahat, M.N. & Mohamed, R. (2018). Chemical constituents and toxicity effects of leaves from several agarwood tree species (*Aquilaria*). *Journal of Tropical Forest Science*, 30(3): 342-353. DOI:10.26525/jtfs2018.30.3.342353

Adhikari, S.R., Pokhrel, K. & Baral, S.D. (2021). Economic value of agarwood and its prospects of cultivation. *International Journal of Applied Sciences and Biotechnology*, 9(1): 23-31. DOI: 10.3126/ijasbt.v9i1.35984

Ahmad, W.N.A.W., Ali, A.M., Wan Mamat, W.N.A. & Mahmod, N.H. (2019). Evaluation of DPPH free radical scavenging, α-glucosidase inhibitory, and antimicrobial activities of *Aquilaria malaccensis* leaf extracts. *Journal of Agrobiotechnology*, 10(1): 36-45. DOI: 10.13140/RG.2.2.25987.35368

American Diabetes Association. (2021). 2. Classification and diagnosis of diabetes: standards of medical care in diabetes—2021. *Diabetes care*, 44(Supplement_1): S15-S33. DOI:10.2337/dc21-S002.

Arulselvan, P., Fard, M.T., Tan, W.S., Gothai, S., Fakurazi, S., Norhaizan, M.E. & Kumar, S.S. (2016). Role of antioxidants and natural products in inflammation. *Oxidative Medicine and Cellular Longevity*, 2016(1): p.5276130. DOI:10.1155/2016/5276130

Azab, A., Nassar, A. & Azab, A.N. (2016). Anti-inflammatory activity of natural products. *Molecules*, 21(10): 1321. DOI:10.3390/molecules21101321

Bahrani, J.M., Paydar, M. & Rothan, H.A. (2014). Isolation and characterisation of acetylcholinesterase inhibitors from *Aquilaria subintegra* for the treatment of Alzheimer's disease (AD). *Current Alzheimer Research*, 11(2): 1-9. DOI:10.2174/1567205011666140130151344

Bashir, A. & Sizar, O. (2019). *Laxatives.* StatPearls Publishing LLC.

Batubara, R., Hanum, T.I., Risnasari, I., Ginting, H. & Lubis, L.A. (2018). Antioxidant activity and preferences test of agarwood leaves tea (*Aquilaria malaccensis lamk*) based on leaves drying methods. *Proceedings of BROMO Conference, Indonesia*, 2018: 159-163. DOI:10.5220/0008359101590163.

Begum, Y. (2016). Study on agarwood (*Aquilaria malaccensis*) to evaluate antibacterial and antioxidant activities of n-hexane, chloroform and ethyl acetate extracts. *PharmaTutor*, 4(2): 47-50. https://www.pharmatutor.org/magazines/articles/february-2016/study-agarwood-aquilaria-malaccensis-evaluate-antibacterial-antioxidant-activities

Blaslov, K., Naranđa, F.S., Kruljac, I. & Renar, I.P. (2018). Treatment approach to type 2 diabetes: Past, present and future. *World Journal of Diabetes*, 9(12): 209. DOI: 10.4239/wjd.v9.i12.209

Chiangsaen, P., Taepavarapruk, P., Wongwad, E., Ingkaninan, K. & Taepavapruk, N. (2016). Screening of the central nervous system action of agarwood leaves extract in female ovariectomized rats. *Proceedings of the Mae Fah Luang University International Conference 2016, Chiang Rai, Thailand* (21-30).

Ciocan, A.G., Tecuceanu, V., Enache-Preoteasa, C., Mitoi, E.M., Helepciuc, F.E., Dimov, T.V., Simon-Gruita, A. & Cogălniceanu, G.C. (2023). Phenological and Environmental Factors' Impact on Secondary Metabolites in Medicinal Plant Cotinus coggygria Scop. *Plants*, 12(9): 1762. DOI:10.3390/plants12091762

Cole, J.B. & Florez, J.C. (2020). Genetics of diabetes mellitus and diabetes complications. *Nature Reviews Nephrology*, 16(7): 377-390. DOI:10.1038/s41581-020-0278-5

Dahham, S.S., Hassan, L.E.A., Ahamed, M.B.K., Majid, A.S.A., Majid, A.M.S.A. & Zulkepli, N.N. (2016). In vivo toxicity and antitumor activity of essential oils extract from agarwood (*Aquilaria crassna*). *BMC Complementary and Alternative Medicine*, 16(1): 1-11. DOI:10.1186/s12906-016-1210-1

Dash, M., Patra, J.K. & Panda, P.P. (2008). Phytochemical and antimicrobial screening of extracts of *Aquilaria agallocha Roxb*. *African Journal of Biotechnology*, 7(20): 3531-3534. DOI: 10.5897/AJB08.623

Desa, A.P., Lee, S.Y., Mustapa, M.Z., Mohamed, R. & Emang, D. (2021). Trends in the agarwood industry of Peninsular Malaysia. *The Malaysian Forester*, 84(1): 152-168. https://malaysianforester.my/forestry/archives_journal_volume.php?volume=84&nombor=1

Duan, Z.W., Li, W.G., Dou, Z.H., Xie, H., He, A. & Shi, M., (2015). Extraction and antioxidant activity of flavonoids from *Aquilaria sinensis (Lour.) Gilg* leaves. *Journal of Food Science.*, 36, 45-50. DOI: 10.7506/spkx1002-6630-201506009.

Eissa, M.A., Hashim, Y.Z.H.Y., Salleh, H.M., Abd-Azziz, S.S., Isa, M.L.M., Warif, N.M.A., Nor, Y.A., El-Kersh D.M. & Sani, M.S.A. (2020). *Aquilaria* species as potential anti-inflammatory agents–A review on in vitro and in vivo studies. *Indian Journal of Natural Products and Resources*, 11(3): 141-154.

Elbashir, S.M.I., Devkota, H.P., Wada, M., Kishimoto, N., Moriuchi, M., Shuto, T., Misumi, S., Kai H. & Watanabe, T. (2018). Free radical scavenging, α-glucosidase inhibitory and lipase inhibitory activities of eighteen Sudanese medicinal plants. *BMC Complementary and Alternative Medicine*, 18: 1-12. DOI:10.1186/s12906-018-2346-y

Ezzat, S.M., Motaal, A.A. & El Awdan, S.A.W. (2017). In vitro and in vivo antidiabetic potential of extracts and a furostanol saponin from *Balanites aegyptiaca*. *Pharmaceutical Biology*, 55(1): 1931-1936. DOI:10.1080/13880209.2017.1 343358

Fayyadh, A.A., Ibrahim, H., Zain, H.H.M. & Al-Qubaisi, M.S. (2020). The effect of agarwood leaf extracts on blood glucose level of type II diabetes mellitus in ICR male mice. *Research Journal of Pharmacy and Technology*, 13(1): 237-242. DOI : 10.5958/0974-360X.2020.00048.7

Feng, J., Yang, X. W. & Wang, R. F. (2011). Bio-assay guided isolation and identification of α-glucosidase inhibitors from the leaves of *Aquilaria sinensis*. *Phytochemistry*, 72(2-3): 242-247. DOI:10.1016/j.phytochem.2010.11.025

Forootan, M., Bagheri, N. & Darvishi, M. (2018). Chronic constipation: A review of literature. *Medicine*, 97(20). DOI: 10.1097/MD.0000000000010631

Ghan, S.Y., Chin, J.H., Thoo, Y.Y., Yim, H.S. & Ho, C.W. (2016). Acute oral toxicity study of *Aquilaria crassna* and [alpha]-tocopherol in mice. *International Journal of Pharmaceutical Sciences and Research*, 7(4): 1456-1461. DOI: 10.13040/IJPSR.0975-8232.7(4).1456-61

Hashim, Y.Z.H.Y., Kerr, P.G., Abbas, P. & Salleh, H.M. (2016). Aquilaria spp.(agarwood) as source of health beneficial compounds: A review of traditional use, phytochemistry and pharmacology. *Journal of Ethnopharmacology*, 189: 331-360. DOI:10.1016/j.jep.2016.06.055

Hara, H., Ise, Y., Morimoto, N., Shimazawa, M., Ichihashi, K., Ohyama, M. & Iinuma, M. (2008). Laxative effect of agarwood leaves and its mechanism. *Bioscience, Biotechnology, and Biochemistry*, 72(2): 335-345. DOI:10.1271/bbb.70361

He, K., Shi, J.C. & Mao, X.M. (2014). Safety and efficacy of acarbose in the treatment of diabetes in Chinese patients. *Therapeutics and Clinical Risk Management*, 505-511. DOI: 10.2147/TCRM.S50362

Hendra, H., Moeljopawiro, S. & Nuringtyas, T. R. (2016). *Antioxidant and antibacterial activities of agarwood (Aquilaria malaccensis Lamk.) leaves.* Advances of Science and Technology for Society: Proceedings of the 1st International Conference on Science and Technology 2015. Yogyakarta, Indonesia. DOI:10.1063/1.4958565

Hsiao, S.W., Wu, Y.C., Mei, H.C., Chen, Y.H., Hsiao, G. & Lee, C.K. (2021). Constituents of *Aquilaria sinensis* leaves upregulate the expression of matrix metalloproteases 2 and 9. *Molecules*, 26(9): 2537. DOI:10.3390/molecules26092537

Huda, A.W.N., Munira, M.A.S., Fitrya, S.D. & Salmah, M. (2009). Antioxidant activity of *Aquilaria malaccensis (Thymelaeaceae)* leaves. *Pharmacognosy Research*, 1(5): 270-273. https://www.phcogres.com/article/2009/1/5/nil-4

Ibrahim, A. (2016). *Comparative analysis of in vitro bioactivities and phenolic content of leaf extracts from six species of Aquilaria* (Doctoral dissertation, Universiti Sains Malaysia).

Ito, T., Kakino, M., Tazawa, S., Watarai, T., Oyama, M., Maruyama, H., Araki, Y., Hara, H. & Iinuma, M. (2012). Quantification of polyphenols and pharmacological analysis of water and ethanol-based extracts of cultivated agarwood leaves. *Journal of Nutritional Science and Vitaminology*, 58(2): 136-142. DOI:10.3177/jnsv.58.136

Jani, B. & Marsicano, E. (2018). Constipation: evaluation and management. *Missouri Medicine*, 115(3): 236-240. https://www.msma.org/Missouri-Medicine-Library

Kahar, E.E.M., Talip, B.A., Mohd Fauzi, N.A., Kamarulzaman, S.N., Zakaria, F., Muhammad, N., Mamat T.N.A.R. & Basri, H. (2021). Properties and potential of agarwood hydrosol as a drink: A review. *Food Research*, 5(3): 29-35. DOI:10.26656/fr.2017.5(3).382

Kakino, M., Tazawa, S., Maruyama, H., Tsuruma, K., Araki, Y., Shimazawa, M. & Hara, H. (2010[a]). Laxative effects of agarwood on low-fiber diet-induced constipation in rats. *BMC Complementary and Alternative Medicine*, 10(68): 1-8. DOI:10.1186/1472-6882-10-68

Kakino, M., Izuta, H., Ito, T., Tsuruma, K., Araki, Y., Shimazawa, M., Oyama, M., Iinuma, M. & Hara, H. (2010[b]). Agarwood induced laxative effects via acetylcholine receptors on loperamide-induced constipation in mice. *Bioscience, Biotechnology, and Biochemistry*, 74(8): 1550-1555. DOI:10.1271/bbb.100122

Kamonwannasit, S., Nantapong, N., Kumkrai, P., Luecha, P., Kupittayanant, S. & Chudapongse, N. (2013). Antibacterial activity of *Aquilaria crassna* leaf extract against *Staphylococcus epidermidis* by disruption of cell wall. *Annals of Clinical Microbiology and Antimicrobials*, 12(20): 1-7. DOI:10.1186/1476-0711-12-20

Kapoor, G., Saigal, S. & Elongavan, A. (2017). Action and resistance mechanisms of antibiotics: A guide for clinicians. *Journal of Anaesthesiology Clinical Pharmacology*, 33(3): 300. DOI: 10.4103/joacp.JOACP_349_15

Kenzo, T., Yoneda, R., Tanaka-Oda, A. & Azani, M.A. (2019). Growth performance and leaf ecophysiological traits in three *Aquilaria* species in Malaysia. *New Forests*, 50: 699-715. DOI:10.1007/s11056-018-09693-7

Krishnaiah, D., Bono, A., Sarbatly, R., Nithyanandam, R. & Anisuzzaman, S.M. (2015). Optimisation of spray drying operating conditions of *Morinda citrifolia L*. fruit extract using response surface methodology. *Journal of King Saud University-Engineering Sciences*, 27(1): 26-36. DOI:10.1016/j.jksues.2012.10.004

Kuntorini, E.M., Nugroho, L.H. & Nuringtyas, T.R. (2022). Maturity effect on the antioxidant activity of leaves and fruits of *Rhodomyrtus tomentosa* (Aiton.) Hassk. *AIMS Agriculture and Food*, 7(2): 282-296. DOI: 10.3934/agrfood.2022018

Lee, S.Y. & Mohamed, R. (2016). The origin and domestication of *Aquilaria*, an important agarwood-producing genus. *Agarwood: Science Behind the Fragrance*, 1-20. Springer, Singapore. DOI:10.1007/978-981-10-0833-7_1

Li, Q., Huang, J., Yang, Y., Chen, M., Liang, Y. & Chen, X. (2015). Research on the acute toxicity and genetic toxicity of *Aquilaria sinensis (Lour.) Gilg: leaf*. *China Journal of Health Laboratory Technology*, 25: 1518-1521.

Maharani, R., Fernandes, A., Turjaman, M., Lukmandaru, G. & Kuspradini, H. (2016). The characterization of Phytochemical and GC-MS analysis on Borneo agarwood (*Aquilaria malaccensis* Lamk) leaves and its utilization as an anti-browning in apple juice. *International Journal of Pharmacognosy and Phytochemical Research*, 8(10): 1576-1582. https://ijppr.com/volume8issue10/

Manukumar, H.M., Shiva Kumar, J., Chandrasekhar, B., Raghava, S. & Umesha, S. (2017). Evidence for diabetes and insulin mimetic activity of medicinal plants: present status and future prospects. *Critical Reviews in Food Science and Nutrition*, 57(12): 2712-2729. DOI:10.1080/10408398.2016.1143446

Marín-Peñalver, J.J., Martín-Timón, I., Sevillano-Collantes, C. & del Cañizo-Gómez, F.J. (2016). Update on the treatment of type 2 diabetes mellitus. *World Journal of Diabetes*, 7(17): 354-395. DOI: 10.4239/wjd.v7.i17.354

Nadeem, M. & Zeb, A. (2018). Impact of maturity on phenolic composition and antioxidant activity of medicinally important leaves of Ficus carica L. *Physiology and molecular biology of plants*, 24: 881-887. DOI: 10.1007/s12298-018-0550-3

Pranakhon, R., Aromdee, C. & Pannangpetch, P. (2015). Effects of iriflophenone 3-C-β-glucoside on fasting blood glucose level and glucose uptake. *Pharmacognosy magazine*, 11(41): 82-89. DOI: 10.4103/0973-1296.149711

Pranakhon, R., Pannangpetch, P. & Aromdee, C. (2011). Antihyperglycemic activity of agarwood leaf extracts in STZ-induced diabetic rats and glucose uptake enhancement activity in rat adipocytes. *Songklanakarin Journal of Science & Technology*, 33(4): 405-410. https://sjst.psu.ac.th/search.php

Portalatin, M. & Winstead, N. (2012). Medical management of constipation. *Clinics in colon and rectal surgery*, 25(01): 012-019. DOI: 10.1055/s-0032-1301754

Qi, J., Lu, J.J., Liu, J.H. & Yu, B.Y. (2009). Flavonoid and a rare benzophenone glycoside from the leaves of *Aquilaria sinensis*. *Chemical and Pharmaceutical Bulletin*, 57(2): 134-137. DOI:10.1248/cpb.57.134

Rashid, Z.M., Nasir, N.N.M., Ahmad, W.N.W. & Mahmod, N.H. (2020). α-glucosidase inhibition, DPPH scavenging and chemical analysis of polysaccharide extracts of *Aquilaria* sp. leaves. *Journal of Agrobiotechnology*, 11(2): 59-69. DOI:10.37231/jab.2020.11.2.225

Razak, R.N.H.A., Ismail, F., Isa, M.L.M., Wahab, A.Y.A., Muhammad, H., Ramli, R. & Ismail, R.A.S.R. (2019). Ameliorative effects of *Aquilaria malaccensis* leaves aqueous extract on reproductive toxicity induced by cyclophosphamide in male rats. *The Malaysian journal of medical sciences: MJMS*, 26(1): 44. DOI: 10.21315/mjms2019.26.1.4

Said, F., Kamaluddin, M.T. & Theodorus, (2016). Efficacy of the *Aquilaria malaccensis* leaves active fraction in glucose uptake in skeletal muscle on diabetic wistar rats. *International Journal of Health Sciences & Research*. 6(7): 162-167. https://www.ijhsr.org/archive_ijhsr_vol.6_issue7.html

Saeedi, P., Petersohn, I., Salpea, P., Malanda, B., Karuranga, S., Unwin, N., Colagiuri, S., Guariguata, L., Motala, A.A., Ogurtsova, K., Shaw, J.E., Dominic B. & Williams R. (2019). Global and regional diabetes prevalence estimates for 2019 and projections for 2030 and 2045: Results from the International Diabetes Federation Diabetes Atlas. *Diabetes research and clinical practice*, 157: 107843. DOI:10.1016/j.diabres.2019.107843

Sari, R., Kartika, E. & Apridamayanti, P. (2019). Antibacterial activity from ethanolic extract karas (*Aquilaria* sp.*)* leaves against pathogenic bacteria. *European Journal of Biomedical and Pharmaceutical Sciences*, 6(2): 80-82. https://www.ejbps.com/ejbps/abstract_id/5413

Su, L.J., Zhang, J.H., Gomez, H., Murugan, R., Hong, X., Xu, D., Jiang, F. & Peng, Z.Y. (2019). Reactive oxygen species-induced lipid peroxidation in apoptosis, autophagy, and ferroptosis. *Oxidative medicine and cellular longevity*, 2019. DOI:10.1155/2019/5080843

Surjanto, Batubara, R., Hanum, T.I. & Pulungan, W. (2019 May). Phytochemical and antioxidant activity of gaharu leaf tea (*Aquilaria malaccensis* Lamk) as raw material of tea from middle Tapanuli Regency, North Sumatera Province. In *IOP Conference Series: Earth and Environmental Science*. 260(1): 012101. IOP Publishing. DOI:10.1088/1755-1315/260/1/012101

Tan, C.S., Isa, N.M., Ismail, I. & Zainal, Z. (2019). Agarwood induction: current developments and future perspectives. *Frontiers in Plant Science*, 10: 122. DOI:10.3389/fpls.2019.00122

Thitikornpong, W., Palanuvej, C. & Ruangrungsi, N. (2019). In vitro antidiabetic, antioxidation and cytotoxicity activities of ethanolic extract of *Aquilaria crassna* leaves and its active compound; mangiferin. *Indian Journal of Traditional. Knowledge*, 18(1): 144-150. https://www.researchgate.net/publication/330668706_In_vitro_antidiabetic_antioxidation_and_cytotoxicity_activities_of_ethanolic_extract_of_aquilaria_crassna_leaves_and_its_active_compound_mangiferin

Tsunoda, T., Samadi, A., Burade, S. & Mahmud, T. (2022). Complete biosynthetic pathway to the antidiabetic drug acarbose. *Nature Communications*, 13(3455): 1-12. DOI:10.1038/s41467-022-31232-4

Wang, S., Yu, Z.X., Wang, C.H., Wu, C.M., Guo, P. & Wei, J.H., (2018). Chemical constituents and pharmacological activity of agarwood and Aquilaria plants. *Molecules*, 23(2): 342–363. DOI:10.3390/molecules23020342

Wangiyana, I.G.A.S., Supriadi, Nikmatullah, A. & Sunarpi., (2022). A mini review on agarwood tea development towards alternative utilization of agarwood commodity in Indonesia: mini review: Agarwood tea development. *Biological Sciences*, 65(2): 189-196. DOI:10.52763/PJSIR.BIOL.SCI.65.2.2022.189.196

Wongwad, E., Pingyod, C., Saesong, T., Waranuch, N., Wisuitiprot, W., Sritularak, B., Temkitthawon, P. & Ingkaninan, K. (2019). Assessment of the bioactive components, antioxidant, antiglycation and anti-inflammatory properties of *Aquilaria crassna* Pierre ex Lecomte leaves. *Industrial crops and products*, 138: 111448. DOI: 10.1016/j.indcrop.2019.06.011

Xu, W., Cheng, Y., Guo, Y., Yao, W. & Qian, H. (2022). Effects of geographical location and environmental factors on metabolite content and immune activity of Echinacea purpurea in China based on metabolomics analysis. *Industrial Crops and Products*, 189: 115782. DOI: 10.1016/j.indcrop.2022.115782

Zainurin, N.A.A., Samsudin, N., Hashim, Y.Z.H.Y., Al-Khatib, M.F.R., Azmin, N.F.M. & Maifiah, M.H.M. (2020). Response surface optimization of the yield of agarwood (*Aquilaria malaccensis*) leaf extract using soxhlet extraction. *International Journal of Recent Technology and Engineering*, 8(6): 1926-1934. DOI: 10.35940/ijrte.F8013.038620

Zakaria, F., Talip, B.A., Kahar, E.E.M., Muhammad, N., Abdullah, N. & Basri, H. (2020). Solvent used in extraction process of agarwood: A systematic review. *Food Research*, 4(3): 731-737. DOI:10.26656/fr.2017.4(3).333

Zhou, M., Wang, H., Kou, J. & Yu, B. (2008). Antinociceptive and anti-inflammatory activities of *Aquilaria sinensis* (Lour.) Gilg. Leaves extract. *Journal of ethnopharmacology*, 117(2): 345-350. DOI:10.1016/j.jep.2008.02.005

Zulkiflie N.L., Omar N.A.M., Tajudin S.N. & Shaari, M.R. (2013, December). Antidiabetic activities of Malaysian agarwood (*Aquilaria* spp.) leaves extract. In *Conference on Industry-Academia Joint Initiatives in Biotechnology CIA: Biotech* (Vol. 13, pp. 5-7).

Borneo Journal of Resource Science and Technology (2025), 15(1): 97-104
DOI: https:doi.org/10.33736/bjrst.7706.2025

The In Vitro Ovicidal Activity of *Cassia alata* Methanolic Extracts on *Aedes aegypti* and *Aedes albopictus* Eggs

AZLINDA ABU BAKAR* AND SHUKI LIM SHUET EN

School of Biological Sciences, Universiti Sains Malaysia, 11800 USM, Pulau Pinang
*Corresponding author: azlindaab@usm.my
Received: 26 August 2024 Accepted: 21 February 2025 Published: 30 June 2025

ABSTRACT

The widespread use of chemical insecticides for controlling *Aedes* mosquitoes has resulted in the development of insecticide resistance, prompting the need for alternative solutions. Botanical insecticides have gained attention as a promising approach in modern pest control. This study focuses on evaluating the ovicidal effects of methanol extracts from *Cassia alata* leaves on *Aedes* mosquitoes. The extracts were produced through the maceration-filtration technique, followed by the preparation of various concentrations (0.05-2.00 mg/ml) These concentrations were then tested to assess their impact on the fertility and egg viability of *Aedes aegypti* and *Aedes albopictus*. From the results obtained in the bioassay on egg fertility and viability, a significant difference in fertility was observed between *Ae*. *aegypti* and *Ae*. *albopictus* ($p<0.05$, $p = 0.044$). However, no significant difference was observed in overall egg viability between the two species ($p>0.05$, $p = 0.468$). The LC50 and LC90 values for *Ae*. *albopictus* were 0.323 mg/ml and 5.280 mg/ml, respectively, which were lower than those for *Ae*. *aegypti* 0.560 mg/ml and 11.480 mg/ml. This indicates that, *Ae*. *albopictus* is more susceptible to the methanolic *C. alata* extracts. These findings suggest that *C. alata* extracts could be a viable alternative to chemical insecticides in mosquito control programs, particularly for targeting *Ae*. *albopictus*.

Keywords: *Aedes*, *Cassia alata*, extracts, methanolic, ovicidal

INTRODUCTION

The increasing prevalence of mosquito-borne diseases, such as dengue, chikungunya, and Zika, has become a significant public health concern in Malaysia and other tropical regions of Southeast Asia (AbuBakar *et al*., 2022). These diseases are primarily transmitted by *Aedes aegypti* and *Aedes albopictus*, which have shown remarkable adaptability to urban environments and a high reproductive rate, contributing to their widespread distribution (Soni *et al*., 2023). To combat this, traditional chemical insecticides have been the mainstay in controlling mosquito populations. However, their prolonged use has led to the development of resistance among mosquito species, which reduces the effectiveness of insecticides and its becoming a critical global issue impacting public health and increasing the risk of diseases such as dengue and malaria (Richards *et al*., 2020). This resistance often arises from the frequent and repeated use of synthetic insecticides. To address this challenge, exploring alternative strategies, such as the use of bioinsecticides, is essential. Bioinsecticides offer a promising alternative to conventional synthetic insecticides like pyrethroids and organophosphates, posing challenges to their effectiveness. Additionally, the adverse effects of chemical insecticides on non-target organisms, including beneficial insects and aquatic life, as well as the potential for environmental contamination, have raised concerns about their continued use (Gan *et al*., 2021).

In response to these challenges, there is a growing interest in exploring alternative, environmentally friendly strategies for mosquito control. One promising approach is the use of natural plant extracts as insecticides. Plants have evolved a wide range of chemical defenses against herbivores and pathogens, many of which have been found to exhibit insecticidal properties (Şengül Demirak & Conpolat, 2022). Among these, *Cassia alata*, a medicinal plant native to tropical regions, has attracted attention for its potential as a natural ovicide against *Aedes* mosquitoes. In Southeast Asia, *C. alata* is commonly consumed as both food and spices.

However, they have also been traditionally utilized by local communities, particularly in countries such as Malaysia, Thailand, Indonesia, and Brunei, for medicinal purposes. One notable application among these communities is the management of skin diseases (Fatmawati *et al*., 2020). A comprehensive review of the traditional uses, phytochemical composition, and primary pharmacological activities of these herbs highlights their role in managing skin conditions, particularly atopic dermatitis (AD) (Chew *et al*., 2022).

Recent studies have demonstrated the efficacy of *Cassia* sp. extracts in inhibiting the development of mosquito larv*ae*, suggesting its potential as a viable alternative to chemical insecticides (Raman Ibrahim *et al*., 2022). While significant research has focused on plant-derived larvicides and adult repellents, there has been relatively little investigation into the ovicidal activity of plant extracts for controlling mosquito eggs (Giovanni, 2015). Furthermore, the active compounds found in *C. alata*, such as anthraquinones and flavonoids (Fatmawati *et al*., 2020), have been reported to possess ovicidal properties that could disrupt the reproductive cycle of mosquitoes, thereby could reducing their population density (Lengai *et al*., 2020). This study aims to fill this gap by evaluating the potential of botanical insecticides as effective ovicides for mosquito vector control, potentially offering a new approach to managing mosquito populations and mitigating the spread of mosquito-borne diseases.

Ovicides are a class of insecticides specifically designed to target and eliminate mosquito eggs within their breeding habitats, thereby preventing the development and growth of mosquito populations. These substances work by either disrupting the oviposition process, thereby preventing adult mosquitoes from laying eggs, or by directly killing the eggs, preventing them from hatching into larv*ae*. Ovicides are particularly useful in breeding sites that are challenging to manage through source reduction or larvicide application, such as in wash basins (Andrew *et al*., 2016). Plant-derived compounds, including essential oils, have shown promise as effective ovicides for controlling mosquito populations (Ephantus *et al*., 2018). Hence, the use of *C. alata* as a mosquito ovicide is particularly relevant in Malaysia, where the plant is abundant and easily accessible. Despite the promising results from preliminary studies, there remains a gap in understanding the full potential of *C. alata* extracts in mosquito control, particularly concerning their ovicidal effects on *Aedes* species. This study aims to fill this gap by investigating the ovicidal activity of *C. alata* extracts against *Ae*. *aegypti* and *Ae*. *albopictus*, focusing on the efficacy, optimal concentrations, and potential mechanisms of action. By evaluating the effectiveness of *C. alata* as a natural ovicide, this research contributes to the ongoing efforts to develop sustainable mosquito control strategies that align with public health and environmental safety goals. Given the increasing resistance to chemical insecticides and the ecological hazards they pose, the exploration of plant-based insecticides like *C. alata* offers a promising alternative for mosquito control in Malaysia and other tropical regions. The findings of this study are expected to provide valuable insights into the potential of *C. alata* as part of an integrated vector management strategy, ultimately contributing to the reduction of mosquito-borne diseases in affected communities.

MATERIALS AND METHOD

Plant Preparation

Fresh, mature *C. alata* leaves were obtained from a local supplier and brought to the laboratory at the School of Biological Sciences, Universiti Sains Malaysia, Pulau Pinang. The leaves were thoroughly washed with tap water to remove any debris. After cleaning, they were spread out on newspapers on a laboratory table and left to air-dry at room temperature (27 ± 2 °C) for 5 - 7 days.

Plant Extractions

The extraction of *C. alata* leaves was performed using the maceration technique, which involves immersing coarsely powdered leaves in a solvent. Initially, the leaves were air-dried and then mechanically ground into a fine powder using an electric blender (Khind 1.2L BL1012). The powdered leaves were then subjected to maceration, where they were soaked in methanol at a ratio of 10 ml of solvent (methanol) per gram of leaf powder. A total of 160 g of powdered leaves were used, requiring 1600 ml of methanol for the extraction. To begin the extraction, 100 ml of methanol, serving as the menstruum, was

measured using a graduated cylinder and poured into a beaker containing the powdered leaves. The mixture was stirred thoroughly, covered tightly with aluminum foil, and left to macerate for at least three days in the laboratory. During this period, the beaker was occasionally shaken to enhance the extraction process. After the three-day maceration process, the mixture was filtered through filter paper to obtain the plant extract via the filtrate (Abdullahi & Mainul, 2020; Seng *et al*., 2023). The filtered extract was then placed in an oven set at 40 °C and left to evaporate for at least two days, allowing the solvent to fully evaporate and leaving a concentrated plant paste at the bottom of the beaker. This paste was carefully scraped out using a spatula, transferred to a Petri dish, and sealed with parafilm tape. The Petri dishes were then stored in a refrigerator to slow down the decay of the paste/extract, while sealing and moisture control were used to prevent microbial contamination.

Rearing and Culturing *Aedes* Mosquitoes in the Laboratory

The laboratory strains of *Ae*. *aegypti* and *Ae*. *albopictus* mosquitoes were obtained from the Vector Control Research Unit (VCRU) at Universiti Sains Malaysia (USM). The mosquito eggs were placed in containers and reared with seasoned water under controlled room temperature (27 ± 2 °C). To maintain optimal conditions, the seasoned water was replaced twice a week, and the larv*ae* were fed fish food pellets once every two days to minimise bacterial growth, which could contaminate the water and harm the larv*ae*. Upon reaching the pupal stage, they were carefully transferred to small containers with seasoned water using a dropper. To prevent the emerging adult mosquitoes from escaping, the containers with pup*ae* were then placed inside a mosquito cage. Additionally, a small beaker with cotton soaked in a 10% sucrose solution was provided inside the cage to nourish the adult mosquitoes before they were subjected to blood feeding with rats.

Preparation of Stock Solution and Bioassay Concentrations

A stock solution with a concentration of 250 mg/ml was prepared by mixing 5000 mg of *C. alata* leaf extract paste with 20 ml of methanol in a beaker. The beaker was sealed with aluminum foil and stored in the fridge to prevent contamination. Ten (10) serial dilutions were performed from the stock solution by diluting it with methanol. The volumes of stock solution and methanol required for each concentration were calculated using the formula $M_1V_1=M_2V_2$ where V_1 is the volume of the stock solution needed. This was determined by dividing the desired concentrations and final volume by the concentration of the stock solution (M_1). The concentration of *C. alata* prepared for the ovicidal bioassay ranged from 0, 0.05, 0.10, 0.15, 0.20, 0.25, 0.50, 1.00, 1.50, and 2.00 mg/ml.

Ovicidal Bioassay of *Cassia alata* Extracts Against *Aedes* Eggs (Fertility)

The adult female mosquitoes were deprived of sucrose solution for 24 hours before being sent for the blood-feeding procedure. The blood-feeding procedure was conducted by the Animal Ethics unit of the School of Biological Sciences. Each session required at least 30 starved female mosquitoes and lasted between 30 to 60 minutes to ensure adequate feeding. Simultaneously, ten Petri dishes were prepared: one with 5 ml of seasoned water as a control and nine with 5 ml of *C. alata* methanol extracts at concentrations ranging from 0.05 to 2.00 mg/ml. Cone-shaped filter papers were placed in each Petri dish to serve as egg-laying substrates. After feeding, the mosquitoes were transferred to a cage containing the Petri dishes with the *C. alata* extracts where they were exposed to these extracts for 24 to 72 hours at 22.5 °C.

To maintain the moisture of the filter papers and ensure suitable breeding conditions, 2 mL of the respective test concentrations (0, 0.05, 0.10, 0.15, 0.20, 0.25, 0.50, 1.00, 1.50, and 2.00 mg/mL) was added daily to ensure consistency and comparability. Additionally, a sucrose solution was provided to prevent starvation. The filter papers with laid eggs were collected, dried (Figure 1), and stored in closed, labeled containers corresponding to their respective concentrations. The total number of eggs was counted under a stereo microscope (Model SZX16-CCD) and recorded. The bioassay was replicated five times.

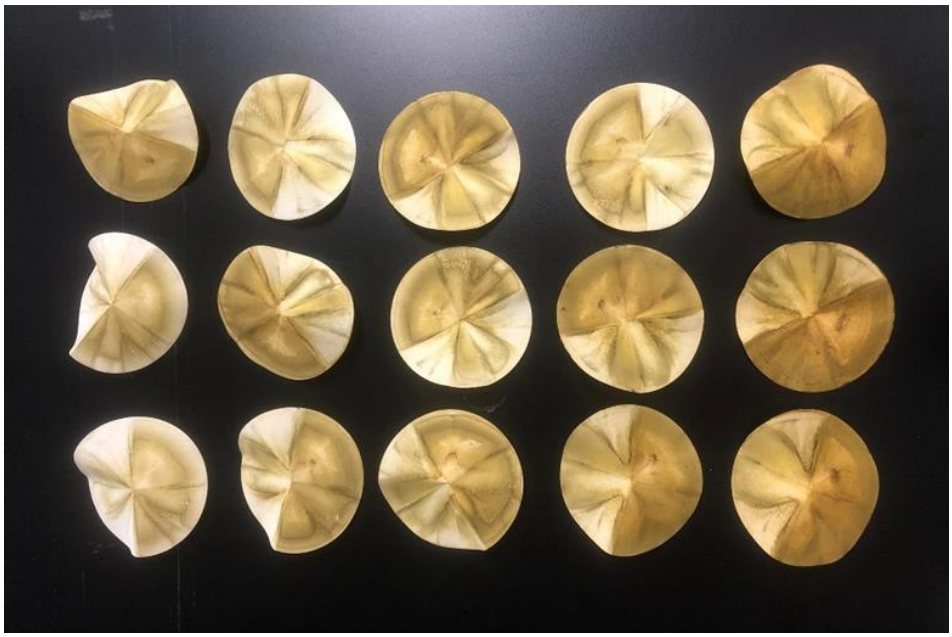

Figure 1. Cone-shaped filter paper used as a substrate for egg laying. The filter papers were removed from the cage for egg counting

Ovicidal Bioassay of *Cassia alata* Extracts against *Aedes* Eggs (Viability)

The viability assay was conducted to evaluate the effectiveness of *C. alata* extracts in controlling *Aedes* eggs over a seven-day period. The assay followed WHO guidelines (2005), with slight modifications. Unlike the standard procedure, which uses larv*ae* as the testing specimens, this assay utilised mosquito eggs. Targeting the egg stage allows to assess their fertility and viability after treatment, providing key insights into how treatments affect early development and helping to tailor mosquito control strategies to different life stages. Ten plastic cups were prepared with varying concentrations of the plant extracts, including a control. The control cup was filled with 200 ml of seasoned water, while the remaining nine cups contained 199 ml of seasoned water and 1 ml of plant extract at concentrations ranging from 0.05 to 2.00 mg/ml Four additional replicates were set up following the same procedure. Each cup was stocked with 125 mosquito eggs which were exposed to the test solutions for one week at approximately 22.5°C. During the assay, larv*ae* were provided with fish food pellets.

Data and Statistical Analysis

The number of eggs hatched was recorded by counting the larvae present in each plastic cup. Egg mortality was determined by using the following formula; Eq.(1):

$$Egg\ mortality\ (\%) = \frac{Total\ number\ of\ eggs - Total\ number\ of\ eggs\ hatched}{Total\ number\ of\ eggs} \times 100\% \quad \textbf{Eq.(1)}$$

The data were analysed using SPSS v27. A t-test was conducted to compare the fertility rates of *Ae*. *aegypti* and *Ae*. *albopictus*. The Mann-Whitney U Test was applied to assess significant differences in fertility rates and egg viability between the two species under different concentrations of *C. alata* extracts. The data were log-transformed prior to analysis. Additionally, lethal concentrations that kill 50% (LC50) and 90% (LC90) of the tested populations for egg viability of *C. alata* extracts were calculated using Probit analysis.

RESULTS AND DISCUSSION

Figure 2 shows the mean number of eggs laid by *Aedes* mosquitoes across the tested concentrations of methanolic *C. alata* extract. The results indicate that the fertility of both *Ae*. *aegypti* and *Ae*. *albopictus* decreases as the concentration of the extract increases. For *Ae*. *aegypti*, the highest mean number of eggs laid was 35.2 in the control group, while the lowest was 1.00 at 2.00 mg/ml. In contrast, *Ae*. *albopictus* laid the highest mean number of eggs (42.4) in the control group but none at concentrations of 0.50 mg/ml and higher.

Statistical analysis revealed a significant difference in fertility between the two species (Z = -2.012, p = 0.044), with *Ae*. *albopictus* showing lower fertility compared to *Ae*. *aegypti* at all concentrations except the control. These findings suggest that methanolic *C. alata* extracts are more effective in deterring oviposition *Ae*. *albopictus* than in *Ae*. *aegypti*, particularly at concentrations of 0.50 mg/ml and above.

Figure 3 presents a bar graph depicting the mean number of eggs hatched (egg viability) in *Ae*. *aegypti* and *Ae*. *albopictus* across various concentrations of methanolic *C. alata* extract (ranging from 0 to 2.00 mg/ml). The data show that the egg viability of *Ae*. *albopictus* decreases steadily with increasing extract concentration, with the highest mean number of eggs hatched being 22.0 in the control group and the lowest at 1.2 eggs at 2.00 mg/ml. For *Ae*. *aegypti*, while there is some fluctuation in egg viability, the overall trend also indicates a decrease as the concentration of the extract increases. The highest mean number of eggs hatched was 22.4 in the control group, with the lowest being 1.4 eggs at 2.00 mg/ml. Statistical analysis (t=0.741, P=0.468) reveals no significant difference in egg viability between *Ae*. *aegypti* and *Ae*. *albopictus*. However, *Ae*. *albopictus* generally exhibits lower egg viability compared to *Ae*. *aegypti*, showing similar trends in the fertility assay.

In this study, a significant reduction in the fertility and egg viability of *Ae*. *aegypti* and *Ae*. *albopictus* was observed with the application of methanolic *C. alata* extracts. This ovicidal activity is likely driven by the diverse phytochemical compounds in the leaves, including flavonoids and alkaloids, which are known for their insecticidal, repellent, and oviposition- inhibitory properties (Meryem & Emel, 2022). Solvent polarity significantly affects the extraction of bioactive compounds, with methanol being particularly effective due to its higher polarity (Anabela *et al*., 2020). Truong *et al*. (2019) found that methanol effectively extracts key phytochemicals, which may explain the strong ovicidal effects observed. Flavonoids like quercetin and k*ae*mpferol disrupt embryogenesis, while alkaloids such as berberine and quinine exhibit insecticidal properties that reduce egg viability (Simmonds, 2001). Similarly, Govindarajan (2011) reported that methanolic extracts of Cassia fistula reduced *Ae*. *aegypti* egg viability. Given the similarity to *C. alata*, its ovicidal activity may stem from the same bioactive compounds. Further analysis is needed to confirm their role in mosquito control. These findings highlight the potential of methanolic *C. alata* extracts as an effective natural ovicide for controlling *Aedes* mosquito populations.

To quantify this potential, Table 1 presents the LC50 and LC90 obtained from assays of egg mortality with varying concentrations of *C. alata* extracts. At a 95% confidence level, the LC50 and LC90 values for *Ae*. *albopictus* were lower than those for *Ae*. *aegypti*. Specifically, the LC50 for *Ae*. *albopictus* was 0.323 mg/ml, and the LC90 was 5.280 mg/ml while for *Ae*. *aegypti* the LC50 was 0.560 mg/ml and an LC90 of 11.480 mg/ml. These results indicate that a lower concentration of methanolic *C. alata* extracts is sufficient to achieve lethal effects on the egg populations of *Ae*. *albopictus* compared to *Ae*. *aegypti*. This research highlights that *Ae*. *albopictus* is more susceptible to these methanolic *C. alata* extracts.

The reduced susceptibility of *Ae*. *aegypti* might be due to genetic resistance developed over successive laboratory generations, with resistance genes potentially being passed down. Meryem & Emel (2022) reported that mosquitoes surviving insecticide exposure can transmit resistance traits to their offspring, resulting in increased resistance in subsequent generations. This resistance is often mediated by detoxifying enzymes like cytochrome P450 monooxygenases, which degrade insecticides and reduce their effectiveness. Continuous exposure can lead to increased enzyme activity, further contributing to resistance development. Dong-jiang *et al*. (2022) observed that plant secondary metabolites could induce cytochrome P450 gene expression, aiding in the detoxification of toxic compounds. Kamal *et al*. (2022) corroborated this by demonstrating that the LC50 values of eugenol (a component of basil and clove oils) for *Ae*. *aegypti* increased from the F10 to the F24 generation, paralleling a rise in cytochrome P450 activity.

Table 1. Lethal concentrations (LC50 and LC90), of *Ae. aegypti* and *Ae. albopictus* eggs against *C. alata* extracts

Species	LC_{50} (mg/ml)	95% Confidence		LC_{90} (mg/ml)	95% Confidence	
		Lower	Upper		Lower	Upper
Ae. aegypti	0.560	0.465	0.690	11.480	6.973	22.502
Ae. albopictus	0.323	0.272	0.382	5.280	3.582	8.793

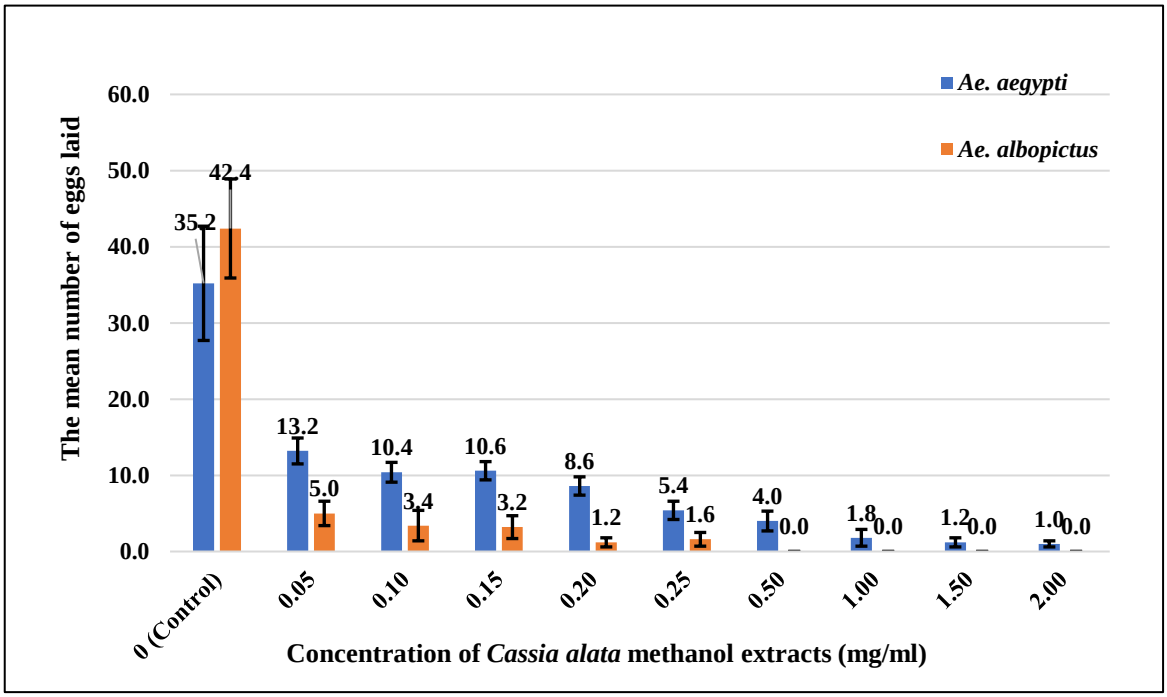

Figure 2. The mean number of eggs laid by *Aedes* mosquitoes across concentration (mg/ml)

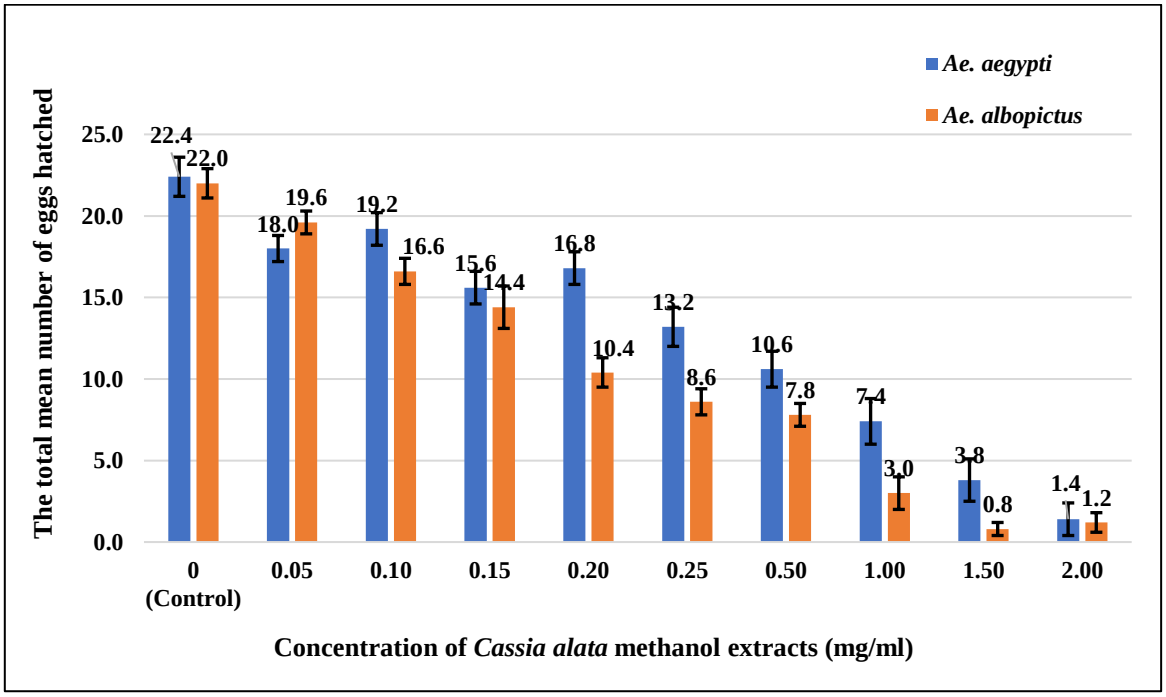

Figure 3. The mean number of eggs hatched by *Aedes* mosquitoes across concentrations (mg/ml)

As reported, *C. alata* contains flavonoid compounds, that likely interact with cytochrome P450 enzymes. Petr *et al*. (2002) found that flavonoids can either induce or inhibit cytochrome P450 expression affecting its metabolic activity. This interaction suggests that *Ae*. *aegypti* may have developed genetic adaptations to enhance survival against *C. alata* extracts potentially through cytochrome P450 mechanisms. Senthil-Nathan (2020) identified cytochrome P450 as a key indicator of metabolic resistance, which can lead to cross-resistance, a significant challenge in managing insecticide resistance. In this study, *C. alata* extracts were less effective against *Ae*. *aegypti* than *Ae*. *albopictus*. This difference in susceptibility warrants further investigation, as it may be influenced by species-specific physiology, detoxification mechanisms, or prior exposure to similar compounds, including potential cross-resistance to synthetic insecticides (Lin *et al*., 2024).

CONCLUSION

In conclusion, methanolic *C. alata* extracts are promising botanical insecticides with the potential to replace chemical insecticides in *Aedes* control. These extracts have shown high effectiveness, particularly against *Ae*. *albopictus*, achieving 100% repellency with no eggs laid at concentrations ranging from 0.50 to 2.00 mg/ml. The LC50 and LC90 values for *Ae*. *albopictus* were significantly lower than those for *Ae*. *aegypti*, indicating greater susceptibility. These eco-friendly, biodegradable extracts are less persistent and less toxic to non-target organisms, making them suitable for integrated pest management (IPM) programs (Şengül Demirak *et al*., 2022). Future research should focus on improving the extraction methods and solvents used for *C. alata* to maximize its effectiveness. It is also important to investigate its potential as a larvicide or adulticide against *Aedes* mosquitoes under different environmental conditions. These efforts could help establish *C. alata* as a reliable and sustainable option for mosquito control.

ACKNOWLEDGEMENT

We extend our gratitude to the School of Biological Sciences, USM Pulau Pinang, for their facilitation and support during this study. We also wish to acknowledge that this research did not receive funding from the university or any other agency.

REFERENCES

Abdullahi, R.A. & Mainul, H. (2020). Preparation of Medicinal Plants: Basic Extraction and Fractionation Procedures for Experimental Purposes. *Journal of Pharmacy & Bioallied Sciences*, 12(1): 1–10. DOI:10.4103/jpbs.JPBS_175_19

AbuBakar, S., Wan Puteh, S.E., Kastner, R., Oliver, L., Lim, S.H., Hanley, R. & Gallagher, E. (2022). Epidemiology (2012-2019) and costs (2009-2019) of dengue in Malaysia: a systematic literature review. *International Journal of Infectious Diseases*, 124: 240-247. DOI:10.1016/j.ijid.2022.09.006.

Anabela, B., Helena, J., Vera, H. & Manuel, S. (2020). Comparison of Techniques and Solvents on the Antimicrobial and Antioxidant Potential of Extracts from Acacia dealbata and Olea europ*ae*a. *Antibiotics*, 9(2):48. DOI:10.3390/antibiotics9020048

Andrew, J.M., Manuel, A., Gilberto, F., Veronica, A. & Roberto, B. (2016). Evaluation of Household Bleach as an Ovicide for the Control of *Aedes aegypti*. *Journal of the American Mosquito Control Association*, 31(1): 77-84. DOI:10.2987/14-6427R.1

Chew, Y.L., Khor, M.A., Xu, Z., Lee, S.K., Keng, J.W., Sang, S.H., Akowuah, G.A., Goh, K.W., Liew, K.B. & Ming, L.C. (2022). Cassia alata, Coriandrum sativum, Curcuma longa and Azadirachta indica: Food Ingredients as Complementary and Alternative Therapies for Atopic Dermatitis-A Comprehensive Review. *Molecules*, 27(17): 5475. DOI:10.3390/molecules27175475

Dong-jiang, L., Yong, F., Ling-yun, L., Li-zhao, Z., San-ji, G., Ran, W. & Jin-da, W. (2022). The insecticidal effect of the botanical insecticide chlorogenic acid on Mythimna separata (Walker) is related to changes in MsCYP450 gene expression. *Frontiers in Plant Science*, 13:1015095. DOI: 10.3389/fpls.2022.1015095

Ephantus, J.M., Jose, L.R., Bruce, Z., Lina, B.F. & Alejandro, P.R. (2018). Ovicidal and Larvicidal Effects of Garlic and Asofoetida Essential Oils Against West Nile Virus Vectors. *Journal of Insect Science*, 18(2): 43. DOI:10.1093/jisesa/iey036

Fatmawati, S., Yuliana, Purnomo, A.S. & Abu Bakar, M.F. (2020). Chemical constituents, usage and pharmacological activity of Cassia alata. *Heliyon*, 6(7): e04396. DOI:10.1016/j.heliyon.2020.e04396

Gan, S.J., Leong, Y.Q., Barhanuddin, M.F.H, Wong, S.T., Wong, S.F., Mak, J.W. & Ahmad, R. (2021). Dengue fever and insecticide resistance in *Aedes* mosquitoes in Southeast Asia: a review. *Parasites Vectors*, 14: 315. DOI:10.1186/s13071-021-04785-4.

Giovanni, B. (2015). Plant-borne ovicides in the fight against mosquito vectors of medical and veterinary importance: a systematic review. *Parasitology Research*, 114: 3201–3212. DOI:10.1007/s00436-015-4656-z

Govindarajan, M., Mathivanan, T., Elumalai, K., Krishnappa, K. & Anandan, A. (2011). Ovicidal and repellent activities of botanical extracts against Culex quinquefasciatus, *Aedes aegypti* and Anopheles stephensi (Diptera: Culicid*ae*). *Asian Pacific journal of tropical biomedicine*, 1(1): 43–48. DOI:10.1016/S2221-1691(11)60066-X

Kamal, A., Bulbuli, K. & Riju, S. (2022). Persistent susceptibility of *Aedes aegypti* to eugenol. *Scientific Reports*, 12: 2277. DOI:10.1038/s41598-022-06302-8

Lengai, G.M.W., Muthomi, J.W. & Mbega, E.R. (2020). Phytochemical activity and role of botanical pesticides in pest management for sustainable agricultural crop production, *Scientific African*, 7: e00239. DOI:10.1016/j.sciaf.2019.e00239.

Lin, L.Q., Chen, Y.H., Tian, Y.F., Zheng, Z.Y., Wu, J.X., Hu, F., Wu, C. & Xie, L.H. (2024). Study on the cross-resistance of *Aedes albopictus* (Skuse) (Diptera: Culicid*ae*) to deltamethrin and pyriproxyfen, *Parasites Vectors*, 17: 403. DOI:10.1186/s13071-024-06485-1

Meryem, S.S.D. & Emel, C. (2022). Plant-Based Bioinsecticides for Mosquito Control: Control:Impact on Insecticide Resistance and Disease Transmission. *Insects*, 13(2):162. DOI:10.3390/insects13020162

Petr, H., Pavel, T. & Marie, S. (2002). Flavonoids-potent and versatile biologically active compounds interacting with cytochromes P450. *Chemico-Biological Interactions*, 139(1): 1-21. DOI:10.1016/S0009-2797(01)00285-X

Raman Ibrahim, N.B., Puchooa, D., Govinden-Soulange, J. & Facknath, S. (2022). Chemical profiling and biological activity of Cassia abbreviata Oliv. *South African Journal of Botany*, 146: 325-339. DOI:10.1016/j.sajb.2021.11.004.

Richards, S.L., Byrd, B.D., Reiskind, M.H. & White, A.V. (2020). Assessing Insecticide Resistance in Adult Mosquitoes: Perspectives on Current Methods. *Environmental Health Insights*, 14. DOI:10.1177/1178630220952790

Seng, C.T., Samuel, L., Scholastica, R.B. & Sui, S.L. (2023). In vitro antimicrobial efficacy of Cassia alata (Linn.) leaves, stem, and root extracts against cellulitis causative agent Staphylococcus aureus. *BMC Complementary Medicine and Therapies*, 23: 85. DOI:10.1186/s12906-023-03914-z

Şengül Demirak, M.Ş. & Canpolat, E. (2022). Plant-Based Bioinsecticides for Mosquito Control: Impact on Insecticide Resistance and Disease Transmission. *Insects*, 13(2): 162. DOI:10.3390/insects13020162

Senthil-Nathan S. (2020). A Review of Resistance Mechanisms of Synthetic Insecticides and Botanicals, Phytochemicals, and Essential Oils as Alternative Larvicidal Agents Against Mosquitoes. *Frontiers in Physiology*, 10: 1591. DOI:10.3389/fphys.2019.01591

Simmonds, M.S.J. (2001). Importance of flavonoids in insect–plant interactions: feeding and oviposition. *Phytochemistry*, 56, (3): 245-252. DOI:10.1016/S0031-9422(00)00453-2.

Soni, S., Gill, V.J.S., Anusheel, Singh, J., Chhabra, J., Gill, G.J.S. & Bakshi, R. (2023). Dengue, Chikungunya, and Zika: The Causes and Threats of Emerging and Re-emerging Arboviral Diseases. *Cureus*, 15(7): e41717. DOI:10.7759/cureus.41717

Truong, D.H., Dinh, H.N., Nhat, T.A.T., Anh, V.B., Tuong, H.D. & Hoang, C.N. (2019). Evaluation of the use of different solvents for phytochemical constituents, antioxidants, and in vitro anti-inflammatory activities of Severinia buxifolia. *Journal of Food Quality*, 2019(1): 8178294. DOI:10.1155/2019/8178294

World Health Organization (2005). Guidelines and field testing of mosquito larvicides. World Health Organization. https://iris.who.int/handle/10665/69101

Borneo Journal of Resource Science and Technology (2025), 15(1): 105-115
DOI: https:doi.org/10.33736/bjrst.8965.2025

Physicochemical, Thermal, and Polymorphic Properties of Binary Blends from Bambangan Stearin and Palm Stearin

NORAZLINA MOHAMMAD RIDHWAN[1], HASMADI MAMAT*[1], MD JAHURUL HAQUE AKANDA[2], MACDALYNA ESTER RONIE[1], AHMAD HAZIM ABDUL AZIZ[1]

[1] Food Security Research Laboratory, Faculty of Food Science and Nutrition, Universiti Malaysia Sabah, 88400 Kota Kinabalu, Sabah, Malaysia [2]Department of Agriculture, School of Agriculture, University of Arkansas, 1200 North University Dr., M/S 4913, Pine Bluff, AR 71601.
*Corresponding author: idamsah@ums.edu.my
Received: 6 February 2025 Accepted: 9 May 2025 Published: 30 June 2025

ABSTRACT

Increasing demand for sustainable and functional fat alternatives in the food industry has prompted research into fat modification resulting in specialty fats production that can imitate cocoa butter. This study investigates the binary blends of bambangan and palm stearin, focusing on their physicochemical, thermal, and morphological properties. The blends were blended in five different ratios, with the addition of palm stearin not exceeding 30%. The results show that the iodine value (33.78 to 34.24 g iodine+/g), slip melting point (33.25 to 38.35 °C), and acid value (1.31 to 1.59 mgKOH/g) of the blends were influenced by the palm stearin content. The melting behaviour and crystallisation properties of the blends analysed using differential scanning calorimetry revealed an improved melting profile compared to the palm stearin. The binary blends exhibited desirable polymorphic transitions to the stable β(v) form, preferred for chocolate applications. Notably, the blend with 70% bambangan stearin and 30% palm stearin (BS5) demonstrated an improved triglyceride profile with a reduction of tripalmitin content and melting properties similar to cocoa butter, reducing the waxy texture typically associated with palm stearin. The findings suggest that BS5 produced from bambangan seed waste is a functional, cost-effective alternative confectionery product, offering stability and desirable thermal properties.

Keywords: Palm stearin**,** bambangan stearin, blending, cocoa butter alternatives

INTRODUCTION

Global demand for cocoa butter (CB) has risen steadily, but current production levels are not sufficient to meet this growing demand. The demand for sustainable and functional fat alternatives in the food industry has driven research into innovative fat blends that mimic the properties of CB. The global demand for CB keep on increasing and the production cannot meet on the global demand. It is used extensively in the food, cosmetics, and pharmaceutical industries. Its special fatty acid composition and triglyceride structure result in an exceptionally low melting point, which is only between 32 °C and 35 °C (Ying & Youk, 2022). CB is a valuable by-product used for chocolate processing, facilitating the dispersion, liquefaction, and diffusion of cocoa powder, paste, sugar, and other additives, helping to create a smooth, homogeneous, continuous phase. It consists mainly of 24.50 to 33.70 % palmitic acid, 3.30 to 40.20 % stearic acid, and 26.30 to 36.50 % oleic acid (Norazura, Sivaruby, & Noor Lida, 2020; Kadivar *et al*., 2016), which contribute to its desirable melting properties. Despite that, CB has limited supply and increased demand, which causes the price to fluctuate (Biswas *et al.,* 2018). Therefore, an alternative from other vegetable sources, such as bambangan seed fat, is plausible.

Bambangan stearin (BS) was produced from the fractionation of bambangan seed fat. It is an underutilized resource distributed around the Borneo region including Malaysia (Jahurul *et al.*, 2019) but has promising potential due to its unique triglyceride composition (TAG) and physicochemical properties. The stearin fraction consists of three dominant fatty acids: palmitic acid (7.26 to 6.76%), stearic acid (44.72 to 48.50%), and oleic acid (33.76 to 36.02%), which are comparable to those of CB (Norazlina *et al.*, 2020). However, the palmitic content in BS is lower than in the commercial CB. It also exhibited more than 50% of 1,3-distearoyl-2-

oleoyl-glycerol, which contributes to the high melting properties. Hence, the direct application of BS is limited by its melting behaviour and thermal stability. Blending of BS with a high palmitic fat content, such as palm stearin (PS), could influence the composition of BS and thus improve its properties.

PS is the most important product from the fractionation of palm oil. Palm oil is obtained from the mesocarp of palm fruit, which is naturally semi-solid at room temperature and then fractionated into different fractions with different physical and chemical properties through fractionation processes (Ahmad Bustamam *et al.,* 2022). In 2024, Malaysia produced 2.367 million tonnes of PS (MPOB, 2024) which is characterised by a higher saturated fatty acid content and a TAG profile with a melting point between 48 °C and 50 °C. Thus, Malaysia plays a crucial role in meeting the increasing global demand for fats sustainably (Roslan, Gerusu, & Mustafa Kamal, 2018). PS obtained by crystallisation at controlled temperatures, is widely used in edible and non-edible products. It serves as a natural source of fat without the need for hydrogenation and increases the plasticity of products. It is a valuable source of solid fats and is used in a range of foods such as margarine, shortenings, and vanaspati, as well as in the production of trans-free fats. However, it exhibits waxy characteristics at higher concentrations.

Blending BS and PS offers an opportunity to create binary fat blends with optimised physicochemical, thermal, and structural properties applicable to confectionery and food applications. The blending also offers the utilization of bambangan seed from agricultural waste into a functional application. Therefore, blending PS with BS could further extend the application of PS in confectionery products as an alternative to cocoa butter, offering functional and economic benefits. In this study, the blending ratio was carefully selected to ensure that the PS content in the mixture did not exceed 30%. This is because a higher PS content could lead to a hard fat with waxy properties due to its high saturation, which is undesirable for confectionery applications. A controlled addition of PS helps to increase the palmitic acid content while maintaining the desired melting and textural properties of the final fat blend.

MATERIALS AND METHODS

Samples and Materials

Matured bambangan fruits were collected from an orchid (kampung Pandasan) in Kota Belud (Sabah), Malaysia, and the palm stearin (Iodine value: 37 g iodine/g) was provided by Sime Darby Malaysia (Selangor, Malaysia). Acetone, cyclohexane, diethyl ether, ethanol, hexane, potassium iodide, phenolphthalein, potassium hydroxide, starch, sodium thiosulphate, and Wijs solution were supplied from Merck (Germany) and Fisher (United Kingdom). All chemicals and reagents used are of the highest purity available.

Sample Preparation

Bambangan fruits were collected, placed in a large basket, and stored at 5 °C before sample preparation. The seeds were carefully separated using a strong household knife, washed, and cut into uniform pieces (2 cm × 1 cm × 0.1 cm) to accelerate drying. The seeds were dried in a cabinet at 60 °C for 48 hours and ground into fine powder (<250 μm) using a mill grinder (MX-898M, Panasonic). The moisture content of the dried seed powder was determined following the official method Ca 2d-25 (AOCS, 2003) yielding a result of 5.08 ± 0.67%, indicating excellent quality. Crude bambangan fat was extracted from the powdered seeds using Soxhlet extraction, following the official method of AOAC (2005). For each extraction, 80.00 ± 0.03 g of bambangan seed powder was extracted with 400 ml of hexane (1:5, w/v) at 40 °C. The crude fat was then fractionated with acetone using the method described by Jin *et al.* (2016) to isolate high-melting-point symmetric triglycerides (stearin). 100.00 ± 0.02 g of extracted bambangan kernel fat was mixed with 500 ml of preheated acetone (40 °C, 1:5 w/v). Fractionation was performed at 18 °C for 180 minutes, after which the first stearin fraction was separated via vacuum filtration. The remaining solvent was evaporated at 45 °C using a rotary evaporator (4001, HEIDOLPH LABORTA, Germany). The second stearin (BS) was produced following the same procedure utilizing the fractionation of the first stearin.

Blending of BS and PS

The preparation for blended fat was performed following the method described by Sonwai *et al.* (2014) with slight modification. BS was blended with PS by gradually increasing PS content in 5% increments. The resulting blend ratios were designated as BS1 (90:10%, SS: PS), BS2 (85:15%, SS: PS), BS3 (80:20%, SS: PS), BS4 (75:25% SS: PS) and BS5 (70:30% SS: PS). The PS content was restricted to 30% to avoid elevated melting points or the development of waxy states due to the high PPP content in PS. Each mixture was melted at 80 °C while continuously stirred at 200 rpm for 10 minutes on a hot plate with a magnetic stirrer (SP131320-33-V, Thermo Scientific, China) to achieve uniform homogenization. The binary mixtures were then stored at 4 °C for further analysis.

Physicochemical Properties

Physicochemical properties such as iodine value (IV), slip melting point (SMP), and acid value (AV) were determined according to the AOCS (2023) established method of Cd 1b-87, Cc 3b-92 and Cd 3a-63, described by Norazlina *et al.* (2020).

TAG Content

The TAG content of the samples was determined following the official AOCS method Ce 5c-93 (AOCS, 2003) with minor modifications using high performance liquid chromatography (HPLC; 1200, Agilent, Canada) with a refractive index detector (RID). Approximately 0.20 ± 0.02 g of the fat sample was dissolved in 10 mL of acetonitrile and dichloromethane (3:2, v/v). The mixture was then filtered using a 0.45 µm PTFE syringe filter (WHATMAN, 47 mm diameter). The analysis was performed with an injection volume of 10 µL, a column temperature set at 30 °C, a detector temperature of 40 °C, a pressure range of 8–9 mPa and a mobile phase flow rate of 0.8 mL/min. The TAG compounds were identified by comparing their elution profiles with those of TAG standards, including a mixed TAG-lipid standard and known PS and BS control standards, and expressed %.

Thermal Behaviour

The melting and crystallisation properties of the samples were evaluated by differential scanning calorimetry (DSC, Diamond, Perkin Elmer, USA) according to recommended practice Cj 1-94 (AOCS, 2003). The binary blends were melted at 80 °C for 30 minutes and then 3–5 mg of the sample was placed in a volatile aluminium pan (0219-0062, Perkin Elmer, USA), which was then sealed. The samples were heated (80 °C for 30 minutes) and incubated at 25 °C for one week to stabilize and temper the fat. The samples were transferred to the sample cell for analysis using an empty dish as a reference. The melting profiles were determined by heating the samples at 10 °C per minute from -40 °C to 80 °C and then hold for 2 minutes. Whereas, the crystallisation profiles were analysed at 10 °C per minute from 80 °C to -40 °C. The initial, offset, and maximum melting and crystallisation temperatures as well as the enthalpy of the fat samples were recorded in °C and J/g.

Polymorphic Behaviour

The polymorphic form of the fat samples was examined using an X-ray diffractometer (XRD Rigaku Smartlab, Rigaku, USA) following the official method Cj 2-95 (AOCS, 2009). Fat blends melted at 80 ºC were placed in glass sample holders, maintained at 25 ºC for 24 hours, and subsequently analysed with the XRD. The analysis parameters included a wavelength (λ) of 1.54178 Å, voltage of 40 kV, and current of 40 mA. Fingerprint measurements were recorded over a range of 14 – 26° (2θ), and the polymorphic forms were identified based on the short spacings observed in the blends.

Statistical Analysis

All analyses were performed in triplicate. The obtained data were processed using SPSS software (version 29), using Analysis of Variance (ANOVA) followed by Tukey's test. Results are presented as mean ± standard deviation, with a significance difference of $p < 0.05$.

RESULTS AND DISCUSSION

The BS and PS mixtures were analysed with regard to their physicochemical properties as well as their thermal and polymorphic behaviour. The physicochemical properties of the binary blends (BS: PS), such as IV, SMP, and AV, are shown in Table 1. These results are complemented by the TAG profiles shown in

Figure 2 and the thermal behaviour described by DSC analysis in Table 2. The crystallisation properties of the blends are listed in Table 2, while the polymorphic forms observed are shown in Figure 3. The results show that the IV value of the blends decreases with the addition of PS, leading to values similar to CB. The SMP values were affected by the PS content and showed a proportional decrease with increasing PS concentration. AV values also showed slight variations, with BS1 having the highest AV content due to the higher stearic and oleic acid composition. Figure 2 shows significant changes in the TAG composition of the binary blends after mixing, with notable proportions of SOS, POS, and POP contributing to the melting and textural properties of the blends. The results of the thermal analysis (Table 2) show changes in the initial, offset, and peak melting temperatures, with the binary blends exhibiting a more consistent melting profile compared to PS alone. The crystallisation data (Table 3) show distinct crystallisation peaks, with the blends containing more than 20 % PS showing two separate peaks that correlate with the melting thermograms. The polymorphic behaviour of the blends, as shown in Figure 3, shows a transition to the stable β(v) polymorphic form, which is desirable for chocolate and confectionery applications.

Table 1. Physicochemical properties of bambangan stearin and palm stearin blends

	Iodine value (g iodine/g)	Slip melting point (˚C)	Acid value (mgKOH/g)
Bambangan stearin (BS)	38.89 ± 0.01^{e}	35.00 ± 0.04^{c}	2.89 ± 0.16^{f}
Palm stearin (PS)	35.79 ± 0.01^{d}	51.67 ± 0.28^{g}	1.03 ± 0.16^{a}
Cocoa butter (CB)	34.00 ± 0.11^{c}	$33.80 \pm 0.28^{a,b}$	2.81 ± 0.09^{f}
BS1 (90 % BS: 10 % PS)	33.78 ± 0.01^{a}	38.35 ± 0.40^{f}	1.59 ± 0.16^{e}
BS2 (85 % BS: 15 % PS)	33.78 ± 0.01^{a}	37.75 ± 0.25^{e}	1.31 ± 0.16^{b}
BS3 (80 % BS: 20 % PS)	$33.92 \pm 0.05^{a,b}$	36.75 ± 0.25^{d}	1.40 ± 0.01^{c}
BS4 (75 % BS: 25 % PS)	34.24 ± 0.02^{c}	35.00 ± 0.00^{c}	1.40 ± 0.07^{c}
BS5 (70 % BS: 30 % PS)	33.99 ± 0.02^{b}	33.25 ± 0.25^{a}	$1.49 \pm 0.16^{c,d}$

Values are the mean±standard deviation of triplicate; means a different letter within a column is significantly different ($p<0.05$) as measured by Tukey test.

Physicochemical Properties

The binary blends produced a solid white fat (Figure 1) at room temperature, indicating they have high saturated fatty acids because they solidify rapidly. This solidification contributes to the product's hardness, maintaining texture, and hardness during storage and transportation. PS is more saturated and harder makes it solidifies rapidly at room temperature and takes longer to liquefy during melting. It has low IV because PS has high saturated FA content (44.50 – 54.28% of palmitic and 4.47 – 4.78% of stearic acids) and ~ 30% of POP, with a significant presence of high melting TAG such as PPP. Thus, contributing to its waxy texture (Biswas *et al.* 2016; Oliveira *et al.*, 2017). The oleic content in PS is also relatively low. Table 2 shows that the IV of the blends is significantly ($p<0.05$) improved with the proportion of the PS in BS.

The IV for the binary mixtures decreased after adding PS, resulting in IVs ranging from 33.78 to 34.24, which are similar to CB. The decrease in the unsaturated fatty acid composition may reduce the unsaturation level of the binary blends. The low IV value in the CB and the binary blends obtained from this study are correlated with improved fat quality, long-term stability properties of oil that are essential for storage such as longer shelf life, and reduced susceptibility to oxidation (Ishaka, Aliyu, & Mohmmad Hassan, 2020; Kittiphoom & Sutasinee, 2013). High IV values are usually associated with unsaturated fatty acids with low melting points; thus, fat with high IV values also has a low melting point. PS in this study has an SMP of 51.67 °C, higher than BS: PS blends. The SMP in this study is consistent with the palmitic (64.0 °C) and PPP (66.4 °C) content of the blends, which required a higher melting temperature for a complete melting state. The

results can also be supported by Nusantoro (2009), who reported that the final non-isothermal melting point of PS is 49.8 °C.

However, the SMP of PS blends decreased after the blending process. PS was used only up to 30% in this study; thus, the physicochemical properties were mainly dominated by the BS fat. The blends have melting points between 33.25 °C and 38.35 °C, with values decreasing proportionally to the increase in PS ratios. The SMP for BS1 to BS3 (36.75 °C to 38.35 °C) is relatively higher than that of CB in this study, and CB (25.3 °C to 35.0 °C) reported by Sonwai, Kaphuekngam, & Flood (2014) and Jin *et al.* (2018), but BS2 to BS5 showed melting at body temperature (33.25 °C to 37.75 °C). BS5 (33.25 °C) also has comparable SMP values with the CB (33.80 °C). The changes were presumably correlated to the fatty acid content of the blends, which caused the SMP values to differ. Adding high saturated fatty acid PS into BS blends increases the saturated palmitic content, thus explaining the increase in SMP values. BS1 might contain more stearic than the other blends because 90 % of the composition is BS. An increase in the palmitic in BS1 increases the saturated fatty acid content; thus, it is prone to a higher temperature. In contrast, the stearic acid in the other blends decreased proportionally to the PS ratio; therefore, the blends have a lower SMP than BS1.

PS and the binary blends in this study showed low AV. More than 60 % of PS composition was dominated by saturated fatty acid (Biswas *et al.*, 2016; Oliveira *et al.*, 2017), owing to low unstable oleic (22.8%) and linoleic (4.6%) acids making it more stable. The stearic content is also less in PS. Therefore, it is less prone to rancidity and is thus considered higher quality. After blending BS and PS, the AV of the blends slightly increased than the values of individual PS, but they showed variation. Although PS has shallow AV content, BS contains relatively high stearic and oleic acids that cause the blends to have high AV; thus, BS1 showed higher AV (1.59%) than PS. BS5, on the other hand, had low AV values.

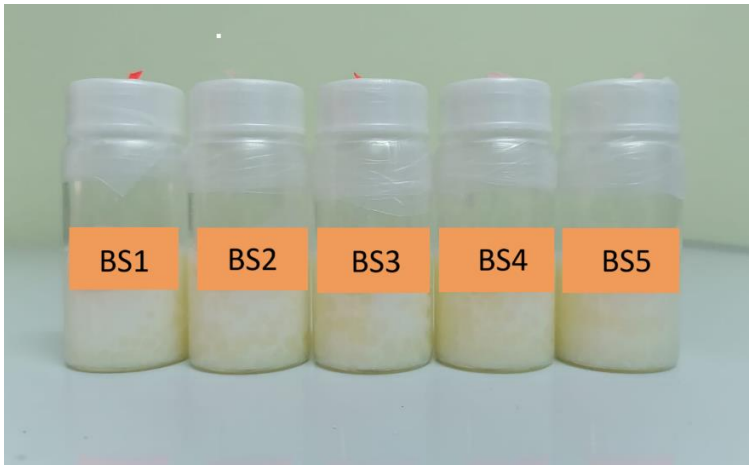

Figure 1. Binary blends produced from the blending of bambangan stearin and palm stearin

Triglycerides (TAG) Profiles

PS exhibited a significant ($P<0.05$) level of PPP, a high-melting TAG, resulting into incomplete melting state at 37 °C. The PPP (melting point: 66.4 °C) was attributed to the very high palmitic acid content (>50%), which impacts the fat's digestibility due to its elevated overall melting point (Biswas *et al.*, 2016; Berry & Sander, 2005; Oliveira *et al.*, 2017). Consequently, the direct use of PS as a specialty fat poses challenges due to its high melting properties, which may lead to a waxy texture. Blending PS with BS offers a way to modify its properties, making it a potential alternative to CB. Commercial CB typically contains symmetrically disaturated (SUS)-TAGs, such as POP, POS, and SOS (Bootello *et al.*, 2018). Similarly, the CB analysed in this study comprised POP (14.25%), POS (33.36%), and SOS (25.65%).

The binary blends were also dominated by these three TAGs but included a notable amount

of high-melting TAGs like SSS and PPP. Compared to CB, PS had a higher POP content (32.65%), followed by PPP (19.30%), POO (14.21%), PLL (7.71%), and POS (6.55%). Blending PS with BS resulted in significant ($p<0.05$) changes to the TAG profiles (Figure 2). SOS (30.22% to 37.73%) was the most abundant TAG in all mixtures, followed by POS (10.95% to 12.43%) and POP (5.66% to 10.35%). However, the binary blends showed reduced POP and POS levels compared to CB, presumably due to the dominance of BS in the mixtures. The SOS content in BS contributed significantly to this observation.

Furthermore, while the blends retained some PPP content from PS, it was significantly ($p<0.05$) lower than in pure PS, likely due to the influence of oleic and stearic acids in BS, which led to increased low-melting TAGs such as SOO and POO. Among the blends, BS1 had the highest SOS, POP, PPP, and SSS levels, indicating a higher melting point. The SSS content in BS1 was also 5% higher than in CB, potentially affecting CB's melting behaviour. Both PPP and SSS, with melting points above 60 °C, may contribute to a waxy texture in the fat. Previous studies (Norazura, Sivaruby, & Noor Lida, 2020; Yanty *et al.*, 2016) have shown that PPP levels above 4% can lead to waxiness, reducing the quality of the final product.

Notably, BS5, comprising 70% BS and 30% PS, demonstrated improved TAG profiles. Although its POS and POP contents were slightly lower than those in CB, BS5 had the lowest SOS range, indicating lower melting properties compared to other blends. The POP content of BS5 was also closer to that of CB. These findings align with previous reports on CB-Equivalent composition, including POP (10.70 – 30.33%), POS (4.60 – 49.53%), and SOS (3.26 – 27.53%) as noted by Bootello *et al*. (2018), Kadivar *et al*. (2016), and Sonwai *et al*. (2014).

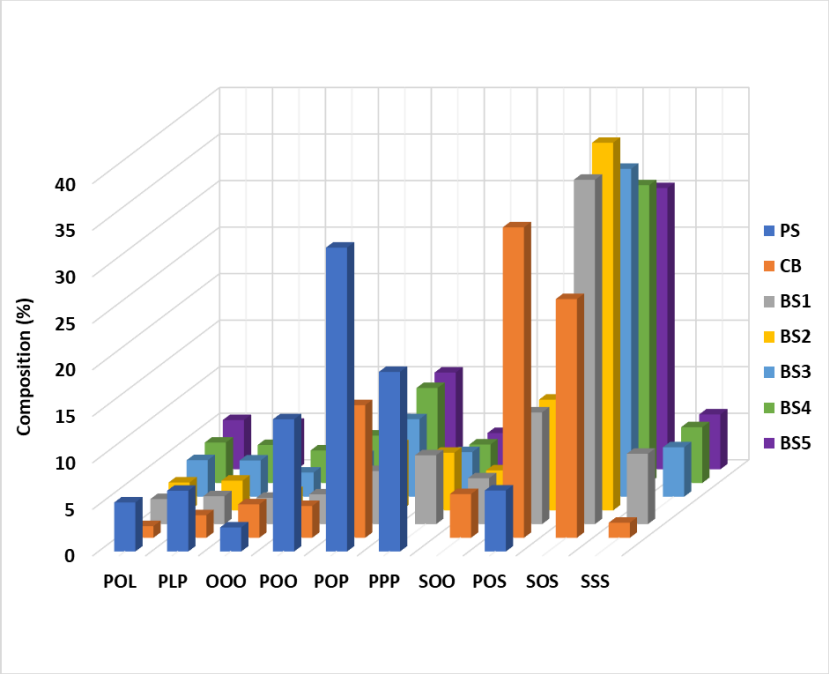

Figure 2. Diffraction pattern and short spacing of bambangan and palm stearin blends

Melting Properties

The individual and blended fat samples in this study were stabilized by incubating fat samples at room temperature for seven days. The stabilization of the fat is needed because the TAG can exist in a few crystalline forms such as (I) γ, (II) α, (III) β'_2, (IV) β'_1, (V) β_2, *and* (VI) β_1 while in a state of solid. Among these forms, (I) γ is the least stable, and (VI) β_1 is the most stable (Talhat *et al.*, 2015). According to Sagiri, Sharma, Basak, and Pal (2014), a peak at ~20 °C suggests the presence of the α-polymorph, which is followed by the β' and β states at increasing temperatures. The TAG is primarily crystallised in the (V) β_2 form, which is more stable and

contributes to a high melting peak temperature in a stabilized fat (Sullo, Arellano, & Norton, 2014). Additionally, the less stable forms may change into more stable ones after being stored for a long enough time. As a result, the melting characteristics of the fat blends have improved after stabilizing for seven days resulting in a melting curve that is sharp and narrow and less likely to cause a waxy mouthfeel (Kadivar *et al.*, 2016).

The melting properties of PS and its mixture are shown in Table 2. The interpretation of the thermal DSC curve is complex for BS, and PS blends due to the complexity of the TAG mixtures in the PS samples and the polymorphic transitions that may occur during melting (Bootello *et al.*, 2018). PS has a broad melting range at a higher temperature, starting at 31.26 °C and ending at 61.58 °C. It shows that this PS is harder, and the melting properties are because the POP and PPP are abundant in PS, which results in a high melting point and incomplete melting at body temperature Kang *et al.* (2013). Additionally, low-fat plasticity in PS results in challenges in generating edible fats like shortening and margarine. Due to its excessively high melting characteristics, which leave a waxy aftertaste, producing alternatives for cocoa butter is also affected (Sellami *et al.*, 2011; Edy & Rizki, 2020). Therefore PS is blended with BS to lower the melting properties. Significant ($p<0.05$) changes can be seen in the melting properties of PS after blending with BS.

The onset, offset, and maximum temperature of PS gradually declined with the blending of BKF-SS. The onset temperature showed an increasing trend proportional to the increment of the PS in the blends. In contrast, constant trends are observed in the offset and maximum temperature of the binary blends. The DSC melting curve for BS: PS blends obtained in this study showed two endothermic peaks but were less broad than the PS. The observation is consistent with the melting curve for PS blending reported by Jahurul *et al.* (2019). The TAG of PS contributed to the presence of the two peaks with a high melting temperature. The onset and offset values for the blends range from 23.05 °C to 26.06 °C and 39.66 °C to 39.71 °C, respectively.

Table 2. Melting properties of bambangan stearin and palm stearin blends

	Melting properties			
	Onset temperature (˚C)	Maximum temperature (˚C)	Offset temperature (˚C)	Enthalpy (J/g)
Bambangan stearin (BS)	22.19 ± 0.02^{b}	31.20 ± 0.01^{b}	37.82 ± 0.01^{b}	66.14 ± 0.56^{h}
Palm stearin (PS)	31.26 ± 0.36^{g}	60.25 ± 0.02^{g}	62.58 ± 0.67^{f}	40.97 ± 0.07^{c}
Cocoa butter (CB)	21.00 ± 0.60^{a}	28.20 ± 0.11^{a}	37.10 ± 0.08^{a}	56.30 ± 0.30^{g}
BS1 (90% BS: 10% PS)	23.05 ± 0.26^{c}	33.45 ± 0.02^{e}	39.66 ± 0.23^{c}	47.34 ± 0.11^{e}
BS2 (85% BS: 15% PS)	25.81 ± 0.19^{e}	35.27 ± 0.01^{f}	39.65 ± 0.34^{c}	45.40 ± 0.48^{d}
BS3 (80% BS: 20% PS)	25.95 ± 0.11^{e}	32.16 ± 0.03^{d}	39.80 ± 0.36^{e}	23.09 ± 0.16^{a}
BS4 (75% BS: 25% PS)	26.06 ± 0.12^{f}	32.13 ± 0.09^{d}	39.71 ± 0.34^{d}	28.43 ± 0.15^{b}
BS5 (70% BS: 30% PS)	25.07 ± 0.23^{d}	31.95 ± 0.02^{c}	39.71 ± 0.21^{d}	54.11± 0.49^{f}

Values are the mean±standard deviation of triplicate; means a different letter within a column is significantly different ($p<0.05$) as measured by Tukey test

The results are significantly ($p<0.05$) higher than the CB, indicating the blends (melting range: 13.65 °C to 16.61 °C) showed more rapid melting than the CB (melting range: 16.1 °C). According to Shetty, Reddy, & Khatoon (2014) and Rebecca *et al.* (2020), the melting temperature for SSS, PPP, POP, POS, and SOS are 73.1 °C, 66.4 °C, 35.2 °C, 37.5 °C to 58 °C and 41.6 °C, respectively. BS: PS blends in this study have higher SOS thus, the offset values for the blends are closer to 40 °C.

Crystallisation Profiles

Table 3 shows the changes in the crystallisation properties for BS: PS blends. PS showed a sharp crystallisation curve with the crystallisation starting at 26.36 ºC and ending at 23.57 ºC. The

crystallisation process occurs fast (crystallisation range: 2.79 ºC) because the high melting TAG dominated 50% of PS composition. Therefore, PS tends to crystallise faster below its melting temperature. Compared to CB, the PS crystallises at room temperature faster than CB and its blends. The onset and offset values for the blends were significantly higher than the CB observed in this study. The binary blends contain higher palmitic and POP content thus the blends have a rapid crystallisation range. The increase in the PS ratio induced the crystallisation peak of the binary blends to move toward lower temperatures.

The results correlate with the decrease of trisaturated TAG and the increase of disaturated TAG. The SSS and PPP content in the binary blends decreased proportionally to the increase in the PS ratio, lowering the melting and crystallisation properties of the blends. BS2 and BS3 showed a mixture of two crystallisation peaks, and blends with more than 20% of PS ratios showed two separate peaks. The thermogram is consistent with their melting thermogram, which indicates a mixture of two distinct TAGs. Among the blends, BS5 showed a comparable crystallisation value with CB (onset: 16.6 ºC and offset: 7.4 ºC) reported by Kang *et al.* (2013), indicating this blend resembled CB the most.

Table 3. Crystallization properties of bambangan stearin and palm stearin blends

	Crystallization properties			
	Onset Temperature (ºC)	Offset Temperature (ºC)	Max Temperature (ºC)	Enthalpy (J/g)
Cocoa butter (CB)	14.77 ± 0.23^{a}	3.42 ± 0.07^{a}	11.17 ± 0.56^{a}	-140.53 ± 1.46^{d}
Palm stearin (PS)	26.36 ± 0.18^{g}	23.57 ± 0.43^{h}	25.18 ± 0.11^{h}	-148.76 ± 0.81^{c}
Bambangan stearin (BS)	18.24 ± 0.01^{c}	7.92 ± 0.01^{b}	15.05 ± 0.13^{c}	-118.92 ± 0.04^{h}
BS1 (90% BS: 10% PS)	20.42 ± 0.18^{f}	11.58 ± 0.07^{g}	16.62 ± 0.23^{g}	-156.13 ± 1.85^{b}
BS2 (85% BS: 15% PS)	19.47 ± 0.14^{e}	8.28 ± 0.18^{c}	14.64 ± 0.05^{b}	-163.71 ± 2.81^{a}
BS3 (80% BS: 20% PS)	18.67 ± 0.04^{d}	11.37 ± 0.08^{f}	16.55 ± 0.07^{f}	-127.88 ± 2.13^{g}
BS4 (75% BS: 25% PS)	18.00 ± 0.03^{c}	10.48 ± 0.09^{e}	15.99 ± 0.32^{e}	-133.16 ± 2.01^{f}
BS5 (70% BS: 30% PS)	17.53 ± 0.01^{b}	9.18 ± 0.01^{d}	15.32 ± 0.32^{d}	-136.29 ± 2.01^{e}

Values are the mean±standard deviation of triplicate; means a different letter within a column is significantly different ($p<0.05$) as measured by Tukey test

Polymorphic Form

The effect of blending PS in the BS polymorphic behaviour is presented in Figure 3. Unlike BS, PS in this study has a different TAG composition with very high palmitic content that leads to the presence of PPP-TAG. Hence, the PS in this study exhibited *β'* (d-spacing of 4.13 Å) peak and a weak *β* peak at a d-spacing of 4.58 Å with *β'* peak being dominant. This finding is consistent with the fingerprint pattern of PS reported by Omar *et al.* (2018), who reported the *β'* form in PS. This is associated with grainy structure, and tripalmitin is the *β* form-tending. The polymorphic form for BS: PS blends changed significantly ($p<0.05$), resulting in a similar fingerprint pattern to the CB after integrating BS in the binary blends which showed a sharp *β* (v) form at 4.58 Å. This form is commonly associated with the desirable polymorphic form of chocolate. The stable *β* (v) form is preferred for chocolates and coatings because it melts at high temperatures and has a small to moderate crystal structure, providing a smooth mouthfeel effect.

Therefore, the blends might exhibit small to moderate crystal structures that result in the abovementioned properties. The binary blends exhibited a dominant *β* (v) form closer to the CB polymorphic form, with BS5 showing equal intensity and pattern. This behaviour was presumably due to the BS fingerprint pattern, which has a similar polymorphic pattern to the CB as well as the changes in the FA composition contributing to the presence of the three main TAGs (POP, POS, and SOS). The binary blends showed a mixture of *β'* and *β* polymorphic

forms, with the stable β form being dominant because a random TAG distribution in fat can independently present the β' form (Ribeiro *et al.*, 2009). BS1 showed an inseparable peak pattern at 22 to 24 Θ degrees, similar to the fingerprint pattern as BS. The intensity of the β peak is also the highest due to the high SOS content in this blend. The polymorphic form for these blends is also identical to the polymorphic behaviour CBE produced from high oleic high stearic sunflower-based CBE (Bootello *et al.*, 2018). These results indicate that the binary blend produced from the blending of 70% BS and 30% PS exhibited the desirable β (v) form of CB suggested for chocolate or confectionery production.

Overall, the BS: PS blends, especially at the PS content of 30% (BS5), exhibited physicochemical and thermal properties comparable to those of commercial CB. The IV (33.78 – 34.24 g iodine/g) and slip melting point (33.25 °C – 38.35 °C) of the blends were within the typical range for cocoa butter IV: 31.30 to 38.40 g iodine/g and SMP: 25.30 °C to 35.00 °C (Jin *et al*., 2018, 2017, 2016). In terms of TAG composition, the mixtures had a high content of SOS, a low content of POS, and POP. Although the POP and POS content was slightly lower than in cocoa butter, the melting and crystallisation profiles of BS5 were similar to those of cocoa butter, which exhibited a sharp melting range and stable β(V) polymorphism. This behaviour is essential for the desired mouthfeel and snapping properties in chocolate applications. These results suggest that the optimised BS: PS blends could be a potential alternative fat source to commercial cocoa butter.

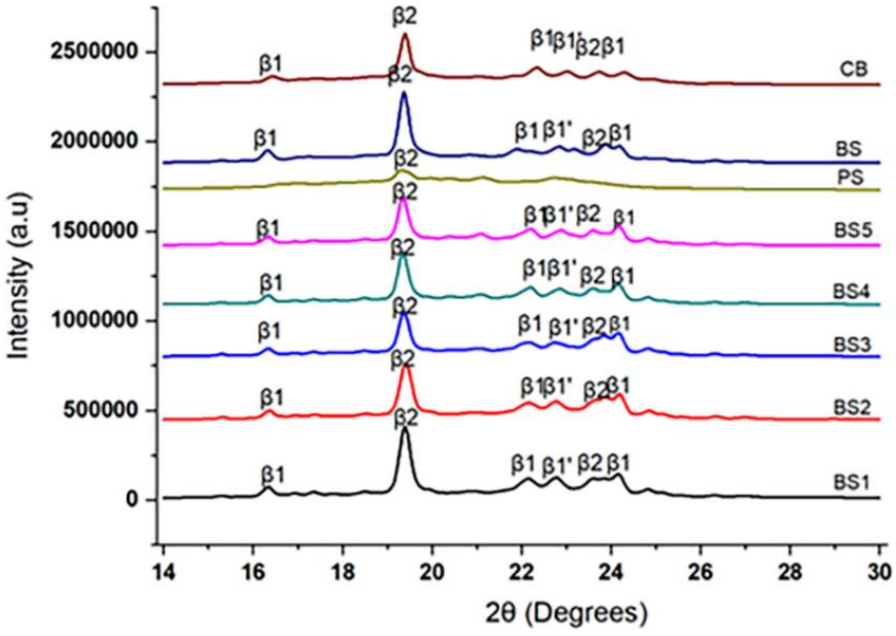

Figure 3. Diffraction pattern and short spacing of bambangan and palm stearin blends

CONCLUSION

This study successfully demonstrated that blending BS with PS can effectively modify the physicochemical and thermal properties of the resulting fat blends. The blends exhibited improved IV, SMP, and AV compared to individual PS, with BS5 (70% BS:30% PS) showing the most promising TAG profile and melting properties similar to commercial CB. The optimized blend reduces the waxy texture often associated with PS while maintaining desirable thermal stability and crystallisation behaviour. These findings suggest that BS: PS blends, specifically BS5, have significant potential as a functional alternative to CB in improving the thermal stability of products and confectionery applications. Further studies on sensory evaluation and product-specific performance are recommended to validate their commercial feasibility.

ACKNOWLEDGEMENTS

All authors thank the Centre for Research and Innovation for Research Grant (SDN0061-2019). The authors also acknowledge Sime Darby Malaysia and the Malaysian Cocoa Board for the sample of PS and CB.

REFERENCES

Ahmad Bustamam, F.K., Yeoh, C.B., Sulaiman, N. & Saw, M.H. (2022). Evaluation on the quality of Malaysian refined palm stearin. *Oil Seeds and fats, Crops and Lipids*, 29. DOI: DOI:10.1051/ocl/2022030

American Oils Chemists' Society. (2003). *Official methods and recommended practices of the American Oils Chemists' Society*. (5th Ed.). (Champaign, Illinois, USA).

AOAC Official Method of Analysis. (2005). Method 945.16, *Oil in Cereal Adjuncts*. (18th Ed). AOAC International, Gaithersburg, MD.

American Oil Chemists' Society. (2009). Official methods and recommended practices of the American Oil Chemist's Society (6th Ed.). Champaign, IL: AOCS Press.

Bootello, M.A., Chong, P.S., Manez, A., Garces, R., Martinez-Force, E. & Salas, J.J. (2018). Characterization of sunflower stearin based confectionery fats in bulk and in compound coatings. *Journal of American Oil Chemist Society*. 94: 235-245. DOI:10.1002/aocs.12126

Biswas, N., Cheow, Y.L., Tan, C.P., & Siow, L.F. (2018). Physical, rheological and sensorial properties, and bloom formation of dark chocolate made with cocoa butter substitutes. *LWT-Food Science and Technology*, 82: 420-428. DOI:10.1016/j.lwt.2017.04.039

Biswas, N., Cheow, Y.L., Tan, C.P., & Siow, L.F. (2016). Blending of palm oil mid fraction, refined deodorized palm kernel oil, or palm stearin for cocoa butter alternative. *Journal of American Oil Chemist Society*, 93: 1415-1427. DOI:10.1007/s11746-016-2880-z

Ishaka, A., Aliyu, A.G. & Mohammad Hassan, Y. (2020). Physico-chemical characteristics of Sokoto Locally grown Cucumis melo L (honeydew Melon) seed oil. *Annals of Clinical Experimental Medicine*, 1: 58-62. DOI:10.47838/ACEM.26011977.11162020.ASMEDA.9.0

Jahurul, M.H.A., Zaidul, I.S.M., Leykey, B., Sharifudin, M.S., Shafiquzzaman, S., Hasmadi, M., Sahena, F., Mansoor,A.H., Lee, J.S. & Jinap, S. (2019). Valuable components of bambangan fruit (*Mangifera pajang*) and its co-products: A review. *Food Research International*, 11: 105-115. DOI:10.1016/j.foodres.2018.08.017

Jin, J., Akoh, C.K., Jin, Q. & Wang, X. (2018). Preparation of mango kernel fat stearin-based hard chocolate fats via physical blending and enzymatic interesterification. *LWT- Food Science and Technology*, 97: 308-316. DOI:10.1016/j.lwt.2018.07.018

Jin. J., Zheng, L., Pembe, W.M., Zhang, J., Xie, D., Wang, X., Huang, J., Jin, Q. & Wang, X. (2017). Production of sn-1,3-distearoyl-2-oleoyl-glycerol-rich fats from mango kernel fat by selective fractionation using 2-methlupentane based isohexane. *Food Chemistry*, 234: 46-54. DOI:10.1016/j.foodchem.2017.04.165

Jin, J., Warda, P., Qi, C., Sun, C., jie, L., Xie, D., Huang, J., Jin, Q. & Xinggua, W. (2016). Mango kernel fat based chocolate fat with heat resistant triacylglycerols: production via blending using mango kernel fat mid-fraction and palm mid-fractions produced in different fractionation paths. *Royal Society Chemistry*, 6: 108981. DOI:10.1039/C6RA19438A

Kadivar, S., De Clercq, N., Mokbul, M. & Dewettinck, K. (2016). Influence of enzymatically produced sunflower oil-based cocoa butter equivalents on the phase behaviour of cocoa butter and quality of dark chocolate. *LWT-Food Science and Technology*, 66: 48-55. DOI:10.1016/j.lwt.2015.10.006

Kang, K.K., Jeon, H., Kim, I.H. & Kim, B.H. (2013). Cocoa butter equivalents prepared by blending fractionated palm stearin and shea stearin. *Food Science Biotechnology*, 22: 347-352. DOI:10.1007/s10068-013-0087-8

Kitiphoom, S. & Sutasinee, S. (2013). Mango seed kernel oil and its physicochemical properties. *International Food Research Journal*, 20: 1145-1149.DOI 10.5281/zenodo.1147522.

MPOB. (2024). Refinery: Monthly production of selected processed palm oil for December 2024. Available from https://bepi.mpob.gov.my/index.php/import/1171-production-of-selected-processed-palm-oil-2024.

Norazlina, M.R., Jahurul, M.H.A., Hasmadi, M., Sharifudin, M.S., Patricia, M., Mansoor, A.H. & Lee, J.S., (2020). Characteristics of bambangan kernel fat fractions produced by solvent fractionation and their potential industrial applications. *Journal of Food Processing and Preservation*, 44 (6): p.e14446. DOI: 10.1111/jfpp.14446

Norazura, A.M.H., Sivaruby, K. & Noor Lida, H.M.D. (2020). Blended palm fractions as confectionery fats: a preliminary study. *Journal of Oil Palm Research*, 0101. DOI:10.21894/jopr.2020.0101

Oma, Z., Hishamudin, E., Kanagaratnam, S., Abd Rashid, N. & Alejndro, G.M. (2018). Dynamics of polymorphic transformation in palm oil, palm stearin and palm kernel oil characterized by coupled powder XRD-DSC. *Journal of Oleo Science*, 6: 737-744. DOI:10.5650/jos.ess17168

Oliveira, P.D., Rodrigues, A.M., Bezerra, C.V. & Silva, L.H. (2017). Chemical intresterification of blends with palm stearin and patawa oil. *Food Chemistry*, 215: 369-376. DOI:10.1016/j.foodchem.2016.07.165

Roslan, M.S., Gerusu, G.J. & Mustafa Kamal, A.H. (2018). Rainwater interception pattern of a regenerated secondary topical forest an oil palm (*Elaeis guineesis* Jacq.) Canopies in Bintulu, Sarawak. *Borneo Journal of Resource Science and Technology*, 8 (1): 41-55. DOI:10.33736/bjrst.823.2018

Ribeiro, A.P.B., Basso, R.C., Gimaldi, R., Gioielli, L.A. & Goncalves, L.P.A. (2009). Instrumental methods for the evaluation of interested fats. *Food analytical Method*, 2: 282-302. DOI:10.1007/s12161-009-9073-4

Sonwai, S., Kaphuekngam, P. & Flood. (2014). Blending of mango kernel fat and palm oil mid-fraction to obtain cocoa butter equivalent. *Journal of Food Science Technology*, 51: 2357-2369. DOI:10.1007/s13197-012-0808-7

Yanty, N., Nazrim, M., Shuhai,I, M. & Miskandar, M.S. (2016). Composition and thermal analysis of ternary mixtures of avocado fat: palm stearin: cocoa butter (Avo: PS:CB). *International Journal of Food Properties*. 1094-2912.DOI:10.1080/10942912.2016.1166130

Borneo Journal of Resource Science and Technology (2025), 15(1): 116-129
DOI: https:doi.org/10.33736/bjrst.6872.2025

Volatile Components, Antibacterial and Antioxidant Activities of Komburongoh (*Acorus calamus* L.) Essential Oils as Potential Medicinal Herbs from Sabah, Malaysia

MOHAMMAD AMIL ZULHILMI BENJAMIN[1], JACQUELINE VINCENT[2], HAJA NURSADAH BINSALI[2], AHMAD ASNAWI MUS[3], MOHD AZRIE AWANG[4] & NOR AZIZUN RUSDI*[2]

[1]Borneo Research on Algesia, Inflammation and Neurodegeneration (BRAIN) Group, Faculty of Medicine and Health Sciences, Universiti Malaysia Sabah, Jalan UMS, 88400, Kota Kinabalu, Sabah, Malaysia; [2]Institute for Tropical Biology and Conservation, Universiti Malaysia Sabah, Jalan UMS, 88400, Kota Kinabalu, Sabah, Malaysia; [3]Faculty of Science and Technology, Universiti Malaysia Sabah, Jalan UMS, 88400, Kota Kinabalu, Sabah, Malaysia; [4]Innovative Food Processing and Ingredients Research Group, Faculty of Food Science and Nutrition, Universiti Malaysia Sabah, Jalan UMS, 88400, Kota Kinabalu, Sabah, Malaysia
*Corresponding authors: azizun@ums.edu.my
Received: 1 April 2024 Accepted: 10 February 2025 Published: 30 June 2025

ABSTRACT

Acorus calamus L., known for diverse therapeutic applications, was studied for its volatile components, antibacterial and antioxidant potential in essential oils from Sabah, Malaysia. Employing hydrodistillation with a Clevenger apparatus, the oils were analysed through gas chromatography-mass spectrometry. Antibacterial activity was assessed via disc diffusion against methicillin-resistant *Staphylococcus aureus* (MRSA) and *Escherichia coli*. Antioxidant properties were evaluated using the 2,2-diphenyl-1-picrylhydrazyl (DPPH) and ferric reducing antioxidant power (FRAP) assays. Both leaf and rhizome oils were rich in phenylpropanoids, oxygenated sesquiterpenes, and sesquiterpenes including α-asarone, γ-asarone, methyl isoeugenol, 6-epi-shyobunone, and (E)-β-farnesene. They demonstrated significant antibacterial activity at 400 µg/mL, while displaying lower DPPH (IC_{50} = 28.20 ± 4.99 µg/mL) and excelling in the FRAP (150.12 ± 0.10 mg TE/g). This ongoing phytochemical analysis of *A. calamus* holds promise for enhancing quality control, ensuring safety, and validating its traditional applications.

Keywords: *Acorus calamus*; antibacterial; antioxidant; essential oil; volatile components

INTRODUCTION

In recent years, there has been a notable increase in research focused on medicinal plants such as *Coleus forskohlii*, *Ranunculus isthmicus* subsp. *tenuifolius*, and *Ranunculus rumelicus*, mostly driven by their wide-ranging pharmacological potential (Khatun *et al.*, 2011; Fafal *et al.*, 2022). The increasing popularity of *Acorus* proliferates due to their medicinally and pharmacologically vital active components (Mukherjee *et al.*, 2007; Mittal *et al.*, 2009). These plants yield numerous natural compounds with therapeutic and pharmacological characteristics such as terpenoids, flavonoids, phenolics, and alkaloids (Sharma *et al.*, 2014; Sharma *et al.*, 2020). Thus, the various beneficial biological activities of natural plant products were extensively investigated. These well-documented advantages involved antibacterial, antioxidant, anti-inflammatory, antifungal, cytotoxicity, herbicide, and insecticide activities (Liu *et al.*, 2013; Ganesan and Gurumallesh Prabu, 2019; Loying *et al.*, 2019; Dinev *et al.*, 2021; Vakayil *et al.*, 2021).

According to Rajput *et al.* (2014), the Acoraceae family contained approximately 110 genera and 1,800 species. Moreover, the morphological and anatomical distinctions of this family indicated that it was originally a member of the Araceae family (Grayum, 1987). Nonetheless, this family was viewed as a relatively primitive group within the family before its reclassification as Acoraceae (Heng *et al.*, 2010). Although the genus *Acorus* comprised 40 species, only several were identified based on their volatile components and bioactivities. These species included *A. calamus* L., *A. tatarinowii* Schott, and *A. gramineus* Solandin

Ait. (Ganjewala and Srivastava, 2011). These plants have been used in traditional medicine systems for centuries.

The *A. calamus* monocot plant is observed as grass-like with long and perennial characteristics. This plant typically thrives in moist and watery semi-aquatic habitats in tropical and subtropical climates (Sharma *et al.*, 2014). According to Ahmad and Holdsworth (2003), the Kadazan-Dusun communities in Sabah, Malaysia, employed around 50 plants (including *A. calamus*) as traditional herbal medicines daily. Furthermore, this plant is also known as 'sweet flag' or 'komburongoh' in the Dusun language, offering advantageous traditional medicine properties in healing various ailments including diarrhoea, insect repellent, poison antidote, and relieving gastritis (Kulip, 1997; Ahmad and Holdsworth, 2003). The leaves and rhizomes produce essential oils in the ethnobotany, phytochemistry, and biological fields, which were also widely investigated (Rajput *et al.*, 2014; Sharma *et al.*, 2014).

Both the leaves and the rhizomes of *A. calamus* contain various bioactive compounds that are believed to offer potential benefits in the pharmaceutical and nutraceutical industries. The antibacterial, antioxidant, antifungal, cardiovascular, and immunosuppressive effects of *A. calamus* essential oil were demonstrated in previous studies (Rajput *et al.*, 2014; Sharma *et al.*, 2014). Numerous researchers have investigated the volatile components of *A. calamus* essential oil due to its medicinal properties, leading to the identification of β-asarone as the primary constituent. However, the concentration of β-asarone in the essential oil varies depending on the geographical area and ploidy level of the plant (Raina *et al.*, 2003; Raal *et al.*, 2016).

α-Asarone (**1**), β-asarone (**2**), and γ-asarone (**3**) (Figure 1) are phenylpropenes that occur naturally in various plant groups, primarily in Acoraceae, Aristolochiaceae, and Lauraceae (Ganjewala and Srivastava, 2011; Uebel *et al.*, 2021). Plants containing asarone are commonly used for flavouring alcoholic beverages such as bitters. Research on the mutagenic effects of propenylic α-asarone and β-asarone has produced inconsistent findings, and there is a lack of available data regarding the potential carcinogenicity or genotoxicity of allylic γ-asarone (Varma *et al.*, 2002; Berg *et al.*, 2016; Atalar and Türkan, 2018).

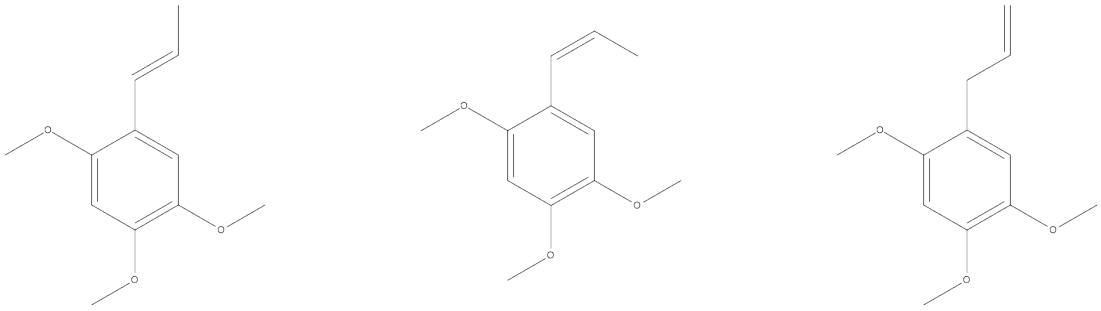

(1) **(2)** **(3)**

Figure 1. Chemical structures of α-asarone (**1**), β-asarone (**2**), and γ-asarone (**3**)

There are no published studies on the antibacterial and antioxidant properties of essential oils derived from various parts of *A. calamus* plants. Furthermore, no prior findings on the chemical composition, antibacterial and antioxidant properties of essential oils produced from these plants have been reported in Sabah, Malaysia. Different studies may employ varied extraction methods or analytical techniques, making it challenging to directly compare results. Despite the extensive research conducted on *A. calamus*, there may still be undiscovered phytochemicals or components with potential therapeutic benefits. Hence, this research was undertaken to investigate the antibacterial activity using the disc diffusion method, as well as the antioxidant activity using the 2,2-diphenyl-1-picrylhydrazyl (DPPH) radical scavenging and ferric reducing antioxidant power (FRAP) assays of essential oils isolated from various components of *A. calamus*. Additionally, the essential oils from different parts of *A. calamus* were evaluated using gas chromatography-mass spectrometry (GC-MS) analysis to identify their volatile components and determine which factors contribute to their

antibacterial and antioxidant properties. Overall, studying the phytochemical analysis of *A. calamus* is an ongoing process that can improve quality control and safety considerations, and further validate the traditional uses of this plant.

MATERIALS AND METHODS

Chemicals and Reagents

The ferric chloride ($FeCl_3$) heptahydrate and pentane were procured from Merck (Darmstadt, Germany). Subsequently, 2,4,6-tris(2-pyridyl)-1,3,5-triazine (TPTZ) reagent, kanamycin, and glycerol were obtained from Sigma-Aldrich (Burlington, MA, USA). Meanwhile, acetic acid, anhydrous sodium acetate, hydrochloric acid, and methanol were sourced from Chemiz (Selangor, Malaysia). This study also utilised Trolox (Targetmol, Boston, MA, USA), dimethyl sulfoxide (DMSO) (Systerm, Selangor, Malaysia), and DPPH reagent (Tokyo Chemical Industry, Tokyo, Japan). Finally, all chemicals and reagents acquired from Bio3 Scientific Sdn. Bhd. and Apical Scientific Sdn. Bhd., Malaysia, were of analytical grade.

Plant Material

Whole plants of *A. calamus* were purchased from local farms in Ranau, Sabah, Malaysia (Coordinate: 5°57'26.4" N 116°40'24.0" E). The samples were not subjected to herbarium identification, as their identity was already well-established. *A. calamus* leaves and rhizomes were rinsed with distilled water to eliminate extraneous contaminants from the sample. After drying the samples in an oven at 50 °C (ED 23, Binder, Neckarsulm, Germany) until reaching a constant weight, the weights of each sample were measured. After collection, 250 to 300 g of *A. calamus* leaves and rhizomes were ground and pulverised using a grinder (EBM-9182, Elba, Borso Del Grappa, Italy). This increased the surface area, facilitating the extraction process and making it easier to fill the round flask.

Essential Oil Extraction

Following the method described by Cheng *et al.* (2005) with minor modifications, the dried *A. calamus* leaves and rhizomes were individually obtained using the hydrodistillation process. The ground samples were added to a 500 mL round flask with a capacity of 1000–2000 mL of distilled water. Subsequently, the substance was subjected to a six-hour hydrodistillation technique using a glass Clevenger-type apparatus. After the pentane dehydration process, the essential oil was transferred into dark-brown glass vials, sealed with aluminium foil, and stored at 4 °C until further analysis. The quantities of essential oil obtained were measured and expressed as a percentage (%) of the weight of the initial samples, following the established protocol described by Park *et al.* (2021). The oil yield was determined using the following equation, Eq.(1):

$$\text{Oil yield (\%, w/w)} = \frac{\text{Mass of oil extracted (g)}}{\text{Mass of sample (g)}} \times 100 \qquad \text{Eq.(1)}$$

Volatile Component Analysis

A fused silica capillary column (SH-Stabilwax-DA, Shimadzu, Kyoto, Japan) with dimensions of 30 m × 0.25 mm × 0.25 µm was connected to a GC-MS (GCMS-QP2010 SE, Shimadzu, Kyoto, Japan) for the analysis of the volatile components in the extracted oil. The injector was programmed to reach an injection volume of 1 µL, a split ratio of 1:40, and a target temperature of 250 °C. Initially, the GC oven temperature was set to 50 °C for 20 min, then ramped up to 250 °C at a rate of 3 °C per min, followed by a slower ramp to 300 °C at a rate of 1 °C per min. Helium was used as the carrier gas at a steady flow rate of 0.8 mL/min. Other analytical parameters included an ionisation potential of 70 eV and mass scanning from 35 to 450 m/z. In full scan mode, the MS detector revealed unique peak fragmentation patterns for several metabolites. The identification of volatile components from each peak was matched with reference mass spectra obtained from the National Institute of Standards and Technology (NIST) (MS Search Program Version 2.0) databases. The individual component concentrations were determined using a percentage of peak area (Adams, 2000).

Antibacterial Analysis

Bacterial strain growth

The American Type Culture Collection (ATCC) reference strains were received from the Faculty of Science and Technology, Universiti Malaysia Sabah. Two human pathogenic bacterial strains

were used: methicillin-resistant *Staphylococcus aureus* (MRSA) (Gram-positive, ATCC 43300) and *Escherichia coli* (Gram-negative, ATCC 25922).

Media preparation

The powdered 38 g Mueller-Hinton Agar (MHA) (Becton Dickinson, Franklin Lakes, NJ, USA) was added to 1 L distilled water. Subsequently, the media was carefully dissolved by shaking the conical flask. The media were then sterilised for 20 min at 121 °C in an autoclave (HMC Hiclave HV-25L, Gemini BV, Apeldoorn, Netherlands). Finally, the media were cooled before being transferred to separate 25 mL-capacity Petri dishes (nutrient agar).

Disc diffusion method

Using a modified version of the disc diffusion method outlined by Hong *et al.* (2021), the extracted oils were tested against two human pathogens. The 90 mm Petri dishes were prepared with 20 mL MHA and a 100 µL bacterial suspension, distributing them evenly. Sterilised filter paper discs with a 6 mm diameter were impregnated with 20 µL of essential oil. The oil was serially diluted with DMSO to achieve varying concentrations (100, 200, 300, and 400 µg/mL), following the protocol of Pintatum *et al.* (2020). Subsequently, the discs were left to dry for 15 min before being transferred using sterile forceps and then injected with two controls. These controls included a kanamycin susceptibility disc (100 µg/mL) for the positive control, and a DMSO susceptibility disc (100 µg/mL) for the negative control. The Petri dishes were then incubated at 37 °C for approximately 24 h. Finally, the diameters of the zone of inhibition (ZOI) were measured to determine the growth inhibition zones in millimetres (mm).

Antioxidant Analysis

DPPH assay

Based on the study by Benjamin *et al.* (2022), the DPPH free radical scavenging activity of the essential oil was assessed with minor adjustments. In a 96-well culture plate, 50 µL of dissolved essential oil was reacted at respective doses with 0.1 mM DPPH-methanolic solution (195 µL). The mixture was then gently stirred for 1 min before resting for 1 h. Finally, the absorbance of the final product was measured against a blank (methanol) using a microplate reader (Multiskan SkyHigh, Thermo Fisher Scientific, Waltham, MA, USA) at 540 nm absorbance units. The positive control used was Trolox within a range of 6.25 to 100 µg/mL. Regression analysis was employed to determine the IC_{50} values (the concentration of a sample necessary to neutralise half of the DPPH radicals).

FRAP assay

The FRAP assay used in this investigation was modified based on the method outlined by Jinoni *et al.* (2024). The FRAP reagent was prepared by combining 300 mM acetate buffer (pH 3.6), TPTZ, and 20 mM $FeCl_3$ in a 10:1:1 ratio. In a 96-well culture plate placed in a water bath (WB-11, Daihan Scientific, Wonju, South Korea), 20 µL of dissolved essential oil and 180 µL of FRAP reagent were mixed and subjected to incubation at 37 °C for 40 min in the dark. The resulting absorbance readings of the combination were measured at 593 nm using a microplate reader, with a blank reference of methanol. The antioxidant positive control Trolox was used within a range of 0 to 100 µg/mL. The value was expressed as mg of Trolox per g (mg TE/g) of extract.

Statistical Analysis

This study performed each procedure in triplicate. The findings were then denoted as mean ± standard deviation. Subsequently, independent samples t-tests (with a significance level of $p<0.05$) were applied in the antibacterial analysis to compare the statistical data. Statistical analysis was performed using IBM SPSS Statistics version 19.0 for Windows.

RESULTS AND DISCUSSION

Extraction Yield

When subject to hydrodistillation, both the *A. calamus* leaves and rhizomes yielded yellow-coloured essential oils with strong aromatic fragrances (Figure 2). On a fresh weight basis, the essential oil yield was 0.043%, w/w, for leaves and 0.370%, w/w, for rhizomes (Table 1). Notably, factors such as genotype and agronomic variables (including harvesting

period, plant age, soil fertility, and crop density) can significantly impact production (Marotti *et al.*, 1994). Additionally, Parki *et al.* (2017) pointed out that the oil output from *A. calamus* leaves and rhizomes varies based on climate, season, and geographic location.

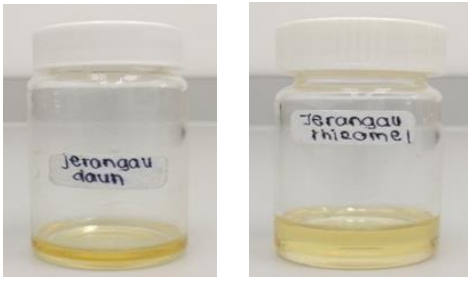

(a) (b)

Figure 2. Essential oil extract from *A. calamus* leaves (a) and rhizomes (b)

Table 1. Essential oil yields from different tissues of *A. calamus*

Tissue	Fresh weight (g)	Yields (%, w/w)	Physical properties
Leaf	3293.79	0.043	Yellow
Rhizome	2229.08	0.370	Yellow

The *A. calamus* leaves and rhizomes exhibit a decreased oil yield compared to the findings published in prior research studies. For example, from a 500 g sample of fresh rhizomes, they managed to produce 1.30% and 1.23% to 4.80% oil yield (Raina *et al.*, 2003; Parki *et al.*, 2017).

Volatile Components of Essential Oils

A total of 78 volatile components were detected in both *A. calamus* leaf and rhizome essential oils. The identified components in *A. calamus* essential oils obtained separately from leaves and rhizomes, along with their relative percentages, retention times, and compound classes, are presented in Table 2. Moreover, the chromatographic oil profiles of *A. calamus* leaves and rhizomes are depicted in Figure 3 and Figure 4, respectively.

Fifty-nine (59) components were identified in the *A. calamus* leaf essential oil, comprising two monoterpenes (0.17%), 14 sesquiterpenes (8.09%), seven oxygenated monoterpenes (2.26%), one oxygenated diterpene (0.02%), 23 oxygenated sesquiterpenes (7.42%), five phenylpropanoids (80.07%), and seven miscellaneous (1.81%), accounting for 99.84% of the volatile components. Among the 41 components identified in the *A. calamus* rhizome essential oil, four were monoterpenes (2.90%), 11 were sesquiterpenes (2.97%), five were oxygenated monoterpenes (1.38%), 12 were oxygenated sesquiterpenes (6.78%), five were phenylpropanoids (84.66%), and four were miscellaneous (0.98%), representing 99.67% of the volatile components. The leaf essential oil was characterised by the presence of α-asarone (73.39%), (E)-β-farnesene (5.12%), methyl isoeugenol (4.63%), 6-epi-shyobunone (2.63%), γ-asarone (1.60%), linalool (1.43%), and Z-3-hexadecen-7-yne (1.21%) as the major components. Similarly, the rhizome essential oil was rich α-asarone (76.70%), methyl isoeugenol (6.38%), 6-epi-shyobunone (3.20%), trans-β-ocimene (2.02%), 4,6,6-trimethyl-2-(3-methylbuta-1,3-dienyl)-3-oxatricyclo[5.1.0.02,4]octane (1.96%), and γ-asarone (1.55%).

Previous research has extensively documented the diverse array of volatile components found in the leaves and rhizomes of *A. calamus* essential oils from various regions across the globe. For instance, Chaubey *et al.* (2018) reported the presence of 37 volatile components in the *A. calamus* leaf essential oil from the Himalayan region of Uttarakhand, India, with β-asarone constituting the highest proportion (77.7%), followed by α-asarone (6.8%). Raal *et al.* (2016) conducted research specifically on the essential oil extracted from *A. calamus* rhizomes and found it to be primarily composed of oxygenated sesquiterpenes (81.7 – 97.0%). The most abundant component in this oil was β-asarone, accounting for a substantial proportion ranging from 9.3% to 85.3%.

Table 2. Volatile components identified in the *A. calamus* leaf and rhizome essential oils

No.	Rt (min)[a]	Component[b]	Molecular formula	Percentage (%)[c]	
				Leaves	Rhizomes
1	8.206	α-Pinene	$C_{10}H_{16}$	–	0.13
2	8.918	Camphene	$C_{10}H_{16}$	–	0.53
3	9.059	1-Methylpentyl hydroperoxide	$C_6H_{14}O$	0.38	0.40
4	9.816	Sabinene	$C_{10}H_{16}$	–	0.22
5	10.06	β-Pinene oxide	$C_{10}H_{16}O$	–	0.05
6	12.34	Limonene	$C_{10}H_{16}$	0.06	–
7	12.562	trans-β-Ocimene	$C_{10}H_{16}$	0.11	2.02
8	15.659	Linalool	$C_{10}H_{18}O$	1.43	0.39
9	18.285	Camphor	$C_{10}H_{16}O$	0.27	0.78
10	19.753	Terpinen-4-ol	$C_{10}H_{18}O$	0.07	0.08
11	20.233	(E)-1,4-Undecadiene	$C_{11}H_2O$	0.06	–
12	20.526	α-Terpineol	$C_{10}H_{18}O$	0.06	–
13	24.241	Isopiperitenone	$C_{10}H_{14}O$	0.07	–
14	24.600	Bornyl acetate	$C_{12}H_{20}O_2$	0.34	0.08
15	26.761	δ-Elemene	$C_{15}H_{24}$	0.01	–
16	29.302	β-Elemene	$C_{15}H_{24}$	0.12	0.08
17	30.155	Methyl eugenol	$C_{11}H_{14}O_2$	0.03	0.01
18	30.677	Aristolene	$C_{15}H_{24}$	–	0.68
19	30.682	cis-β-Guaiene	$C_{15}H_{24}$	–	0.17
20	30.754	Isocaryophyllene	$C_{15}H_{24}$	0.96	–
21	31.200	β-Copaene	$C_{15}H_{24}$	–	0.62
22	31.207	β-Gurjunene	$C_{15}H_{24}$	–	0.29
23	32.009	(E)-β-Farnesene	$C_{15}H_{24}$	5.12	–
24	32.380	α-Humulene	$C_{15}H_{24}$	0.92	–
25	32.555	Methyl isoeugenol	$C_{11}H_{14}O_2$	4.63	6.38
26	33.490	Germacrene D	$C_{15}H_{24}$	0.12	0.03
27	33.833	6-epi-Shyobunone	$C_{15}H_{24}O$	2.63	3.20
28	34.113	Bicyclogermacrene	$C_{15}H_{24}$	0.04	0.06
29	34.114	γ-Elemene	$C_{15}H_{24}$	0.09	0.02
30	34.663	Dihydro-β-agarofuran	$C_{15}H_{26}O$	0.01	–
31	34.811	Shyobunone	$C_{15}H_{24}O$	0.49	–
32	35.004	δ-Cadinene	$C_{15}H_{24}$	0.27	0.51
33	35.634	Kessane	$C_{15}H_{26}O$	0.17	0.12
34	36.157	α-Calacorene	$C_{15}H_{20}$	0.02	0.39
35	36.381	α-Elemol	$C_{15}H_{26}O$	0.22	–
36	36.404	Elimicin	$C_{12}H_{16}O_3$	–	0.02
37	36.405	Cyclopentanecarboxylic acid, 3-methylene-2,2-dimethyl-5-[(E)-1-propenyl]-, methyl ester	$C_{13}H_{20}O_2$	–	0.03
38	36.733	Nerolidol	$C_{15}H_{26}O$	0.35	–
39	36.721	(E)-Farnesene epoxide	$C_{15}H_{24}O$	0.50	–
40	37.126	γ-Asarone	$C_{12}H_{16}O_3$	1.60	1.55
41	37.604	epi-Cubebol	$C_{15}H_{26}O$	0.12	–
42	37.667	Spathulenol	$C_{15}H_{24}O$	–	0.04
43	37.596	Germacra-diene-4-ol	$C_{15}H_{24}O$	0.22	–
44	37.897	Germacra-4(15),5,10(14)-trien-1-α-ol	$C_{15}H_{24}O$	0.04	–
45	37.907	Caryophyllene oxide	$C_{15}H_{24}O$	0.05	–
46	38.911	Z-3-Hexadecen-7-yne	$C_{16}H_{28}$	1.21	0.44
47	39.313	α-Asarone	$C_{12}H_{16}O_3$	73.39	76.70
48	39.907	Tetradecahydrophenanthrene	$C_{14}H_{24}$	0.05	–
49	39.928	Shyobunone @(2S,3S,6S)	$C_{15}H_{24}O$	0.05	–
50	39.922	Selina-3,11-dien-6-α-ol	$C_{15}H_{24}O$	0.14	–
51	40.177	Ledane	$C_{15}H_{26}$	0.03	–
52	40.307	Cadina-1(6),4-diene	$C_{15}H_{24}$	0.02	–
53	40.337	τ-Cadinol	$C_{15}H_{26}O$	0.30	0.21

Table 2. (continued)

No.	Rt (min)[a]	Component[b]	Molecular formula	Percentage (%)[c] Leaf	Rhizome
54	40.877	τ-Muurolol	$C_{15}H_{26}O$	0.11	0.07
55	40.879	α-Cadinol	$C_{15}H_{26}O$	0.63	–
56	41.21	Khusinol acetate	$C_{17}H_{26}O_2$	–	0.24
57	41.402	(Z)-Isogeraniol	$C_{10}H_{18}O$	0.02	–
58	41.441	Isolongifolol acetate	$C_{17}H_{28}O_2$	0.05	–
59	41.567	β-Asarone	$C_{12}H_{16}O_3$	0.42	–
60	41.572	4,6,6-Trimethyl-2-(3-methylbuta-1,3-dienyl)-3-oxatricyclo[5.1.0.02,4]octane	$C_{15}H_{22}O$	–	1.96
61	41.620	Aromadendrene	$C_{15}H_{24}$	0.23	–
62	41.668	Cyclocolorenone	$C_{15}H_{22}O$	0.63	–
63	42.035	Bulnesol	$C_{15}H_{26}O$	0.03	–
64	42.210	7-Tetracyclo[6.2.1.0(3.8)0(3.9)]undecanol, 4,4,11,11-tetramethyl-	$C_{15}H_{24}O$	–	0.05
65	42.418	Isogermacrene D	$C_{16}H_{26}$	0.14	–
66	42.421	β-Vatirenene	$C_{15}H_{22}$	–	0.12
67	42.457	6-epi-Shyobunol	$C_{15}H_{26}O$	0.15	–
68	42.460	Shyobunol	$C_{15}H_{26}O$	0.45	–
69	42.896	N-Dodecanal	$C_{12}H_{24}O$	0.01	–
70	42.905	Octadecanal	$C_{18}H_{36}O$	0.04	–
71	43.202	Asaronaldehyde	$C_{10}H_{12}O_4$	0.06	0.11
72	43.703	Lippifoli-1(6)-en-5-one	$C_{15}H_{22}O$	–	0.33
73	44.513	Isocalamendiol	$C_{15}H_{26}O_2$	–	0.38
74	44.520	α-Bisabolol	$C_{15}H_{26}O$	0.02	–
75	44.530	Isocalamenediol	$C_{15}H_{26}O_2$	0.06	–
76	46.459	Cyperotundone	$C_{15}H_{22}O$	–	0.05
77	46.473	8-Isopropenyl-1,3,3,7-tetramethyl-bicyclo[5.1.0]oct-5-en-2-one	$C_{15}H_{22}O$	–	0.13
78	56.346	Phytol	$C_{20}H_{40}O$	0.02	–
		Monoterpenes		0.17	2.90
		Sesquiterpenes		8.09	2.97
		Oxygenated monoterpenes		2.26	1.38
		Oxygenated diterpenes		0.02	–
		Oxygenated sesquiterpenes		7.42	6.78
		Phenylpropanoids		80.07	84.66
		Miscellaneous		1.81	0.98
		Total		99.84	99.67

[a]Retention time (RT) identified using the NIST mass spectral library. [b]Compound are listed in order of elution from the SH-Stabilwax-DA column. [c]Percentage of components was calculated as the peak area of each component divided by the peak area of the total ion chromatogram × 100. (–) = Not detected.

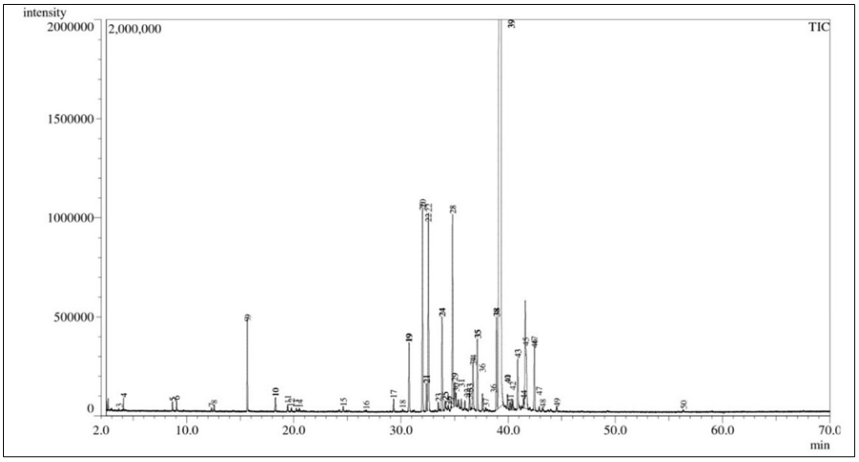

Figure 3. The chromatographic profiles of *A. calamus* leaf essential oil

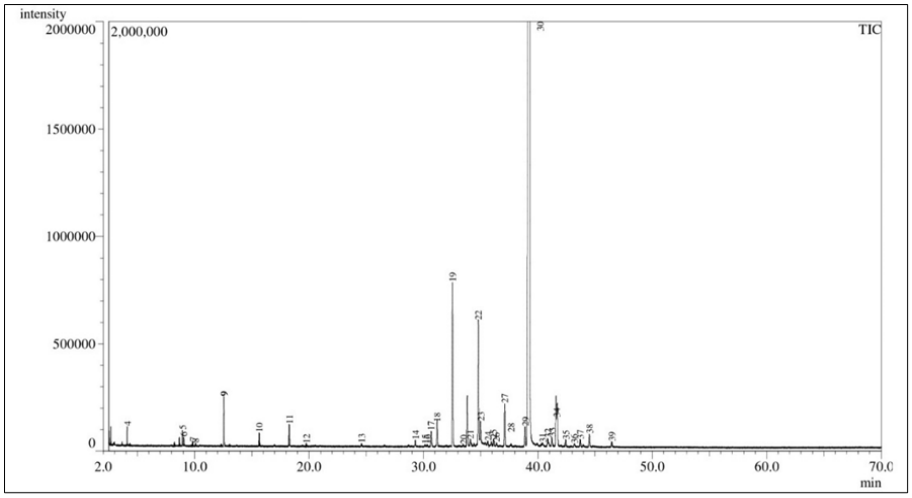

Figure 4. The chromatographic profiles of *A. calamus* rhizome essential oil

Additionally, α-acorenone, shyobunone, 6-epi-shyobunone, dehydroisocalamendiol, preisocalamendiol, and isoacorone were identified as notable constituents in the oil across four different accessions. Similarly, Venskutonis and Dagilyte (2003) reported that β-asarone was the predominant compound in *A. calamus* leaf essential oil, making up 27.0–45.5% of the total composition. Other studies have reported varying dominant compounds in *A. calamus* essential oil. For example, in a collection of triploid European calamus (*A. calamus*) oil, Mazza (1985) identified β-asarone (77.68%) and α-asarone (6.80%) as the primary constituents. Raina *et al.* (2003) found the tetraploid characteristic of *A. calamus* leaf and rhizome essential oils from Utaranchal, India, to contain β-asarone (83.2–85.6%), α-asarone (9.7%), and linalool (4.7%). Moreover, compounds like β-asarone, (Z)-methyl isoeugenol, (E)-caryophyllene, α-humulene, germacrene, linalool, camphor, and isoborneol have also been reported in the *A. calamus* leaf essential oil from Lithuania (Radušiene *et al.*, 2007). Furthermore, studies by Satyal *et al.* (2013), Parki *et al.* (2017), and Loying *et al.* (2019) consistently noted the presence of β-asarone as principal components in *A. calamus* leaf and rhizome essential oils.

The variability of volatile components within different plant parts is influenced by various factors such as geographical conditions, plant age, climate, and plant ploidy (Venskutonis and Dagilyte, 2003; Parki *et al.*, 2017). Various species of *A. calamus* demonstrate a global distribution pattern that correlates with their respective ploidy levels (Ogra *et al.*, 2009). Among the various research findings, Liu *et al.* (2013) reported the presence of α-asarone (50.09%) as the predominant constituent in *A. calamus* rhizome essential oil found in Hebei Province, China. This discovery aligns with the results obtained in this study, where it was observed that the *A. calamus* leaf and rhizome oils from Sabah, Malaysia, are predominantly composed of α-asarone. Furthermore, the identification of allylic γ-asarone in the essential oils derived from the leaves and rhizomes of *A. calamus* in Sabah, Malaysia, at concentrations of 1.60% and 1.55% respectively, provides compelling evidence for the exceptional distinctiveness of these oils compared to those obtained from *A. calamus* in different regions. Notably, β-asarone has consistently been associated with potential toxicity and carcinogenicity. However, as of now, there are no existing restrictions in place to prohibit the utilisation of α-asarone and γ-asarone (Uebel *et al.*, 2021).

The use of retention index (RI) in this analysis was limited by several factors. The main limitation was the analytical setup, which lacked the required standard compounds for RI calibration, making RI measurement impractical. Therefore, RT was used, along with mass spectral matching and similarity measures, which provided sufficient reliability for compound identification, as demonstrated in previous studies (Mus *et al.*, 2021; Manjarrez-Quintero *et al.*, 2024). Additionally, the consistent and well-documented conditions of the GC column ensured that RT remained a reliable metric across similar analyses, supporting its use in this study.

Antibacterial Activity

The ZOI against the Gram-positive bacterial strain (MRSA) and Gram-negative bacterial strain (*E. coli*) are presented in Table 3 and Table 4, respectively. The antibacterial activity of *A. calamus* leaf and rhizome essential oils was successfully assessed. The ZOI against MRSA ranged from 8.67 ± 0.58 mm to 11.00 ± 0.00 mm for leaves, and from 9.33 ± 0.58 mm to 11.33 ± 0.58 mm for rhizomes, respectively. Similarly, both *A. calamus* leaf and rhizome essential oils exhibited inhibitory effects against *E. coli*, with ZOI ranging from 8.67 ± 0.58 mm to 9.67 ± 0.58 mm, and from 8.67 ± 0.58 mm to 10.00 ± 0.00 mm, respectively. These values demonstrated a steady increase with increasing oil concentration, from 100 µg/mL to 400 µg/mL.

Table 3. ZOI of *A. calamus* leaf and rhizome essential oils against MRSA

Plant part	ZOI (mm)					
	Concentration of essential oil (µg/mL)				Control (µg/mL)	
	100	200	300	400	Kanamycin	DMSO
Leaves	8.67 ± 0.58	9.33 ± 0.58	10.00 ± 0.00	11.00 ± 0.00	10.33 ± 0.58	0.00
Rhizomes	9.33 ± 0.58	9.67 ± 0.58	10.33 ± 0.58	11.33 ± 0.58	10.67 ± 0.58	0.00

Values are expressed as means ± standard deviations based on three replicates. Significant differences were observed among concentrations within each plant part (independent samples t-test, $p<0.05$).

Table 4. ZOI of *A. calamus* leaf and rhizome essential oils against *E. coli*

Plant part	ZOI (mm)					
	Concentration of essential oil (µg/mL)				Control (µg/mL)	
	100	200	300	400	Kanamycin	DMSO
Leaves	8.67 ± 0.58	9.00 ± 1.00	9.33 ± 0.58	9.67 ± 0.58	8.67 ± 0.58	0.00
Rhizomes	8.67 ± 0.58	9.33 ± 0.58	9.67 ± 0.58	10.00 ± 0.00	8.67 ± 0.58	0.00

Values are expressed as means ± standard deviations based on three replicates. Significant differences were observed among concentrations within each plant part (independent samples t-test, $p<0.05$).

From the leaves and rhizomes at 400 µg/mL, the *E. coli* (9.67 ± 0.58 mm and 10.00 ± 0.00 mm) produced a significantly ($p<0.05$) lower ZOI than MRSA (11.00 ± 0.00 mm and 11.33 ± 0.58 mm), respectively. In addition, the kanamycin susceptibility disc (100 µg/mL) was a positive control against MRSA with ZOI values for the leaves (10.33 ± 0.58 mm) and rhizomes (10.67 ± 0.58 mm), respectively. Likewise, the ZOI values for the leaves (8.67 ± 0.58 mm) and rhizomes (8.67 ± 0.58 mm) were obtained based on *E. coli*. Consequently, the leaves and rhizomes acquired oil at the largest required concentration (400 µg/mL). Hence, this concentration was necessary to create a ZOI for both antibacterial strains greater than the positive control.

In the current investigation, *A. calamus* leaf and rhizome essential oils exhibited significantly ($p<0.05$) high susceptibility against MRSA and *E. coli* from the lowest to the highest, ranging from 100–400 µg/mL concentration. Vakayil *et al.* (2021) reported that the *A. calamus* rhizome essential oil was effective against *S. aureus*, *E. coli*, *Pseudomonas aeruginosa*, *Klebsiella pneumoniae*, *K. oxytoca*, and *Acinetobacter baumanii*, ranging from 20–60 µg to produce a ZOI. Loying *et al.* (2019) also mentioned that the *A. calamus* rhizome essential oil succeeded against *S. aureus*, *Salmonella typhimurium*, *Bacillus subtilis*, and *B. cereus*, at 500 µg/mL required to yield a ZOI. However, little is known about *A. calamus* leaf essential oil used in ZOI applications with different concentrations against bacterial pathogens.

Based on the current research findings, it has been observed that a significant proportion of the volatile components under investigation exhibit notable biological activity. Notably, asaronaldehyde, detected in both *A. calamus* leaf (0.06%) and rhizome (0.11%) essential oils, demonstrates particularly high levels of biological activity. Its bactericidal efficacy has been observed against several soil bacteria elucidated from *Piper cubeba* berries (Alqadeeri *et al.*, 2019). Furthermore, the *in vitro* antibacterial effects of the essential oil could also be attributed to a high concentration of α-asarone, which is known to occur at higher concentrations in *A. calamus* leaves and rhizomes as reported by Kumar *et al.* (2015).

Antioxidant Activity

The antioxidant activity of whole *A. calamus* (leaf and rhizome) essential oil was assessed using two methodologies: DPPH and FRAP assays. Employing multiple methods provides a comprehensive evaluation of the antioxidant properties in the sample, as a single method offers only basic insights (Číž *et al.*, 2010). Therefore, the results are summarised in Table 5. In the DPPH assay, the essential oil demonstrated strong radical scavenging effects with an IC_{50} value of 28.20 ± 4.99 µg/mL when compared to Trolox (IC_{50} = 62.40 ± 0.29 µg/mL). The essential oil also demonstrated a potent FRAP value, registering at 150.12 ± 0.10 mg TE/g.

Table 5. Antioxidant activity of *A. calamus* leaf and rhizome essential oils

Plant part	DPPH (µg/mL)	FRAP (mg TE/g)
Leaves Rhizomes	IC_{50} = 28.20 ± 4.99	150.12 ± 0.10
Trolox	IC_{50} = 62.40 ± 0.29	NA

Values are expressed as means ± standard deviations based on three replicates. NA = Not applicable.

Various studies have reported on the antioxidant activities of essential oils derived from *A. calamus* plants. Loying *et al.* (2019) found a DPPH radical scavenging activity of 1.68 µg/mL for *A. calamus* rhizomes, compared to the standard, ascorbic acid (IC_{50} = 1.48 µg/mL). Parki *et al.* (2017) described varying DPPH radical scavenging activity in *A. calamus* leaf and rhizome essential oils, with IC_{50} values ranging from 37.31 ± 0.19 µg/mL to 198.06 ± 0.07 µg/mL based on different seasons. In contrast, Devi and Ganjewala (2011) demonstrated that the methanolic extract derived from *A. calamus* leaves and rhizomes exhibited significant DPPH radical and superoxide anion-scavenging activities, as well as displayed the capacity to chelate ferrous ions.

Evidently, the significant antioxidant activity shown in *A. calamus* leaf and rhizome essential oils could be attributed to the presence of two primary volatile components, namely α-asarone and methyl isoeugenol. Both chemical substances are phenylpropanoids that have been found to exhibit diverse biological functions (Ilijeva and Buchbauer, 2016; Sharma *et al.*, 2020). This component possesses numerous biological activities with potential neurological and metabolic disorders for antimicrobial (Asha and Ganjewala, 2009; Kumar *et al.*, 2015), antioxidant (Manikandan and Devi, 2005), anti-inflammatory (Manikandan and Devi, 2005; Sundaramahalingam *et al.*, 2013; Jo *et al.*, 2018), anti-depression (Chellian *et al.*, 2016), anti-epilepsy (Wang *et al.*, 2014), antidiabetic (Das *et al.*, 2019a), and anticancer (Das *et al.*, 2019b) properties. Synthetic methyl eugenol has been extensively employed as an adjunctive flavouring agent in a diverse range of processed food products, beverages, sauces, fragrances, and aromatherapy oils, as evidenced by previous studies (Vargas *et al.*, 2010; Tan and Nishida, 2012).

The presence of epi-shyobunone had recently been identified in the essential oil of *Siparuna guianensis* (Siparunaceae). The essential oil derived from this species has demonstrated significant efficacy in safeguarding the brain and combatting Alzheimer's disease. This mechanism was achieved through the inhibition of cholinesterase, an enzyme that is closely linked to the pathogenesis of Alzheimer's disease, facilitated by the presence of certain shyobunone derivatives (Martins *et al.*, 2021). In this investigation, it was shown that the 6-epi-shyobunone was present in significant quantities (2.63% and 3.20%) in the respective leaves and rhizomes of *A. calamus*, which are part of the massive composites. Furthermore, it can be inferred that the *A. calamus* in Sabah, Malaysia, exhibits significant promise for use in the field of medicine. Due to the richness and active phytoconstituents of the volatile components, particularly α-asarone, γ-asarone, methyl isoeugenol, 6-epi-shyobunone, and (E)-β-farnesene, *A. calamus* can serve as benchmark research for modifying metabolic and neurological illnesses (based on compelling *in vitro*, *in vivo*, and clinical evidence).

CONCLUSION

This study successfully identified the essential oil extracted from *A. calamus* leaves and rhizomes. This study included 78 volatile

components, with α-asarone predominating the outcome. Based on prior studies, the volatile components possessed potent antibacterial and antioxidant effects. The identification of other unique components, namely γ-asarone, methyl isoeugenol, 6-epi-shyobunone, and (E)-β-farnesene, in significant quantities within the *A. calamus* leaves and rhizomes from Sabah, Malaysia, represents a novel finding not previously reported in samples obtained from other regions. Hence, undertaking comprehensive investigations into the molecular mechanisms underlying the distinct volatile components mentioned remains imperative, as these compounds have not yet been thoroughly studied. These endeavours aim to elucidate the untapped potential of these components in several domains, including pharmaceuticals, cosmeceuticals, and other related fields.

The extracted oil exhibited excellent antibacterial activity on MRSA and *E. coli*, with a maximum concentration necessary to demonstrate a ZOI of 400 µg/mL. Therefore, *A. calamus* can be a viable alternative for treating certain infectious disorders caused by human pathogenic bacteria. Additionally, the essential oil displayed significant antioxidant activity in radical scavenging, making it a potential anti-aging component. For future studies, the antioxidant activities of *A. calamus* leaf and rhizome should be analysed individually to provide more detailed insights and to assess mechanisms *in vitro* and *in vivo*. The toxicity of *A. calamus* leaves and rhizomes also needs to be emphasised using acute and subacute toxicity studies. These crucial steps will underscore the considerable potential for commercialisation of *A. calamus* from Sabah, Malaysia.

ACKNOWLEDGEMENTS

This study was supported by Universiti Malaysia Sabah through the Geran Bantuan Penyelidikan Pascasiswazah (UMSGreat) [GUG0460-1/2020]. The authors would like to thank the Institute for Tropical Biology and Conservation, Universiti Malaysia Sabah, for providing the necessary facilities.

REFERENCES

Adams, R.P. (2000). Systematics of *Juniperus* section *Juniperus* based on leaf essential oils and random amplified polymorphic DNAs (RAPDs). *Biochemical Systematics and Ecology*. 28(6): 515–528. DOI: 10.1016/S0305-1978(99)00089-7

Ahmad, F.B. & Holdsworth, D.K. (2003). Medicinal plants of Sabah, East Malaysia – Part I. *Pharmaceutical Biology*. 41(5): 340–346. DOI: 10.1076/phbi.41.5.340.15940

Alqadeeri, F., Rukayadi, Y., Abbas, F. & Shaari, K. (2019). Antibacterial and antispore activities of isolated compounds from *Piper cubeba* L. *Molecules*. 24(17): 3095. DOI: 10.3390/molecules24173095

Asha, D.S. & Ganjewala, D. (2009). Antimicrobial activity of *Acorus calamus* (L.) rhizome and leaf extract. *Acta Biologica Szegediensis*. 53(1): 45–49

Atalar, M.N. & Türkan, F. (2018). Identification of chemical components from the rhizomes of *Acorus calamus* L. with gas chromatography-tandem mass spectrometry (GC-MS\MS). *Journal of the Institute of Science and Technology*. 8(4): 181–187. DOI: 10.21597/jist.433743

Benjamin, M.A.Z., Ng, S.Y., Saikim, F.H. & Rusdi, N.A. (2022). The effects of drying techniques on phytochemical contents and biological activities on selected bamboo leaves. *Molecules*. 27(19): 6458. DOI: 10.3390/molecules27196458

Berg, K., Bischoff, R., Stegmüller, S., Cartus, A. & Schrenk, D. (2016). Comparative investigation of the mutagenicity of propenylic and allylic asarone isomers in the Ames fluctuation assay. *Mutagenesis*. 31(4): 443–451. DOI: 10.1093/mutage/gew007

Chaubey, P., Parki, A., Prakash, O., Kumar, R. & Pant, A.K. (2018). Comparative study of chemical composition and antioxidant activity of essential oil extracted from *Acorus calamus* L. leaves. *Journal of Herbal Drugs*. 8(4): 203–211. DOI: 10.14196/jhd.2018.203

Chellian, R., Pandy, V. & Mohamed, Z. (2016). Biphasic effects of α-asarone on immobility in the tail suspension test: Evidence for the involvement of the noradrenergic and serotonergic systems in its antidepressant-like activity. *Frontiers in Pharmacology*. 7: 72. DOI: 10.3389/fphar.2016.00072

Cheng, S.S., Lin, H.Y. & Chang, S.T. (2005). Chemical composition and antifungal activity of essential oils from different tissues of Japanese cedar (*Cryptomeria japonica*). *Journal of Agricultural and Food Chemistry*. 53(3): 614–619. DOI: 10.1021/jf0484529

Číž, M., Čížová, H., Denev, P., Kratchanova, M., Slavov, A. & Lojek, A. (2010). Different methods for control and comparison of the antioxidant properties of vegetables. *Food Control*. 21(4): 518–523. DOI: 10.1016/j.foodcont.2009.07.017

Das, B.K., Choukimath, S.M. & Gadad, P.C. (2019a). Asarone and metformin delays experimentally induced hepatocellular carcinoma in diabetic milieu. *Life Sciences*. 230: 10–18. DOI: 10.1016/j.lfs.2019.05.046

Das, B.K., Swamy, A.V., Koti, B.C. & Gadad, P.C. (2019b). Experimental evidence for use of *Acorus calamus* (asarone) for cancer chemoprevention. *Heliyon*. 5(5): e01585. DOI: 10.1016/j.heliyon.2019.e01585

Devi, S.A. & Ganjewala, D. (2011). Antioxidant activities of methanolic extracts of sweet-flag (*Acorus calamus*) leaves and rhizomes. *Journal of Herbs, Spices and Medicinal Plants*. 17(1): 1–11. DOI: 10.1080/10496475.2010.509659.

Dinev, T., Tzanova, M., Velichkova, K., Dermendzhieva, D. & Beev, G. (2021). Antifungal and antioxidant potential of methanolic extracts from *Acorus calamus* L., *Chlorella vulgaris* Beijerinck, *Lemna minuta* Kunth and *Scenedesmus dimorphus* (Turpin) Kützing. *Applied Sciences*. 11(11): 4745. DOI: 10.3390/app11114745

Fafal, T., Sümer Tüzün, B. & Kıvçak, B. (2022). Fatty acid compositions and antioxidant activities of *Ranunculus isthmicus* subsp. *tenuifolius* and *Ranunculus rumelicus*. *International Journal of Nature and Life Sciences*. 6(2): 151–159. DOI: 10.47947/ijnls.1173088

Ganesan, R.M. & Gurumallesh Prabu, H. (2019). Synthesis of gold nanoparticles using herbal *Acorus calamus* rhizome extract and coating on cotton fabric for antibacterial and UV blocking applications. *Arabian Journal of Chemistry*. 12(8): 2166–2174. DOI: 10.1016/j.arabjc.2014.12.017

Ganjewala, D. & Srivastava, A.K. (2011). An update on chemical composition and bioactivities of *Acorus* species. *Asian Journal of Plant Sciences*. 10(3): 182–189. DOI: 10.3923/ajps.2011.182.189

Grayum, M.H. (1987). A summary of evidence and arguments supporting the removal of *Acorus* from the Araceae. *Taxon*. 36(4): 723–729. DOI: 10.2307/1221123

Heng, L., Guanghua, Z. & Bogner, J. (2010). Acoraceae. In Wu, Z.Y., Raven, P.H. and Hong, D.Y. (eds.). *Flora of China*, vol. 23. St. Louis, MO, USA, Missouri Botanical Garden Press. pp. 1–2

Hong, Y., Liu, X., Wang, H., Zhang, M. & Tian, M. (2021). Chemical composition, antibacterial, enzyme-inhibitory, and anti-inflammatory activities of essential oil from *Hedychium puerense* rhizome. *Agronomy*. 11(12): 2506. DOI: 10.3390/agronomy11122506

Ilijeva, R. & Buchbauer, G. (2016). Biological properties of some volatile phenylpropanoids. *Natural Product Communications*. 11(10): 1619–1629. DOI: 10.1177/1934578x1601101041

Jinoni, D.A., Benjamin, M.A.Z., Mus, A.A., Goh, L.P.W., Rusdi, N.A. & Awang, M.A. (2024). *Phaleria macrocarpa* (Scheff.) Boerl. (mahkota dewa) seed essential oils: Extraction yield, volatile components, antibacterial, and antioxidant activities based on different solvents using Soxhlet extraction. *Kuwait Journal of Science*. 51: 100173. DOI: 10.1016/j.kjs.2023.100173

Jo, M.-J., Kumar, H., Joshi, H.P., Choi, H., Ko, W.-K., Kim, J.M., Hwang, S.S.S., Park, S.Y., Sohn, S., Bello, A.B., Kim, K.-T., Lee, S.-H., Zeng, X. & Han, I. (2018). Oral administration of α-asarone promotes functional recovery in rats with spinal cord injury. *Frontiers in Pharmacology*. 9: 445. DOI: 10.3389/fphar.2018.00445.

Khatun, S., Chatterjee, N.C. & Cakilcioglu, U. (2011). Antioxidant activity of the medicinal plant *Coleus forskohlii* Briq. *African Journal of Biotechnology*. 10(13): 2530–2535. DOI: 10.5897/AJB10.2526

Kulip, J. (1997). A preliminary survey of traditional medicinal plants in the West Coast and Interior of Sabah. *Journal of Tropical Forest Science*. 10(2): 271–274.

Kumar, S.N., Aravind, S.R., Sreelekha, T.T., Jacob, J. & Kumar, B.S.D. (2015). Asarones from *Acorus calamus* in combination with azoles and amphotericin B: A novel synergistic combination to compete against human pathogenic *Candida* species *in vitro*. *Applied Biochemistry and Biotechnology*. 175(8): 3683–3695. DOI: 10.1007/s12010-015-1537-y

Liu, X.C., Zhou, L.G., Liu, Z.L. & Du, S.S. (2013). Identification of insecticidal constituents of the essential oil of *Acorus calamus* rhizomes against *Liposcelis bostrychophila* Badonnel. *Molecules*. 18(5): 5684–5696. DOI: 10.3390/molecules18055684

Loying, R., Gogoi, R., Sarma, N., Borah, A., Munda, S., Pandey, S.K. & Lal, M. (2019). Chemical compositions, in-vitro antioxidant, anti-microbial, anti-inflammatory and cytotoxic activities of essential oil of *Acorus calamus* L. rhizome from North-East India. *Journal of Essential Oil-Bearing Plants*. 22(5): 1299–1312. DOI: 10.1080/0972060X.2019.1696236

Manikandan, S. & Devi, R.S. (2005). Antioxidant property of α-asarone against noise-stress-induced changes in different regions of rat brain. *Pharmacological Research*. 52(6): 467–474. DOI: 10.1016/j.phrs.2005.07.007

Manjarrez-Quintero, J.P., Valdez-Baro, O., García-Estrada, R.S., Contreras-Angulo, L.A., Bastidas-Bastidas, P.de.J., Heredia, J.B., Cabanillas-Bojórquez, L.A. & Gutiérrez-Grijalva, E.P. (2024) Optimized ultrasonic extraction of essential oil from the biomass of *Lippia graveolens* Kunth using deep eutectic solvents and their effect on *Colletotrichum asianum*. *Processes*. 12(7): 1525, DOI: 10.3390/pr12071525

Marotti, M., Piccaglia, R., Giovanelli, E., Deans, S.G. & Eaglesham, E. (1994). Effects of planting time and mineral fertilization on peppermint (*Mentha* x *piperita* L.) essential oil composition and its biological activity. *Flavour and Fragrance Journal*. 9(3): 125–129. DOI: 10.1002/ffj.2730090307

Martins, R.M.G., Xavier-Júnior, F.H., Barros, M.R., Menezes, T.M., de Assis, C.R.D., de Melo, A.C.G.R., Veras, B.O., Ferraz, V.P., Filho, A.A.M., Yogui, G.T., Bezerra, R.S., Seabra, G.M., Neves, J.L. & Tadei, W.P. (2021). Impact on cholinesterase-inhibition and in silico investigations of sesquiterpenoids from Amazonian *Siparuna guianensis* Aubl. *Spectrochimica Acta - Part A: Molecular and Biomolecular Spectroscopy*. 252: 119511. DOI: 10.1016/j.saa.2021.119511

Mazza, G. (1985). Gas chromatographic and mass spectrometric studies of the constituents of the rhizome of calamus. I. The volatile constituents of the essential oil. *Journal of Chromatography A*. 328: 179–194. DOI: 10.1016/S0021-9673(01)87390-8

Mittal, N., Ginwal, H.S. & Varshney, V.K. (2009). Pharmaceutical and biotechnological potential of *Acorus calamus* Linn.: An indigenous highly valued medicinal plant species. *Pharmacognosy Reviews*. 3(5): 83–93

Mukherjee, P.K., Kumar, V., Mal, M. & Houghton, P.J. (2007). *Acorus calamus*: Scientific validation of Ayurvedic tradition from natural resources. *Pharmaceutical Biology*. 45(8): 651–666. DOI: 10.1080/13880200701538724

Mus, A.A., Gansau, J.A., Kumar, V.S. & Rusdi N.A. (2020) The variation of volatile compounds emitted from aromatic orchid (*Phalaenopsis bellina*) at different timing and flowering stages. *Plant OMICS*. 13(2): 78–85, DOI: 10.21475/POJ.13.02.20.2271

Ogra, R.K., Mohanpuria, P., Sharma, U.K., Sharma, M., Sinha, A.K. & Ahuja, P.S. (2009). Indian calamus (*Acorus calamus* L.): Not a tetraploid. *Current Science*. 97(11): 1644–1647

Park, Y.-S., Kim, I., Dhungana, S.K., Park, E.-J., Park, J.-J., Kim, J.-H. & Shin, D.-H. (2021). Quality characteristics and antioxidant potential of lemon (*Citrus limon* Burm. f.) seed oil extracted by different methods. *Frontiers in Nutrition*. 8: 644406. DOI: 10.3389/fnut.2021.644406

Parki, A., Chaubey, P., Prakash, O., Kumar, R. & Pant, A.K. (2017). Seasonal variation in essential oil compositions and antioxidant properties of *Acorus calamus* L. accessions. *Medicines*. 4(4): 81. DOI: 10.3390/medicines4040081

Pintatum, A., Laphookhieo, S., Logie, E., Berghe, W. Vanden & Maneerat, W. (2020). Chemical composition of essential oils from different parts of *Zingiber kerrii* Craib and their antibacterial, antioxidant, and tyrosinase inhibitory activities. *Biomolecules*. 10(2): 228. DOI: 10.3390/biom10020228

Raal, A., Orav, A. & Gretchushnikova, T. (2016). β-Asarone content and essential oil composition of *Acorus calamus* L. rhizomes from Estonia. *Journal of Essential Oil Research*. 28(4): 299–304. DOI: 10.1080/10412905.2016.1147391

Radušiene, J., Judžentiene, A., Pečiulyte, D. & Janulis, V. (2007). Essential oil composition and antimicrobial assay of *Acorus calamus* leaves from different wild populations. *Plant Genetic Resources: Characterisation and Utilisation*. 5(1): 37–44. DOI: 10.1017/S1479262107390928

Raina, V.K., Srivastava, S.K. & Syamasunder, K. V. (2003). Essential oil composition of *Acorus calamus* L. from the lower region of the Himalayas. *Flavour and Fragrance Journal*. 18(1): 18–20. DOI: 10.1002/ffj.1136

Rajput, S.B., Tonge, M.B. & Karuppayil, S.M. (2014). An overview on traditional uses and pharmacological profile of *Acorus calamus* Linn. (sweet flag) and other *Acorus* species. *Phytomedicine*. 21(3): 268–276. DOI: 10.1016/j.phymed.2013.09.020

Satyal, P., Paudel, P., Poudel, A., Dosoky, N.S., Moriarity, D.M., Vogler, B. & Setzer, W.N. (2013). Chemical compositions, phytotoxicity, and biological activities of *Acorus calamus* essential oils from Nepal. *Natural Product Communications*. 8(8): 1179–1181. DOI: 10.1177/1934578x1300800839

Sharma, V., Singh, I. & Chaudhary, P. (2014). *Acorus calamus* (the healing plant): A review on its medicinal potential, micropropagation and conservation. *Natural Product Research*. 28(18): 1454–1466. DOI: 10.1080/14786419.2014.915827

Sharma, V., Sharma, R., Gautam, D.N.S., Kuca, K., Nepovimova, E. & Martins, N. (2020). Role of Vacha (*Acorus calamus* Linn.) in neurological and metabolic disorders: Evidence from ethnopharmacology, phytochemistry, pharmacology and clinical study. *Journal of Clinical Medicine*. 9(4): 1176. DOI: 10.3390/jcm9041176

Sundaramahalingam, M., Ramasundaram, S., Rathinasamy, S.D., Natarajan, R.P. & Somasundaram, T. (2013). Role of *Acorus calamus* and α-asarone on hippocampal dependent memory in noise stress exposed rats. *Pakistan Journal of Biological Sciences*. 16(16): 770–778. DOI: 10.3923/pjbs.2013.770.778

Tan, K.H. & Nishida, R. (2012). Methyl eugenol: Its occurrence, distribution, and role in nature, especially in relation to insect behavior and pollination. *Journal of Insect Science*. 12: 56. DOI: 10.1673/031.012.5601

Uebel, T., Hermes, L., Haupenthal, S., Müller, L. & Esselen, M. (2021). α-Asarone, β-asarone, and γ-asarone: Current status of toxicological evaluation. *Journal of Applied Toxicology*. 41(8): 1166–1179. DOI: 10.1002/jat.4112

Vakayil, R., Nazeer, T.A. & Mathanmohun, M. (2021). Evaluation of the antimicrobial activity of extracts from *Acorus calamus* rhizome against multidrug-resistant nosocomial pathogens. *Research Journal of Agricultural Sciences*. 12(5): 1613–1617.

Vargas, R.I., Shelly, T.E., Leblanc, L. & Piñero, J.C. (2010). Recent advances in methyl eugenol and cue-lure technologies for fruit fly detection, monitoring, and control in Hawaii. In Litwack, G. (ed.). *Vitamins and Hormones*, vol. 83, Cambridge, MA, USA, Academic Press. pp. 575–595. DOI: 10.1016/S0083-6729(10)83023-7

Varma, J., Tripathi, M., Ram, V.J., Pandey, V.B. & Dubey, N.K. (2002). γ-Asarone – The fungitoxic principle of the essential oil of *Caesulia axillaris*. *World Journal of Microbiology and Biotechnology*. 18(3): 277–279. DOI: 10.1023/A:1014905111973

Venskutonis, P.R. & Dagilyte, A. (2003). Composition of essential oil of sweet flag (*Acorus calamus* L.) leaves at different growing phases. *Journal of Essential Oil Research*. 15(5): 313–318. DOI: 10.1080/10412905.2003.9698598

Wang, Z.-J., Levinson, S.R., Sun, L. & Heinbockel, T. (2014). Identification of both GABAA receptors and voltage-activated Na^+ channels as molecular targets of anticonvulsant α-asarone. *Frontiers in Pharmacology*. 5: 40. DOI: 10.3389/fphar.2014.00040

Borneo Journal of Resource Science and Technology (2025), 15(1): 130-145
DOI: https:doi.org/10.33736/bjrst.7237.2025

Recognition of Sesquiterpenoids and Piperidine Alkamides as Two Discerning Metabolite Classes in the Fruits of *Piper nigrum* 'Semongok Aman'

MUHAMAD FARIS OSMAN*[1], SITI MUNIRAH MOHD FAUDZI [2,3], KHOZIRAH SHAARI[2], SHAHRUL RAZID SARBINI[4] & SHAMSUL KHAMIS[5,6]

[1]Pharmacognosy Research Group, Department of Pharmaceutical Chemistry, Kulliyyah of Pharmacy, International Islamic University Malaysia, Kuantan 25200, Pahang, Malaysia; [2]Natural Medicines and Products Research Laboratory, Institute of Bioscience, Universiti Putra Malaysia, 43400 UPM Serdang, Selangor, Malaysia; [3]Department of Chemistry, Faculty of Science, Universiti Putra Malaysia, 43400 UPM, Serdang. Selangor, Malaysia; [4]Department of Crop Science, Faculty of Agricultural and Forestry Sciences, Universiti Putra Malaysia, Bintulu 97008, Sarawak, Malaysia; [5]Department of Biological Sciences and Biotechnology, Faculty of Science and Technology, Universiti Kebangsaan Malaysia, UKM, Bangi 43600, Selangor, Malaysia; [6]Fraser's Hill Research Center, Natural and Physical Laboratory Management Center (ALAF-UKM) Research Complex, Universiti Kebangsaan Malaysia, UKM, Bangi 43600, Selangor, Malaysia
*Corresponding author: farisosman@iium.edu.my
Received: 24 June 2024 Accepted: 5 February 2025 Published: 30 June 2025

ABSTRACT

The Malaysian Pepper Board (MPB) has recommended the plantation of three over seven *Piper nigrum* L. cultivars, owing to their beneficial agronomic traits. Currently, distinction between the cultivars is assessed based on morphological characters. The MPB has also proposed the concept of monovarietal farm, which is believed to have the potential of strengthening the quality of pepper in the global market. However, there remains a need for a fair assessment of the specialised metabolites' variation among *P. nigrum* cultivars in search of a cultivar with distinctive metabolites profile, which may be the most suitable candidate for the application of such concept. We hereby describe revised protocols aimed at minimising the oxidation of the fruits of five *P. nigrum* cultivars and reducing the experimental run time that allowed utilisation of the same samples in GC-MS and ^{1}H-NMR metabolomics. Subsequently, feature-based molecular network (FBMN) was used to verify the patterns observed in the principal component analysis (PCA) of the ^{1}H-NMR and GC-MS data. PCA of both datasets revealed that the clustering pattern of the five cultivars paralleled the origin of their parent plants, with the genetically more similar cultivars, 'Kuching', 'Semongok Emas', 'India', and 'Yong Petai', being closer to each other compared to 'Semongok Aman'. 'Semongok Aman' was found to contain a higher abundance of the sesquiterpenoids germacrene B and γ-elemene, as well as the piperidine alkamides piperine and its isomers. FBMN further highlighted the higher abundance of the two metabolite classes in the fruits of 'Semongok Aman'. 'Semongok Aman' might be a suitable cultivar for the implementation of monovarietal pepper farm concept owing to its distinctive metabolite profile.

Keywords: Alkamides, cultivar, FBMN, metabolomics, *Piper nigrum*, sesquiterpenoids

INTRODUCTION

Recognised as the 'King of Spices', black or white pepper, the fruit of *Piper nigrum* L., is traded globally for its culinary and medicinal uses (Ashokkumar *et al.*, 2021; Takooree *et al.*, 2019). In Malaysia, the state of Sarawak is the largest pepper producer and boasts the prestigious geographical indication (GI)-certified Sarawak pepper, which is responsible for about 98% of the country's pepper harvest (Entebang *et al.*, 2021). Sarawak pepper is a final product obtained from the processed fruits of several cultivars of *P. nigrum* grown in Sarawak. Presently, it consists of a mixture of the fruits of different cultivars, as the concept of monovarietal pepper cultivation is not currently practised in Malaysia (Chen *et al.*, 2018).

The differences between the cultivars are discerned by manual assessment of a set of six diagnostic morphological characters, which include the qualitative and quantitative traits of leaves, inflorescences, fruits, seeds, and shoot

tips (Chen & Tawan, 2020a). Notwithstanding the morphological diversity and distributional variation of the cultivars, the Malaysian Pepper Board (MPB) has maintained its recommendation for the cultivation of 'Kuching', 'Semongok Emas', and 'Semongok Aman' (Fong & Liang, 2011; Gaweng & Lai, 2017; Johny *et al.*, 2020; Entebang *et al.*, 2021). This recommendation is based on the results of extensive yield verification studies that demonstrated the superiority of the three cultivars over seven other non-recommended cultivars in several positive agronomic aspects. These include consistent percentage yields of green, black, and white pepper, uniform fruit ripening, and increased resistance to pest infestation and fatal diseases (Fong & Liang, 2011; Gaweng & Lai, 2017).

Of the three cultivars, 'Semongok Aman' demonstrates superior chemical properties, having the highest contents of piperine, oleoresin, and volatile and non-volatile oils in its fruits (Fong & Liang, 2011; Gaweng & Lai, 2017). Nevertheless, a comparative analysis of the piperine content and essential oil composition in the fruits of the ten cultivars revealed the highest piperine content was in a non-recommended cultivar, while six out of seven non-recommended cultivars had the highest amount of certain monoterpenoids and sesquiterpenoids (Chen & Tawan, 2020b). Although studies have examined the correlation between pharmacological properties and specialised metabolites (Ashokkumar *et al.*, 2021; Luca *et al.*, 2021; Wang *et al.*, 2021) and the variation in specialised metabolite profiles among different origins (Ahmad *et al.*, 2020; Hashimoto *et al.*, 2021; Jaidee *et al.*, 2022; Liang *et al.*, 2021; Rivera-Pérez *et al.*, 2021) and cultivars (Barata *et al.*, 2021) of *P. nigrum* fruits, data on metabolite profiles of *P. nigrum* fruits from recommended and non-recommended cultivars grown in a single farm are currently lacking.

Therefore, the aim of the present research was to study the variations in metabolite fingerprints and profiles of fruits from three recommended and two non-recommended *P. nigrum* cultivars grown on a farm in Sarawak. Since previous studies have demonstrated that polyphenol oxidase (PPO) in the fruit's skin is the enzyme responsible for blackening of freshly harvested green *P. nigrum* fruits (Bandyopadhyay *et al.*, 1990; Gu *et al.*, 2013), which can obfuscate a fair comparative analysis between the cultivars, the specific objectives of the present research were to: (1) establish a revised protocol for the preparation of plant material and extracts for reliable comparative analysis of metabolite fingerprints and profiles *P. nigrum* fruits of the five selected cultivars; (2) analyse the metabolite classes contributing to the observed variation; and (3) determine the cultivar exhibiting the most distinctive metabolite fingerprints and profiles. The findings may shed light on the application of monovarietal cultivation concept, which is believed to improve the quality of peppers in the global market (Chen *et al.*, 2018).

MATERIALS & METHODS

The methods described in the following subsections were improvised based on the findings from preliminary GC-MS and ^{1}H-NMR metabolomics of *P. nigrum* 'Kuching', 'Semongok Emas', 'Semongok Aman', 'India', and 'Yong Petai' fruits, collected from a pepper farm in Sebauh, Bintulu, Sarawak, Malaysia on 10th October 2018.

Collection of Plant Materials

Fresh fruit spikes bearing healthy mature fruits of the selected *P. nigrum* cultivars were collected from 13-year-old vines (as of 2023) on the same pepper farm on 25th October 2019 between 9:00 and 11:00 a.m. (Figure S1). The fruits were at developmental stage eight (8), i.e., early hard dough stage (i.e., firm, difficult to press open, and all parts of the exocarp were dark green) (Fong & Liang, 2011). The vines were planted by the farm owner on one of the farm plots. The different cultivars were identified by the owner, based on the morphological features of the leaves (Figure S2) and the fruit spikes (Figure S3).

Except for 'Kuching', the fruits spikes of eight vines were sampled for all cultivars, with one vine representing a biological replicate. For 'Kuching', only four biological replicates were available as most vines of the cultivar were in poor condition at the time of sampling. At minimum, six healthy fruit spikes were harvested from each vine. The fruit spikes from each vine were kept in labelled zip-lock bags in

an ice box and transported to a laboratory in UPM Bintulu.

In the laboratory, three fruit spikes bearing green fruits of uniform size were selected for each vine. The fruit spikes were cleaned with tap water to remove dirt and insects and dried for one hour at room temperature on unbleached parchment paper (Figure S4). To facilitate subsequent handling of the fruit spikes, the three fruit spikes representing each vine were carefully tied together with a metal wire (Figure S5). To minimise PPO activity, the bundled fruit spikes were frozen overnight at −80 °C, quenched in liquid nitrogen, and refrozen at −80 °C for 48 hours. All bundled fruit spikes were lyophilised for 48 hours and transported via air to another laboratory at the Institute of Bioscience, UPM Serdang. Then, 30 lyophilised green fruits of similar size were selected from each bundle to represent a sample (Figure S6). A dummy sample (sample code B4) was obtained from a 'Semongok Emas' sample, which was used for optimisation of GC-MS parameters and determination of representative fruit parts based on GC-MS metabolite profiles.

To further minimise fruit oxidation and facilitate their handling, fruits were stored in 15 mL polypropylene centrifuge tubes (Figure S7) in a desiccator and protected from sunlight. All samples were randomised by an individual unrelated to the study, with each sample assigned unique codes known only to the individual. Hence, the experimenters were blinded, i.e., they did not know which sample was labelled with a particular sample code, from the preparation of the extracts until the completion of the analytical procedures of the samples (Beger *et al.*, 2019; Evans *et al.*, 2020; Phapale *et al.*, 2020). The lyophilisation was carried out prior to grinding of the fruits because, as observed in the preliminary study, quenching the fresh fruits in liquid nitrogen followed by grinding them manually using mortar and pestle resulted in browning (oxidation) of the green fruits. Other than that, unlike the flat leaves, the fresh fruits were round, thus requiring more grinding time. A longer grinding time may lead to greater degree of oxidation, which can vary between the samples as the grinding was done manually. To reduce the grinding time, the lyophilised fruits were ground with a mortar and pestle, instead of the fresh fruits for each sample. Besides, of the 30 fruits per sample, only 10 fruits were ground to powder.

GC-MS Metabolomics of *P. nigrum* Fruit Extracts

GC-MS parameters in the current research were modified from previous studies (Gul *et al.*, 2017; Matsuo *et al.*, 2017; Singh *et al.*, 2013) and improvised based on the findings of the GC-MS analysis of dummy sample B4 in the preliminary study (Figures S8−S11).

Acquisition of GC-MS Data

First, 10 mg of the ground samples were weighed, extracted using 1 mL LC grade *n*-hexane containing 5 ppm *n*-nonane as an internal standard, followed by 15 min of sonication and filtration with 0.22 µm PTFE syringe filters into 1.5 mL screw-cap vials. The GC-MS system used was the 7890A Gas Chromatograph equipped with 7000 Series Triple Quadrupole Mass Spectrometer operated in electron ionisation (EI) mode at 70 eV and an ion source temperature of 200 °C. The following parameters were set for data acquisition: mode = full scan, scan rate = 10 scans/s, mass range = 30–350 Da, and solvent delay = 5 min. The inlet temperature was set at 250 °C. Then, 1 µL of extract was injected in splitless mode into a HP-5MS column of 30.00 m length × 0.25 mm internal diameter × 0.25 µm film thickness. The helium flow rate was maintained at 1 mL/min. The oven temperature was programmed as follows: 50 °C (1.0 min) and 4 °C/min to 280 °C (3.0 min), making a total run time of 61.50 min. The post-run column temperature was set at 310 °C for 1 min.

The GC-MS metabolomics workflow was adapted from a previous study, describing a four-step strategy for metabolite identification of unknown GC-MS peaks (Matsuo *et al.*, 2017). Next, noisy chromatographic peaks were excluded from further analysis by generating a calibration curve from dilution series of a pooled QC sample (sample code QCP0). For the preparation of calibration curve's QC samples (sample codes QCC1–QCC5), 5 mg of each sample (n = 36) was added to a 15 mL centrifuge tube, shaken vigorously, and the resulting mixture QCP0 (total weight: 180 mg) was divided into five 2 mL centrifuge tubes such that each tube contained 2.5 (QCC1), 3.75 (QCC2),

5.0 (QCC3), 7.5 (QCC4), and 10.0 mg (QCC5) of QCP0, respectively. The remaining QCP0 was divided into six analytical QC samples (sample codes QCP1–QCP6, 10 mg QCP0 each), which were injected after the injection of five or six samples. All QC samples (i.e., QCC1–QCC5 and QCP1–QCP6) were extracted using 1 mL LC grade *n*-hexane containing 5 ppm *n*-nonane. Three tubes containing extraction solvent blank (LC grade *n*-hexane containing 5 ppm *n*-nonane) were also prepared, labelled NH0 (not sonicated), and NH1 and NH2 (sonicated together with the samples) to monitor the background signals from the GC-MS instrument and to assess the suitability of using the signal from the internal standard to normalise the data set in PCA (Figure S12). For calculation of the LRI and the examination of the retention time shift, the alkane standard (code ALK) was injected after the first two injections of the extraction solvent blank (NH0 and NH1) and at the end of the run sequence (after the NH2 injection) (Jumhawan *et al.*, 2013). The calibration curve QC samples (QCC1–QCC5) were injected after the first injection of ALK, followed by the injection of *P. nigrum* fruit extracts and QCP1–QCP6.

Preprocessing and Principal Components Analysis (PCA) of GC-MS Data

Metabolite identification (Adams, 2017; Andriamaharavo, 2014; Babushok *et al.*, 2011; Miyazaki *et al.*, 2011), data preprocessing, and PCA followed the procedures described in a previous publication (Osman *et al.*, 2021), with modifications of several parameters in MS-DIAL version 4.60 as follows: retention time begin = min 5.48, retention time end = min 60.25, mass range begin = 40 Da, mass range end = 345 Da, number of threads = 25, amplitude cut off = 100, alignment reference file = QCC5, and normalisation = internal standard. In contrast to a previous study in which the coefficient of determination (r^2) was used to remove noisy chromatographic features (Matsuo *et al.*, 2017), the bivariate Pearson correlation coefficient (r) was used in the present research as r is more informative in modelling a linearly increasing or decreasing trend in feature intensities. A cut-off value of 0.700 was set for r when filtering the QC calibration curve (Figure S13).

^{1}H-NMR Metabolomics of *P. nigrum* Fruit Extracts

In the preliminary study, following the extraction protocol described in (Osman *et al.*, 2021), it was discovered that the aqueous methanolic fruit extracts of *P. nigrum* were unstable approximately six hours after preparation. This was evident from the formation of dark precipitates at the bottom of the NMR tubes (see Figure S14). Therefore, the sequence of steps for preparing the extracts and acquiring spectral data for 1H NMR metabolomics in the present study was designed to complete the steps involved in less than six hours. To achieve this, the procedures were carried out by two experimenters A and B in two batches of 18 extracts for each batch. All extracts (n = 36) were prepared by experimenter A and all spectral data were acquired by experimenter B. The extracts preparation for the second batch was started by experimenter A at the same time that spectral data for the extracts for the first batch were acquired by experimenter B. ^{1}H-NMR spectra were acquired, preprocessed, and analysed following the protocols detailed in the previous publication (Osman *et al.*, 2021).

LC-MS/MS Analysis

LC-MS/MS data acquisition was performed following the method described in (Osman *et al.*, 2022). The Feature-Based Molecular Network (FBMN) workflow was employed to visualise unique features in the fruit metabolite profiles of *P. nigrum* cultivars. Compared to the classical MN, which uses the summed precursor ion count or spectral count, FBMN provides more accurate quantification of relative ion intensities because FBMN uses LC-MS feature abundance such as peak area or peak height (Nothias *et al.*, 2020). To generate a feature list file for FBMN, the converted raw data were first preprocessed with MZmine 2.53 using the settings listed in Table S1. The data preprocessing settings were adjusted to match the instrument settings based on previous studies (Afzan *et al.*, 2019; Houriet *et al.*, 2020). Spectral library searches using the GNPS platform were performed following the procedure described in (Osman *et al.*, 2022). The FBMN and GNPS job parameters are publicly accessible at http://bit.ly/3ZINOFE (sample codes for the online FBMN are as follows: 01B = 'Semongok Emas', 03L = 'Semongok Aman',

03Z = 'India', 18P = 'Kuching', and 27J = 'Yong Petai').

RESULTS & DISCUSSION

GC-MS Fruit Metabolite Profiles of *P. nigrum* Cultivars

The BPCs of all 36 fruit samples of *P. nigrum* cultivars are depicted in Figure 1. All cultivars revealed similar chromatographic patterns over a run time of 61.5 min. In addition, the chromatographic peak intensities of monoterpenoids (**1**–**3**), sesquiterpenoids (**4**–**7**), and alkamides (**8**–**10**) exhibited small to moderate variations. A complete list of identified metabolites and magnified view of metabolite peaks are shown in Table S2 and Figure S15, respectively. As only representative samples are shown, the peak intensities in Figure 1 could be unique to a particular sample and do not reflect the distribution of peak intensities for all samples of the selected *P. nigrum* cultivars. Therefore, PCA was carried out to identify discriminating metabolites while accounting the distribution of peak intensities across all *P. nigrum* fruit samples.

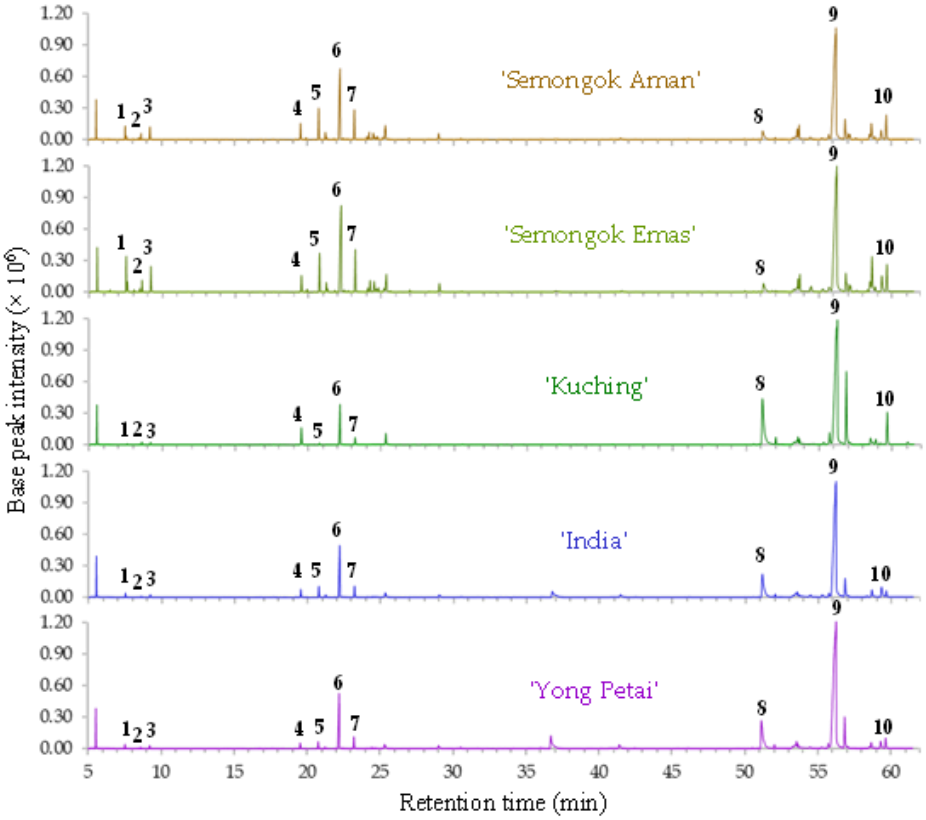

Figure 1. Representative GC-MS BPC of *n*-hexane fruit extracts of the selected *Piper nigrum* cultivars: (1) sabinene, (2) 3-carene, (3) D-limonene, (4) δ-elemene, (5) α-copaene, (6) (*E*)-β-caryophyllene, (7) α-humulene, (8) piperanine, (9) piperine, and (10) piperolein B

PCA of GC-MS Data of *P. nigrum* Fruit Extracts

Preprocessing of the GC-MS BPCs using QC samples calibration curve with r = 0.700, followed by exclusion of variables with a relative standard deviation (RSD) greater than 30% in all six QC samples, reduced the number of variables in the data set from 557 to 370. As shown in Figure 2A, with 66.6% of the total variation explained by the PCA model (see also Figure S16), the samples could be divided into three clusters: (A) a cluster of five 'Semongok Aman' samples; (B) a cluster comprising all 'Kuching' and 'Yong Petai', two 'Semongok Aman', and four 'India' samples; and (C) another cluster consisting of all 'Semongok Emas', four 'India', and one 'Semongok Aman' samples. The higher abundance of sesquiterpenoids α-copaene, β-cubebene, β-elemene, α-gurjunene,

(*E*)-β-caryophyllene, and α-humulene strongly contributes to the segregation of all 'Semongok Emas' samples (cluster C) from most other samples along the first PC, accounting 47.2% of the total variation. In addition, the lower abundance of the alkamide piperanine in the 'Semongok Emas' samples discriminates them from samples in the other two clusters. The second PC, which explains 19.4% of the total variation in the data set, highlights the significantly higher abundance of two sesquiterpenoids: germacrene B and γ-elemene (Figures 2Bviii and 2Bix) in five 'Semongok Aman' samples (cluster A) in comparison to all other samples.

Moreover, Figure 2A also shows that 'Kuching', 'Semongok Emas' and 'Semongok Aman', although they are three varieties recommended for pepper cultivation in Malaysia, have remarkable quantitative variations in their fruit metabolite profiles and are therefore not clustered in the first two PCs. Disregarding the three 'Semongok Aman' samples that deviate from the 'Semongok Aman' cluster, the clustering patterns in the PCA biplot in Figure 2A coincide well with the origins of the selected cultivars; historically, how the cultivars originated. To further highlight, *P. nigrum* is reported to have originated in the tropical forests of the Western Ghats, South India (Krishnamoorthy & Parthasarathy, 2010) and was first introduced to Sarawak by the Hakka Chinese in the 1840s Fong & Liang, 2011). 'Kuching' is one of the earliest *P. nigrum* cultivars in Sarawak and was the only commercial cultivar planted by local pepper farmers prior to introduction of the non-recommended cultivar 'India' (or 'Uthirancotta') from India in 1957. 'Kuching' and 'India' are quite similar morphologically. Both cultivars have leaves with a smooth adaxial surface and bear abundant pale-yellow flowers. Nonetheless, 'India' is considered inferior to 'Kuching' due to smaller fruit size and bear insufficient fruit caused by lower proportion of hermaphroditic flower (Fong & Liang, 2011) s.

'Yong Petai', another non-recommended cultivar in the 'Kuching' cluster (cluster B), is derived from local selection and is believed to originated from seedlings of 'Kuching'. It was found that 'Yong Petai' was grown together with 'Kuching' when it was first acquired by a pepper grower in Sungai Petai, Sarikei Division, Sarawak, in 1999 (Fong & Liang, 2011). This is supported by the finding of genetic relatedness using Directed Amplification of Minisatellite-region DNA (DAMD) markers of pepper cultivar accessions maintained at Agriculture Research Centre (ARC) Semongok, where cultivars grown in the same geographic region appear to be clustered together and 'Yong Petai' (accession no. PN129) falls in the same cluster as 'Kuching' (Ho *et al.*, 2005).

Inclusion of another half of the 'India' samples in the 'Semongok Emas' cluster reveals the genotype of 'Semongok Emas', a recommended cultivar released for cultivation by pepper farmers in 1991 after 26 years of field trials and evaluations. 'Semongok Emas' is genetically related to 'India' and 'Kuching' as it is a back-cross hybrid between 'Balancotta' (i.e., one of the four cultivars introduced from India in 1957) as the female parent and 'Kuching' as the male parent (Fong & Liang, 2011). The exclusivity of the recommended cultivar 'Semongok Aman' can be related to its country of origin, Costa Rica, where accession PN106 was collected on 21st January 1992. After several years of field evaluations, the cultivar 'Semongok Aman', resulting from clonal propagation of the germplasm of accession PN106, was released to pepper farmers in 2006 (Fong & Liang, 2011). In the aforementioned study utilising the DAMD marker, accession PN106 was separated from other accessions from Sarawak, India, and Indonesia and clustered together with several accessions from Costa Rica (PN107–112) and Honduras (PN113–116) (Ho *et al.*, 2005).

PCA of ^{1}H-NMR Spectra of *P. nigrum* Fruit Extracts

To corroborate whether the same clustering patterns are replicated by aqueous methanolic fruit extracts of the selected *P. nigrum* cultivars, the ^{1}H-NMR spectra of all samples were analysed using PCA. Figure 3A shows that the ^{1}H-NMR spectra of the different *P. nigrum* cultivars are also qualitatively similar, and no cultivar has signals that are absent in other cultivars.

The scatter plot of PCA scores in Figure 3B shows that the majority samples of 'Semongok Aman' and 'Yong Petai' can be grouped together (cluster 1) and separated from the other samples

(cluster 2) by the first PC axis. In contrast to the PCA model of the GC-MS data in Figure 2A (R^2X [cum. PC 2] = 94.9% and Q^2X [cum. PC 2] = 87.8%), the first two PCs of the ^{1}H-NMR spectral data explained only 76.4% of the total variation and the PCA model proved to be weakly predictive (Q^2X [cum. PC 2] = 63.0%). Therefore, the binned ^{1}H-NMR spectral data set subjected to power two-transformed prior to mean-centring, resulting in an improved PCA model with better fit and predictive power (Figure 3B). The power two transformation resulted in intensity changes in the variables of the data set (i.e., the binned ^{1}H-NMR signals), with only slight increases in the low-intensity variables and significant increases in the high-intensity variables. Consequently, the new PCA model was built with a greater emphasis on the variation among the high-intensity signals, which proved to be beneficial as can be seen from the improvement in the goodness of fit and prediction of the model.

Inspection of the variable loadings of the improved PCA model in Figure 3C revealed that the discrimination of the two clusters by the first PC axis was influenced by a higher abundance of variables δ 1.60, 1.68, 3.60, and 6.88 in the samples of cluster 1. As these discriminating variables are 0.04 ppm-width bins of the ^{1}H-NMR spectra of the aqueous methanolic fruit extracts of the selected *P. nigrum* cultivars, their labels in Figure 3C are the midpoints of the bins. For instance, the variable δ 3.60 in Figure 3C denotes a bin that starts at δ 3.58 and ends at δ 3.62, where δ 3.60 is the midpoint (see Figure S17). Hence, the annotation of the metabolite/s eliciting the ^{1}H-NMR signals in Figure S17 considered the whole range of signals represented by the variables δ 1.60, 1.68, 3.60, and 6.88. Besides, as the samples analysed were extracts of *P. nigrum* fruits, the probability of overlapping metabolite signals in the ^{1}H-NMR spectra was also taken into consideration.

Comparison of the ^{1}H-NMR signals in Figure S17 with the reference spectra in the Chenomx Spectral Reference Library in Chenomx Profiler version 8.2, which contain mainly ^{1}H-NMR spectra of primary metabolites and a minimal number of ^{1}H-NMR spectra of specialised metabolites in biofluids, did not show good agreement, implying that the ^{1}H-NMR signals could belong to specialised metabolite/s of *P. nigrum* fruits. Therefore, the signals were annotated based on comparison with literature data, focussing on piperine. Piperine, is a major specialised metabolite that has been utilised as a chemical marker in fingerprinting techniques for quality control of *P. nigrum* fruits (Mayr *et al.*, 2021). The annotation of the discriminatory signals largely contributed by piperine can be found in Table S3. It is possible that the discriminatory signals also originated to some extent from the three geometric isomers isochavicine, isopiperine, and chavicine, formed by photoisomerisation of piperine (Hashimoto *et al.*, 1996; Kozukue *et al.*, 2007) and the piperine analogue piperanine (Gómez-Calvario & Rios, 2019) due to co-occurrence of 1,3-benzodioxole, an unsaturated aliphatic chain, and piperidine moieties in their chemical structures. Hence, the first two PCs revealed that the aqueous methanolic fruit extracts of the recommended cultivar 'Semongok Aman' and non-recommended cultivar 'Yong Petai' had higher content of piperine and/or its geometric isomers isochavicine, isopiperine, and chavicine and/or piperanine compared to the fruit extracts of the recommended cultivars 'Kuching' and 'Semongok Emas', and non-recommended cultivar 'India'.

LC-MS/MS Metabolite Profiles of *P. nigrum* Fruits

The requirement of power two transformation of the binned ^{1}H-NMR spectra and the interpretation of the resulting PCA model with respect to the unprocessed ^{1}H-NMR spectra in Figure S17 suggest that the variation between ^{1}H-NMR fingerprints of 'Semongok Aman', 'Yong Petai', and other cultivars is small. This is evidenced by the fact that a large percentage (93.5%) of the total variation between the ^{1}H-NMR fingerprints is well-governed by merely 3.0% of the data set's variables (11 out of 370). To further investigate the nature of the variation in metabolite profiles in more polar (i.e., methanol) extracts of the selected *P. nigrum* cultivars, a sample located approximately in the centre of a cultivar's distribution of PC 1 and 2 scores in Figure 3B was selected for the acquisition of metabolite profiles with positive and negative ionisation LC-MS/MS. The fruit metabolite profiles of each cultivar were examined to select representative profiles (Figure 4), which were then visualised in the form of an FBMN. Figure 4 shows that more metabolites in methanolic fruit extracts of

selected *P. nigrum* cultivars were ionised in positive ionisation mode compared to the negative mode. While the maximum intensity of the base peak reached 12.8×10^9 ('Semongok Aman') in positive ionisation, the maximum intensity of the base peak was much lower at 1.27×10^9 ('India') in negative ionisation.

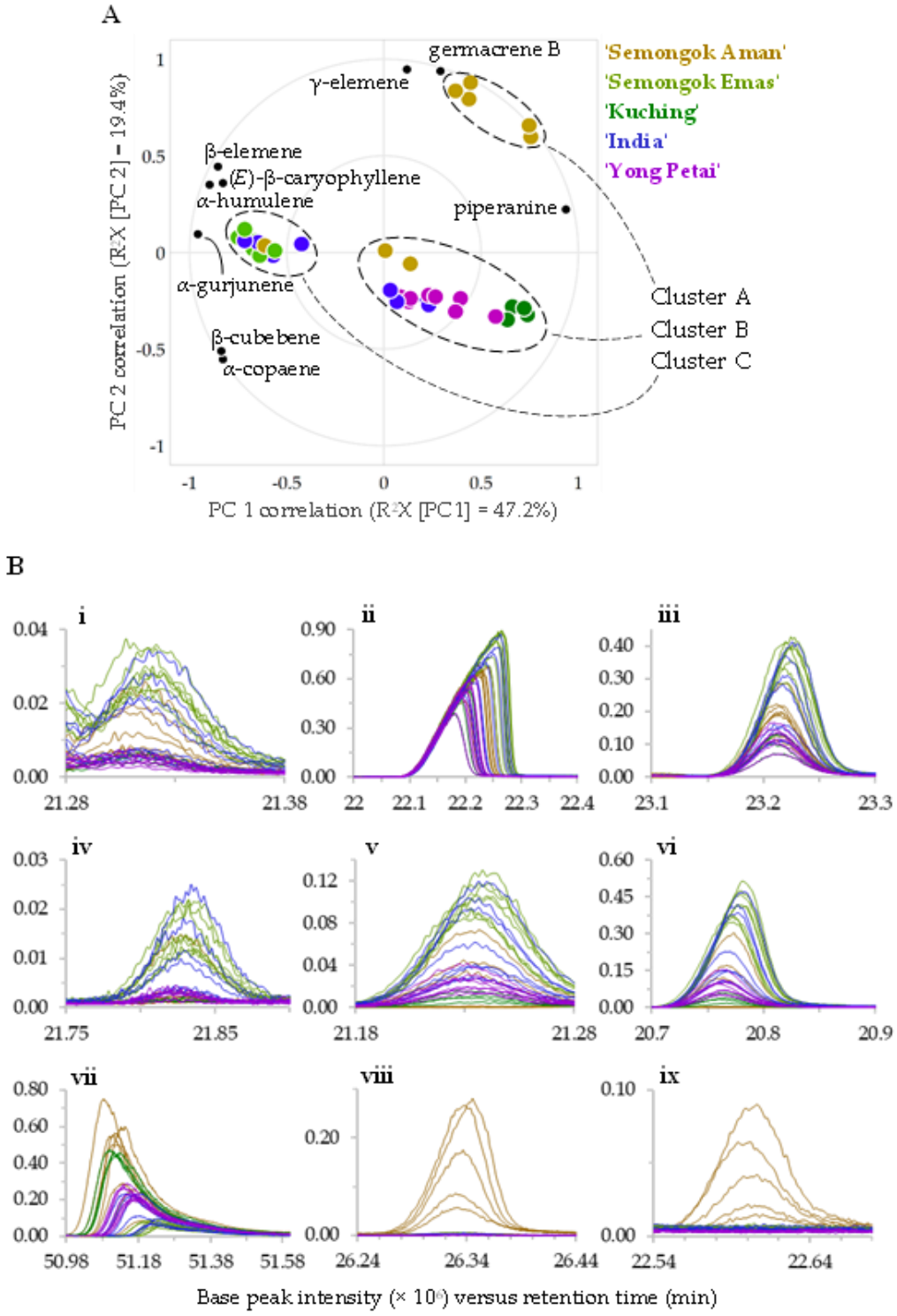

Figure 2. (A) Correlation-scaled PCA biplot of preprocessed GC-MS BPCs of *n*-hexane fruit extracts of *Piper nigrum* cultivars (Q^2X [cum. PC 2] = 61.7%) and (B) magnified views of discriminant metabolite peaks. Only well-modelled variables are shown on the biplot (Q^2VX [cum. PC 2] ≥ 80%). Dimension of data matrix = 36 × 370. (i) β-Elemene, (ii) (*E*)-β-caryophyllene, (iii) α-humulene, (iv) α-gurjunene (v) β-cubebene, (vi) α-copaene, (vii) piperanine, (viii) germacrene B, and (ix) γ-elemene

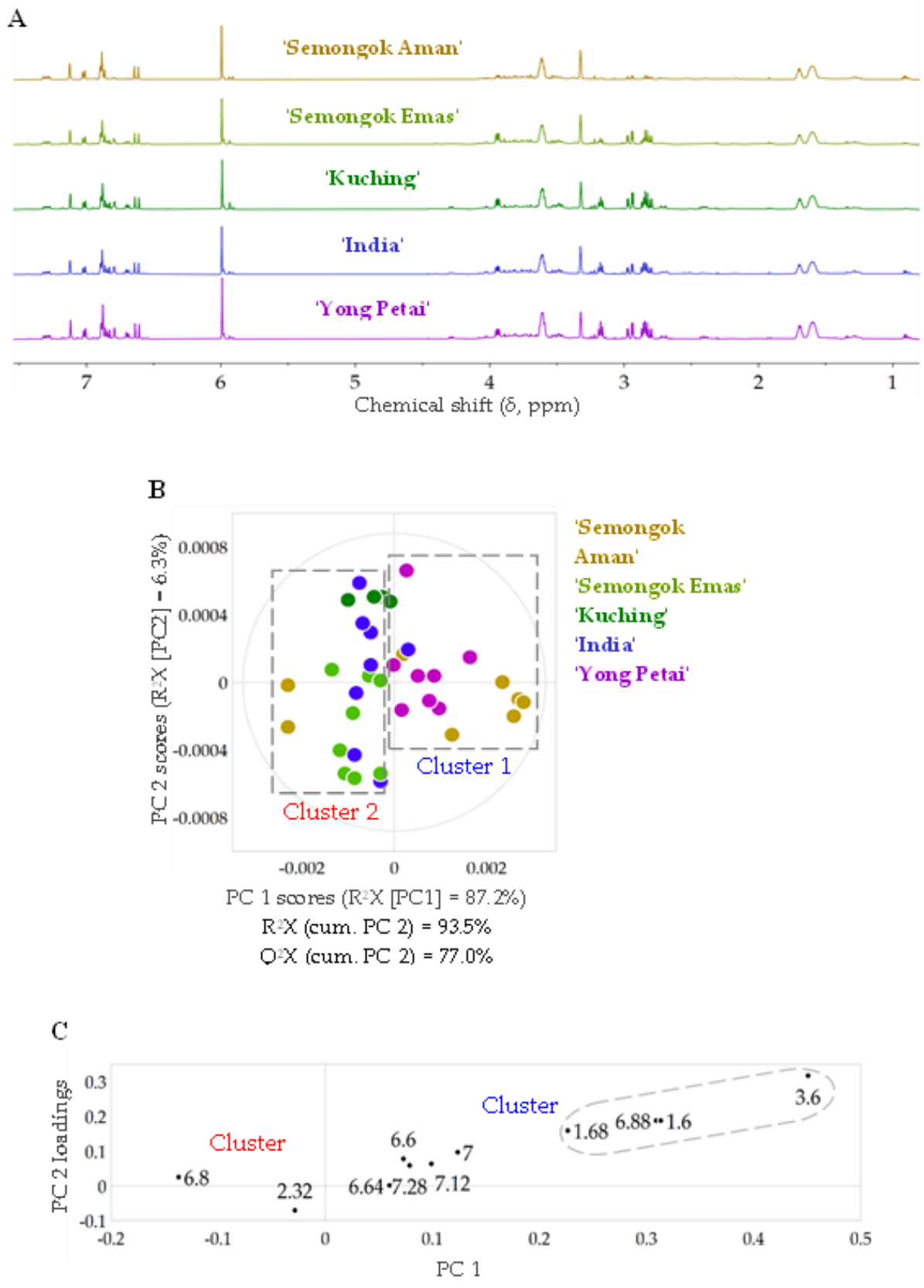

Figure 3. (A) Representative ^{1}H-NMR spectra of aqueous methanolic fruit extracts of *Piper nigrum* cultivars, (B) PCA scores scatter plot (B), and (C) loadings scatter plot of binned, power two-transformed, and mean-centred ^{1}H-NMR spectral data matrix. Dimension of data matrix = 36 × 211. All spectra in (A) were normalised to the TSP signal (δ 0.00, intensity = 100), with a maximum signal intensity = 67 (δ 6.00, 'Yong Petai'). Only well-modelled variables (Q^2VX [cum. PC 2] ≥ 80%) are shown in (C). A magnified view of the ^{1}H-NMR signals corresponding to the four high-magnitude variables circled in (C) is depicted in Figure S17

Moreover, the reproducibility of the retention time in the positive ionisation mode was found to be better than that in the negative ionisation, as the retention time shift for the base peaks at min 7.81 and by min 20.0 in the BPCs with negative ionisation can be seen in Figure 4. For these reasons, the BPCs with positive ionisation were considered to be more representative of the metabolite profiles of *P. nigrum* fruit than the BPCs with negative ionisation and were therefore selected for further examination of intercultivar metabolite profiles variation via FBMN (Figure 5 and Table 1).

Clusters A and B in the FBMN in Figure 5 were annotated as belonging to the alkamides of the *P. nigrum* fruit, whereas cluster C was annotated as belonging to the bisabolane sesquiterpene α-bisabolol. Based on GNPS spectral libraries search, the feature with the highest intensity in the positively ionised BPCs was annotated as a protonated adduct of the piperidine alkamide piperine (cluster B, node ID 1). Therefore, the higher base peak intensities of protonated piperine in 'Semongok Aman' (12.8×10^9) and 'Yong Petai' (12.5×10^9) relative to the other cultivars ($11.4–12.0 \times 10^9$) in Figure 4 support the grouping of the two cultivars into cluster 1 in ^{1}H-NMR metabolomics. Nevertheless, the ID 1 node in Figure 5 implies that the intensity of the base peaks of protonated piperine for each cultivar differs only slightly. This is parallel with the findings described previously, i.e., the contribution of piperine signals to the intercultivar metabolite profile variation is minimal. Apart from piperine, the intensity of the base peaks of other specialised metabolites is also similar in each cultivar, with the exception of node IDs 226 and 4 of cluster A, node 21 of cluster B and node 1285 of cluster C. These four FBMN nodes have significantly higher base peak intensities of the piperidine alkamide piperanine, two isobutylamine alkamides, namely (*E*)-5-(1,3-benzodioxol-5-yl)-*N*-(2-methylpropyl)pent-4-enamide and piperlonguminine, and the sesquiterpene α-bisabolol in the recommended cultivar 'Semongok Aman'.

The experimental and data analysis workflow in this exploratory research enabled the detection of fruit metabolite profiles and fingerprint patterns of the recommended and non-recommended Malaysian *P. nigrum* cultivars via utilisation of GC-MS and ^{1}H-NMR, respectively. In addition, FBMN of the fruit's LC-MS/MS data was employed to carry out automated metabolite annotation, focusing on the metabolites that led to the discriminating ^{1}H-NMR signals.

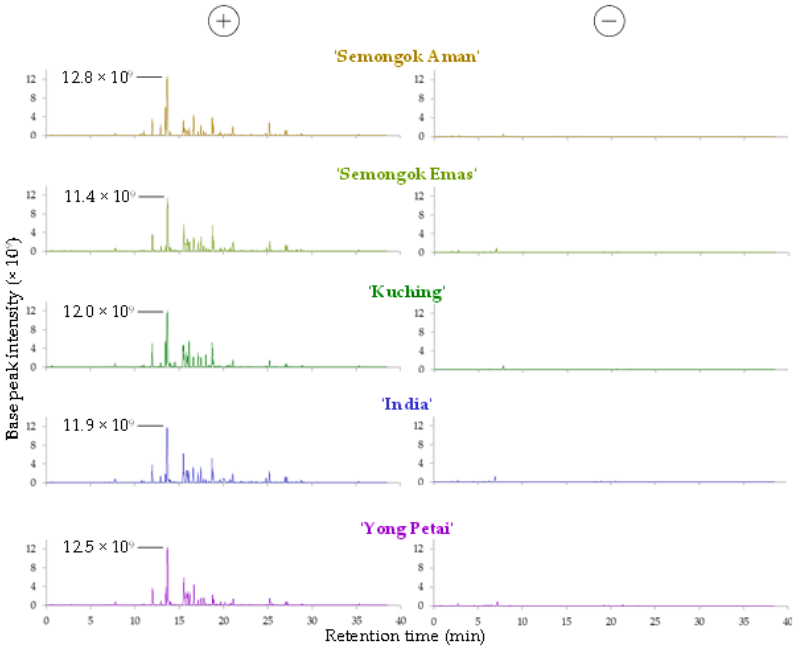

Figure 4. Positive (left) and negative (right) ionisation LC-MS BPCs of methanolic fruit extracts of *Piper nigrum* cultivars

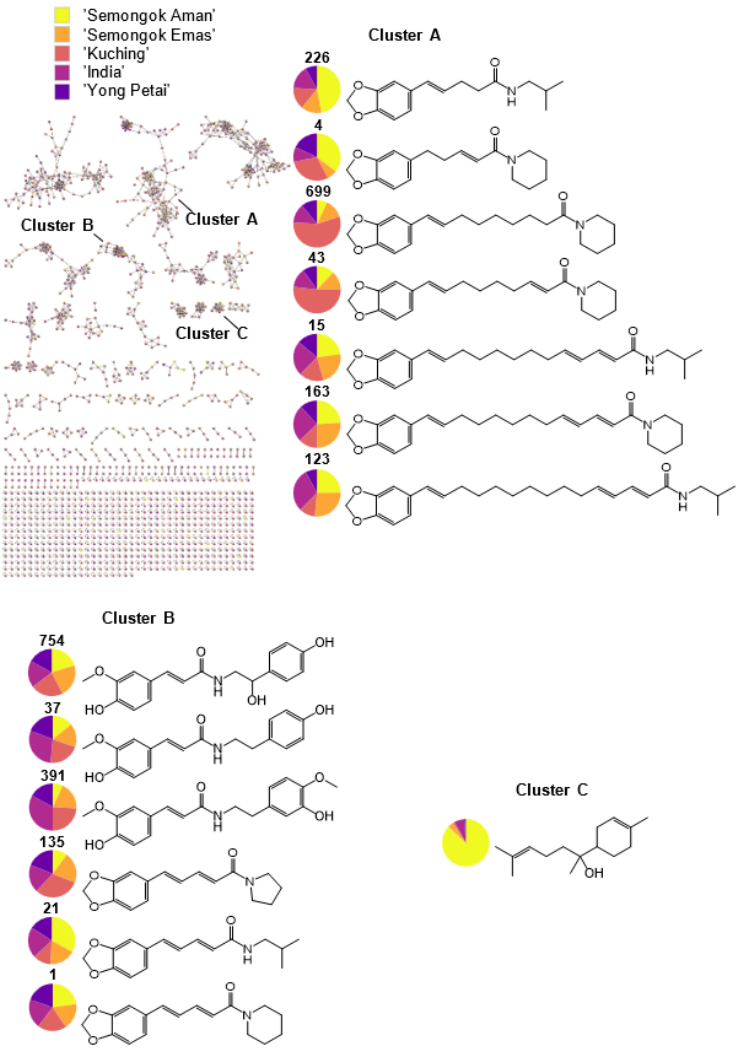

Figure 5. Positive ionisation BPCs FBMN of methanolic fruit extracts of *Piper nigrum* cultivars. The numbers above the FBMN nodes are the node IDs. The FBMN nodes indicate the percent intensity of precursor ions in all samples. See Table 1 for the description of the metabolites

In this research, GC-MS was preferred over ^{1}H-NMR spectroscopy because, apart from the analytical challenge due to the lack of ^{1}H-NMR reference spectra of specialised metabolites in the Chenomx spectral library and the computational challenge of deconvoluting the ^{1}H-NMR fingerprint, to annotate metabolites in complex mixtures (Häckl *et al.*, 2021; Mehr *et al.*, 2023; Schmid *et al.*, 2023), the annotation of discriminative metabolite signals in the fingerprint generated from a small sample size (30 mg) is even more challenging when the percentage of variation to be examined (i.e., infraspecific variation) is much smaller than the interspecific variation. Moreover, previous studies have pointed out the issue of low solubility of piperine in methanol and water (Traxler *et al.*, 2020) and the potential problem of locking and shimming during NMR spectra acquisition due to the use of mixed solvents (Rivera-Pérez *et al.*, 2022). Nevertheless, considering the rapid acquisition of ^{1}H-NMR spectra (whose file sizes are much smaller than those of LC-MS/MS), which precludes time-consuming optimisation of instrument settings and multiple steps of data preprocessing as in LC-MS metabolomics. It is important to highlight that the ^{1}H-NMR metabolomics allowed further overview of clustering of the *P. nigrum* cultivars apart from GC-MS metabolomics. While the same clustering pattern was recognised in both GC-MS and ^{1}H-NMR metabolomics, the inclusion of chromatography and *m/z* dimensions in the GC-MS and LC-MS/MS datasets facilitated the annotation of the discriminating metabolites underlying the observed clustering patterns.

Table 1. List of metabolites identified via GNPS spectral library searches in the FBMN workflow

Average RT (min)	Node ID	Metabolite	Molecular formula	Adduct	*m/z*	Chemical class
Cluster A						
12.87	226	(*E*)-5-(1,3-benzodioxol-5-yl)-*N*-(2-methylpropyl)pent-4-enamide	$C_{16}H_{21}NO_3$	$[M+H]^+$	276.159	Isobutylamine alkamide
13.50	4	Piperanine	$C_{17}H_{21}NO_3$	$[M+H]^+$	288.159	Piperidine alkamide
18.06	699	Piperolein B	$C_{21}H_{29}NO_3$	$[M+H]^+$	344.223	Piperidine alkamide
18.07	43	Pipernonaline	$C_{21}H_{27}NO_3$	$[M+H]^+$	342.206	Piperidine alkamide
21.10	15	Guineensine	$C_{24}H_{33}NO_3$	$[M+H]^+$	384.253	Isobutylamine alkamide
22.16	163	Piperchabamide C	$C_{25}H_{33}NO_3$	$[M+H]^+$	396.253	Piperidine alkamide
23.21	123	Brachystamide B	$C_{26}H_{37}NO_3$	$[M+H]^+$	412.285	Isobutylamine alkamide
Cluster B						
6.87	754	(*E*)-*N*-[2-hydroxy-2-(4-hydroxyphenyl)ethyl]-3-(4-hydroxy-3-methoxyphenyl)prop-2-enamide	$C_{18}H_{19}NO_5$	$[M+H]^+$	330.133	Tyramine alkamide
7.81	37	Moupinamide	$C_{18}H_{19}NO_4$	$[M+H]^+$	314.139	Tyramine alkamide
8.12	391	(*E*)-3-(4-hydroxy-3-methoxyphenyl)-*N*-(3-hydroxy-4-methoxyphenethyl)acrylamide	$C_{19}H_{21}NO_5$	$[M+H]^+$	344.149	Tyramine alkamide
12.30	135	Trichostachine	$C_{16}H_{17}NO_3$	$[M+H]^+$	272.120	Pyrrolidine alkamide
12.96	21	Piperlonguminine	$C_{16}H_{19}NO_3$	$[M+H]^+$	274.144	Isobutylamine alkamide
13.69	1	Piperine	$C_{17}H_{19}NO_3$	$[M+H]^+$	286.144	Piperidine alkamide
Cluster C						
19.93	1285	α-Bisabolol	$C_{15}H_{26}O$	$[M+H-H_2O]^+$	205.195	Bisabolane sesquiterpene

Although three of the eight 'Semongok Aman' samples exhibited individual variations that led to their segregation from the main cluster, the fruits of 'Semongok Aman' originating from Costa Rica were generally found to have a more distinct metabolite profile and fingerprint than the four other, more genetically similar cultivars. The difference was evident in two metabolite classes, namely sesquiterpenoids (germacrene B, γ-elemene, and α-bisabolol) and piperidine alkamides (piperanine, piperine, and piperine isomers). Apart from having better tolerance than 'Kuching' to Phytophthora foot rot caused by the oomycete *Phytophthora capsici* and blackberry diseases caused by the fungal plant pathogens *Colletotrichum truncatum*, *gloeosporioides*, and *orchidearum* species complexes (Jayawardena *et al.*, 2021), and infestation by the pepper stem borer (*Lophobaris piperis*), 'Semongok Aman' is considered a cultivar with satisfactory fruit yield, uniform fruit ripening, and good chemical quality (Fong & Liang, 2011). However, 'Semongok Aman' and 'Kuching' are equally susceptible to the major disease known as slow decay/wilt. This is a debilitating disease complex between the root-knot nematode *Meloidogyne* spp. and the plant-pathogenic fungus *Fusarium* spp. (Fong & Liang, 2011). In one study, the significant increase in sesquiterpenoids α-bisabolol and δ-elemene in the leaves of 'Bragantina' and 'Cingapura', respectively (two important *P. nigrum* cultivars in Brazil), observed after infection with *Fusarium solani* f.

sp. piperis, was postulated to be a response to plant-pathogen interaction (Trindade *et al.*, 2021). Therefore, from the viewpoint of biotechnological approach for the improvement of *P. nigrum* cultivars, future research focusing on the biosynthetic pathways of sesquiterpenes in existing *P. nigrum* cultivars with a significantly higher content of sesquiterpenoids content may assist in the identification of candidate genes for resistance to *Fusarium* spp.

CONCLUSION

The current research provided further information regarding the unique chemical quality of 'Semongok Aman', which was characterised by a higher abundance of the sesquiterpenoids germacrene B, γ-elemene, and α-bisabolol, and the piperidine alkamides piperanine, piperine, and piperine isomers than the other four Malaysian *P. nigrum* cultivars. The findings are parallel with the current recommendation of the Malaysian Pepper Board that 'Semongok Aman' should be grown in local pepper farms over the other non-recommended cultivars due to its good disease tolerance profile, superior chemical quality, and better annual fruit yield and fruit ripening uniformity. In terms of monovarietal pepper cultivation to boost Malaysian pepper production in the world market, 'Semongok Aman' could be considered as a suitable cultivar for future implementation of such an approach.

ACKNOWLEDGEMENTS

The authors acknowledge Sarawak Biodiversity Centre for the approval of plant materials' collection (application ID 2019071), Chen Yi Shang (Malaysian Pepper Board) for his sharing of experience and insights on pepper research in Malaysia, Fidelia Johny, Muhamad Hanif Rawi, Siti Maisarah Mohd Nashri for their assistance in the collection of plant materials, as well as Izzahtul Afiqah Kamarullail and Anis Zulaika Roslan for their contribution in the preliminary GC-MS and ^{1}H-NMR metabolomics of the *P. nigrum* cultivar's fruits. This study was funded by Universiti Putra Malaysia (grant number GP-IPS/2018/9664600).

DATA AVAILABILITY

Metabolomics data have been deposited in the EMBL-EBI MetaboLights database with identifier number MTBLS7768 (https://www.ebi.ac.uk/metabolights/editor/study/MTBLS7768/descriptors).

REFERENCES

Adams, R.P. (2017). *Identification of essential oil components by gas chromatography/mass spectrometry*. Fourth Edition. DuPage County: Allured Business Media.

Afzan, A., Kasim, N., Ismail, N.H., Azmi, N., Ali, A.M., Mat, N. & Wolfender, J.L. (2019). Differentiation of *Ficus deltoidea* varieties and chemical marker determination by UHPLC-TOFMS metabolomics for establishing quality control criteria of this popular Malaysian medicinal herb. *Metabolomics*, 15(3): 1-11. DOI: 10.1007/s11306-019-1489-2

Ahmad, R., Ahmad, N., Amir, M., Aljishi, F., Alamer, M.H., Al- Shaban, H.R., Alsadah, Z.A., Alsultan, B.M., Aldawood, N.A., Chathoth, S. & Almofty, S.A. (2020). Quality variation and standardization of black pepper (*Piper nigrum*): A comparative geographical evaluation based on instrumental and metabolomics analysis. *Biomedical Chromatography*, 34(3): e4772. DOI: 10.1002/bmc.4772

Andriamaharavo, N.R. (2014). Retention Data. NIST Mass Spectrometry Data Center. https://webbook.nist.gov/cgi/cbook.cgi?Source=2014AND%2319410M&Mask=2000

Ashokkumar, K., Murugan, M., Dhanya, M.K., Pandian, A. & Warkentin, T.D. (2021). Phytochemistry and therapeutic potential of black pepper [*Piper nigrum* (L.)] essential oil and piperine: A review. *Clinical Phytoscience*, 7(1): 52. DOI: 10.1186/s40816-021-00292-2

Babushok, V.I., Linstrom, P.J. & Zenkevich, I.G. (2011). Retention indices for frequently reported compounds of plant essential oils. *Journal of Physical and Chemical Reference Data*, 40(4): 043101. DOI: 10.1063/1.3653552

Bandyopadhyay, C., Narayan, V.S. & Variyar, P.S. (1990). Phenolics of green pepper berries (*Piper nigrum* L.). *Journal of Agricultural and Food Chemistry*, 38(8): 1696–1699. DOI: 10.1021/jf00098a015

Barata, L.M., Andrade, E.H., Ramos, A.R., De Lemos, O.F., Setzer, W.N., Byler, K.G., Maia, J.G.S. & Da Silva, J.K.R. (2021). Secondary metabolic profile as a tool for distinction and characterization of cultivars of black pepper (*Piper nigrum* L.) cultivated in Pará State, Brazil. *International Journal of Molecular Sciences*, *22*(2): 890. DOI: 10.3390/ijms22020890

Beger, R.D., Dunn, W.B., Bandukwala, A., Bethan, B., Broadhurst, D., Clish, C.B., Dasari, S., Derr, L., Evans, A., Fischer, S., Flynn, T., Hartung, T., Herrington, D., Higashi, R., Hsu, P.C., Jones, C., Kachman, M., Karuso, H., Kruppa, G., Lippa, K., Maruvada, P., Mosley, J., Ntai, I., O'Donovan, C., Playdon, M., Raftery, D., Shaughnessy, D., Souza, A., Spaeder, T., Spalholz, B., Tayyari, F., Ubhi, B., Verma, M., Walk, T., Wilson, I., Witkin, K., Bearden, D.W. & Zanetti, K.A. (2019). Towards quality assurance and quality control in untargeted metabolomics studies. *Metabolomics*, 15(1): 4. DOI: 10.1007/s11306-018-1460-7

Chen, Y.S., Dayod, M. & Tawan, C.S. (2018). Phenetic analysis of cultivated black pepper (*Piper nigrum* L.) in Malaysia. *International Journal of Agronomy*, 2018. DOI: 10.1155/2018/3894924

Chen, Y.S. & Tawan, C.S. (2020a). Analysis of qualitative and quantitative trait variability among black pepper (*Piper nigrum* L.) cultivars in Malaysia. *Pertanika Journal of Tropical Agricultural Science*, 43(3): 257–274.

Chen, Y.S. & Tawan, C.S. (2020b). *Phenotypic, taxonomy, phytochemical and physiological characterization of black pepper (Piper nigrum L.) cultivars in Malaysia* (PhD thesis). Universiti Malaysia Sarawak.

Entebang, H., Wong, S.-K. & Mercer, Z.J.A. (2021). Development and performance of the pepper industry in Malaysia: A critical review. *International Journal of Business and Society*, 21(3): 1402–1423. DOI: 10.33736/ijbs.3361.2020

Evans, A.M., O'Donovan, C., Playdon, M., Beecher, C., Beger, R.D., Bowden, J.A., Broadhurst, D., Clish, C.B., Dasari, S., Dunn, W.B., Griffin, J.L., Hartung, T., Hsu, P.C., Huan, T., Jans, J., Jones, C.M., Kachman, M., Kleensang, A., Lewis, M.R., Monge, M.E., Mosley, J.D., Taylor, E., Tayyari, F., Theodoridis, G., Torta, F., Ubhi, B.K. & Vuckovic, D. (2020). Dissemination and analysis of the quality assurance (QA) and quality control (QC) practices of LC–MS based untargeted metabolomics practitioners. *Metabolomics*, 16(10): 113. DOI: 10.1007/s11306-020-01728-5

Fong, L.K. & Liang, S.S. (Eds). (2011). *Pepper production technology in Malaysia*. Kuching: Lembaga Lada Malaysia.

Gaweng, P. & Lai, J.C. (Eds). (2017). *Manual penanaman lada*. Kuching: Lembaga Lada Malaysia.

Gómez-Calvario, V. & Rios, M.Y. (2019). ^{1}H and ^{13}C NMR data, occurrence, biosynthesis, and biological activity of *Piper* amides. *Magnetic Resonance in Chemistry*, 57(12): 994–1070. DOI: 10.1002/mrc.4857

Gu, F., Tan, L., Wu, H., Fang, Y. & Wang, Q. (2013). Analysis of the blackening of green pepper (*Piper nigrum* Linnaeus) berries. *Food Chemistry*, 138(2–3): 797–801. DOI: 10.1016/j.foodchem.2012.11.033

Gul, I., Nasrullah, N., Nissar, U., Saifi, M. & Abdin, M.Z. (2017). Development of DNA and GC-MS fingerprints for authentication and quality control of *Piper nigrum* L. and its adulterant *Carica papaya* L. *Food Analytical Methods*, 11: 1209–1222. DOI: 10.1007/s12161-017-1088-7

Häckl, M., Tauber, P., Schweda, F., Zacharias, H.U., Altenbuchinger, M., Oefner, P.J. & Gronwald, W. (2021). An R-package for the deconvolution and integration of 1D NMR data: MetaboDecon1D. *Metabolites*, 11(7): 452. DOI: 10.3390/metabo11070452

Hashimoto, K., Yaoi, T., Koshiba, H., Yoshida, T., Maoka, T., Fujiwara, Y., Yamamoto, Y. & Mori, K. (1996). Photochemical isomerization of piperine, a pungent constituent in pepper. *Food Science and Technology International, Tokyo*, 2(1): 24–29. DOI: 10.3136/fsti9596t9798.2.24

Hashimoto, K., Yaoi, T., Koshiba, H., Yoshida, T., Maoka, T., Fujiwara, Y., Yamamoto, Y. & Mori, K. (2021). Feasibility of applying untargeted metabolomics with GC-Orbitrap-HRMS and chemometrics for authentication of black pepper (*Piper nigrum* L.) and identification of geographical and processing markers. *Journal of Agricultural and Food Chemistry*, 69(19): 5547–5558. DOI: 10.1021/acs.jafc.1c01515

Ho, W.S., Lau, E.T., Jafar, H.R., Sim, S.L. & Paulus, A.D. (2005). Evaluation of genetic relatedness among pepper (*Piper nigrum* L.) accessions using Direct Amplification of Minisatellite-Region DNA (DAMD). *Proceedings of the 6th National Congress on Genetics*, 12-14 May 2005, Kuala Lumpur, Malaysia. pp. 299–302.

Houriet, J., Allard, P.M., Queiroz, E.F., Marcourt, L., Gaudry, A., Vallin, L., Li, S., Lin, Y., Wang, R., Kuchta, K. & Wolfender, J.L. (2020). A mass spectrometry-based metabolite profiling workflow for selecting abundant specific markers and their structurally related multi-component signatures in traditional chinese medicine multi-herb formulae. *Frontiers in Pharmacology*, 11: 578346. DOI: 10.3389/fphar.2020.578346

Jaidee, W., Maneerat, T., Rujanapun, N., Paojumroon, N., Duangyod, T., Banerjee, S., Kar, A., Mukherjee, P.K. & Charoensup, R. (2022). Metabolite fingerprinting of *Piper nigrum* L. from different regions of Thailand by UHPLC-QTOF-MS approach and *in vitro* bioactivities. *Trends in Sciences*, 19(22): 1520. https://doi.org/10.48048/tis.2022.1520

Jayawardena, R.S., Bhunjun, C.S., Hyde, K.D., Gentekaki, E. & Itthayakorn, P. (2021). *Colletotrichum*: Lifestyles, biology, morpho-species, species complexes and accepted species. *Mycosphere*, 12(1): 519–669. DOI: 10.5943/mycosphere/12/1/7

Johny, F., Saupi, N. & Ramaiya, S.D. (2020). Status of pepper farming and flower composition of different pepper varieties in Sarawak. *Pertanika Journal of Tropical Agricultural Science*, 43(4): 467–476. DOI: 10.47836/PJTAS.43.4.04

Jumhawan, U., Putri, S.P., Yusianto, Marwani, E., Bamba, T. & Fukusaki, E. (2013). Selection of discriminant markers for authentication of asian palm civet coffee (Kopi Luwak): A metabolomics approach. *Journal of Agricultural and Food Chemistry*, 61(33): 7994–8001. DOI: 10.1021/jf401819s

Kozukue, N., Park, M.S., Choi, S.H., Lee, S.U., Ohnishi-Kameyama, M., Levin, C.E. & Friedman, M. (2007). Kinetics of light-induced cis-trans isomerization of four piperines and their levels in ground black peppers as determined by HPLC and LC/MS. *Journal of Agricultural and Food Chemistry*, 55(17): 7131–7139. DOI: 10.1021/jf070831p

Krishnamoorthy, B. & Parthasarathy, V.A. (2010). Improvement of black pepper. *CABI Reviews*, 2010. DOI: 10.1079/PAVSNNR20105003

Liang, J., Sun, J., Chen, P., Frazier, J., Benefield, V. & Zhang, M. (2021). Chemical analysis and classification of black pepper (*Piper nigrum* L.) based on their country of origin using mass spectrometric methods and chemometrics. *Food Research International*, 140: 109877. DOI: 10.1016/j.foodres.2020.109877

Luca, S.V., Minceva, M., Gertsch, J. & Skalicka-Woźniak, K. (2021). LC-HRMS/MS-based phytochemical profiling of *Piper* spices: Global association of piperamides with endocannabinoid system modulation. *Food Research International*, 141: 11012. DOI: 10.1016/j.foodres.2021.110123

Matsuo, T., Tsugawa, H., Miyagawa, H. & Fukusaki, E. (2017). Integrated strategy for unknown EI-MS identification using quality control calibration curve, multivariate analysis, EI-MS spectral database, and retention index prediction. *Analytical Chemistry*, 89(12): 6766–6773. DOI: 10.1021/acs.analchem.7b01010

Mayr, S., Beć, K.B., Grabska, J., Schneckenreiter, E. & Huck, C.W. (2021). Near-infrared spectroscopy in quality control of *Piper nigrum*: A comparison of performance of benchtop and handheld spectrometers. *Talanta*, 223(Part 2): 121809. DOI: 10.1016/j.talanta.2020.121809

Mehr, S.H.M., Tang, A.W. & Laing, R.R. (2023). Automated qualitative and quantitative analysis of complex forensic drug samples using ^{1}H NMR. *Magnetic Resonance in Chemistry*, 61(2): 95–105. DOI: 10.1002/mrc.5265

Miyazaki, T., Plotto, A., Goodner, K. & Gmitter, F.G. (2011). Distribution of aroma volatile compounds in tangerine hybrids and proposed inheritance. *Journal of the Science of Food and Agriculture*, 91(3): 449–460. DOI: 10.1002/jsfa.4205

Nothias, L.F., Petras, D., Schmid, R., Dührkop, K., Rainer, J., Sarvepalli, A., Protsyuk, I., Ernst, M., Tsugawa, H., Fleischauer, M., Aicheler, F., Aksenov, A.A., Alka, O., Allard, P.M., Barsch, A., Cachet, X., Caraballo-Rodriguez, A.M., Da Silva, R.R., Dang, T., … Dorrestein, P.C. (2020). Feature-based molecular networking in the GNPS analysis environment. *Nature Methods*, 17(9): 905–908. DOI: 10.1038/s41592-020-0933-6

Osman, M.F., Lee, S.Y., Sarbini, S.R., Mohd Faudzi, S.M., Khamis, S., Zainudin, B.H. & Shaari, K. (2021). Metabolomics-driven discovery of an introduced species and two Malaysian *Piper betle* L. variants. *Plants*, 10(11): 2510. DOI: 10.3390/plants10112510

Osman, M.F., Mohd Faudzi, S.M., Khamis, S., Sarbini, S.R. & Shaari, K. (2022). Shedding light on *Piper*'s identity via computational mass spectrometry. *Malaysian Journal of Chemistry*, 24(4): 150–160.

Phapale, P., Rai, V., Mohanty, A.K. & Srivastava, S. (2020). Untargeted metabolomics workshop report: Quality control considerations from sample preparation to data analysis. *Journal of the American Society for Mass Spectrometry*, 31(9): 2006–2010. DOI: 10.1021/jasms.0c00224

Rivera-Pérez, A., Romero-González, R. & Garrido Frenich, A. (2021). Application of an innovative metabolomics approach to discriminate geographical origin and processing of black pepper by untargeted UHPLC-Q-Orbitrap-HRMS analysis and mid-level data fusion. *Food Research International*, 150(Part A): 110722. DOI: 10.1016/j.foodres.2021.110722

Rivera-Pérez, A., Romero-González, R. & Garrido Frenich, A. (2022). A metabolomics approach based on ^{1}H NMR fingerprinting and chemometrics for quality control and geographical discrimination of black pepper. *Journal of Food Composition and Analysis*, 105: 104235. DOI: 10.1016/j.jfca.2021.104235

Schmid, N., Bruderer, S., Paruzzo, F., Fischetti, G., Toscano, G., Graf, D., Fey, M., Henrici, A., Ziebart, V., Heitmann, B., Grabner, H., Wegner, J.D., Sigel, R.K.O. & Wilhelm, D. (2023). Deconvolution of 1D NMR spectra: A deep learning-based approach. *Journal of Magnetic Resonance*, 347: 107357. DOI: 10.1016/j.jmr.2022.107357

Singh, S., Kapoor, I.P.S., Singh, G., Schuff, C., Lampasona, M.P.De, & Catalan, C.A.N. (2013). Chemistry, antioxidant and antimicrobial potentials of white pepper (*Piper nigrum* L.) essential oil and oleoresins. *Proceedings of the National Academy of Sciences, India Section B: Biological Sciences*, 83(3): 357–366. DOI: 10.1007/s40011-012-0148-4

Takooree, H., Aumeeruddy, M.Z., Rengasamy, K.R.R., Venugopala, K.N., Jeewon, R., Zengin, G. & Mahomoodally, M.F. (2019). A systematic review on black pepper (*Piper nigrum* L.): From folk uses to pharmacological applications. *Critical Reviews in Food Science and Nutrition*, 59(sup1): S210–S243. DOI: 10.1080/10408398.2019.1565489

Traxler, F., Schinnerl, J. & Brecker, L. (2020). Spectroscopic studies on the molecular interactions of curcumin and piperine. *Monatshefte Fur Chemie*, 151(3): 325–330. DOI: 10.1007/s00706-020-02563-z

Trindade, R., Almeida, L., Xavier, L., Andrade, E.H., Maia, J.G., Mello, A., Setzer, W.N., Ramos, A. & da Silva, J.K.R. (2021). Influence on secondary metabolism of *Piper nigrum* L. by co-inoculation with arbuscular mycorrhizal fungi and *Fusarium solani* f. sp. *piperis*. *Microorganisms*, 9(3): 484. DOI: 10.3390/microorganisms9030484

Wang, D., Zhang, L., Huang, J., Himabindu, K., Tewari, D., Horbańczuk, J.O., Xu, S., Chen, Z. & Atanasov, A.G. (2021). Cardiovascular protective effect of black pepper (*Piper nigrum* L.) and its major bioactive constituent piperine. *Trends in Food Science and Technology*, 117: 34–45. DOI: 10.1016/j.tifs.2020.11.024

Borneo Journal of Resource Science and Technology (2025), 15(1): 146-155
DOI: https:doi.org/10.33736/bjrst.6982.2025

Essential Oil from *Citrus medica* Waste and Its Repellent Activity Against Mosquitoes (Diptera: Culicidae)

NUR HISAM ZAMAKSHSHARI[1], NURHAZIQAH MD YAZID[1], KHO SWEN JACK[1], SURISA PHORNVILLAY*[1], DIANA KERTINI MONIR[1] & NURAINEE SALAEMAE[2]

[1]Faculty of Resource Science and Technology, Universiti Malaysia Sarawak, 94300 Kota Samarahan, Sarawak, Malaysia; [2]Department of Agricultural and Fishery Science, Faculty of Science and Technology, Prince of Songkla University, Pattani 94000, Thailand
Corresponding author: psurisa@unimas.my
Received: 19 April 2024 Accepted: 28 August 2024 Published: 30 June 2025

ABSTRACT

Citrus medica is enriched with beneficial antioxidant agents and has promising potential as a mosquito repellent. Most commercial mosquito repellents contain N,N,-diethyl-3-methybenzamide (DEET), damaging the synthetic fabric and plastic, thus producing toxic reactions. This study was conducted to identify the application of *C. medica* peels as new mosquito repellents formulated using essential oil of *C. medica* peels. Methodologically, the essential oil of *C. medica* peels was extracted via hydro-distillation method and analysed by gas chromatography-mass spectrometry. The insect repellent of *C. medica* essential oil nanoemulsion (EON) spray was formulated. This EON was further characterized and assessed for its stability as well as mosquito repellency properties. Major chemical constituents were successfully identified in *C. medica* peels, in which D-Limonene constituted almost 64.57%. The formulated EON was found to be slightly turbid, bluish-white, and isotropic. The pH of EON was 5.45, which was skin-friendly, with 0.8896 ± 0.0016 cP viscosity at 27 °C, which was lower than water (0.8539 cP). The conductivity readings (- 234V) used to establish the oil-in-water nanoemulsion were substantiated by spherical and homogenous shapes with no aggregation seen on a scanning electron microscope. From the repellency test, EON showed good potential with more than 70% mosquito repellency. In conclusion, mosquito repellents formulated from *C. medica* peel essential oil showed good mosquito repellency that effectively reduces vector-borne diseases, which significantly threaten many lives.

Keywords: Citrus, essential oil, food waste, mosquito repellency, nanoemulsion spray

INTRODUCTION

Citrus medica is a member of the Rutaceae family and is referred to as 'limau susu' locally (Mahdi *et al*., 2020). The *C. medica* is a short tree with an oblong fruit of 8 cm to 12 cm in length (Onyeyirichi *et al*., 2014). This species abundantly grows in Malaysia, India, China, Japan, and other tropical and subtropical areas (Langgut, 2015; Onyeyirichi *et al*., 2014). The fruit has long been known to contain many secondary metabolites such as ascorbic acid (vitamin C), retinol (vitamin A), niacin, and thiamine, which are recognized as good antioxidant agents (Bhuiyan *et al*., 2009). These metabolites were also essential nutrients for humans. While the fruit is consumed worldwide as fresh fruit and juice, the peel is often discarded as food waste (Muhd Rodhi *et al*., 2020). It is estimated that 48 million tons of *C. medica* wastes (seeds and peels) are produced globally (Badalamenti *et al*., 2022). Until recently, this circumstance prompted a fresh shift in direction through the enhancement and utilization of previously disregarded by-products, which were once seen as having limited commercial worth and were otherwise left unused (Boccia *et al*., 2021). The essential oil extracted from *C. medica* peel is well-known for its pleasant odor and flavor intensity (Li *et al*., 2019). In contemporary times, there exists a significant need for this vital oil across various sectors such as food production, pharmaceuticals, cosmetics, and perfumery industries (Zamakshshari *et al*., 2023). Its established properties encompass pain relief, anxiety reduction, neuroprotective effects, and demonstrating antibacterial and antifungal effectiveness (Yen & Failloux, 2020).

The vector-borne diseases (malaria, dengue, Chagas disease, yellow fever, Japanese encephalitis, and onchocerciasis) affect millions

globally through mosquitoes transmitting infectious pathogens from animals to humans. The World Health Organization (WHO) reports that more than 700,000 people die annually from vector-borne diseases (WHO, 2020). Finding a safe, effective, and affordable tool to fight these diseases is urgent. Mosquito repellent is one of the tools that can be used to tackle this problem. The mechanism of mosquito repellent is to minimise contact with mosquitoes and avoid the transmission of infectious pathogens (Yen & Failloux, 2020). A synthetic repellent of N, N, -diethyl-3-methybenzamide (DEET) is used commercially as a mosquito repellent (Tan *et al*., 2019). However, DEET application will lead to toxic reactions and cause damage to plastic and synthesis fabric (Gillij *et al*., 2008). A wonderful and potent protein target for the mosquito would be the odorant binding protein (OBP) as this protein, initially identified from moths, could be used as molecular targets for the creation of mosquito and moth repellent (Leite *et al*., 2009).

The application of plant-based repellents has become popular because they are free of toxicity and adverse reactions (Ojewumi *et al*., 2021). The essential oil isolated from plants has shown excellent repellent activity in several phytophagous insects and hematophagous such as mosquitoes. Studies showed that essential oil nanoemulsion (EON) repellent from *Eucalyptus globulus* and *Mentha piperita* is efficient compared to synthetic repellent, with lower protection times against mosquitoes (Mohammadi *et al*., 2019; Navayan *et al*., 2017). The essential oil contains secondary metabolites such as limonene, citronella, 1,8-cineole, geraniol, and eugenol and these compounds have a good insect repellent activity as the compounds pose unbearable odour for the insects (da Silva & Ricci-Júnior, 2020). To date, the EONs from *C. medica* have been developed by researchers for food and beverage applications. The development is due to their biological activities, such as antibacterial, anti-inflammatory, antioxidant, antibiofilm, followed by human gut protective activity (Li *et al*., 2018; Liu *et al*., 2021; Lou *et al*., 2017). However, no EON formulation of *C. medica* has been reported specifically for mosquito repellent application (Diptera: Culicidae). Therefore, this study aimed to identify the application of *C. medica* waste in developing new mosquito repellents.

MATERIALS AND METHODS

Chemicals

Each chemical substance was procured from Merck (Darmstadt, Germany) and Sigma-Aldrich (Chemie, Steinheim, Germany). Additionally, all solvents employed held the chromatographic or analytical grade quality standard.

Sample Collection and Preparation

Citrus medica fruits were purchased from the local market, Kota Samarahan, Malaysia, in January to March 2023. The fruit underwent multiple rinses with distilled water to eliminate surface impurities such as dirt, dust, microorganisms and any lingering pesticide traces. Subsequently, the peels were sliced into small fragments using a stainless-steel knife.

Extraction of Essential Oil from *Citrus medica*

The methodology of hydro-distillation via the Clevenger-type apparatus was employed in this work according to Zamakshshari *et al*. (2023). About 2.198 kg of freshly cut *C. medica* peel was placed in a 5 L round bottom flask with the addition of ultrapure water. The sample was heated for 4 h. The resulting steam, carrying the oil, was channelled through a condenser, and collected within the Clevenger-type apparatus. The condensate (including oil) in the conical flask was collected. For separation, liquid-liquid extraction was performed using 150 mL of ethyl acetate. The resulting supernatant was collected, and subsequent removal of any residual water molecules was achieved by introducing anhydrous sodium sulfate. Further purification involved the removal of ethyl acetate through a rotary evaporator (Buchi, Germany) to yield the essential oil. The procedure was repeated several times, and the essential oil was stored in a small vial covered with aluminum foil before gas chromatography-mass spectrometry (GC-MS) analysis (Zamakshshari *et al*., 2023). The essential oil's percentage yield was determined using the formula provided accordingly; Eq. (1):

Essential oil percentage yield (w/w) % = Mass of essential oil (g) / Mass of sample (g) x 100 Eq.(1)

Chemical Profiling Using Gas Chromatography-Mass Spectrometry (GC-MS)

The essential oil of *C. medica* peels was analysed using GC-MS (Agilent 7890B) equipped with capillary column HP-5 MS (30 m × 250 μm × 0.25 μm) coupled with a quadrupole mass spectrometer (Agilent 5977) as reported by Mohammed *et al*. (2022) with slight modifications. An aliquot of 1 μL of the sample was injected in splitless mode. Then, the temperature of the column, initially 50 °C (1 min hold), was increased to 280 °C at the rate of 5 °C min^{-1} and maintained at this temperature for 10 min, injection temperature of 280 °C, detector temperature of 300 °C. Helium was the carrier gas with a constant flow rate at 1 mL min^{-1} and the total analysis time was 57 min. Electron ionization at 70 eV determined the mass spectra in the m/z range of 50-500 Da. The chromatogram percentage area was measured and identified using the MassHunter Qualitative Analysis software. The matching percentage was assigned to greater than 79% by comparing their mass ionization spectra with the NIST17 library (National Institute of Standards and Technology, 2017) without any correction factors (Dob *et al*., 2005).

Insect Repellent of Oily-Based Nanoemulsion Spray Formulation

The spray was formulated using the emulsion phase inversion method of Ostertag *et al*. (2012) with slight modifications. The essential oil was immersed with Tween 80 to activate the surfactant, followed by the co-surfactant glycerin. The EON was formulated according to a ratio of 1:1.5:10 of essential oil, surfactant and co-surfactant, respectively. The nanoemulsion was stirred using a magnetic stirrer for 30 min. About 1.25 g of the nanoemulsion was diluted to 100X with a 100 Mm acetate buffer and 0.5 g of tocopherol as the final EON spray product.

Characterisation and Stability Test On Nanoemulsion Spray

pH

EON spray's pH was determined at room temperature by a pH meter (MW 102 pH, Milwaukee Instruments, Hungary, Budapest). The pH measurements were taken in triplicate for the sample tested. The pH meter was calibrated using a buffer solution with pH 10.01, 7.01 and 4.01 as quality control before measurements were made.

Conductivity

The conductivity of the EON spray was measured at ambient temperature using a digital conductivity measuring device (Jenway 4510 Conductivity/TDS Meter). This test determined the emulsion's continuous phase, whether it was o/w emulsions (conductive) or w/o emulsions (unconducive) (Azmi *et al*., 2019). The conductivity test was carried out in triplicate for the sample tested. Before any measurements were taken, the meter was calibrated using deionised water.

Thermodynamic and Shelf Stability

The stability studies were based on Shafiq-un-Nabi *et al*. (2007) with slight modifications. The thermodynamic stability test can be divided into three parts: (i) centrifugal separation, in which the EON was centrifuged at 1350 rpm for 5 min, (ii) temperature cycling, involving six cycles, alternating between refrigerated conditions at 4 ℃ and elevated temperature at 40 ℃, were conducted (the samples were stored at each temperature for a minimum of 24 h) and (iii) freeze-thaw cycling, in which the formulations were subjected to three freeze-thaw cycles, alternating between temperatures of -21 ℃ and 25 ℃ (the samples were stored at each temperature for a minimum of 24 h). The thermodynamically stable EON formulation was subjected to shelf-life stability; EON was assessed for cracking, creaming or phase separation via macroscopy for 84 days.

Viscosity Measurement and Scanning Electron Microscope (SEM)

A U-tube viscometer was utilised to determine the viscosity of the EON spray at 27 ℃. Morphology of the nanostructure of the EON was characterised using SEM (JEOL JSM-6390LA, Japan). The EON was subjected to serial dilution using ethanol. A sample drop was smeared onto a zinc plate, air-dried, and subjected to platinum coating before the SEM imaging.

Mosquito Repellent Assay

The excito chamber method was used to observe the mosquito behavior change in the form according to Anuar and Yusof (2016) with slight modifications. The excito chamber is shown in Figure 1. Both chambers A and B were constructed with transparent plastic, with each side measurement of 30 cm × 30 cm × 30 cm, forming a cube. A small entry opening (5 cm × 5 cm) equipped with a short netting sleeve on the outside was made at chamber A to lead mosquitos into the chamber. A transparent plastic cylinder was placed as a bridge connecting chamber A and B. A fabric (4 cm × 4 cm) was treated with insect repellent spray or cream. Prior to the test, the mosquitoes were fasted overnight or for a minimum duration of 4 h. The behaviour of the mosquitoes was monitored in relation to the count of mosquitoes that managed to move to a different area and the mosquitoes that remained within the enclosure containing the treated substance. This observation was documented after a 30 min exposure period. The experiments were carried out during daylight hours in triplicates. The percentage of mosquito repellency was computed using the subsequent formula, Eq.(2):

Mosquito repellency (%):

$$(NME + NMD)/(N_{total}) \times 100 \qquad \text{Eq.(2)}$$

Whereby, NME = the count of mosquitoes that managed to escape, NMD = number of deceased mosquitoes, and Ntotal = number of mosquitoes that were exposed.

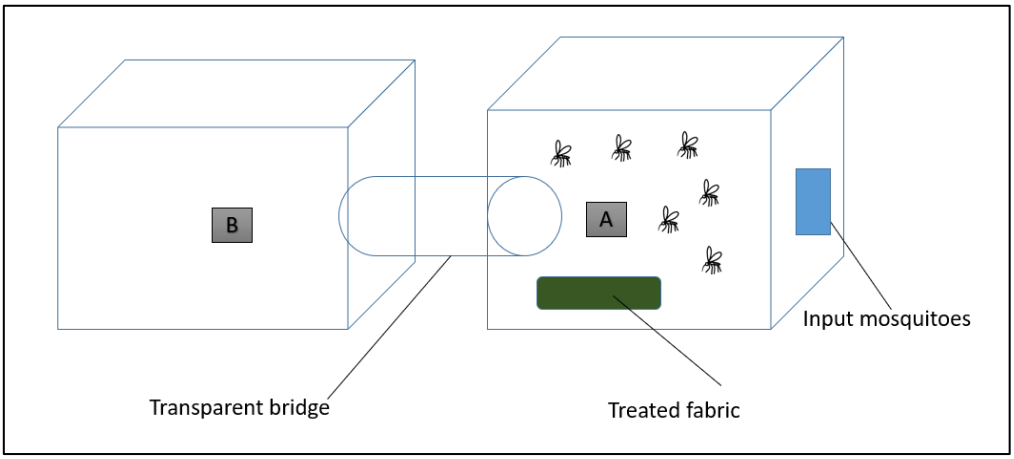

Figure 1. Excito chamber

Statistical Analysis

The data on the extraction of essential oil, stability test, and mosquito repellent assays were represented as mean ± standard deviation and were conducted in three replicates analyses.

RESULTS AND DISCUSSION

Yield of Essential Oil Extract and Qualitative Analysis of Essential Oil Using GC-MS

The *C. medica* peel essential oil was extracted using the hydro-distillation process for 4 h, yielding 0.23% (w/w) (Table 1). The essential oil obtained was pale yellow. Similarly, Venturini *et al*. (2014) reported that 0.40 - 0.72% (w/w) essential oil was extracted from *C. medica* peels using the same method. However, the percentage yield of essential oil obtained in this study is slightly different from previously reported extractions (Amelia *et al*., 2017). This suggests that factors might be due to the *C. medica* origin, sample preparation technique before hydro-distillation, duration of hydro-distillation, diversity of various *C. medica* genetics, and environmental factors such as terrestrial factors (drought, water, soil), climate factors (temperature, light, stressors), and human factors (fertilizers, pollution, deforestation) (Upadhyay *et al*., 2022).

The library score matched with a percentage greater than 80% was selected by comparing their mass ionisation spectra with the NIST17 library (National Institute of Standards and

Technology, 2017) without any correction factors (Dob *et al*., 2005). A total of 11 compounds comprising 99.99% of the essential oil content were identified (Figure 2). Monoterpenes were the major constituent in essential oil (76.50%), followed by oxygenated monoterpenes (5.28%). Specifically, three major constituents abundantly found in essential oil were D-limonene (64.57%), γ-terpinene (10.58%), and linalool (6.08%). Other chemical constituents present in the essential oil were (S)-(+)-5-methyl-1-heptanol (1.36%), 1,3-cyclohexadiene, 1-methyl-4-(1-methylethyl)- (1.35%), terpinen-4-ol (1.17%), α-terpineol (2.50%), decanal (1.18%), 6-oct-1-ol,3,7-dimethyl-, formate (1.70%), 1-cyclohexene-1-carboxaldehyde, 4-(1-methylethenyl)- (0.43%) and dodecanal (0.41%), as shown in Table 2. A value of less than 0.1% was denoted as traces (Dob *et al*., 2005). In *C. medica*, D-limonene is known to have high biological activity; thus, to improve the high biological activity of the extract it needs to contain high D-limonene. According to Santiago *et al*. (2020), the hydro distillation method can result in high levels of D-limonene in the extract, which is a compound with potential biological activity (Amelia *et al*., 2017). Figure 3 shows the chemical structure of chemical constituents that are present in essential oil.

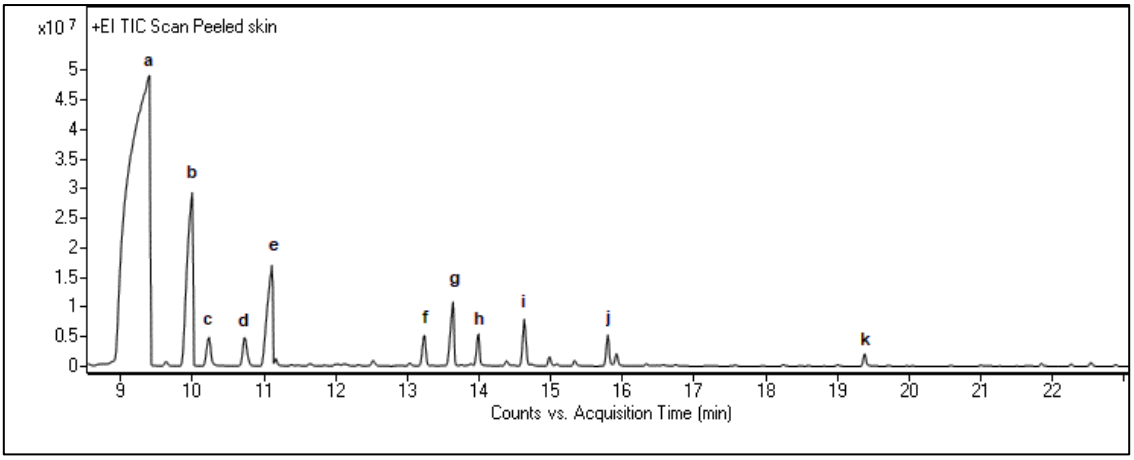

Figure 2. Chromatogram of *Citrus medica* peels

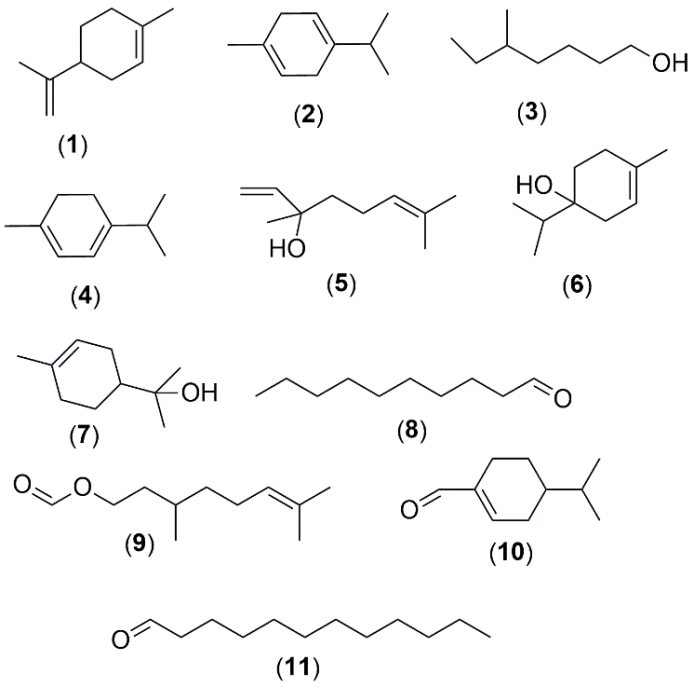

Figure 3. Chemical structures of the compounds obtained from *Citrus medica* essential oil from hydro-distillation method

Table 1. Percentage yield of *Citrus medica* peels essential oil

Sample	Sample mass (kg)	Weight of essential oil (g)	Percentage yield (w/w) %	Colour of essential oil
Citrus medica peels	2.198	4.52	0.23	Pale yellow

Table 2. Chemical composition of *Citrus medica* peels

Peak no.	Retention time	Compound name	Molecular formula	Percentage area (%)	Library score
a	9.39	D-Limonene (**1**)	$C_{10}H_{16}$	64.57	91.35
b	9.97	γ-Terpinene (**2**)	$C_{10}H_{16}$	10.58	90.01
c	10.23	(S)-(+)-5-methyl-1-heptanol (**3**)	$C_8H_{18}O$	1.36	90.41
d	10.73	1,3-cyclohexadiene, 1-methyl-4-(1-methylethyl) (**4**)	$C_{10}H_{16}$	1.35	90.41
e	11.10	Linalool (**5**)	$C_{10}H_{18}O$	6.08	84.45
f	13.23	Terpinene-4-ol (**6**)	$C_{10}H_{18}O$	1.17	87.61
g	13.63	α-Terpineol (**7**)	$C_{10}H_{18}O$	2.50	83.35
h	13.99	Decanal (**8**)	$C_{10}H_{20}O$	1.18	85.49
i	14.63	6-Oct-1-ol,3,7-dimethyl-, formate (**9**)	$C_{11}H_{20}O_2$	1.70	85.49
j	15.92	1-Cyclohexene-1-carboxaldehyde, 4-(1-methylethenyl) (**10**)	$C_{10}H_{14}O$	0.43	91.64
k	19.38	Dodecanal (**11**)	$C_{12}H_{24}O$	0.41	85.00
Total					99.99

Formulation and Characterisation of EON Spray

The essential oil of *C. medica* is insoluble in water; thus, limiting its usage. To overcome this situation Tween 80 and glycerol were used as surfactant and cosurfactant (Saberi *et al*., 2013). The final EON formulation was obtained in the ratio of 1:1.5:10 of essential oil, surfactant and co-surfactant in 100 mL of acetate buffer (pH 5.45) as the aqueous phase. The formulation was chosen in the specific ratio because studies have proven that 1000 mg L^{-1} or 0.1 mL of this similar essential oil is effective as a mosquito repellent (Choochote *et al*., 2007; Nascimento *et al*., 2017). The visual observation of the EON spray showed as a slightly turbid, bluish-white, and isotropic solution which are characteristics of good nanoemulsion formation (Shafiq *et al*., 2007). The extensive freeze-thaw, cooling, and heating centrifugation test were also performed to determine the thermodynamic stability. The SEM results (Figure 4) confirmed that the EON formulated has high thermodynamic stability as there was no visual evidence of creaming, cracking, coalescence, phase separation and inversion in the finished product, indicating that the preliminary stability of the EON is acceptable. The EON remained stable for two months at room temperature as none of the above-mentioned physical properties were observed. The essential oil degradation led to some colour fading of the EON after six months, but the strong citric aroma of the spray remained unchanged.

The additional characterisation of the formulation was evaluated, including pH, viscosity and conductivity, as exhibited in Table 3. The formulated EON exhibited a skin-friendly pH of which is 5.45, as the general optimal pH value of human skin is around pH 4 to 6 (Lukić *et al*., 2021). The viscosity of the formulation was detected as 0.8896 ± 0.0016 cP, slightly thicker than water at 0.8539 cP at 27 ℃, as this is a phenomenon caused by emulsification whereby it thickens the liquid (Geetanjali *et al*., 2021). A slightly higher viscosity than water is favourable as the EON is not too thickened, which would affect its transmittance as a repellent. This is proven by Okpalaku *et al*. (2022) as the lemon nanoemulsion had the lowest viscosity and the highest transmittance percentage when compared to turmeric and coconut nanoemulsion.

Besides that, the SEM results also showed that EON's supportive oil-in-water (o/w) nanoemulsion character with bright droplets appearing in the dark background (Figure 4).

The EON exhibited spherical and homogenous shapes, which was also a justification for the conductivity measurements (-234 ± 5V) for o/w nanoemulsion confirmation. The results exhibited no evidence of the emulsion droplets coalescing with each other and aggregating into larger clusters, suggesting the oil droplets are stably dispersed (Chuesiang *et al*., 2018; Geetanjali *et al*., 2021; Okpalaku *et al*., 2022). The conductivity of o/w nanoemulsions is higher than that of w/o nanoemulsions (Okpalaku *et al*., 2022). Therefore, EON must be of the o/w type, as their high conductivity values indicate. Nanoemulsion components, such as oil, water and surfactants, each impact their viscosity to varying degrees.

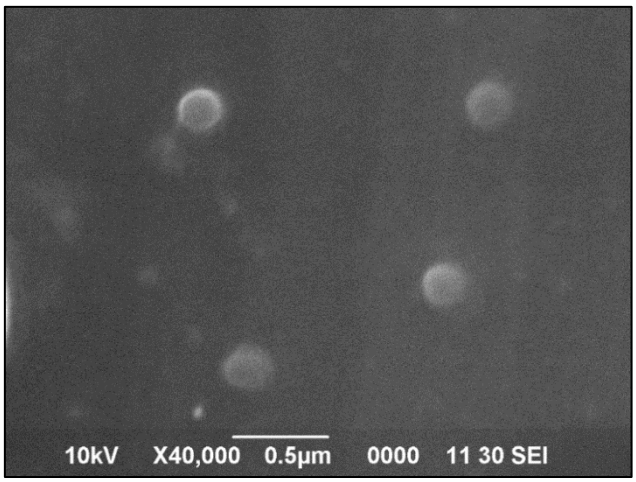

Figure 4. Scanning electron microscopic image of essential oil nanoemulsion (EON)

Table 3. Physicochemical characterization and shelf stability of essential oil nanoemulsion (EON)

Physicochemical Properties	Results
pH	5.45
Conductivity	-234 ± 5 V
Viscosity	0.8896 ± 0.0016 cP
Centrifugation	Pass
Heating cooling cycle	Pass
Freeze-thaw cycle	Pass
Shelf Stability (days)	
1	Pass
7	Pass
14	Pass
28	Pass
56	Pass
84	Pass

Mosquito Repellent Activity

The formulated oily-based nanoemulsion spray from *C. medica* peel essential oil was tested for its mosquito repellent activity using the excito chamber (Nararak *et al*., 2019). Ten mosquitoes were used for each set of experiments. The first set of the experiment gave 70% mosquito repellence, with four deaths and three mosquitoes escaping to the next box. Meanwhile, the second set of experiments gives 90% mosquito repellence, with five deaths and four mosquitoes escaping to the next box. The third trial gives 80% mosquito repellence, with six deaths and two mosquitoes escaping to another box. All sets of experiments showed that the EON spray has above 50% mosquito repellent activity, suggesting good mosquito repellence properties. The repellent activity is believed due to the presence of D-limonene, α-terpineol, 6-oct-1-ol,3,7-dimethyl-, formate, γ-terpinene and 1,3-cyclohexadiene, 1-methyl-4-(1-methylethyl)- as a constituent in the essential oil of *C. medica* peels. Additionally, D-Limonene was used in the organic agriculture industry as pest control due to its good repellent activity against two insect pests: *Tribolium castaneum* and *Lasioderma serricorne* (Pang *et*

al., 2021). Meanwhile, the γ-terpinene, also found in wild carrot essential oil, shows excellent cytotoxic activity against three types of mosquito larva: *Aedes aegypti* L., *Culex pipiens* L. and *Culex restuans* Theobald larvae (Muturi *et al*., 2019). All sets of experiments showed a high mortality rate of mosquitoes. α-Terpineol is an aromatic agent widely used in the food industry and exhibits bio properties including antioxidative, growth-inhibiting, antimicrobial, anti-inflammatory, and pain-relieving properties as pharmaceutic (Sales *et al*., 2020).

CONCLUSION

In conclusion, this study successfully demonstrated the potential of *C. mdeica* peel waste as an effective natural mosquito repellent. The hydro-distillation method efficiently extracted essential oil, predominantly containing D-limonene, which was identified as a major active component. The formulated EON spray exhibited promising mosquito repellent properties, achieving over 70% repellency. Furthermore, the EON spray was characterised by skin-friendly pH, suitable viscosity and stable thermodynamic properties, making it a viable alternative to synthetic repellent like DEET. These findings underscore the dual benefits of utilising food waste for sustainable repellent production and offering a safer solution to mitigate mosquito-borne diseases. Future research should focus on large-scale production and comprehensive field testing to further validate the efficacy and safety of *C. medica* essential oil-based repellents.

ACKNOWLEDGEMENTS

The authors would like to acknowledge Universiti Malaysia Sarawak (UNIMAS) for the PILOT Research Grant Scheme (UNI/F07/PILOT/85369/2022) and the Sarawak Biodiversity Centre (SBC) for granting the permission to conduct this research.

REFERENCES

Amelia, B., Saepudin, E., Cahyana, A.H., Rahayu, D.U., Sulistyoningrum, A.S. & Haib, J. (2017). GC-MS analysis of clove (*Syzygium aromaticum*) bud essential oil from Java and Manado. *AIP Conference Proceeding*, 1862, 030082. DOI: 10.1063/1.4991186

Anuar, A.A. & Yusof, N. (2016). Methods of imparting mosquito repellent agents and the assessing mosquito repellency on textile. *Fashion and Textiles*, 3(1): 12. DOI:10.1186/s40691-016-0064-y

Azmi, N.A.N., Elgharbawy, A.A.M., Motlagh, S.R., Samsudin, M. & Salleh, H.M. (2019). Nanoemulsion: Factory for food, pharmaceutical and cosmetics. *Processes*, 7(9): 617. DOI: 10.3390/pr7090617

Badalamenti, N., Bruno, M., Schicchi, R., Geraci, A., Leporini, M., Tundis, R. & Loizzo, M.R. (2022). Reuse of food waste: The chemical composition and health properties of pomelo (*Citrus maxima*) cultivar essential oils. *Molecules*, 27(10): 3273. DOI:10.3390/molecules27103273

Bhuiyan, M.N.I., Begum, J., Sardar, P.K. & Rahman, M.S. (2009). Constituents of peel and leaf essential oils of *Citrus medica* L. *Journal of Scientific Research*, 1(2): 387-392. DOI:10.3329/jsr.v1i2.1760

Boccia, F., Di Pietro, B. & Covino, D. (2021). Food waste and environmental-sustainable innovation: A scenario for the Italian *Citrus* market. *Quality-Access to Success*, 182: 145-153.

Choochote, W., Chaithong, U., Kamsuk, K., Jitpakdi, A., Tippawangkosol, P., Tuetun, B., Champakaew, D. & Pitasawat, B. (2007). Repellent activity of selected essential oils against *Aedes aegypti*. *Fitoterapia*, 78(5): 359-364. DOI:10.1016/j.fitote.2007.02.006

Chuesiang, P., Siripatrawan, U., Sanguandeekul, R., McLandsborough, L. & Julian McClements, D. (2018). Optimization of cinnamon oil nanoemulsions using phase inversion temperature method: Impact of oil phase composition and surfactant concentration. *Journal of Colloid and Interface Science*, 514: 208-216. DOI:10.1016/j.jcis.2017.11.084

da Silva, M.R.M. & Ricci-Júnior, E. (2020). An approach to natural insect repellent formulations: from basic research to technological development. *Acta Tropica*, 212: 105419. DOI:10.1016/j.actatropica.2020.105419

Dob, T., Dahmane, D., Berramdane, T. & Chelghoum, C. (2005). Chemical composition of the essential oil of *Artemisia campestris* L. from Algeria. *Pharmaceutical Biology*, 43(6): 512-514. DOI:10.1080/13880200500220664

Geetanjali, R., Sreejit, V., Sandip, P. & Preetha, R. (2021). Preparation of aloe vera mucilage-ethyl vanillin nano-emulsion and its characterization. *Materials Today: Proceedings*, 43: 3766-3773. DOI:10.1016/j.matpr.2020.10.990

Gillij, Y.G., Gleiser, R.M. & Zygadlo, J.A. (2008). Mosquito repellent activity of essential oils of aromatic plants growing in Argentina. *Bioresource Technology*, 99(7): 2507-2515. DOI:10.1016/j.biortech.2007.04.066

Langgut, D. (2015). Prestigious fruit trees in ancient Israel: first palynological evidence for growing *Juglans regia* and *Citrus medica*. *Israel Journal of Plant Sciences*, 62(1-2): 98-110. DOI:10.1080/07929978.2014.950067

Leite, N. R., Krogh, R., Xu, W., Ishida, Y., Iulek, J., Leal, W. S., & Oliva, G. (2009). Structure of an odorant-binding protein from the mosquito *Aedes aegypti* suggests a binding pocket covered by a pH-sensitive "lid." *PLoS ONE*, 4(11): e8006. DOI:10.1371/journal.pone.0008006

Li, Z., Cai, M., Liu, Y. & Sun, P. (2018). Development of finger citron (*Citrus medica* L. var. *sarcodactylis*) essential oil loaded nanoemulsion and its antimicrobial activity. *Food Control*, 94: 317-323. DOI:10.1016/j.foodcont.2018.07.009

Li, Z.H., Cai, M., Liu, Y.S., Sun, P.L. and Luo, S.L., 2019. Antibacterial activity and mechanisms of essential oil from *Citrus medica* L. var. *sarcodactylis*. *Molecules*, 24(8): p.1577. DOI:10.3390/molecules24081577

Liu, W., Li, Z., Yang, K., Sun, P. & Cai, M. (2021). Effect of nanoemulsion loading finger citron (*Citrus medica* L. var. *Sarcodactylis*) essential oil on human gut microbiota. *Journal of Functional Foods*, 77: 104336. DOI:10.1016/j.jff.2020.104336

Lou, Z., Chen, J., Yu, F., Wang, H., Kou, X., Ma, C. & Zhu, S. (2017). The antioxidant, antibacterial, antibiofilm activity of essential oil from *Citrus medica* L. var. *sarcodactylis* and its nanoemulsion. *LWT*, 80: 371-377. DOI:10.1016/j.lwt.2017.02.037

Lukić, M., Pantelić, I. & Savić, S.D. (2021). Towards optimal pH of the skin and topical formulations: From the current state of the art to tailored products. *Cosmetics*, *8*(3): 69. DOI:10.3390/cosmetics8030069

Mahdi, A.A., Al-Ansi, W., Ahmed, M.I., Xiaoyun, C., Mohammed, J.K., Sulieman, A.A., Mushtaq, B.S., Harimana, Y. & Wang, H. (2020). Microwave assisted extraction of the bioactive compounds from peel/pulp of *Citrus medica* L. var. *sarcodactylis* swingle along with its nutritional profiling. *Journal of Food Measurement and Characterization*, 14(1): 283-292. DOI:10.1007/s11694-019-00290-6

Mohammadi, R., Khoobdel, M., Negahban, M., & Khani, S. (2019). Nanoemulsified Mentha piperita and Eucalyptus globulus oils exhibit enhanced repellent activities against *Anopheles stephensi*. *Asian Pacific Journal of Tropical Medicine*, 12(11): 520. DOI:10.4103/1995-7645.271292

Mohammed, H.H., Laftah, W.A., Noel Ibrahim, A. & Che Yunus, M.A. (2022). Extraction of essential oil from *Zingiber officinale* and statistical optimization of process parameters. *RSC Advances*, 12(8): 4843-4851. DOI:10.1039/D1RA06711G

Muhd Rodhi, M.N., Saifuddin, P.N.S. & Veny, H. (2020). Characterisation of used cooking oil (UCO) and orange peels as the medium of insect repellent. *Malaysian Journal of Chemical Engineering and Technology*, 3(2): 67-75. DOI:10.24191/mjcet.v3i2.10947

Muturi, E.J., Doll, K., Ramirez, J.L. & Rooney, A. P. (2019). Bioactivity of wild carrot (*Daucus carota*, Apiaceae) essential oil against mosquito larvae. *Journal of Medical Entomology*, 56(3): 784-789. DOI:10.1093/jme/tjy226

Nararak, J., Sathantripop, S., Kongmee, M., Mahiou-Leddet, V., Olliver, E., Manguin, S. & Chareonviriyaphap, T. (2019). Excito-repellent activity of β-caryophyllene oxide against *Aedes aegypti* and *Anopheles minimus*. *Acta Tropica*, 197: 105030. DOI:10.1016/j.actatropica.2019.05.021

Nascimento, A.M.D., Maia, T.D.S., Soares, T.E.S., Menezes, L.R.A., Scher, R., Costa, E.V., Cavalcanti, S.C.H. & La Corte, R. (2017). Repellency and larvicidal activity of essential oils from *Xylopia laevigata*, *Xylopia frutescens*, *Lippia pedunculosa*, and their individual compounds against *Aedes aegypti* Linnaeus. *Neotropical Entomology*, 46(2): 223-230. DOI:10.1007/s13744-016-0457-z

Navayan, A., Moghimipour, E., Khodayar, M.J., Vazirianzadeh, B., Siahpoosh, A., Valizadeh, M. & Mansourzadeh, Z. (2017). Evaluation of the mosquito repellent activity of nano-sized

microemulsion of *Eucalyptus globulus* essential oil against Culicinae. *Jundishapur Journal of Natural Pharmaceutical Products*, 12(4): e55626. DOI:10.5812/jjnpp.55626

Ojewumi, M.E., Obanla, O.R. & Atauba, D.M. (2021). A review on the efficacy of *Ocimum gratissimum*, *Mentha spicata*, and *Moringa oleifera* leaf extracts in repelling mosquito. *Beni-Suef University Journal of Basic and Applied Sciences*, 10(1): 87. DOI:10.1186/s43088-021-00176-x

Okpalaku, O., Uronnachi, E., Okoye, E., Umeyor, C., Nwakile, C., Okeke, T. & Attama, A. (2022). Evaluating some essential oils-based and coconut oil nanoemulgels for the management of rheumatoid arthritis. *Letters in Applied NanoBioScience*, 12(3): 75. DOI:10.33263/LIANBS123.075

Onyeyirichi, I., Ogechi, N., Oche, O., Jerry, U. & Gero, M. (2014). Evaluation of chemical constituent of *Citrus medica* Limonium leaf essential oil. *Journal of Pharmaceutical and Scientific Innovation*, 3(4): 306-309. DOI:10.7897/2277-4572.034161

Ostertag, F., Weiss, J. & McClements, D.J. (2012). Low-energy formation of edible nanoemulsions: Factors influencing droplet size produced by emulsion phase inversion. *Journal of Colloid and Interface Science*, 388(1): 95-102. DOI:10.1016/j.jcis.2012.07.089

Pang, X., Feng, Y., Qi, X., Xi, C. & Du, S. (2021). Acute toxicity and repellent activity of essential oil from *Atalantia guillauminii* Swingle fruits and its main monoterpenes against two stored product insects. *International Journal of Food Properties*, 24: 304-315. DOI:10.1080/10942912.2021.1876088

Saberi, A.H., Fang, Y. & McClements, D.J. (2013). Effects of glycerol on formation, stability, and properties of vitamin-E enriched nanoemulsions produced using spontaneous emulsification. *Journal of Colloid and Interface Science*, 411: 105-113. DOI: 10.1016./j.jcis.2013.08.041

Sales, A., Felipe, L. de O. & Bicas, J.L. (2020). Production, properties, and applications of α-terpineol. *Food and Bioprocess Technology*, 13(8): 1261-1279. DOI:10.1007/s11947-020-02461-6

Santiago, B., Moreira, M.T., Feijoo, G. & González-García, S. (2020). Identification of environmental aspects of citrus waste valorization into D-limonene from a biorefinery approach. *Biomass and Bioenergy*, 143: 105844. DOI:10.1016/j.biombioe.2020.105844

Shafiq, S., Shakeel, F., Talegaonkar, S., Ahmad, F. J., Khar, R.K. & Ali, M. (2007). Development and bioavailability assessment of ramipril nanoemulsion formulation. *European Journal of Pharmaceutics and Biopharmaceutics*, 66(2): 227-243. DOI:10.1016/j.ejpb.2006.10.014

Shafiq-un-Nabi, S., Shakeel, F., Talegaonkar, S., Ali, J., Baboota, S., Ahuja, A., Khar, R.K. & Ali, M. (2007). Formulation development and optimization using nanoemulsion technique: A technical note. *AAPS pharmscitech*, 8(2): E12-E17. DOI:10.1208/pt0802028

Tan, K., Faierstein, G.B., Xu, P., Barbosa, R.M.R., Buss, G.K. & Leal, W.S. (2019). A popular Indian clove-based mosquito repellent is less effective against *Culex quinquefasciatus* and *Aedes aegypti* than DEET. *PLOS ONE*, 14(11): e0224810. DOI:10.1371/journal.pone.0224810

Upadhyay, H., Juneja, A., Turabieh, H., Malik, S., Gupta, A., Bitsue, Z.K. & Upadhyay, C. (2022). Exploration of crucial factors involved in plants development using the fuzzy AHP method. *Mathematical Problems in Engineering*, 2022: 1-9. DOI:10.1155/2022/4279694

Venturini, N., Barboni, T., Curk, F., Costa, J. & Paolini, J. (2014). Volatile and flavonoid composition of the peel of *Citrus medica* L. var. corsican fruit for quality assessment of its liqueur. *Food Technology and Biotechnology*, 52(4): 403-410. DOI:10.17113/ftb.52.04.14.3717

WHO (World Health Organization). (2020, March). *Vector-borne diseases*.

Yen, P.-S. & Failloux, A.-B. (2020). A Review: Wolbachia-based population replacement for mosquito control shares common points with genetically modified control approaches. *Pathogens*, 9(5): 404. DOI: 10.3390/pathogens9050404

Zamakshshari, N.H., Ahmed, I.A., Didik, N.A.M., Nasharuddin, M.N.A., Hashim, N.M., & Abdullah, R. (2023). Chemical profile and antimicrobial activity of essential oil and methanol extract from peels of four *Durio zibethinus* L. varieties. *Biomass Conversion and Biorefinery*, 13(15): 13995-14003. DOI:10.1007/s13399-021-02134

Borneo Journal of Resource Science and Technology (2025), 15(1): 156-166
DOI: https:doi.org/10.33736/bjrst.7475.2025

Characterisation of Soilless Substrates Blended from Coco Peat and Burned Rice Husk via Particle Size Distribution Analysis

MOHD FAUZIE JUSOH*[1,2], MUHAMMAD FIRDAUS ABDUL MUTTALIB[1], NUR SAKINAH SAEDIN[1], CH'NG HUCK YWIH[2] & AYOB KATIMON[1]

[1]Faculty of Mechanical Engineering Technology, Universiti Malaysia Perlis, 02600 Arau, Perlis, Malaysia; [2]Faculty of Agro Based Industry, Universiti Malaysia Kelantan, Jeli Campus, Locked Bag No 100, 17600 Jeli, Kelantan, Malaysia

*Corresponding authors: fauzie.j@umk.edu.my
Received: 27 July 2024 Accepted: 10 February 2025 Published: 30 June 2025

ABSTRACT

Soilless media is widely employed in modern agriculture to facilitate efficient water management, enhance nutrient uptake, and mitigate soil-borne diseases. When different soilless media are blended in varying compositions, their physical and hydrological properties change, directly impacting crop yield and growth performance. Understanding the combination effect of coco peat (CP) and burn rice husk (BRH) concerning particle size distribution suitability for the potting medium is essential. This study aims to evaluate the particle size distribution of blended soilless substrates composed of CP and BRH at various compositions. The analysis of variance (ANOVA) test was deployed to assess significant differences between particle sizes among the treatments. Particle distribution curves were further analysed for particle diameter at selected cumulative mass distribution, median, standard deviation, mass relative span, kurtosis and skewness. Results indicated that most samples consist of fines and medium particle size, positive fine skewed, and signified by mesokurtic and leptokurtic. The combination of CP and RBH at different ratios has changed the coarse (> 2.3 mm), medium (2.3 to 0.6 mm) and fine (< 0.6 mm) particle size composition. This study demonstrated that the combination of CP and BRH improved particle distribution size by increasing the medium and fine-size particles. This finding provides valuable information on physical changes in particle size due to the blend of CP and BRH for potting soilless media. Understanding soilless media characteristics would guide farmers in managing better irrigation practices for precision irrigation or IoT smart farming for optimum agricultural production.

Keywords: Burn rice husk, coco peat, particle size, sieve analysis, soilless

INTRODUCTION

Soilless substrate cultivation in agriculture refers to planting crops without soil as growing media. It is reported that 3.5% of the crop production in the world utilised soilless media as cultivation media (Joshi *et al*., 2022). The soilless substrate as growing media has been applied by modern farmers since around 40 years ago (Gruda, 2022), where soilless cultivation practice saves irrigation water, eases plant nutrition monitoring and increases crop production (Joshi *et al*., 2022). With the rapid advancement of nanotechnology, soilless substrates have been enhanced and enriched for the production of nanoproducts, as well as amended with biochar to increase their value (Igiebor *et al*., 2023; Gruda, 2020; Huang & Gu, 2019). In horticulture, soilless media is commonly used in two forms: either in solid media, such as coco peat, vermiculite, perlite, pine bark, sawdust, gravel, and rockwool, or in liquid systems (nutrient film technique, deep water culture, deep flow technique, aeroponic, and wicking). The application of soilless media in horticulture can enhance sustainability and promote the optimum use of agricultural waste production (Gruda, 2020).

The irrigated agriculture sector is facing pressure due to global water scarcity. It is estimated that approximately 1.2 billion people live in areas of physical scarcity, while another 1.6 billion faces economic water scarcity (Zhu & Wang, 2013). The shortage and limitation of water

resources for irrigation and the lack of a clear understanding of the properties of soilless media have decreased water use efficiency and crop water productivity (Kanda *et al*., 2020). A comprehensive and intensive knowledge of the particle size distribution and soilless substrate properties is vital in designing and managing irrigation systems to maximise crop water use efficiency and water productivity. Enhancing water use efficiency in crops requires assessing a substrate's ability to retain and release water for plant use (Fields *et al*., 2014).

Coco peat (CP) is a relatively new growing medium (Duggan-Jones *et al*., 2013), and it has been produced and applied in modern agriculture for soilless media worldwide. Although coco peat have almost the same microstructure regardless of their country of production, their particle size and physical properties vary (Fornes *et al*., 2003; Duggan-Jones *et al*., 2013). Coco peat is characterised by low hydraulic conductivity (0.1 cm/s) and low bulk density (0.09 g/cm^3), but its water-holding capacity is high as 912.54% (Yahya *et al*., 1997; Ilahi & Ahmad 2017). Due to these properties, it can hold the water for longer. Burn rice husk (BRH) is a biochar produced from the pyrolysis process and is another alternative for soilless media (Jusoh *et al*., 2021). The CP and BRH are agricultural wastes that are widely available in Malaysia since paddy and coconut are among the essential major crops in Malaysia. It is estimated that the area cultivated with paddy and coconut in Malaysia in 2020 is 644,854 hectares and 84,942 hectares, respectively (Department of Agriculture, 2021).

Fornes *et al*. (2017) reported that variations in biochar particle size did not alter its chemical properties or microporosity but significantly affected its water-holding capacity. The biochar's pH and electrical conductivity ranges are still within the acceptable tolerance for plant-growing substrates (León-Ovelar *et al*., 2022). Biochar can also be used as a soil amendment in growing media to change the substrate's physical properties by reducing the larger-sized components and altering the chemical properties of the substrate (Huang & Gu, 2019; Jahromi *et al*., 2020). In Malaysia, past research was carried out, and soilless media was used to test the crop in the field. Among the crops tested are chilli (Berahim *et al*., 2016; Zakaria *et al*., 2020), Misai Kucing (Ya'Acob *et al*., 2021), tomato (Ali *et al*., 2003a, 2003b; Mahamud & Manisah, 2007), vegetables (Ismail *et al*., 2004; Ismail & Ann, 2004) and rice (Samsuddin *et al*., 2014). However, various soilless media were used, such as coconut coir dust, sago waste, rice straw compost and empty fruit bunch compost. As Duggan-Jones, Nichols, and Woolley (2013) mentioned, particle size distribution's impact on agricultural productivity involving various soilless media and their combination in different ratios is poorly understood.

Although the literature reports the application of various soilless media, there is still a dearth of knowledge and paucity of data on the possibilities of coco peat, burn rice husk and their combination to create appropriate potting media for the production of horticulture crops in the Asian region. We hypothesised that different combinations of CP and BRH could change the particle distribution size of soilless media and hence change the soilless media properties. This study aimed to characterise the particle size distribution of the blended soilless substrate from CP and BRH at different compositions. In addition, this study sought to answer the questions: a) What is the characteristic of blended soilless media on percent finer and volumetric distribution subjected to particle size separation and b) What is the effect of leaving oven-dried soilless media on its weight.

MATERIALS & METHODS

The study was conducted at the Process Laboratory Unit, Faculty of Chemical Engineering Technology, Universiti Malaysia Perlis, Arau, Perlis, Malaysia (6º26'27" N, 100º13'59'' E). The experiment was conducted in July 2022.

Soilless Media Preparation

The CP and BRH were supplied by Pertubuhan Peladang Titi Tinggi (Padang Besar, Perlis) and Nurain Athirah Company (Ayer Hitam, Kedah), respectively. Before application, CP was screened

and passed through a 3.5 x 0.5 cm sieve at the initial level to separate CP from coco coir and debris. CP and BRH were air-dried for at least seven days under a rainhouse shelter to reduce moisture. CP and BRH were used in this study since both soilless media are common and readily available to Malaysian farmers in tropical countries (Shanmugasundaram *et al*., 2014). The mixture or composition of the treatments was based on dry weight, and the detailed description is shown in Table 1.

Table 1. The composition of the treatments

Treatment	Media Compositions
1	100% Coco peat
2	100% Burn Rice Husk
3	50% Coco peat + 50% Burn Rice Husk
4	30% Coco peat + 70% Burn Rice Husk
5	70% Coco peat + 30% Burn Rice Husk

Particle Size Determination and Data Analysis

The particle size of the soilless samples (T1, T2, T3, T4 and T5) was analysed using a 2.5 horsepower automatic sieve shaker (NL Scientific, Model NL 1015X/005, Malaysia). The procedures of particle size distribution were based on EN 15428 (2007). Before sieving, the samples were oven dried at 105 ^{o}C for 72 hours using a drying oven (Binder, Model FD 115, Germany). The oven-dried moisture content of the samples was calculated based on Equation 1, (Eq. 1).

$$\text{Moisture Content (\%)} = \frac{(\text{Wet Weight Sample-Dried Weight Sample})}{\text{Dried Weight Sample}} \times 100 \quad \text{Eq. (1)}$$

A set of 10 individual woven sieves with stainless steel frames, excluding pan with the size of 10, 5, 2.3, 1.18, 0.6, 0.3, 0.25, 0.15, 0.075, and 0.025 mm, were stacked with the larger opening diameter on the top and smaller diameter on the bottom. The pan was positioned at the lowest part of the sieve arrangement to collect the finest particles. The automatic sieve shaker was set to shake for 5 minutes, and all samples were repeated thrice, as suggested by Bartley *et al*. (2022). The weight of the empty sieve and soil retained in each sieve at two decimal places were measured using a digital balance (Kern, Model 572-39, Germany). The total mass of the initial and final samples should be nearly identical, where a loss of more than 2% is considered unsatisfactory. The sieving process is repeated if the sample loss exceeds 2%. Before beginning of a new sieving process and reweighing the sieves, they were meticulously cleaned three times: first using a brush, followed by empty sieving with a mechanical shaker, and finally, another thorough brushing before their subsequent use in the sieving operation.

The percent finer for each sample was plotted against aperture size on the semi-logarithmic scale to obtain a respective particle size distribution. The semi-logarithmic scale was applied to the aperture size to ease the reading of smaller particle sizes. The mass relative span (MRS) was calculated using Equation 2 (Eq. 2). The median was measured as the distribution at D_{50}. Standard deviation (SD) was measured using Equation 3 (Eq. 3). Skewness (SK) and kurtosis (KU) represented distribution shape and were formulated in Equation 4 (Eq. 4) and Equation 5 (Eq. 5), respectively. The D_5, D_{10}, D_{16}, D_{25}, D_{50}, D_{75}, D_{84}, D_{90} and D_{95} are the particle diameters (in mm) at 5%, 10%, 16%, 25%, 50%, 75%, 84%, 90% and 95% of the cumulative mass distribution respectively calculated from particles distribution curve.

$$MRS = \frac{(D_{90} - D_{10})}{D_{50}} \quad Eq. (2)$$

$$SD = D_{84} - \left(\frac{D_{16}}{2}\right) \quad Eq. (3)$$

$$SK = \frac{D_{16} + D_{84} - 2D_{50}}{2(D_{84} - D_{16})} + \frac{D_5 + D_{95} - 2D_{50}}{2(D_{95} - D_5)} \quad Eq. (4)$$

$$KU = \frac{D_{95} - D_5}{2.44\,(D_{75} - D_{25})} \quad Eq. (5)$$

In a separate experiment, the soilless samples were placed in a plastic container of 11 cm diameter and 5 cm height with three replications to observe the weight changes of dried soilless media. All the samples were arranged in a completely randomised design with three replications and placed into the trays at room temperature. The weight measurement was made at 10:00 a.m. daily for seven days. The container was loosely covered with a lid to prevent media losses caused by wind.

Statistical Analysis

One-way analysis of variance (ANOVA) test via SPSS software Version 25 was deployed to assess significant differences between particle sizes. The Duncan Multiple Range Test was carried out for mean comparison at p=0.05 if significant differences were detected from the ANOVA model. A paired sample T-test was also conducted to compare the mean volume and weight of soilless media before and after sieving work. The descriptive analysis reported in this study was based on the selected parameters suggested by Bartley *et al*. (2022).

RESULTS & DISCUSSION

Figure 1 illustrates particle distribution curves of the different soilless media compositions. The particle size distribution curve describes the sample percentage that passes through each selected sieve size. Most tested samples retained the middle-range sieve size, whereas some retained the finer size. Single BRH has the highest fine particle percentage, whereas CP has the highest percentage of coarse particles. Regarding uniformity, single BRH samples are uniformly graded soilless media that can be noticed from steeper curves compared to the other treatments. Conversely, a single CP sample consisted of more particle size heterogeneity where the distribution curve is broader compared to other treatments. From this study, adding BRH increases the medium and fine particle size percentage, where it can be observed that the combined ratio treatment curves have shifted between the single CP and single BRH curves.

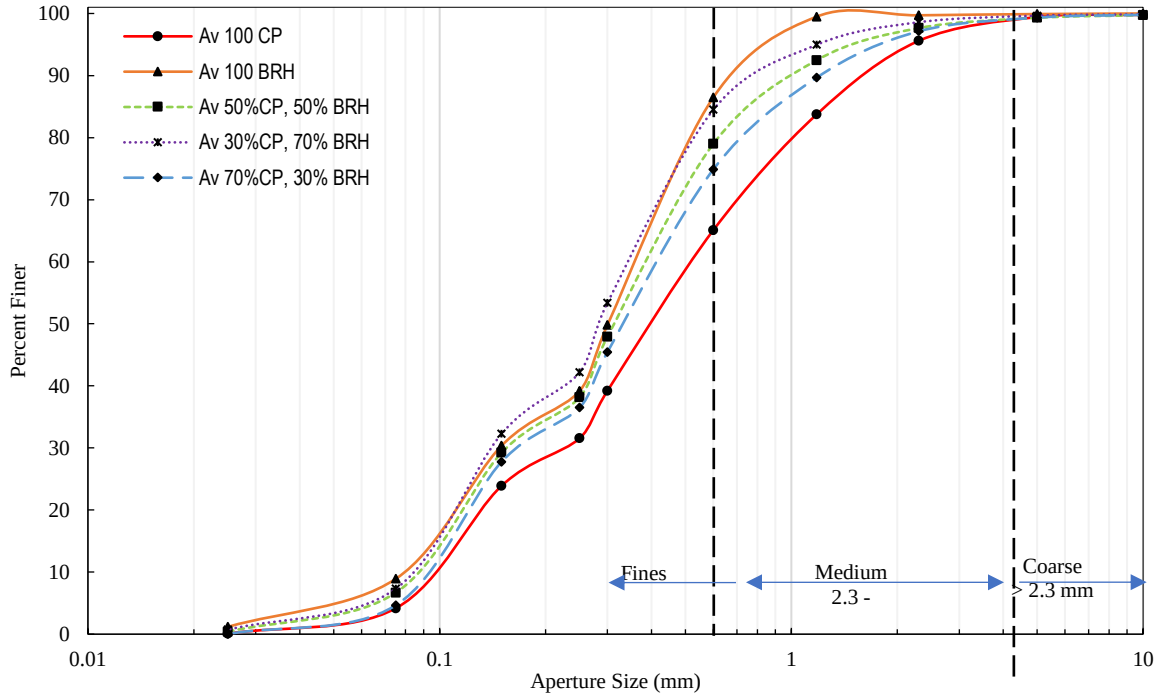

Figure 1. Particle distribution curve of soilless media based on average (av) samples replication. The vertical dash lines separate the aperture size according to categories

Table 2. Descriptive statistics and selected particle size diameter from particle distribution curve

Parameters	Treatment				
	T1	T2	T3	T4	T5
D_5 (mm)	0.079±0.002 ^{a}	0.050±0.001^{b}	0.065±0.002^{c}	0.063±0.001^{c}	0.075±0.001^{a}
D_{10} (mm)	0.098±0.001^{a}	0.080±0.000^{b}	0.087±0.002^{c}	0.084±0.001^{c}	0.092±0.001^{d}
D_{16} (mm)	0.127±0.003^{a}	0.100±0.000^{b}	0.113±0.003^{cd}	0.106±0.004^{bc}	0.120±0.000^{ad}
D_{25} (mm)	0.167±0.007^{a}	0.137±0.003^{b}	0.137±0.003^{b}	0.133±0.003^{b}	0.153±0.003^{c}
D_{50} (mm)	0.393±0.009^{a}	0.303±0.003^{b}	0.310±0.006^{b}	0.287±0.003^{c}	0.330±0.000^{d}
D_{75} (mm)	0.827±0.017^{a}	0.480±0.000^{b}	0.537±0.009^{c}	0.477±0.003^{b}	0.600±0.010^{d}
D_{84} (mm)	1.267±0.033^{a}	0.563±0.003^{b}	0.707±0.017^{c}	0.587±0.007^{b}	0.863±0.022^{d}
D_{90} (mm)	1.667±0.033^{a}	0.670±0.010^{b}	1.030±0.085^{c}	0.750±0.017^{b}	1.300±0.000^{d}
D_{95} (mm)	2.267±0.176^{a}	0.813±0.007^{b}	1.500±0.100^{cd}	1.267±0.033^{c}	1.767±0.033^{d}
SD	1.203±0.034^{a}	0.513±0.003^{b}	0.650±0.015^{c}	0.5343±0.006^{b}	0.803±0.022^{d}
MRS	3.992±0.117^{a}	1.945±0.029^{b}	3.035±0.221^{c}	2.324±0.067^{d}	3.661±0.002^{a}
SK	0.600±0.013^{a}	0.218±0.006^{b}	0.474±0.015^{c}	0.418±0.005^{d}	0.542±0.008^{e}
KU	1.356±0.089^{a}	0.912±0.017^{b}	1.470±0.086^{a}	1.436±0.036^{a}	1.554±0.058^{a}

The values are represented as mean ± standard error. The values with different superscript letters in the same row represent significant differences ($p < 0.05$). T1 is 100% Coco peat, T2 is 100% Burn Rice Husk, T3 is 50% Coco peat + 50% Burn Rice Husk, T4 is 30% Coco peat + 70% Burn Rice Husk, T5 is 70% Coco peat + 30% Burn Rice Husk, SD is standard deviation, MRS is Mass Relative Span, SK is skewness, and KU is kurtosis. D_5, D_{10}, D_{16}, D_{25}, D_{50}, D_{75}, D_{84}, D_{90} and D_{95} are the particle diameters in mm at 5%, 10%, 16%, 25%, 50%, 75%, 84%, 90% and 95% of the cumulative mass distribution respectively.

The combination between CP and BRH resulted in the diversity of particle size composition. The particle sizes of soilless substrate were categorised into three groups, which are coarse particle size (> 2.3 mm), medium particle size (2.3 to 0.6 mm) and fines particle size (< 0.6 mm).

More parameters were extracted from the particle distribution curve to understand the tested samples further and get more detailed information. Table 2 summarises the descriptive statistics and selected particle size diameter of the samples. The single CP and BRH have differed significantly regardless of their particle size diameters (D_5 until D_{95}). Their particle diameter sizes also varied, where CP had a particle size diameter range between 0.079 and 2.267 mm while BRH ranged between 0.050 and 0.813 mm. The composition of CP and BRH at the same level (T3) showed that particle size diameter at around median size (D_{25} and D_{50}) is not significant compared to the single composition of BRH. Inversely, the smaller (D_5 until D_{16}) and higher (D_{75} until D_{95}) particle size diameters showed significant differences compared to the single composition of BRH. At median size (D_{50}), both T4 and T5 significantly differ from single CP and single BRH, indicating that all treatments consist of various particle sizes at the median point. T4 showed almost no significant difference at the fine and medium size compared to single BRH, where it inherits the particle size distribution nearly the same as single BRH. The bigger portion of CP in T5 makes it differ significantly at medium size instead of finer size.

The standard deviation (SD) indicated a significant difference between T1, T3 and T5. However, no differences in SD values in T2 and T4. As the proportion of BRH increased, the soilless media showed a deviation in particle size from a single CP. The mass relative span (MRS) for T1 and T5 was insignificant, whereas MRS for T2, T3 and T4 differed significantly. The magnitude of MRS is an indicator of distribution width (Bitra *et al*., 2009). An increasing proportion of BRH increased the SD and MRS values of the soilless media. It is reasonable and parallel to the effective size parameter (D_{10}), where adding fine-size particles gives significant effective size values except for minor changes in T3 & T4. The effective size for all samples indicated that 10% of the particle size of soilless media is smaller than 0.08 mm, and 90% is larger than 0.08 mm. Based on Boggs (2009) classification, the soilless media from T2, T3, and T5 were identified as moderately well-sorted, while T5 and T1 were classified as moderately sorted and poorly sorted, respectively. Lower values of SD and MRS generally suggest a more uniform and well-graded particle size distribution, which is often preferred for consistent and predictable media properties.

All soilless media yielded strongly fine skewed (SK >+0.3) except T2, which was classified as fine skewed. The mean skewness showed a significant difference for all treatments, and T1 had the highest skewness value. Lowering the CP proportion shifted the soilless media towards a fine-skewed characteristic due to the availability of a finer texture. Interestingly, lowering CP in the soilless media composition did not result in a significant difference in mean kurtosis (KU), as shown in T1, T3, T4, and T5. The KU value of T2 differs significantly compared to others. KU signifies the sharpness or peakedness of a grain size distribution curve. Single BRH (T2) was classified as "mesokurtic" since the KU value was 0.912, indicating a normal particle size distribution. Soilless media of T1, T3 and T4 were classified as "leptokurtic" since KU values varied between 1.356 and 1.554. The result indicates that "leptokurtic" soilless media had positive kurtosis where particle size is distributed larger at the tail, and the tail is fatter than the normal distribution curve. Determining skewness, kurtosis, and leptokurtic characteristics is important for understanding particle size distribution and its impact on the physical properties of soilless media. Fine-skewed media indicates that most particles are smaller, which can affect water retention and drainage. Such distributions may help retain more water, benefiting plants that require a consistent moisture supply. In the context of soilless media, leptokurtic distributions suggest a predominance of certain particle sizes, which can help create consistent air spaces and ensure predictable water movement. Media with leptokurtic characteristics may provide stable physical properties, reducing the risk of waterlogging or excessive drying. This stability is especially beneficial for young plants or seedlings that need consistent moisture levels.

Table 3. Comparison between volume and weight before and after sieving

Treatment	Volume (mL)		Weight (g)	
	Before Sieving	After Sieving	Before Sieving	After Sieving
T1	1183.33±16.67^{a}	1514.10±9.61^{b}	100.26±0.08^{a}	100.42±0.19^{a}
T2	780.00±0.00^{a}	894.40±8.96^{b}	100.36±0.10^{a}	100.48±0.05^{a}
T3	810.00±20.82^{a}	972.17±40.30^{b}	100.48±0.21^{a}	100.53±0.14^{a}
T4	746.67±20.28^{a}	916.00 ± 8.79^{b}	100.19 ± 0.10^{a}	100.34 ± 0.05^{a}
T5	916.67 ± 12.02^{a}	1192.87 ± 42.45^{b}	100.27 ± 0.04^{a}	100.51 ± 0.17^{a}

The volume and weight values are displayed as mean ±standard error. The values with different superscript letters in the same row represent significant differences at the 95% confidence interval. T1 is 100% Coco peat, T2 is 100% Burn Rice Husk, T3 is 50% Coco peat + 50% Burn Rice Husk, T4 is 30% Coco peat + 70% Burn Rice Husk, T5 is 70% Coco peat + 30% Burn Rice Husk.

Adding BRH could increase water-holding capacity by increasing micropore space between soilless media particles (Gonnella & Renna, 2021). The particle size distribution indicates that adding BRH increases the medium and fine particle size percentage where the combination ratio treatment curves have shifted between the CP and BRH curves. As explained by Altland *et al*. (2018) and Fields *et al*. (2018), manipulation of soilless properties is possible by mixing different types of soilless media. The properties of soilless media, such as available water, air space, bulk density, total porosity, container capacity, nutrient availability, pH, electrical conductivity, microbial activities and cation exchange capacity, deviate from its original conditions (Gabriel *et al*., 2009; Huang & Gu, 2019). This result also indicated that although all the samples have a particle size smaller than 2.0 mm, they are composed of various fine particle sizes. The suitable particle size of soilless media is between 0.25 and 0.5mm (CANNA, 2021).

Volumetric analysis is one of the alternative presentations of soilless media, which can give more explicit pictures of the tested samples (Albaghdady & Alabadi, 2021). Figure 2 presents the distribution of soilless volume and weight based on their respective aperture size. All treatments have the highest volume and weight at the particle size of 0.3 mm. Table 3 shows the volume and weight comparison before and after the sieve analysis. A Paired samples t-test was performed to determine the effect of sieving on volume and weight changes of soilless media. The results indicate a significant difference between the original and after-sieving volumes.

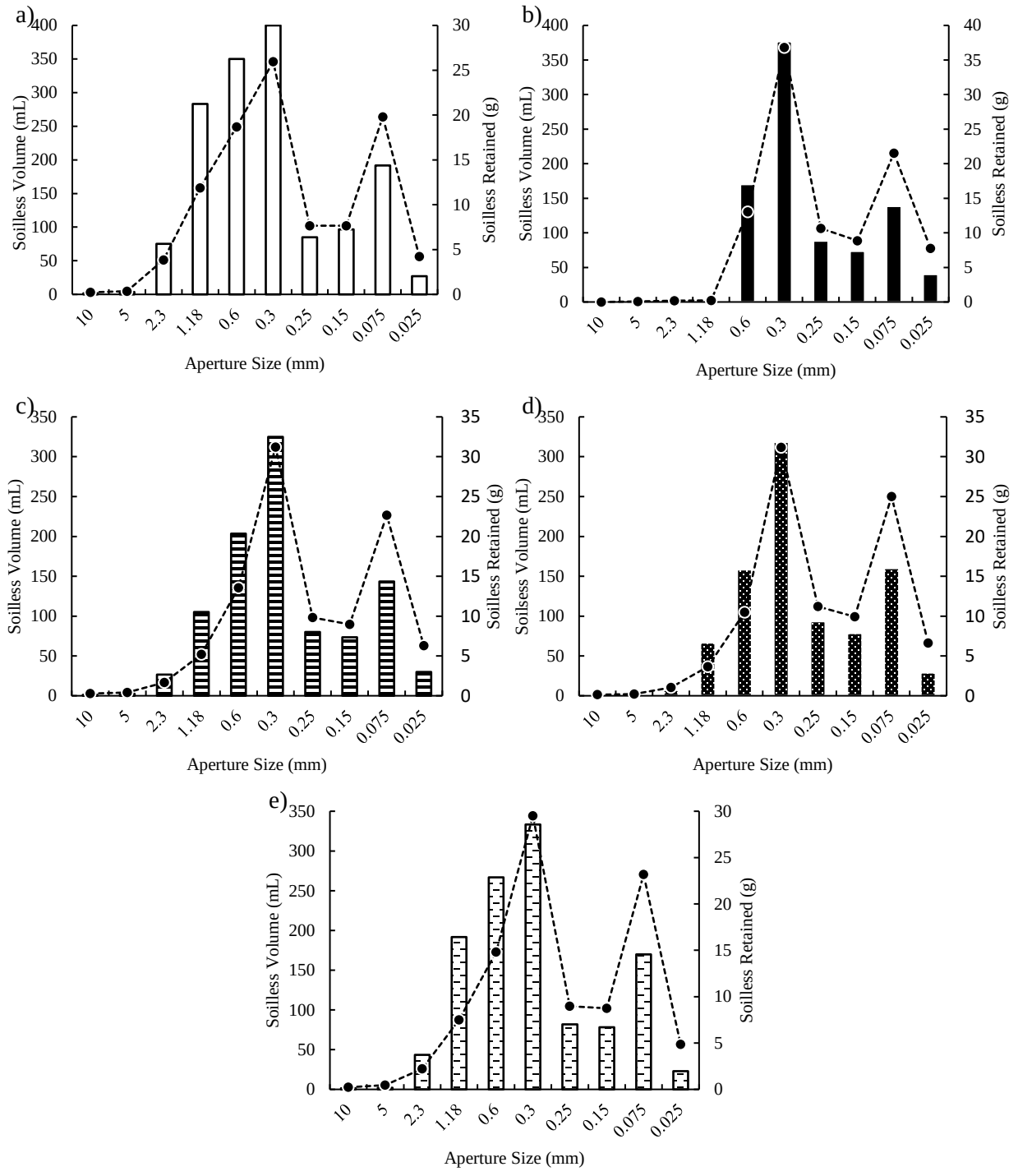

Figure 2. The volume of soilless media in individual sieve aperture size for a) T1-100% CP, b) T2- 100% BRH, c) T3-50% CP & 50% BRH, d) T4-30% CP& 70% BRH, and e) T5-70% CP& 30%BRH. The bar shows the soilless volume (mL), while the dashed line represents the weight of soilless retained (g)

However, no significant difference was detected between weight values before and after sieving.

Although the weight of the samples has no changes in their magnitude before and after the sieving process, the volume of the sample might change significantly. Similarly, the same result was reported by Zazirska *et al*. (2021), where there were statistical differences in particle size distribution in volumetric distribution. By separating particle sizes according to their respective size, the volume of soilless media has increased between 14 and 30%. The lowest and highest increment volumes were detected in single BRH (T2) and 70% coco peat + 30% burn rice husk (T5), respectively. It can be understood that if the proportion of BRH decreases while the ratio of CP increases in a soilless container in dry condition, the volume of soilless media will automatically increase. This is due to the larger coarse particle size of CP, which occupies more space. BRH has almost fine particles, so the volume change is small.

Observation of weight changes of the oven-dried samples for seven days is shown in Figure 3. The range of weight changes of the samples generally varies between 0 and 3%. The weight change trends for combination mixtures (T3, T4 and T5) showed increasing trends up to day four of air drying. After day four, they showed slightly decreasing trends at the constant level. Coco peat media (T4) showed a steady and stable increase in moisture during observation. However, T2, which is 100% BRH, showed different pattern trends of weight changes compared to other treatments. The T2 samples became drier until day four, and the weight changes remained constant (± 0.5). The result indicates that fully CP media can absorb moisture from the air, which causes its weight to increase slightly. However, full BRH showed the opposite result compared to other treatments. BRH media showed almost constant weight, and the air could make the BRH somewhat drier than it was in its initial condition, which is indicated by deficit weight changes.

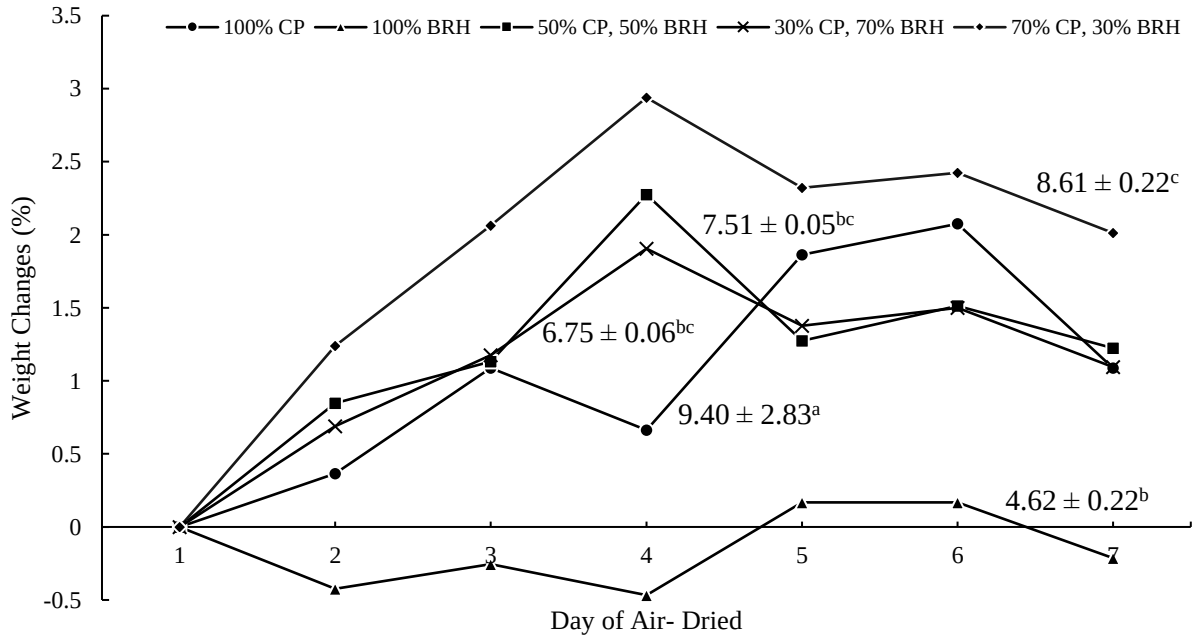

Figure 4. Weight changes of oven-dried samples after seven days of air drying. Mean ± SD with a different letter at the graph line are significantly different at $p<0.05$

Although this study provides valuable information on the particle distribution curve, especially for combination or mixture between CP and BRH, it lacks related information on neither the physical nor chemical characteristics of the tested soilless media. This study is limited and valid for clean coco peat since we screened the coco peat from coconut coir and debris before use. In real situations, the coco peat received by the farmer might not be clean, or low quality since the production of coco peat and quality control vary between factories. Deploying different soilless media in horticulture might not affect crop yield but saves irrigation water (Elakiya & Arulmozhiselvan, 2024; Gruda, 2022).

CONCLUSION

This study used the particle size distribution analysis via mechanical sieve analysis to characterise the soilless substrate from coco peat, burn rice husk and its combination. This study scrutinised the effects of mixing coco peat and burn rice husk on the particle distribution curve of soilless media for pot planting. Results have demonstrated that a single coco peat has a heterogeneous particle size distribution, whereas a single burn rice husk is more homogenous in its particle size distribution. Blending coco peat and burn rice husk at different compositions resulted in a shifting particle distribution curve between a single coco peat and burn rice husk. However, all soilless media treatments consist of a major proportion of fines to medium size, which is suitable for growing media. The combination of different media will change the particle size distribution and hence expected to alter the physical, hydrological, chemical, and biological properties of manipulated soilless media. In addition, the high proportion of coco peat (70%) in a mixture sample of soilless media that air dried for more than seven days produced significant weight loss compared to other treatments. This study provides beneficial information on the fundamentals of precision irrigation for crops planted in the soilless substrate. Future research should explore the long-term effects of different coco peat and burned rice husk blends on crop performance, including factors such as water use efficiency, nutrient retention, and root growth. Given that sensor-based moisture measurements often require soil-specific calibration, further studies should assess the suitability of these soilless media for accurate moisture monitoring to ensure precise irrigation control. Additionally, it is recommended to study the chemical properties of these blends to better understand how they interact with plant nutrient uptake.

ACKNOWLEDGEMENT

This study was funded by the Fundamental Research Grant Scheme (FRGS/1/2021/WAB04/UNIMAP/02/1). This study was also supported by Skim Latihan Akademik Bumiputera (474/2019/8). Ministry of Higher Education Malaysia awarded both grants.

REFERENCES

Albaghdady, S.N.S. & Alabadi, L.A.S. (2021). Grain size analysis of sand fractions and the sedimentary environment of selected soil samples from southern and northern Iraq. *Malaysian Journal of Chemistry*, 23(4): 77–88. DOI:10.13140/RG.2.2.10490.47047

Ali, H.I., Ismail, M.R., Manan, M.M. & Saud, H.M. (2003a). Effect of rice straw compost under normal and stressful condition on quality of tomatoes grown in two different media. *Ecology, Environment and Conservation*, 9(4): 533–536.

Ali, H.I., Ismail, M.R., Manan, M.M. & Saud, H.M. (2003b). Rice straw compost used as soilless media for organic tomato transplant production. *Asian Journal of Microbiology, Biotechnology and Environmental Sciences*, 5(1): 31–36.

Altland, J.E., Owen, J.S., Jackson, B.E. & Fields, J.S. (2018). Physical and hydraulic properties of commercial pine-bark substrate products used in production of containerized crops. *HortScience*, 53(12): 1883–1890. DOI:10.21273/HORTSCI13497-18

Bartley, P.C., Fonteno, W.C. & Jackson, B.E. (2022). A review and analysis of horticultural substrate characterization by sieve analysis. *HortScience*, 57(6): 715–725. DOI:10.21273/hortsci16583-22

Berahim, Z., Salamat, S.S., Razak, N.A., Megat Wahab, P.E. & Ismail, M.R. (2016). Efficiency of fertilizer formulation, stock solution volume and media on chili (*Capsicum annum* kulai F1). *Journal of Plant Nutrition*, 39(11): 1570–1577. DOI:10.1080/01904167.2016.1161776

Bitra, V.S.P., Womac, A.R., Cannayen, I., Miu, P.I., Yang, Y.T. & Sokhansanj, S. (2009). Comminution energy consumption of biomass in knife mill and its particle size characterization. *American Society of Agricultural and Biological Engineers Annual International Meeting*, 3(June). DOI:10.13031/2013.26987

Boggs, J.S. (2009). Petrology of Sedimentary Rock. In *Cambridge University Press*. Cambridge University Press.

CANNA. (2021). *What makes a good-quality soilless growing medium*. https://www.canna.ca/articles/what-makes-good-quality-soilless-growing-medium

Department of Agriculture. (2021). Booklet statistik tanaman (sub-sektor tanaman makanan) 2021. In *Kementerian Pertanian & Industri Makanan*. www.doa.gov.my

Duggan-Jones, D.I., Nichols, M.A. & Woolley, D.J. (2013). Effect of physical characteristics of coir on the productivity of greenhouse tomatoes. In W. Zhu & Q. Li (eds.), *In International Symposium on Soilless Cultivation 1004*.pp. 101–106.

EN 15428. (2007). *Soil improvers and growing media - Determination of particle size distribution*. EN 15428. European Committee for Standardization, Brussels, Belgium.

Elakiya, N. & Arulmozhiselvan, K. (2024). Effective media validation, benefits and costs for achieving high yield in Ribbed gourd in soilless culture under matric suction irrigation. *Journal of Advances in Biology & Biotechnology*, 27(8): 416-432.

Fields, J.S., Fonteno, W.C., Jackson, B.E., Heitman, J.L. & Owen, J.S. (2014). Hydrophysical properties, moisture retention, and drainage profiles of wood and traditional components for greenhouse substrates. *HortScience*, 49(6): 827–832. DOI:10.21273/HORTSCI.49.6.827

Fields, J.S., Owen, J.S., Altland, J.E., van Iersel, M.W. & Jackson, B.E. (2018). Soilless substrate hydrology can be engineered to influence plant water status for an ornamental containerized crop grown within optimal water potentials. *Journal of the American Society for Horticultural Science*, 143(4): 268–281. DOI:10.21273/JASHS04251-17

Fornes, F., Belda, R.M., Abad, M., Noguera, P., Puchades, R., Maquieira, A. & Noguera, V. (2003). The microstructure of coconut coir dusts for use as alternatives to peat in soilless growing media. *Australian Journal of Experimental Agriculture*, 43(9): 1171–1179. DOI:10.1071/EA02128

Fornes, F., Belda, R.M., Córdova, P.F. & Cebolla-Cornejo, J. (2017). Assessment of biochar and hydrochar as minor to major constituents of growing media for containerized tomato production. *Journal of the Science of Food and Agriculture*, 9(11): 3675–3684. DOI:10.1002/jsfa.8227

Gabriel, M.Z., Altland, J.E. & Owen, J.S. (2009). The effect of physical and hydraulic properties of peatmoss and pumice on douglas fir bark based soilless substrates. *HortScience*, 44(3): 874–878. DOI:10.21273/hortsci.44.3.874

Gonnella, M. & Renna, M. (2021). The evolution of soilless systems towards ecological sustainability in the perspective of a circular economy. Is it really the opposite of organic agriculture? *Agronomy*, 11(5): 950. DOI:10.3390/agronomy11050950

Gruda, N.S. (2020). Increasing sustainability of growing media constituents and stand-alone substrates in soilless culture systems. *Agronomy*, 10(9): 1–24. DOI:10.3390/agronomy10091384

Gruda, N.S. (2022). Advances in soilless culture and growing media in today's horticulture - An editorial. *Agronomy*, 12(11): 10–15. DOI:10.3390/agronomy12112773

Huang, L. & Gu, M. (2019). Effects of biochar on container substrate properties and growth of plants—a review. *Horticulturae*, 5(1): 1–25. DOI:10.3390/horticulturae5010014

Igiebor, F.A., Asia, M. & Ikhajiagbe, B. (2023). Green nanotechnology: A modern tool for sustainable agriculture – a review. *International Journal of Horticultural Science and Technology*, 10(4): 269–286.

Ilahi, W.F.F. & Ahmad, D. (2017). A study on the physical and hydraulic characteristics of coco peat perlite mixture as a growing media in containerized plant production. *Sains Malaysiana*, 46(6): 975–980. DOI:10.17576/jsm-2017-4606-17

Ismail, M.R. & Ann, L.J. (2004). Effect of root cooling and shading on growth and yield of tropical cauliflower (*Brassica oleraceae* var. Botrytis) in coconut coir dust culture. *Acta Horticulturae*, 644: 269–274. DOI:10.17660/ActaHortic.2004.644.36

Ismail, M.R., Sze, L.Y., Poulus, P. & Ibrahim, H. (2004). The use of empty oil palm fruit bunch (EFB) compost as additive in coconut dust soilless system for vegetable crop production. *Acta Horticulturae*, 644: 193–198. DOI:10.17660/ActaHortic.2004.644.25

Jahromi, N.B., Fulcher, A., Walker, F. & Altland, J. (2020). Photosynthesis, growth, and water use of *Hydrangea paniculata* 'Silver Dollar' using a physiological-based or a substrate physical properties-based irrigation schedule and a biochar substrate amendment. *Irrigation Science*, 38(3): 263–274. DOI:10.1007/s00271-020-00670-7

Joshi, D., Nainabasti, A., Bhandari, R., Awasthi, P., Banjade, D., Malla, S. & Subedi, B. (2022). A review on soilless cultivation: The hope of urban agriculture. *Archives of Agriculture and Environmental Science*, 7(3): 473–481. DOI:10.26832/24566632.2022.0703022

Jusoh, M.F., Xin, L.J., Ywih, C.H., Abdullah, P.S., Radzi, N.M., Zainol Abidin, M.A. & Abdul Muttalib, M.F. (2021). Effect of wood vinegar and rice husk biochar on soil properties and growth performances of immature kenaf (*Hibiscus cannabinus*) planted on BRIS soil. *Journal of Tropical Resources and Sustainable Science*, 9(1): 48–57. DOI:10.47253/jtrss.v9i1.709

Kanda, E.K., Niu, W., Mabhaudhi, T. & Senzanje, A. (2020). Moistube irrigation technology: A review. *Agricultural Research*, 9(2): 139–147. DOI:10.1007/s40003-019-00448-0

León-Ovelar, R., Fernández-Boy, M. E. & Knicker, H. (2022). Characterization of the residue (endocarp) of *Acrocomia aculeata* and Its biochars as a potential source for soilless growing media. *Horticulturae*, 8(8): 739. DOI:10.3390/horticulturae8080739

Mahamud, S. & Manisah, M.D. (2007). Preliminary studies on sago waste as growing medium for tomato. *Acta Hortic*, 742: 163–168. DOI:10.17660/ActaHortic.2007.742.21

Samsuddin, M. F., Mohd Saud, M. H., Ismail, M. R., Omar, M. H., Habib, S. H., Bhuiyan, M. S. H., & Kausar, H. (2014). Effect of different combinations of coconut coir dust and compost on rice grown under soilless culture. *Journal of Food, Agriculture and Environment*, 12(2): 1280–1283.

Shanmugasundaram, R., Jeyalakshmi, T., Mohan, S.S., Saravanan, M., Goparaju, A. & Murthy, P.B. (2014). Coco peat - An alternative artificial soil ingredient for the earthworm toxicity testing. *Journal of Toxicology and Environmental Health Sciences*, 6(1): 5–12. DOI:10.5897/jtehs2013.0289

Ya'Acob, M.E., Othman, N.F., Buda, M., Jani, E. & Su, A.S.M. (2021). Field assessment on agrivoltaic Misai Kucing techno-economical approach in solar farming. *In 2021 International Conference on Electrical, Computer, and Energy Technologies, (ICECET)*. pp. 1–6. DOI:10.1109/ICECET52533.2021.9698511

Yahya, A., Safie, H. & Kahar, S.A. (1997). Properties of coco peat-based growing media and their effects on two annual ornamentals. *Journal of Tropical Agriculture and Food Science*, 25(2): 151–157.

Zakaria, N.I., Ismail, M.R., Awang, Y., Wahab, P.E.M. & Berahim, Z. (2020). Effect of root restriction on the growth, photosynthesis rate, and source and sink relationship of chilli (*Capsicum annuum* L.) grown in soilless culture. *BioMed Research International*, 2020 (1): 2706937. DOI:10.1155/2020/2706937

Zazirska, M., Owen, J.S., Altland, J.E. & Fields, J. S. (2021). Relationship between particle size summation curves and the moisture characteristic curve for soilless substrates. *Acta Horticulturae*, 1305: 209–217. DOI:10.17660/ActaHortic.2021.1305.29

Zhu, W. & Wang, H. (2013). A brief development history of soilless cultivation in China. *Acta Horticulturae*, 1004: 63–70. DOI:10.17660/ActaHortic.2013.1

Borneo Journal of Resource Science and Technology (2025), 15(1): 167-174
DOI: https:doi.org/10.33736/bjrst.7423.2025

Effect of Vermicompost and Molasses on the Phosphorus Adsorption Characteristics of Cow Dung Amended Soil

NITUL CHANDRA SEN[2], MD. ABU JUWEL[2], MD. NURUL ISLAM[2], MD. SHAHIDUL ISLAM[2], MD. ASHRAFUL HOQUE*[1]

[1]Department of Biochemistry and Molecular Biology, University of Rajshahi, Rajshahi-6205, Bangladesh;
[2]Department of Chemistry, University of Rajshahi, Rajshahi-6205, Bangladesh
*Corresponding author: ashraf_bio@ru.ac.bd
Received: 17 July 2024 Accepted: 25 February 2025 Published: 30 June 2025

ABSTRACT

Long term but steady-control release of phosphorus is crucially important for phosphorus fertiliser management and plant growth. In the present study, we aimed to explore the effects of vermicompost and molasses on the phosphorus adsorption characteristics of cow dung amended soil. To achieve this goal, four treatments: control (soil + 10% cow dung), T1: SCV (soil + 9% cow dung + 1% vermicompost), T2: SCM (soil + 10% cow dung + 0.1% molasses), and T3: SCVM (soil + 9% cow dung + 1% vermicompost + 0.1% molasses) with three replicates were investigated. The treatments were incubated for 21 days at room temperature (~30 °C) and the samples were collected at seven days intervals. Phosphorus adsorption behaviour was examined by measuring maximum phosphorus adsorption capacity (MPAC), phosphate bonding energy (PBE) and maximum phosphate buffering capacity (MPBC)with some related physico-chemical parameters e.g., pH, electrical conductivity (EC), organic matter (OM) content. Physico-chemical studies revealed that both vermicompost and molasses have positive impact on pH, EC, and OM confirming the relatively better nutrient availability to plants. Initially, the MPAC values of both vermicompost and molasses amended samples (T1: SCV, T2: SCM and T3: SCVM) showed the highest MPAC (696.18 ± 52.625, 703.94 ± 92.386 and 670.17 ± 33.786 mg/kg respectively) followed by gradual decrease to 436.15 ± 16.346, 448.61± 24.221, and 430.78 ± 6.871 mg/kg respectively with time while cow dung amended control soil showed increasing trend starting from the value 321.52 ± 56.462 to 592.65 ± 53.657 mg/kg. Study of the PBE and MPBC of all amended samples followed the same pattern of change.

Keywords: Cow dung amended soil; molasses; phosphorus adsorption capacity; vermicompost

INTRODUCTION

Agriculture is an important tool for promoting development to achieve the Sustainable Development Goals for agrarian countries like Bangladesh. In order to increase crop production, the most common agricultural practice is to overuse of agrochemicals (Jote, 2023). In addition to causing financial loss, this pollutes the atmosphere, contaminates water supplies, and deteriorates soil qualities. Organic compost has gained popularity as a solution to such issues with the environment, chemical costs and fertility of soil (Sahu & Pradhan, 2023).

Generally, most farmers now use both organic and inorganic fertilisers combinedly due to cost effectiveness and to increase soil fertility. Some farmers also apply fresh cow dung (CD) with inorganic fertiliser to the field and leave it for some time before planting without checking the soil properties. However, the use of fresh cow dung to soil can decrease the phosphorus adsorption capacity (PAC) and may results in loss of phosphorus fertiliser and eutrophication (Seafatullah *et al.*, 2015).

The amount of applied phosphorus fertiliser that is absorbed by the soil is indicated by its PAC (Aini *et al.*, 2022). Higher PAC indicates that phosphorus is tightly bound to the soil and not accessible to plants. While a lower PAC results in more readily available phosphorus for plant absorption that increases phosphorus run off into the water resulting in water pollution and financial loss (Khan *et al.*, 2023). So, the ability of soil to steady-control release of phosphorus is crucially important for better plant growth. To use phosphorus fertiliser effectively, soil must have the highest possible PAC and decreasing properties with time to ensure proper phosphorus management. By adding organic fertilisers to the

soil, the PAC can be increased (Ahmad *et al.*, 2016). CD and vermicompost are well known organic amendments as well as fertiliser used globally to provide essential nutrients (both macro and micro) to soil for plants growth (Ahmad *et al.*, 2016, Rehman *et al.*, 2023). Molasses has also been used as soil improver particularly on sandy soil and soil of poor structure (Pyakurel *et al.*, 2019). Application of vermicompost and molasses may also change the CD amended soil PAC that could be favorable for plant growth. Considering these facts, a short-term effect of vermicompost and molasses on the phosphorus adsorption characteristics of CD amended soil was investigated to find out their importance in phosphorus fertiliser management, environmental protection and sustainable agriculture.

MATERIALS AND METHODS

Materials

The soil sample was collected from the campus area of University of Rajshahi from 10–30 cm depth. The collected soil sample was air-dried for 7 days and then sieved with a net with a diameter of 2.0 mm. The particle size distributions of the soil samples were 45.26% silt, 52.77% sand and 1.97% clay with texture grade of sandy loam. The pH, electrical conductivity (EC) and organic matter (OM) content of the soil were 6.85, 125.09 µS/cm and 2.91% respectively. CD (pH- 7.1, EC- 2065 µS/cm and OM- 73.28%) was obtained from the Agricultural Project of Rajshahi University. Vermicompost (pH- 6.03, EC- 7610 µS/cm and OM- 41.74%) was prepared from rotten CD using Eudrilus eugeniae (African Nightcrawlers) collected from a farm of vermicompost situated near Paba, Rajshahi, Bangladesh. Molasses was collected from Rajshahi Sugar Mills Limited, Rajshahi, Bangladesh.

Sample Treatment

The study was conducted with four treatments; control: (soil + 10% CD), T1: SCV (soil + 9% CD + 1% vermicompost), T2: SCM (soil+ 10% CD + 0.1% molasses), and T3: T3: SCVM (soil + 9% CD + 1% vermicompost + 0.1% molasses) with three replicates. The prepared mixtures of substrates were mixed thoroughly and filled in plastic circular containers of appropriate size (28 cm diameter and 30 cm depth), with pierced lid for aeration. The mixtures were incubated at 30 ℃ for 21 days and moisture content was maintained at 100% of the field capacity. The samples were collected at seven days intervals and air dried for seven days. Then the samples were packed in a plastic zipper bag and kept in freezing condition for analysis.

Measurement of pH and EC

The pH and EC of the samples were measured using a pH meter (Hanna Instruments, HI 2211) and conductivity meter (Jenway conductivity meter 4310) respectively. The amount of each sample was calculated on dry weight basis. A total of 5.0 g of sample equivalent was mixed with 75 ml of deionised distilled water. The mixture was shaken for 60 minutes with a mechanical shaker and then it was filtered using muslin cloth. 50 ml of the filtrate was taken in a 100 ml beaker. The electrode was immersed into the sample and the pH and EC values were recorded.

Measurement of OM

OM was determined by loss-on-ignition (LOI) method. A known weight of oven dried sample was placed in a ceramic crucible which was then heated at 450 °C (ASTM, 2000) for 6 hours in a muffle furnace. The sample was then cooled in a desiccator and weighed. The percentage of OM content was calculated as the difference between the initial and final sample weights divided by the initial sample weight times 100 (Bojko & Kabala, 2014).

Measurement of Adsorbed Phosphorus

The amount of adsorbed phosphorus was determined according to published method (Ahmed *et al.*, 2008). A range of phosphorus solutions (0, 10, 20, 30, 40, 50, 60 and 70 mg P/L) were prepared by dissolving potassium dihydrogen phosphate (KH_2PO_4) in 0.01 M calcium chloride ($CaCl_2.2H_2O$) solution. Then 0, 100, 200, 300, 400, 500, 600 and 700 mg P/kg of soil samples were prepared by 2.5 g of soil samples with 25 mL of these phosphorus solution in 50 mL conical flask. The samples were then shaken for 22 h at room temperature (25 ℃) followed by centrifugation at 5000 rpm for 15 min and filtered using Whatmann No.1 filter paper. The filtrates were analysed for remaining phosphorus in the solutions using

UV-Visible spectrophotometer (V1000, Yoke instrument) adopted from Ibanez et al. (2008). The amount of phosphorus adsorbed (mg/kg soil) was calculated from the difference between the initial amount of phosphorus added and the amount in the equilibrated solution.

Phosphorus Adsorption Isotherms

The phosphorus adsorption data for the soils used in this study were calculated using Langmuir adsorption equation for getting linear curve to determine the parameters describing phosphorus adsorption properties of tested soils. The Langmuir equation is $C/Q = C/Q_m + 1/kQ_m$, where Q (mg/kg) is the amount of phosphorus adsorbed to soil at the equilibrium phosphorus concentration C (mg/L), Q_m (mg/kg) is the maximum amount of phosphorus adsorbed to the soil known as maximum phosphorus adsorption capacity (MPAC), k (L/mg) is a constant related to the binding strength of phosphorus at the adsorption sites known as phosphorus bonding energy (PBE) and $k \cdot Q_m$ is the maximum phosphorus buffering capacity (MPBC, L/kg) (Lair *et al.*, 2009).

Statistical Analysis

Microsoft Excel 2019 was used to perform data processing, linear regression, and other statistical analyses.

RESULTS AND DISCUSSION

In addition to phosphorus adsorption related parameters, three soil fertility parameters e.g., pH, EC and OM were initially monitored with time for better understanding of the effect of vermicompost and molasses on phosphorus adsorption characteristics of the CD amended soil.

Effect on pH

The soil pH of CD amended control soil was changed upon the application of vermicompost and molasses as illustrated in Figure 1. The addition of vermicompost and molasses to the CD amended soil (T1: SCV and T2: SCM) shifted pH towards the favorable range (6.27 ± 0.035 - 6.74 ± 0.031) from the starting day of incubation. The combine application of vermicompost and molasses (T3: SCVM) showed relatively better pH correcting capacity followed by T2: SCM and T1: SCV. From this data, it was revealed that vermicompost and molasses has a positive impact in correcting soil pH. The availability of most macronutrients (nitrogen, phosphorus, potassium, sulfur, calcium, and magnesium) decreases as soil acidity increases (Khaidem *et al.*, 2018). Therefore, application of vermicompost and molasses to moderately acid soils tends to increase the availability of these nutrients.

Effect on EC

The change in EC of different amended samples with time are shown in Figure 2. Highest initial EC was found in T3: SCVM (404.5 ± 12.998 µS/cm) followed by T1: SCV (361.82 ± 9.321), T2: SCM (306.71 ± 12.027) and control (296.04 ± 8.62 µS/cm). The order in EC values was observed to maintain up to 14th day although there was a decreasing trend for all the treatments. The decrease in conductivity of all samples may be related to the reduction of ammonium and other ions due to the rapid expansion of aerobic microbial populations (Kalamdhad & Kazmi, 2009).

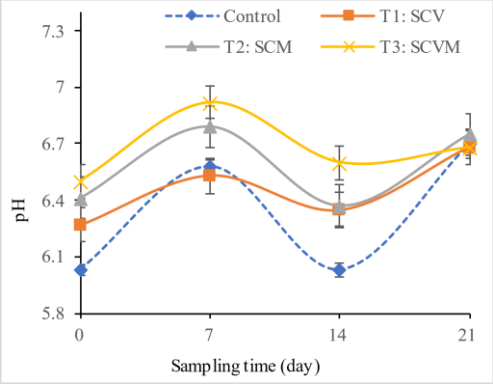

Figure 1. Change in pH of different treatments with incubation time

Effect on OM

The change in OM of different amended samples with time are shown in Figure 3. In our study, the change in OM of all treatments showed decreasing trend with time during incubation. In case of both vermicompost and molasses amended sample (T3: SCVM), the initial OM content found to be the highest (11.59 ± 0.6104 %) followed by control (10.28 ± 0.2193), T2: SCM (10.01 ± 0.0491) and T1: SCV (9.78 ± 0.4263 %). It was implying that both vermicompost and molasses amendment has a positive impact in correcting CD amended soil OM whereas, there was no impact when using only vermicompost or molasses as OM content of both was lower than CD. Therefore, combined application of vermicompost and molasses (T3: SCVM) was suitable soil amendments for soil because of its high OM.

Phosphorus Adsorption Isotherms

The most popular model to quantitatively describe phosphate adsorption is the Langmuir adsorption isotherm (Lair *et al.*, 2009). The data obtained from the experiment, were fitted to the linear form of Langmuir adsorption equation for getting some important parameters to describe phosphate adsorption characteristics (Figure 4). The values of correlation coefficients shown in Table 1 were found between the ranges of 0.87 – 1.00 indicating that adsorbed phosphorus versus equilibrium phosphorus concentration data support this adsorption models for studied. It was observed that vermicompost and molasses clearly influenced the MPAC. The MPAC values for CD amended control soil sample initially was 321.52 ± 56.462 mg/kg while vermicompost and molasses amended soil samples (T1: SCV, T2: SCM and T3: SCVM) were 696.18 ± 52.625, 703.94 ± 92.386 and 670.17 ± 33.786 mg/kg respectively (Table 2).

The MPAC of CD amended control soil showed initially low value and increased gradually to 592.65 ± 53.657 mg/kg during incubation while all vermicompost and molasses amended samples (T1: SCV, T2: SCM and T3: SCVM) showed higher value and gradually decreased to 436.15 ± 16.346, 448.61± 24.221 and 430.78 ± 6.871 mg/kg respectively with time. Seafatullah *et al*. (2015) also demonstrated similar results that vermicompost can significantly enhance the phosphorus adsorption capacity of sandy loam soil, at least initially, and help to regulate the release of phosphorus. The changing tendency of all the samples were attributed by changing physicochemical characteristics of the substrates. The fresh CD contains unstable OMs (Rajdeo Kumar, 2014) which are very poor substrate for adsorption; even it inhibits adsorption by blocking adsorption sites (Delle Site, 2001). However, these unstable organic substances became stable substrate and increased the MPAC by increasing PO_4^{-3} adsorption site (Vijayaraghavan *et al.*, 2016). Vermicompost primarily supplies OM or humus components to the soil that can bound minerals like Fe and Al oxides found in soil. Humic compounds present in vermicompost complexed with Fe-oxide present in soil can enhances PO_4^{3-} adsorption site by forming PO_4^{3-}-Fe-OM ternary complexes, which in turn boosted the PO_4^{-3} adsorption capacity (Yang *et al.*, 2019). The change of PO_4^{3-} sorption capacities of soil (OM/ferrihydrite) systems decreased as they were aged (Kizewski *et al.*, 2010).

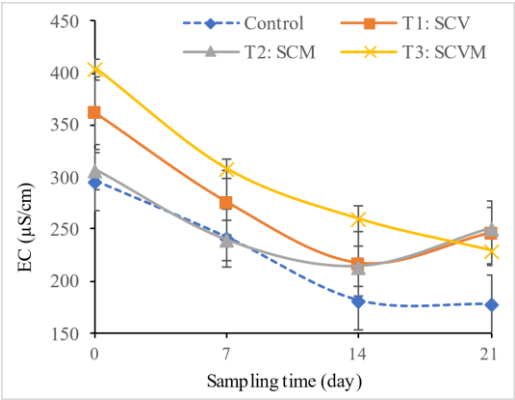

Figure 2. Change in EC of different treatments with incubation time

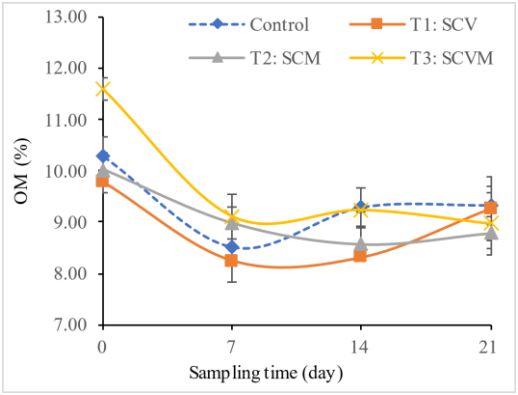

Figure 3. Change in OM of different treatments with incubation time

Table 1. Phosphate adsorption equations for different treatments collected at different intervals

Sampling time	Treatments	Langmuir equation	
		$C/Q = C/Q_m + 1/kQ_m$	R^2
0th day	Control	C/Q = 0.003110C + 0.033550	0.8664
	T1: SCV	C/Q = 0.001436C + 0.008058	0.9722
	T2: SCM	C/Q = 0.001421C + 0.023658	0.9207
	T3: SCVM	C/Q = 0.001492C + 0.006142	0.9875
7th day	Control	C/Q = 0.002152C + 0.007987	0.9978
	T1: SCV	C/Q = 0.001986C + 0.008564	0.9866
	T2: SCM	C/Q = 0.001975C + 0.008779	0.9302
	T3: SCVM	C/Q = 0.001995C + 0.014709	0.9840
14th day	Control	C/Q = 0.001890C + 0.016599	0.9607
	T1: SCV	C/Q = 0.002C + 0.0099	0.9769
	T2: SCM	C/Q = 0.0023C + 0.0287	0.9087
	T3: SCVM	C/Q = 0.0023C + 0.0135	0.9856
21th day	Control	C/Q = 0.0017C + 0.0087	0.9606
	T1: SCV	C/Q = 0.0023C + 0.0081	0.9930
	T2: SCM	C/Q = 0.0022C + 0.0153	0.9856
	T3: SCVM	C/Q = 0.0023C + 0.0092	0.9987

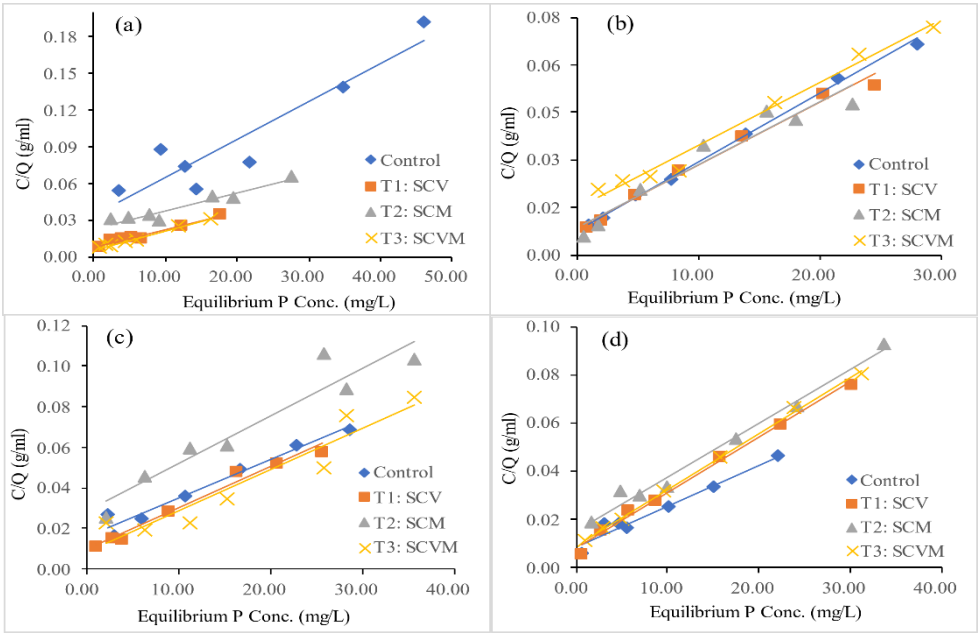

Figure 4. Langmuir phosphorus adsorption isotherm for control, T1: SCV, T2: SCM, T3: SCVM samples collected on (a) 0th day (b) 7th day (c) 14th day and (d) 21th days of incubation

Table 2. Parameters of phosphorus adsorption characteristics described with Langmuir equation (means ± standard deviation)

Sampling time (day)	Parameters	Treatments			
		Control	T1: SCV	T2: SCM	T3: SCVM
0	MPAC (Q_m, mg/kg)	321.52 ± 56.462	696.18 ± 52.625	703.94 ± 92.386	670.17 ± 33.786
	PBE (k, L/mg)	0.0927 ± 0.0847	0.1783 ± 0.0885	0.0600 ± 0.0303	0.2429 ± 0.1099
	MPBC (k × Q_m, L/kg)	29.81 ± 11.983	124.10± 14.955	42.27± 5.031	162.80± 16.451
7	MPAC (Q_m, mg/kg)	464.70 ± 9.8102	503.53 ± 26.2368	506.46 ± 62.0551	501.21 ± 28.5448
	PBE (k, L/mg)	0.2694 ± 0.1107	0.2319 ± 0.1335	0.2249 ± 0.1938	0.1356 ± 0.0679
	MPBC (k × Q_m, L/kg)	125.209 ± 10.538	116.764 ± 19.202	113.906 ± 41.444	67.984 ± 8.410
14	MPAC (Q_m, mg/kg)	528.99 ± 47.880	494.20 ± 34.017	426.81 ± 60.520	488.28 ± 73.058
	PBE (k, L/mg)	0.1139 ± 0.0661	0.2050 ± 0.1314	0.0816 ± 0.0583	0.2514 ± 0.3196
	MPBC (k × Q_m, L/kg)	60.243 ± 9.898	101.300 ± 20.586	34.814 ± 8.530	122.76 ± 97.835
21	MPAC (Q_m, mg/kg)	592.65 ± 53.657	436.15 ± 16.346	448.61± 24.221	430.78 ± 6.871
	PBE (k, L/mg)	0.1945 ± 0.1234	0.2836 ± 0.1654	0.1452 ± 0.0769	0.2531 ± 0.0926
	MPBC (k × Q_m, L/kg)	115.256 ± 22.733	123.696 ± 20.949	65.148 ± 9.046	109.020 ± 7.2810

Furthermore, since it is well-established that competition for adsorption sites occurs between inorganic, specifically adsorbed anions, competition between OM and phosphate leading to decreased phosphate adsorption could be anticipated; however, this is still disputed. Organic matter in solution strongly decreased PO_4^{3-} adsorption onto Al and Fe oxides thus onto soils (Sibanda & Young, 1986). The ability to control release of amended sample make them efficient amendment as it can prevent eutrophication through these properties. The MPAC (Q_m), PBE (k) and MPBC calculated from the product of Q_m and k were used to describe the phosphorus adsorption characteristics of soil phosphorus which is shown in Table 2 and Figure 5.

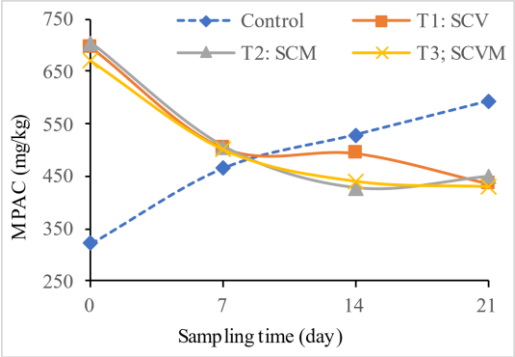

Figure 5. Change in MPAC of the soil samples; control; T1: SCV, T2: SCM, T3: SCVM with incubation

Comparison of Phosphate Bonding Energy and Maximum Phosphate Buffering Capacity

The change in PBE of amended soil samples compared to control soil with time shown in Figure 6(a). From this figure and Table 2, it was found that vermicompost amended soil (T3: SCVM) showed high PBE value (0.2429 ± 0.1099 L/mg) initially followed by T1: SCV (0.1783 ± 0.0885 L/mg), control (0.0927 ± 0.0847 L/mg) and T2: SCM (0.0600 ± 0.0303 L/mg). Vermicompost may enhance the bonding energy of phosphorus in the soil by increasing organic phosphorus adsorption, promoting microbial phosphorus accumulation (Zhang et al., 2020). On the other hand, molasses may indirectly improve phosphorus retention by increasing the CEC and OM content of the soil (Zhou et al., 2020).

MPBC of all samples followed the similar pattern of change with time as occurred in PBE (Figure 6b). Vermicompost amended soil (T3: SCVM) showed the highest MPBC value (162.80 ± 16.451 L/kg) initially followed by T1: SCV (124.10± 14.955), control (42.27± 5.031) and T2: SCM (29.81 ± 11.983 L/kg). The MPBC is an integrated parameter that combines the Q_m and k (Wang & Liang, 2014) and a higher MPBC means more phosphorus will be adsorbed.

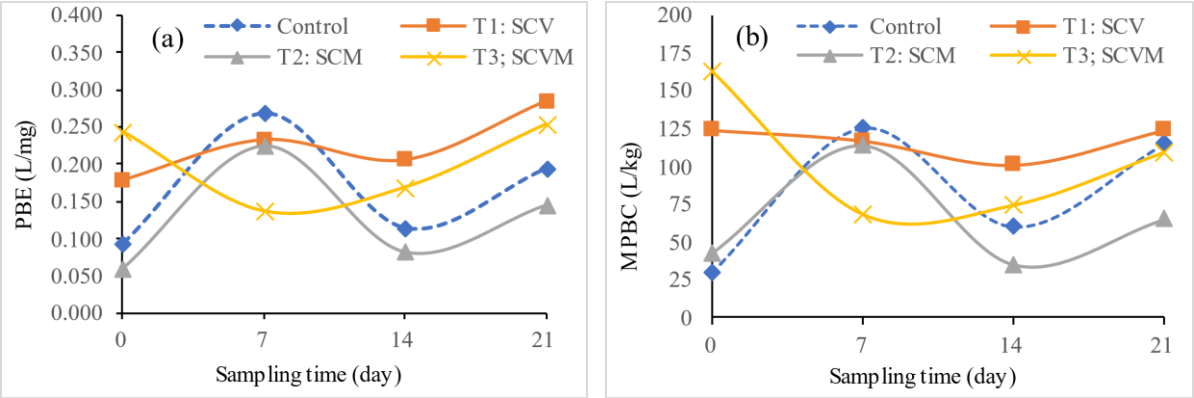

Figure 6. Change in (a) PBE and (b) MPBC of the soil samples; control, T1: SCV, T2: SCM, T3: SCVM with incubation

CONCLUSION

Study on the effects of vermicompost and molasses on the phosphorus adsorption characteristics of CD amended soil was carried out by measuring some parameters related to phosphorus adsorption. The results showed that both vermicompost and molasses have positive impact on the phosphorus adsorption characteristics of CD amended soil. As expected, the combined application of vermicompost and molasses showed further enhancement of that characteristics. Application of cow dung along with phosphate fertiliser seems to increase the loss of the fertiliser through runoff and leaching. Therefore, vermicompost and molasses are recommended to use separately or in combination with cow dung as soil amendment for agro-environmental advantages. Further work is still required to evaluate the efficiency of cow dung, vermicompost and molasses on field experiment and to apply in other soil texture rather than sandy loam.

ACKNOWLEDGEMENTS

We are grateful to the Faculty of Science, University of Rajshahi, Bangladesh for providing financial support to carry out the research work.

REFERENCES

Ahmad, A.A., Radovich, T.J.K., Nguyen, H.V., Uyeda, J., Arakaki, A., Cadby, J., Paull, R., Sugano, J. & Teves, G. (2016). Use of organic fertilisers to enhance soil fertility, plant growth, and yield in a tropical environment. In Larramendy, M.L. and S. Soloneski (Eds.), *Organic Fertilisers—From Basic Concepts to Applied Outcomes*. InTech. DOI: 10.5772/62529

Ahmed, M.F., Kennedy, I.R., Choudhury, A.T.M.A., Kecskés, M.L. & Deaker, R. (2008). Phosphorus adsorption in some Australian soils and influence of bacteria on the desorption of phosphorus. *Communications in Soil Science and Plant Analysis*, 39(9–10): 1269–1294. DOI: 10.1080/00103620802003963

Aini, S.N., Yanti, W., Setiawati, A.R., Prasetyo, D. & Lumbanraja, J. (2022). The behaviour of phosphorus adsorption on soil in the geological formation of Ranau Tuff using the Languir isothermic model to support food security. In *AIP Conference Proceedings* (Vol. 2563, No. 1). AIP Publishing. DOI: 10.1063/5.0103239

Bojko, O. & Kabala, C. (2014). Loss-on-ignition as an estimate of total organic carbon in the mountain soils. *Polish Journal of Soil Science*, 47: 71–79.

Delle Site, A. (2001). Factors affecting sorption of organic compounds in natural sorbent/water systems and sorption coefficients for selected pollutants. *Journal of Physical and Chemical Reference Data*, 30(1): 187–439. DOI: 10.1063/1.1347984

Ibanez, J.G., Hemandez-Esparza, M., Doria-Serrano, C., Fregoso-Infante, A. & Singh, M.M. (2008). Environmental Chemistry: Microscale Laboratory Experiments (Springer, NewYork). DOI: 10.1007/978-0-387-49493-7

Jote, C.A. (2023). The impacts of using inorganic chemical fertilisers on the environment and human health. *Organic and Medicinal Chemistry International Journal*. 13(3): 555864. DOI: 10.19080/OMCIJ.2023.13.555864

Kalamdhad, A.S. & Kazmi, A.A. (2009). Rotary drum composting of different organic waste mixtures. *Waste Management & Research: The Journal for a Sustainable Circular Economy*, 27(2): 129–137. DOI: 10.1177/0734242X08091865

Khaidem, J., Thounaojam, T. & Meetei, T.T. (2018). Influence of soil pH on nutrient availability: A Review. *International Journal of Emerging Technologies and Innovative Research*, 5(12): 707-713.

Khan, F., Siddique, A.B., Shabala, S., Zhou, M. & Zhao, C. (2023). Phosphorus plays key roles in regulating plants' physiological responses to abiotic stresses. *Plants*, 12(15): 2861. DOI: 10.3390/plants12152861

Kizewski, F.R., Hesterberg, D. & Martin, J. (2010). Phosphate sorption to organic matter/ferrihydrite systems as affected by aging time. In *19th World Congress of Soil Science, Soil Solutions for a Changing World 1 – 6 August 2010, Brisbane, Australia. Published on DVD.*

Lair, G.J., Zehetner, F., Khan, Z.H. & Gerzabek, M. H. (2009). Phosphorus sorption–desorption in alluvial soils of a young weathering sequence at the Danube River. *Geoderma*, *149*(1), 39–44. DOI: 10.1016/j.geoderma.2008.11.011

Pyakurel, A., Dahal, B.R. & Rijal, S. (2019). Effect of molasses and organic fertiliser in soil fertility and yield of spinach in Khotang, Nepal. *International Journal of Applied Sciences and Biotechnology*, *7*(1): 49–53. DOI: 10.3126/ijasbt. v7i1.23301

Rajdeo Kumar, N.Y. (2014). Physico-chemical properties of before and after anaerobic digestion of jatropha seed cake and mixed with pure cow dung. *Journal Chemical Engineering & Process Technology*, 5: 186. DOI: 10.4172/2157-7048.1000186

Rehman, S.U., De Castro, F., Aprile, A., Benedetti, M. & Fanizzi, F.P. (2023). Vermicompost: enhancing plant growth and combating abiotic and biotic stress. *Agronomy*, 13(4): 1134. DOI: 10.3390/agronomy13041134

Sahu, B. & Pradhan, M. (2024). Organic farming: a sustainable approach of agriculture. *AgriDristi*. 1(1): 20-21.

Seafatullah, M., Hoque, M.A., Islam, M.S., Islam, M. M., & Islam, M.N. (2015b). Effect of Cow Dung, Biogas Slurry and Vermicompost on Phosphorus Adsorption Behaviour of Soil. *Journal of Scientific Research*, 7(3), 167–175. DOI: 10.3329/jsr. v7i3.23756

Sibanda, H.M. & Young, S.D. (1986). Competitive adsorption of humus acids and phosphate on goethite, gibbsite and two tropical soils. *Journal of Soil Science*, *37*(2): 197–204. DOI: 10.1111/j.1365-2389. 1986.tb00020.x

Vijayaraghavan, P., Arun, A., Vincent, S.G.P., Arasu, M.V. & Al-Dhabi, N.A. (2016). Cow dung is a novel feedstock for fibrinolytic enzyme production from newly isolated bacillus sp. Ind7 and its application in in vitro clot lysis. *Frontiers in Microbiology*, 7: 361. DOI: 10.3389/fmicb.2016.00361

Wang, L. & Liang, T. (2014). Effects of exogenous rare earth elements on phosphorus adsorption and desorption in different types of soils. *Chemosphere*, 103: 148–155. DOI: 10.1016/j.chemosphere.2013.11.050

Yang, X., Chen, X. & Yang, X. (2019). Effect of organic matter on phosphorus adsorption and desorption in a black soil from Northeast China. *Soil and Tillage Research*, 187: 85–91. DOI: 10.1016/j.still.2018.11.016

Zhang, F., Wang, R., Yu, W., Liang, J. & Liao, X. (2020). Influences of a vermicompost application on the phosphorus transformation and microbial activity in a paddy soil. *Soil and Water Research*, 15(4): 199–210. DOI: 10.17221/91/2019-SWR

Zhou, Y., Liu, Y., Feng, L., Xu, Y., Du, Z. & Zhang, L. (2020). Biochar prepared from maize straw and molasses fermentation wastewater: Application for soil improvement. *RSC Advances*, 10(25): 14510–14519. DOI: 10.1039/D0RA02038A

Borneo Journal of Resource Science and Technology (2025), 15(1): 175-188
DOI: https:doi.org/10.33736/bjrst.7584.2025

Enhancing *Barringtonia racemosa* (L.) Streng. Stem Cutting Propagation for Restoration Efforts: Influence of Cutting Position and Substrate Type

EVANIE CLARA FELIX, JULIUS KODOH & ELIA GODOONG*

Faculty of Tropical Forestry, Universiti Malaysia Sabah, Jalan UMS, 88400 Kota Kinabalu, Sabah, Malaysia
*Corresponding author: elia@ums.edu.my
Received: 13 August 2024 Accepted: 25 February 2025 Published: 30 June 2025

ABSTRACT

Barringtonia racemosa (L.) is a common native tropical tree species that grows in adjacent areas of tidal riverbanks, which are slightly beyond the influence of saline waters. This species is commonly associated with mangrove plants, which help prevent erosion, protect water quality, and nourish terrestrial and aquatic habitats. Nevertheless, the seed production of this species has become limited as a result of the severe degradation of riparian areas, thereby making seedling production *via* micropropagation costly. Thus, this study tested the ability of *B. racemosa* to undergo vegetative regeneration in a non-mist poly-propagator under 90% shading in the nursery for three months. The observation primarily focused on the growth performance of cuttings, specifically the shoot and root development, depending on the treatments used. Three different stem cutting positions were used: apical, median, and basal, as well as three types of substrates: sand, cocopeat, and a mixture of sand and cocopeat (1:1). All cuttings were treated with dissolved indole-3-butyric acid (IBA) hormone. The results showed cuttings at the median and basal positions with a mixture of sand and cocopeat sprouted the most with 97.22 ± 4.81% and 83.33 ± 8.36%, respectively. Cuttings at the basal position with the same mixture also rooted the most (97.22 ± 4.81%), followed by the median position with sand (89.00 ± 9.62%). Contradictorily, the apical cuttings in the mixture substrate had lower sprouting and rooting success (13.89 ± 4.82% and 13.98 ± 12.73%). This study concluded that *B. racemosa* can be efficiently propagated using basal and median stem cuttings with suitable substrate type, providing a practical and cost-effective approach for restoration efforts in degraded riparian areas.

Keywords: *Barringtonia racemosa*, non-mist poly-propagator, restoration, seedling production, stem cuttings

INTRODUCTION

Barringtonia racemosa (L.) is a mangrove-associated plant species that belongs to the Lecythideceae family and flourishes well under humid and moist conditions (Kabir *et al*., 2013). This species is distributed along tropical and sub-tropical coasts in various regions, from East and South Africa, Madagascar, the Seychelles Islands, India, Sri Lanka, Myanmar, Thailand, throughout Southeast Asia (including Malaysia), and the Pacific Islands to Northern Australia (Osman *et al*., 2015). It typically occurs near watery areas such as riverbanks and freshwater swamps, occasionally in less sane areas of mangrove swamps (Kabir *et al*., 2013). It has been revised that the *Barringtonia* genus has a total of 69 species, but only three of the species, *B. asiatica*, *B. acutangula*, and *B. racemosa*, are common and occur in lowlands near coastal or along streams and dispersed by water (Aluri *et al*., 2019; Prance, 2012). This tropical higher plant species is native to Malaysia (Hussin *et al*., 2009) and locally known as *Putat Ayer* or *Putat Sungai* in Borneo, Sabah (Soepadmo *et al*., 2002).

B. racemosa is a small to medium sized tree that can grow up to 20 meters tall. Its leaves are arranged in alternate and clustered at the ends of thick twigs. The leaves are characterized by their large size, with shape ranging from obovate-oblong to lanceolate. They typically measure approximately 8 to 35 cm in length and 4 to 13 cm in width. It has a pointed tip with slightly toothed edges and prominent veins. The flowers are attractive, have whitish-pink colours, and are attached to the staminal tube. It has four white petals surrounded by a mass of white filaments, which are arranged in long spikes emerging from the centre of leaf clusters. The fruit is approximately 9 cm long and has an egg-like shape. The bark is typically smooth and greyish (Chantaranothai, 1995; Soepadmo *et al*., 2002; Osman *et al*., 2015; Prance, 2012). In Malaysia, this species has been classified as an under-

utilized crop due to a lack of effort in promoting its development and commercialization (Malaysian Agricultural Research and Development Institute (MARDI) and Ministry of Agriculture of Malaysia, 2007). *B. racemosa* is one of the species that have been extensively documented to function as food and medicine (Chan *et al*., 2017; Kong *et al.*, 2020).

This species has a high tolerance for floods and vaguely saline environments, making it a viable option for mangrove wetlands restoration and an important windbreaker in the coastal zone. According to Liang *et al*. (2022), the riparian zone and the estuarine soil may contain high concentrations of cadmium and lead as a result of sediment contamination, affecting the plant community composition. Hence, it was found that *B. racemosa* has the potential for phytoremediation of cadmium and lead-contaminated soil. However, many riparian forest areas have been reported to be degraded over the last few decades, resulting in soil erosion, habitat loss, poor water quality, and disturbance of terrestrial and aquatic ecosystems (Kabir *et al*., 2013). These challenges, compounded by habitat destruction, have significantly reduced the seed production of *B. racemosa,* hindering large-scale planting stock production necessary for restoration efforts (Kulip *et al*., 2020; Valentine & Chan Kim Lian, 2021).

A study by Behbahani *et al*. (2007) successfully regenerated *B. racemosa* from leaf explants using *in vitro* propagation, with successful establishment achieved after transplantation into mixed soil under greenhouse conditions. While tissue culture has demonstrated potential as a preservation method for tropical tree species, its applications on a large-scale may constrained by high costs and technical demands. Alternatively, *B. racemosa* has been reported to propagate effectively through seeds or stem cuttings (National Parks Board (NParks), 2024). Research on a closely related species, *Barringtonia procera*, has further demonstrated that while seed propagation is common, propagation using leafy stem cuttings in a poly-propagator system is both feasible and efficient (Pauku, 2006). These findings highlight the practicality and cost-effectiveness of stem cutting propagation for *B. racemosa*, making it a compelling alternative to tissue culture for large-scale restoration efforts.

Therefore, this study aimed to establish standardized propagation techniques by examined the influence of stem cutting positions (apical, median, and basal) and substrate type (sand, cocopeat, and a mixture of sand and cocopeat). The goal was to assess the growth performance and root development of *B. racemosa* seedlings using a non-mist poly-propagator under shaded nursery area.

MATERIALS AND METHODS

Study Site

The experiment was conducted from August to November 2023 under 90% shaded nursery of the Faculty of Tropical Forestry, Universiti Malaysia Sabah (6°2'28.68" N, 116°7'46.73" E). Plant material was collected from natural vegetation near the Petagas riparian area in Putatan, about 20 km south-west of Universiti Malaysia Sabah. Both locations experience similar rainfall patterns, with mean annual rainfall ranging from 50 mm and 345 mm. Monthly temperatures typically ranged from 22.9°C to 32.2°C, while relative humidity averages between 78.5% to 83.0% (Malaysia Meteorological Department, 2023).

Plant Material

The plant material consisted of stem cuttings taken from seedlings measuring 20 to 45 cm in height, which had been acclimatized for six months in the nursery at the Faculty of Tropical Forestry, Universiti Malaysia Sabah. Prior to planting, the substrate was treated with Thiram to prevent fungal and parasitic infections. No fertilizer was applied, as the study aimed to develop cost-effective propagation method minimizes environmental disturbances to riparian and aquatic during seedling transplantation. The poly-propagator was secured to prevent pest intrusion, and pesticide was applied selectively as needed. The cuttings were monitored daily to ensure favourable conditions and promptly address any pest or disease issues.

Preparation of Cuttings

The seedlings were watered 24 hours prior to taking the cuttings. Stem were excised 2 cm above the collar region using sterilized secateurs. Each stem was divided into three parts: 1) apical,

2) median, and 3) basal (Figure 1). The average length of these cuttings ranged from 5 to 12 cm (Murugan, 2007), and the average diameter ranged from 4 to 12 mm. Each cutting had at least two axillary buds. For the apical part, two leaves were retained and trimmed to half their size, while the median and basal cuttings were left without leaves. The variation in cutting size can be attributed to the limited availability of suitable plant material due to the scarcity of wildings in its natural habitat and the challenges in sourcing seedlings from the nursery. Consequently, the available plant material was utilized to maximize the potential for successful propagation.

Figure 1. Different stem cuttings position of *B. racemosa* used for propagation; apical cuttings (a), median cuttings (b), and basal cuttings (c)

Experimental Design and Treatments

The experiment was designed as a 3x3 factorial arrangement using a randomized complete block design within a modified non-mist poly-propagator, which inspired by the designs of Leakey (2014), Kouakou *et al*. (2016), and Dao *et al*. (2020). Two factors were tested: 1) cutting position (apical, median, and basal) and 2) substrates (sand, cocopeat, and mixture of sand and cocopeat (1:1)) with nine treatments applied (3 cuttings position x 3 substrates). Each treatment included 36 cuttings arranged in three replicates, with 12 cuttings per replicate. As a treatment, the basal bottom end of each cutting was treated with indole-3-butyric acid (IBA) hormone, briefly dipped into 2.5 g of the IBA dissolved in 1 litre of distilled water for 5 seconds before being placed in the potting trays (Kouakou *et al*., 2016) measuring 54 x 28 x 4 cm (105 holes). While IBA has limited solubility in water, Kroin (1992) suggested that dissolving IBA in water is more effective for rooting compared using alcohol-based solutions, as supported by Kouakou *et al*. (2016).

Nine potting trays were placed inside the non-mist poly-propagator, each containing three types of substrates for each cutting position (Figure 3). The non-mist poly-propagator, measuring 100 x 350 x 80 cm, was positioned on a planting bed under 90% of black plastic netting in the nursery (Figure 2) to protect cuttings from excessive temperatures and direct sunlight (Aminah *et al*., 1997). The non-mist poly-propagator was built using PVC pipe and covered with a transparent polythene plastic sheet to maintain high humidity around the cuttings while allowing light to penetrate. The average temperature and relative humidity recorded inside the non-mist poly-propagator were 29 □ ± 2 □ and 93%, respectively. In order to retain moisture in the substrate, the cuttings were occasionally sprayed with a fine mist of water, 2-3 times per week.

Figure 2. Closed non-mist poly-propagator consisted of cuttings and placed under 90% shading at the nursery

The substrates−sand, cocopeat, and a mixture of sand and cocopeat−were treated with Thiram 80% w/w fungicide to prevent fungal and parasite growth in the substrates (Kodoh *et al*., 2018). Cuttings were planted vertically, with the apical end inserted approximately 3 cm into the substrates (Dao *et al*., 2020) and spaced 3 cm between cuttings. The distance between the trays was set at 9 cm (Figure 3). After 90 days of planting, the cuttings were evaluated for viability, including sprouting percentage, rooting percentage, and growth traits such as shoot length, root collar diameter (RCD), number of shoots, number of leaves, leaf area index (LAI), and root development metrics such as number of primary and secondary roots and primary root length.

Leaf area index (LAI) was measured using Easy Leaf Area software, an automated digital image analysis tool. This method was selected to minimise disturbance to actively growing leaves, ensuring accurate and consistent measurements throughout the study period. Conventional methods for LAI measurement often require destructive sampling, which was deemed unsuitable for this research as it aimed to monitor ongoing leaf development. This software has been demonstrated to provide an accurate and efficient alternative for estimating leaf area from digital images (Easlon & Bloom, 2014), making it a reliable and practical choice for this study. Cuttings were considered to have sprouted or rooted when they had developed at least one bud. To assess the rooting, the rooted cuttings were carefully removed from the substrate (Dao *et al*., 2020). The sprouting was monitored weekly, while the rooting was evaluated at monthly intervals. The final mean data and percentages were calculated at the end of the experiment.

Data Analysis

Means and standard deviations were calculated for each of the parameters based on cutting position and substrates. The effect of the different factors was assessed using one way analysis of variance and their interaction effects between factors were analysed using two way analysis of variance (ANOVA). All statistical analyses were conducted using R software version 12.1 (2023). Tukey's Honestly Significant Different (HSD) test was applied to identify differences between means. Correlation coefficients were analysed using "metan" package in R. One way analysis of variance (ANOVA) was performed to compare the different levels of coppicing nodes.

Figure 3. Sprouted cuttings of *B. racemosa* planted in non-mist poly-propagator; apical cuttings (a), median cuttings (b), basal cuttings (c) with different substrate arranged randomly in replicate block

RESULTS

Effect of Stem Position on Sprouting and Rooting Growth of *B. racemosa*

The result (Table 1) shows that the stem cutting positions significantly influenced the shoot and root development of *B. racemosa* ($p<0.05$) across all parameters. Stem cuttings taken from basal positions presented the highest percentage of sprouting (87.00 ± 14.50%) and rooting (88.90 ± 12.50%). Basal cuttings also presented the greatest number of shoots (0.89 ± 0.17), longest shoot length (4.36 ± 1.70 cm), widest collar diameter (1.59 ± 0.57 mm), largest number of leaves (1.30 ± 0.33), and highest leaf area index (1.24 ± 0.62 cm^2) compared to apical and median position. The formation of roots also presented the best growth when using basal cuttings with highest number of primary roots (3.80 ± 1.58) and secondary roots (6.61 ± 3.44) and longest primary root length (2.96 ± 0.87 cm).

Effect of Substrate on Sprouting and Rooting Growth of *B. racemosa*

Table 2 presents the influence of substrate types on sprouting and rooting growth of *B. racemosa* stem cuttings. The result shows there were no significant differences among the substrate types on the shoot and root growth parameters ($p>0.05$). Despite that, the highest mean sprouting (75.00 ± 17.20%) and rooting (79.60 ± 18.70%) percentages were observed in sand. The number of shoot (0.75 ± 0.17) and number of leaves (1.26 ± 0.43) mean were also presented the highest in sand substrate. In contrast, the shoot length (2.39 ± 2.22 cm), collar diameter (0.87 ± 0.84 mm), and leaf area index (0.87 ± 0.75 cm^2) presented the best in mixture of sand and cocopeat. As for the root formation, the primary (2.85 ± 2.02) and secondary (4.46 ± 4.10) root were observed the best in cocopeat substrate, while primary root length (2.38 ± 1.44 cm) were obtained the better result in a mixture of sand and cocopeat.

Interaction Effect of Cutting Position and Substrate on Sprouting and Rooting Percentage of *B. racemosa*

The interaction effect between cutting position and substrate factors were statistically significant on sprouting ($F = 4.555$, $p = 0.0102$) and rooting ($F = 27.308$, $p = 0.001$) percentage, indicating that the cutting position and substrate on sprouting and rooting percentage were independent. However, Figure 4 shows that there were no significant different among substrates for basal cuttings. Despite that, basal cuttings planted in mixture of sand and cocopeat had the highest sprouting and rooting percentage (97.22 ± 4.81%, 97.22 ± 4.81%, respectively). Conversely, the lowest sprouting and rooting percentage were observed at the apical cuttings with mixture of sand and cocopeat (13.89 ± 4.82 % and 13.98 ± 12.73 %).

Interaction Effect of Cutting Position and Substrate on Growth Traits of Stem Cuttings

Based on Table 4, stem position and substrate significantly affected the number of shoots and shoot length in *B. racemosa* stem cuttings ($p<0.05$). However, no significant effects were observed on collar diameter, number of leaves, and leaf area index ($p>0.05$). The result revealed that the highest mean values for shoot number (1.03 ± 0.09) and shoot length (4.97 ± 1.22 cm) occurred in basal cuttings grown in a sand and

cocopeat mixture. Although other growth parameters did not exhibit significant interactions between stem position and substrate, the overall highest mean values for collar diameter (1.86 ± 0.38 mm) and leaf area index (1.55 ± 0.58 cm^2) were recorded in basal cuttings with a sand and cocopeat mixture. Additionally, the number of leaves had the highest mean (1.47 ± 0.48) in basal cuttings grown in sand substrate. Conversely, cuttings at apical part with mixture of sand and cocopeat show the lowest mean value among the parameters observed, whereas substrate with sand alone generally yielded better mean values for the measured parameters.

Table 1. Effect of stem position on the mean sprouting and rooting growth of stem cuttings from *B. racemose*

Stem position	Apical	Median	Basal	Statistical
Sprouting (%)	35.20 ± 22.40^{b}	78.70 ± 15.70^{a}	87.00 ± 14.50^{a}	$p<0.05$
Rooting (%)	32.40 ± 25.80^{b}	75.00 ± 21.70^{a}	88.90 ± 12.50^{a}	$p<0.05$
Shoot number	0.35 ± 0.22^{b}	0.80 ± 0.15^{a}	0.89 ± 0.17^{a}	$p<0.05$
Shoot length (cm)	0.24 ± 0.16^{c}	1.81 ± 0.62^{b}	4.36 ± 1.70^{a}	$p<0.05$
Collar diameter (mm)	0.00 ± 0.00^{c}	0.65 ± 0.34^{b}	1.59 ± 0.57^{a}	$p<0.05$
Leaves number	0.49 ± 0.40^{b}	1.14 ± 0.45^{a}	1.30 ± 0.33^{a}	$p<0.05$
Leaf area index (cm^2)	0.28 ± 0.19^{b}	0.80 ± 0.41^{a}	1.24 ± 0.62^{a}	$p<0.05$
Number primary root	1.44 ± 1.21^{b}	2.50 ± 0.58^{ab}	3.80 ± 1.58^{a}	$p<0.05$
Number secondary root	1.30 ± 1.47^{b}	2.54 ± 2.37^{b}	6.61 ± 3.44^{a}	$p<0.05$
Primary root length (cm)	1.16 ± 0.81^{b}	2.30 ± 0.70^{a}	2.96 ± 0.87^{a}	$p<0.05$

*Values (means ± SD) within a column followed by different superscript letters are significant different at $p<0.05$ (Tukey's HSD test).

Table 2. Effect of substrate on the mean sprouting and rooting growth of stem cuttings from *B. racemose*

Substrate	Sand	Cocopeat	Sand + Cocopeat (1:1)	Statistical
Sprouting (%)	75.00 ± 17.20^{ns}	61.10 ± 27.60^{ns}	64.80 ± 39.00^{ns}	$p>0.05$
Rooting (%)	79.60 ± 18.70^{ns}	58.30 ± 29.80^{ns}	58.30 ± 40.80^{ns}	$p>0.05$
Shoot number	0.75 ± 0.17^{ns}	0.62 ± 0.28^{ns}	0.67 ± 0.41^{ns}	$p>0.05$
Shoot length (cm)	2.09 ± 1.91^{ns}	1.92 ± 2.08^{ns}	2.39 ± 2.22^{ns}	$p>0.05$
Collar diameter (mm)	0.68 ± 0.77^{ns}	0.69 ± 0.75^{ns}	0.87 ± 0.84^{ns}	$p>0.05$
Leaves number	1.26 ± 0.43^{ns}	0.74 ± 0.42^{ns}	0.94 ± 0.61^{ns}	$p>0.05$
Leaf area index (cm^2)	0.78 ± 0.57^{ns}	0.64 ± 0.44^{ns}	0.87 ± 0.75^{ns}	$p>0.05$
Number primary root	2.65 ± 1.02^{ns}	2.85 ± 2.02^{ns}	2.24 ± 1.45^{ns}	$p>0.05$
Number secondary root	2.06 ± 1.86^{ns}	4.46 ± 4.10^{ns}	3.93 ± 3.62^{ns}	$p>0.05$
Primary root length (cm)	2.07 ± 0.66^{ns}	1.97 ± 1.08^{ns}	2.38 ± 1.44^{ns}	$p>0.05$

*Values (means ± SD) within a column are not significant (ns) different between substrate at $p>0.05$ using Tukey's HSD test.

Table 3. Interaction effect of stem position and substrate on the growth of stem cuttings from *B. racemose*

Stem position	Substrate	Mean shoot number	Mean shoot length (cm)	Mean root collar diameter (mm)	Mean leaf number	Mean leaf area index (cm^2)
Apical	Sand	0.61 ± 0.13^{bc}	0.34 ± 0.14^{ab}	0.00 ± 0.00^{ns}	0.95 ± 0.29^{ns}	0.47 ± 0.07^{ns}
	Cocopeat	0.31 ± 0.10^{cd}	0.30 ± 0.16^{bc}	0.00 ± 0.00^{ns}	0.36 ± 0.21^{ns}	0.24 ± 0.16^{ns}
	Sand + Cocopeat	0.14 ± 0.05^{d}	0.07 ± 0.04^{c}	0.00 ± 0.00^{ns}	0.17 ± 0.09^{ns}	0.09 ± 0.05^{ns}
Median	Sand	0.83 ± 0.17^{ab}	1.81 ± 0.74^{a}	0.60 ± 0.46^{ns}	1.36 ± 0.46^{ns}	0.76 ± 0.42^{ns}
	Cocopeat	0.72 ± 0.21^{ab}	1.49 ± 0.75^{ab}	0.60 ± 0.41^{ns}	0.67 ± 0.30^{ns}	0.65 ± 0.33^{ns}
	Sand + Cocopeat	0.83 ± 0.09^{ab}	2.15 ± 0.27^{a}	0.76 ± 0.26^{ns}	1.39 ± 0.05^{ns}	0.97 ± 0.55^{ns}
Basal	Sand	0.81 ± 0.17^{ab}	4.13 ± 1.75^{a}	1.45 ± 0.26^{ns}	1.47 ± 0.48^{ns}	1.11 ± 0.90^{ns}
	Cocopeat	0.83 ± 0.17^{ab}	3.98 ± 2.48^{a}	1.47 ± 0.67^{ns}	1.19 ± 0.20^{ns}	1.05 ± 0.38^{ns}
	Sand + Cocopeat	1.03 ± 0.09^{a}	4.97 ± 1.22^{a}	1.86 ± 0.38^{ns}	1.25 ± 0.33^{ns}	1.55 ± 0.58^{ns}
	F	4.867	4.555	0.230	2.468	0.704
	p	0.008	0.010	0.918	0.082	0.5997

*Values of means ± SD within a row followed by different superscript letters are significant different at $p<0.05$ (Tukey's HSD test) and are not significant (ns) different at $p>0.005$.

Table 4. Interaction effect of stem position and substrate on the root growth of stem cuttings from *B. racemosa* in a non-mist poly propagator

Stem position	Substrate	Mean primary root number	Mean secondary root number	Mean primary root length (cm)
Apical	Sand	2.50 ± 1.46^{ns}	2.28 ± 2.11^{bc}	2.02 ± 0.65^{abc}
	Cocopeat	1.11 ± 0.85^{ns}	1.28 ± 1.14^{c}	0.64 ± 0.27^{c}
	Sand + Cocopeat	0.72 ± 0.63^{ns}	0.33 ± 0.29^{c}	0.82 ± 0.71^{bc}
Median	Sand	2.50 ± 0.50^{ns}	0.95 ± 0.63^{c}	1.99 ± 0.79^{abc}
	Cocopeat	2.78 ± 0.54^{ns}	2.44 ± 1.64^{bc}	2.36 ± 0.47^{abc}
	Sand + Cocopeat	2.22 ± 0.75^{ns}	4.22 ± 3.35^{abc}	2.55 ± 0.91^{ab}
Basal	Sand	2.94 ± 1.27^{ns}	2.95 ± 2.43^{bc}	2.21 ± 0.80^{abc}
	Cocopeat	4.67 ± 2.40^{ns}	9.67 ± 1.17^{a}	2.91 ± 0.44^{a}
	Sand + Cocopeat	3.78 ± 0.63^{ns}	7.22 ± 2.33^{ab}	3.77 ± 0.59^{a}
	F	1.559	4.28	3.888
	p	0.228	0.013	0.019

*Values of means ± SD within a row followed by different superscript letters are significant different at p<0.05 (Tukey's HSD test) and not significant (ns) different at p>0.005.

Table 5. Effect of node position on the mean coppicing growth of stem cuttings from *Barringtonia racemose*

Node position	1	2	3	p
Mean shoot number	1.05 ± 0.05^{ns}	0.86 ± 0.24^{ns}	0.89 ± 0.19^{ns}	0.136
Mean shoot length (cm)	17.81 ± 3.55^{ns}	13.82 ± 7.93^{ns}	12.99 ± 6.69^{ns}	0.352
Mean root collar diameter (mm)	3.71 ± 0.66^{ns}	2.96 ± 1.47^{ns}	3.32 ± 1.33^{ns}	0.693
Mean leaf number	5.11 ± 0.90^{ns}	4.14 ± 2.49^{ns}	4.75 ± 1.95^{ns}	0.814
Mean leaf area index (cm^2)	3.94 ± 4.24^{ns}	2.45 ± 4.25^{ns}	4.74 ± 4.15^{ns}	0.814

*Values (means ± SD) within a column are not significant (ns) different at p>0.05 using Tukey's HSD test.

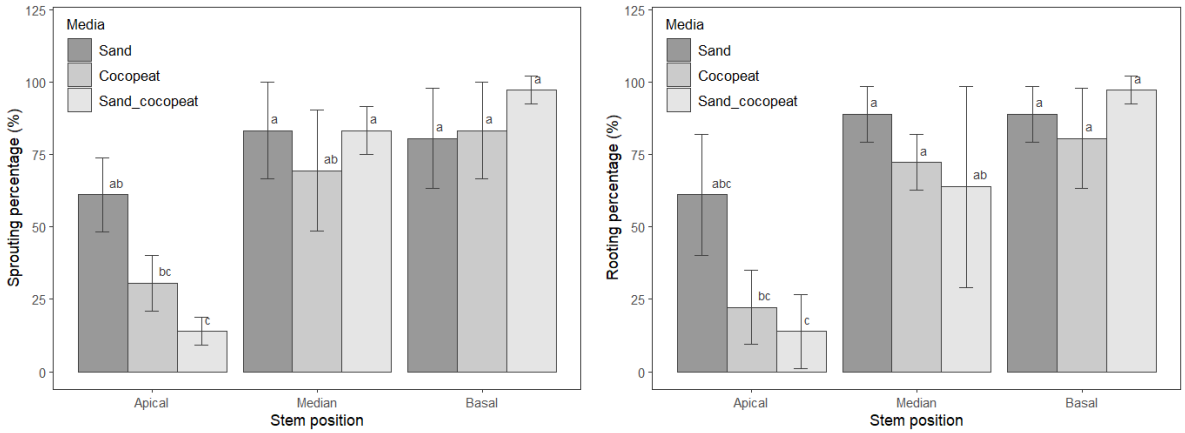

Figure 4. Effect of stem position and substrates on mean sprouting and rooting percentages of *B. racemosa* stem cuttings. The sprouting (F = 4.555, p = 0.0102) and rooting (F = 27.308, p = 0.001) percentage with different superscript letter were significant differences at p<0.005

Interaction Effect of Cutting Position and Substrate on Root Dynamics of Stem Cuttings

A significant interaction was found between the stem cutting position and substrate on the root development for *B. racemosa* (p<0.05) (Table 5), except for number of primary roots (p>0.05). Despite the lack of statistical significance, basal cuttings with a cocopeat substrate exhibited the highest mean number of primary roots (4.67 ± 2.40). Similarly, the mean number of secondary roots were highest in basal cuttings with cocopeat (9.67 ± 1.17). In contrast, apical cuttings grown in a mixture of sand and cocopeat recorded the lowest mean values for both number of primary (0.72 ± 0.63) and secondary roots (0.33 ± 0.29). Regarding root length, the longest primary roots length (3.77 ± 0.59 cm) was observed in basal cuttings with a sand and cocopeat mixture, whereas the shortest primary

roots length (0.64 ± 0.27 cm) were found in apical cuttings with cocopeat.

Correlation Relationship Between Growth and Rooting Traits of *B. racemosa*

The use of different significant levels (p<0.05, p<0.01, and p<0.001) highlights the varying degrees of statistical confidence in the observed relationships as shown in Figure 5. Lower values, such as p<0.001, indicate stronger evidence of a meaningful correlation, providing greater assurance of the strength and reliability of these associations. Significant (p<0.01) and highly significant (p<0.001) positive correlations, ranging from moderately high to very strong (r^2 = 0.49-1.00), were observed among eight (8) shooting and rooting traits based on Figure 5. The strongest positive correlation was between the percentage of sprouting and the number of shoots (r^2 = 1.00; p<0.001), followed by shoot length and root collar diameter (r^2 = 0.98; p<0.001). Meanwhile, the weakest, yet still positive and significant, was between the number of leaves and number of secondary roots (r^2 = 0.49; p<0.01).

Effect of Different Node Position on Coppicing Growth of *B. racemosa*

The formation of coppice shoots was not significantly ($p > 0.05$) influenced by the level of node position. However, the shoot produced by seedlings cut above node 1 was the longest (17.81 ± 3.55) and had the greatest mean number of leaves (5.11 ± 0.90) (Table 6). In addition, seedlings cut above node 1 exhibited the greatest root collar diameter (3.71 ± 0.66). Contradictorily, the mean of leaf area index (4.74 ± 4.15) was recorded the greatest at seedlings cut above node 3.

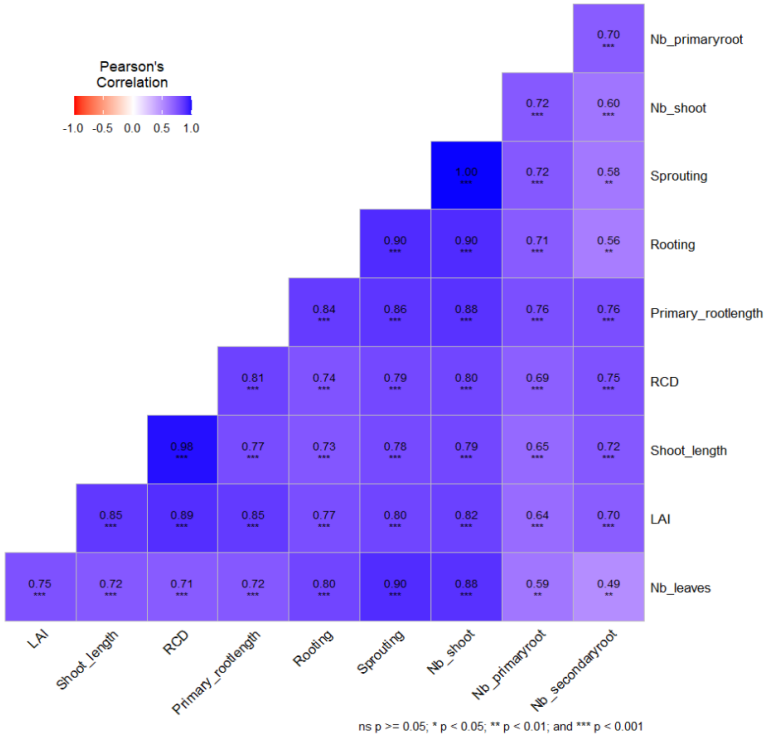

Figure 5. Correlation plot between shoot and root parameters of stem cuttings of *B. racemosa*

DISCUSSION

The different cutting positions of *B. racemosa* seedlings had a significant effect on propagation growth in terms of sprouting and rooting ability. All shoot and root formation parameters increased gradually from the apical to basal cuttings, with the basal cuttings exhibiting the best shoot and root growth. However, this result contradicts the well-recognized convention that cuttings taken from the upper parts of the stem generally have a superior ability to produce new shoots and roots compared to those taken from the lower parts (Leakey, 2014). This phenomenon is probably associated with the interaction between different species and

diameter of stem, which may have different effects on shoot and root development (Leakey, 1983; Dick *et al*., 2004; Kouakou *et al*., 2016). The result showed basal cuttings had the highest shoot and leaf growth as shown in Table 1 compared to apical cuttings, which had the least. The observation aligned with other findings, indicating root-shoot growth is better in the basal cuttings than in the apical cuttings (Zalesny *et al*., 2003; Husen & Pal, 2007b, Herastuti & EK, 2020). Saifuddin *et al*. (2013) also documented that the basal cuttings of *Peltophorum pterocarpum* had the highest survival rate, shoot number, leaf area index (LAI), and root initiation compared to apical cuttings which similar to the study results.

In this study, root formation varied depending on the cutting position. Cuttings taken from the basal position had a greater number of primary (3.80 ± 1.58) and secondary roots (6.61 ± 3.44), as well as longer root length (2.96 ± 0.87 cm), than those from the apical position (Table 1). Dao *et al*. (2020) suggested that basal cuttings of *Garcinia kola* superior growth are due to their higher carbohydrate content or food reserve and increased organogenic activity at different stem positions. Ezekiel (2010) similarly demonstrated that the basal cuttings contained more sugars, which were essential for supplying nutrients needed to initiate new root-shoot tips. Other previous studies indicated that storage capacity is affected by the thickness of stem, or cutting diameter (Leakey & Mohammed, 1985; Rianawati & Siswadi, 2020). Basal cuttings typically have a larger diameter than the apical cuttings, which may lead to better growth. Similar results were found by Rana and Sood (2012), where a larger diameter of *Ficus roxburghii* wall resulted in significantly better growth in the number of primary roots, number of shoots, shoot length, and number of leaves. These authors essentially demonstrated that thicker stems produce more roots number that help boost the water and nutrient absorption, which is essential for plant development.

Piñon *et al*. (2023) found that age-related auxin sensitivity, which is influenced by maturation or ontogenectic aging, has a significant impact. As a result, young and mature tissue respond differently to auxin application, even within the same plant (Pijut *et al*., 2011). The finding showed that basal cuttings have better rooting and sprouting abilities, which is similar to Maanik and Sharma's (2022) results. These abilities may also be attributed to the highest endogenous IBA levels and carbohydrate reserve typically found in the basal region, which play a crucial role in promoting root adventitious development and enhancing starch hydrolysis (Olaniyi *et al*., 2021). It helps facilitate the transport and absorption of carbohydrates and nutrients to the base of the stem. Hardwood cuttings treated with auxin perform better in producing root and shoot due to the auxin application, which enhanced the callus, tissue formation, and cell differentiation (Wendling *et al*., 2014). This variation may be partly explained by the differences in endogenous IBA levels across cutting positions.

Furthermore, the interaction between auxin and carbohydrates has been recognized as vital for root formation (Sorin *et al*., 2005; George *et al*., 2008; Herastuti & EK, 2020). IBA promotes root formation by hydrolyzing polysaccharides, which increases the metabolic activities necessary for the formation and elongation of root meristematic tissues and development of new shoot (Husen & Pal, 2007a; George *et al*., 2008; Kouakou *et al*., 2016). Therefore, the superior growth observed in mature and basal cuttings can be attributed to their higher carbohydrate reserves and the enhanced metabolic activities stimulated by IBA, both of which promote effective root and shoot development. Despite these findings, the reasons behind the decline or loss of rooting competence in physiologically mature cuttings compared to juvenile cuttings remain unclear, necessitating further investigation, potentially through molecular analysis (Piñon *et al*., 2023).

According to the findings of this study, varying maturity levels in different parts of the stem may influence the outcomes. Specifically, the basal part of the stem matures earlier than the apical part. This observation is supported by Corpuz (2013) research on *Hevea brasiliensis* propagation, which demonstrated that brown or older stem cuttings exhibited superior shoot and root formation than green stem cuttings. Rana and Sood (2012) also found that larger diameters of stems treated with IBA showed more successful propagation than smaller diameters of stems treated with IBA hormone. Since all the cuttings in this study were treated with IBA hormone, the effect of hormone might vary depending on the stem's maturity. These

differences become more pronounced with increasing age disparity, highlighting significant variations in the physiological characteristics of cuttings at different developmental stages (Owusu *et al*., 2014).

According to Leakey (2014), the environment and traits of a parent plant are vital in determining the development of roots and shoots in cuttings. The high success rate of sprouting and rooting in the non-mist propagator is due to the constant high humidity and uniform temperature, regardless of stem position or substrate type (Singh *et al*., 2015; Kouakou *et al.*, 2016). The propagator is particularly provided with a favourable environment for better root growth (Selvarajan & Rao, 1982; Singh, 2014).

The results of cuttings using three different substrates revealed that there was no significant effect on the shoot and root growth. However, the interaction of stem cutting position and substrates had a significant effect on the shoot and root parameters. All substrates produced nearly identical results for the shoot and root parameters. Nevertheless, the findings revealed that the substrate using a mixture of sand and cocopeat consistently produced the best results across all parameters (Table 2). Similar results were obtained by Netam *et al*. (2020). This mixture performed best in shoot formation, particularly at the basal stem position (Table 3), where it produced the most shoots (1.03 ± 0.09), shoot length (4.97 ± 1.22 cm), collar diameter (1.86 ± 0.38 mm), and leaf area index (1.55 ± 0.58 cm^2). These results were supported by Shrestha *et al*. (2023). Additionally, the mixture improves root development such as the number of primary and secondary roots and primary root length, particularly at the basal position (Kumar & Malik, 2019).

Overall, the combination of cocopeat and sand proved to be the most optimal substrate, offering a balanced environment that promotes robust root and shoot growth, as evidenced by the present study. This finding aligns with the requirements of an ideal rooting medium that provides sufficient porosity to ensure proper aeration, possesses high water retention capacity while maintaining adequate drainage, and remains free from any fungi and bacteria (Kontoh, 2016). Kontoh (2016) highlighted that mixing coarse river sand and composed oil palm fiber as a rooting medium in equal proportions effectively retained moisture and remained well-aerated. Conversely, a mixture of cocopeat and sand in equal proportions have proven effective for rooting, as demonstrated in the present studies. Similar results were found by Owusu *et al*. (2014) and Cahyo *et al*. (2019), who reported that a mixture of sand and cocopeat promotes the most sprouting and rooting development when compared to other substrate types. This combination may have provided favourable physical conditions and sufficient nutrients to the cuttings, which were necessary for activating enzymatic and metabolic activities (Wazir *et al*., 2003; Shah *et al*., 2021). As other studies have shown, ornamental plants or trees are likely suitable for propagation using a mixture of sand and cocopeat (Shokri *et al.*, 2014; Sedaghathoor *et al.*, 2016; Kumar & Malik, 2019; Shrestha *et al*., 2023).

Cocopeat alone demonstrated moderate to strong root development capabilities, although it was slightly less effective in promoting shoot formation than the mixture, yet root formation showed cocopeat had the highest number of primary and secondary root as shown in Table 2 and Table 4. Aparna *et al*. (2021) reported that cocopeat substrate has high water-holding capacity that helps more water and nutrient absorption from the substrate, which subsequently increases the number of primary and secondary roots. Furthermore, the substrate may protect endogenous IBA from degradation, thereby facilitating the differentiation of meristematic cells into root primordia and increases the number of roots (Rubasinghe *et al*., 2009). In contrast, sand exhibited moderate growth across all parameters, making it less effective than the other two substrates. Sand was reported to have high porosity, low absorptive capacity, and water retentive capacity (Boateng, 2014). Roots that grow in sand tend to develop as thick, brittle structures with minimal lateral branching, making them susceptible to damage during transplantation (Fatemeh & Zaynab, 2015). This could explain why sand substrate has moderate to low growth rates for both shoot and root growth, regardless of the position of the stem cuttings being used.

In terms of coppicing intensity, the results indicate that node position had no significant effect on coppice shoot formation (Table 5). However, other growth parameters varied

notably depending on the node position. Seedlings cut above node 1 produced greater growth in shoot length (17.81 ± 3.55 cm) and number of leaves (5.11 ± 0.90), indicating optimal resource allocation for vigorous shoot growth and leaf development. This finding is consistent with Luostarinen and Kauppi (2005), who reported that less competition for resources leads to stronger and faster shoot development. Additionally, seedlings cut above node 1 had a larger collar diameter (3.71 ± 0.66 mm), indicating a stronger root system and increased nutrient uptake. Furthermore, seedlings cut above node 3 had the highest mean leaf area index (4.74 ± 4.15 cm^2), indicating that while these shoots may not be the longest or have the most leaves, they may have a larger overall leaf surface area, enhancing the plant's photosynthesis capacity (Tschaplinski & Blake, 1995; Kouakou *et al.*, 2016). These findings highlight the different effects of node position on various growth parameters, providing valuable insights for optimizing copping practices and seedling management.

CONCLUSION

This research indicates that *B. racemosa* is highly adaptable to vegetative propagation *via* stem cuttings, providing a viable method for large-scale seedling production aimed at reforestation. The result showed that substrate treatment alone had no significant effect on shoot and root formation. However, some of the shoot parameters and root development had significant interaction between the stem cutting positions and substrates. Basal cuttings with a sand and cocopeat mixture grew significantly faster than median and apical cuttings and adding the IBA application in an aqueous solution boosted growth even more, particularly in basal cuttings. This suggests that using basal in conjunction with IBA treatment is best for the vegetative propagation of *B. racemosa*. Seedling stock plants cut above nodes 1, 2, and 3 have no significant influence on the coppicing growth. However, seedlings cut above node 1 exhibit better shoot growth. Future research should focus on improving environmental and hormonal conditions to further enhance propagation efficiency. While tissue culture methods such as micropropagation have potential for large-scale restoration projects, they may not be feasible for small-scale applications due to resource and technical constraints. This study lays the groundwork for developing effective *B. racemosa* propagation protocols, which will help support long-term reforestation initiatives.

ACKNOWLEDGEMENTS

This study was funded by Skim Dana Khas (SDK0323-2021) of Universiti Malaysia Sabah (UMS).

REFERENCES

Aluri, J.S.R., Palathoti, S.R., Banisetti, D.K. & Samareddy, S.K. (2019). Pollination ecology characteristics of *Barringtonia racemosa* (L.) Spreng.(Lecythidaceae). *Transylvanian Review of Systematical and Ecological Research*, 21(3): 27-34. DOI:10.2478/trser-2019-0017

Aminah, H., Dick, J.M. & Grace, J. (1997). Rooting of *Shorea leprosula* stem cuttings decreases with increasing leaf area. *Forest Ecology and Management*, 91(2-3): 247-254. DOI:10.1016/S0378-1127(96)03857-1

Aparna, D., Reddy, M.L.N., Rao, A.D., Bhaskar, V.V., Subbaramamma, P. & Krishna, K.U. (2021). Effect of media and hormones on rooting of african marigold stem cuttings in mist chamber. *The Journal of Research ANGRAU*, 49(3): 29-44.

Behbahani, M., Ali, A.M. & Muse, R. (2007). Plant regeneration from leaf explants of *Barringtonia racemosa*. *Journal of Medicinal Plants Research*, 5: 103-108.

Boateng, S.K. (2014). Vegetative propagation of Chrysophyllum albidum G. Don by leafy stem cuttings. *Ghana Journal of Agricultural Science*, 47(1): 39-49.

Cahyo, A.N., Sahuri, I.S.N. & Ardika, R. (2019). Cocopeat as soil substitute media for rubber (*Hevea brasiliensis* Müll. Arg.) planting material. *Journal of Tropical Crop Science*, 6(1): 24-29.

Chan, E.W.C., Baba, S., Chan, H.T., Kainuma, M., Inoue, T. & Wong, S.K. (2017). Ulam herbs: A review on the medicinal properties of *Anacardium occidentale* and *Barringtonia racemosa*. *Journal of Applied Pharmaceutical Science*, 7(2): 241-247. DOI:10.7324/JAPS.2017.70235

Chantaranothai, P. (1995). *Barringtonia* (Lecythidaceae) in Thailand. *Kew Bulletin*, 50(4): 677-694. DOI:10.2307/4110230

Corpuz, O.S. (2013). Stem cut: An alternative propagation technology for rubber (*Hevea brasiliensis*) tree species. *International Journal of Biodiversity and Conservation*, 5(2): 78-87. DOI:10.5897/IJBC12.122

Dao, J.P., Kouakou, K.L., Kouakou, C., Cherif, M., Ouedraogo, M.H., Koffi, K.K. & Bi, I.A.Z. (2020). Effect of leafy and leafless greenwood, softwood and hardwood cuttings success of Garcinia kola (Heckel). *Agricultural Sciences*, 11(10): 897-911. DOI:10.4236/as.2020.1110058

Dick, J.M., Leakey, R.R.B., McBeath, C., Harvey, F., Smith, R.I. & Woods, C. (2004). Influence of nutrient application rate on growth and rooting potential of the West African hardwood *Triplochiton scleroxylon*. *Tree Physiology*, 24(1): 35-44. DOI:10.1093/treephys/24.1.35

Easlon, H.M. & Bloom, A.J. (2014). Easy Leaf Area: Automated digital image analysis for rapid and accurate measurement of leaf area. *Applications in plant sciences*, 2(7): 1400033.

Eboy, V., O. & Chan J.K.L. (2021). Application of GIS in identifying potential site for river tourism activities along the Petagas river. *Ilkogretim Online*, 20(4): 743-752. DOI:10.17051/ilkonline.2021.04.78

Ezekiel, A. (2010). Viable options and factors in consideration for low cost vegetative propagation of tropical trees. *International Journal of Botany*, 6: 187-193.

Fatemeh, B. & Zaynab, M. (2015). Influence of rooting substrate and cutting type on rooting of cuttings in *Schefflera arboricola* L. plants. *International Journal of Plant & Soil Science*, 4(3): 281-287. DOI:10.9734/IJPSS/2015/8013

George, E.F., Hall, M.A. & Klerk, G.J.D. (2008). The components of plant tissue culture media I: macro-and micro-nutrients. *In Plant Propagation by Tissue Culture: Volume 1. The Background*. Dordrecht: Springer Netherlands. pp. 65-113.

Herastuti, H. & EK, S.H. (2020). The Influence of Stem Cutting Type and IBA Concentration on Vegetative Growth of *Bougainvillea*. *Journal Techno*, 2(1):12-18.

Husen, A. & Pal, M. (2007a). Metabolic changes during adventitious root primordium development in *Tectona grandis* Linn. f.(teak) cuttings as affected by age of donor plants and auxin (IBA and NAA) treatment. *New Forests*, 33: 309-323. DOI:10.1007/s11056-006-9030-7

Husen, A. & Pal, M. (2007b). Effect of branch position and auxin treatment on clonal propagation of *Tectona grandis* Linn. f. *New Forests*, 34: 223-233. DOI:10.1007/s11056-007-9050-y

Hussin, N.M., Muse, R., Ahmad, S., Ramli, J., Mahmood, M., Sulaiman, M.R., Shukor, M.Y.A., Rahman, M.F.A. & Aziz, K.N.K. (2009). Antifungal activity of extracts and phenolic compounds from *Barringtonia racemosa* L. (Lecythidaceae). *African Journal of Biotechnology*, 8(12): 2835-2842. DOI:10.5897/AJB09.450

Kabir, M.Z., Rahman, S.M., Islam, M.R., Paul, P.K., Rahman, S., Jahan, R. & Rahmatullah, M. (2013). A review on a mangrove species from the Sunderbans, Bangladesh: *Barringtonia racemosa* (L.) Roxb. *American-Eurasian Journal of Sustainable Agriculture*, 7(5): 356-372.

Kodoh, J., Chen, Y.L., Maid, M. & Affendy, H. (2018). Effect of different rooting media on stem cuttings of *Eucalyptus pellita* F. Muell. *Sepilok Bulletin*, 27: 23-29.

Kong, K.W., Junit, S.M., Aminudin, N. & Aziz, A.A. (2020). Phytochemicals in *Barringtonia* species: Linking their traditional uses as food and medicine with current research. *Journal of Herbal Medicine*, 19: 100299.

Kontoh, I.H. (2016). Effect of growth regulators and soil media on the propagation of *Voacanga africana* stem cuttings. *Agroforestry Systems*, 90(3): 479-488. DOI:10.1007/s10457-015-9870-2

Kouakou, K.L., Dao, J.P., Kouassi, K.L., Beugré, M.M., Koné, M., Baudoin, J.P. & Zoro Bi, I.A. (2016). Propagation of Garcinia kola (Heckel) by stem and root cutting. *Silva Fennica*, 50(4): 1588.

Kroin, J. (1992). Advances Using lndole-3-butyric Acid (IBA) Dissolved in Water for-Rooting Cuttings, Transplanting, and Grafting. *In Combined Proceedings International Plant Propagators' Society*, University of Washington, Vol. 42: pp. 345-346.

Kulip, J., Kodoh, J., Lintangah, W., Mojiol, A.R., Godoong, E. & Dawood. M.M. (2020). Project report: Ecological and vegetation studies of riparian habitats for recovery of Petagas and Putatan rivers, Putatan District, Sabah, Malaysia. *Institute Tropical Biology and Conservation*.

Kumar, S. & Malik, A. (2019). Effect of the different rooting media and IBA concentrations on survival percentage and root parameters of carnation (*Dianthus caryophyllus*) cuttings CV. Gaudina. *Journal of Pharmacognosy and Phytochemistry*, 8(5): 953-957.

Leakey, R.R.B. & Mohammed, H.R.S. (1985). The effects of stem length on root initiation in sequential single-node cuttings of *Triplochiton scleroxylon* K. Schum. *Journal of Horticultural Science*, 60(3): 431-437. DOI:10.1080/14620316.1985.11515648

Leakey, R.R.B. (1983). Stockplant factors affecting root initiation in cuttings of *Triplochiton scleroxylon* K. Schum., an indigenous hardwood of West Africa. *Journal of Horticultural science*, 58(2): 277-290.

Leakey, R.R.B. (2014). Plant cloning: macropropagation. In: Van Alfen, N., Ed., *Encyclopedia of Agriculture and Food Systems*. San Diego, Elsevier Publishers. pp. 349-359.

Liang, F., Hu, J., Liu, B., Li, L., Yang, X., Bai, C. & Tan, X. (2022). New Evidence of Semi-Mangrove Plant *Barringtonia racemosa* in Soil Clean-Up: Tolerance and Absorption of Lead and Cadmium. *International Journal of Environmental Research and Public Health*, 19(19): 12947. DOI:10.3390/ijerph191912947

Luostarinen, K. & Kauppi, A. (2005). Effects of coppicing on the root and stump carbohydrate dynamics in birches. *New Forests*, 29: 289-303. DOI:10.1007/s11056-005-5653-3

Maanik & Sharma, R. (2022). Effect of plant growth regulators and different growing media on propagation of fruit crops. *The Pharma Innovation Journal*, 11(12): 4638-4642.

Malaysia Meteorological Department. (2023). From http://www.met.gov.my. Accessed on 04 January 2024.

Malaysian Agricultural Research and Development Institute (MARDI) and Ministry of Agriculture of Malaysia. (2007). *Country Report on the State of Plant Genetic Resources for Food and Agriculture in Malaysia (1997-2007)*. https://www.fao.org/4/i1500e/malaysia.pdf. Downloaded on 19 June 2023.

Murugan, N. (2007). The performance and rooting of *eucalyptus grandis* x nitens cuttings (Doctoral dissertation), University of KwaZulu-Natal, Durban, South Africa.

National Parks Board (NParks). (2024). Flora and Fauna Web. A Singapore Government Agency Website. Retrieved January 01, 2025, from https://www.nparks.gov.sg/florafaunaweb/flora/2/7/2747.

Netam, S.R., Sahu, G.D., Markam, P.S. & Minz, A.P. (2020). Effect of different growing media on rooting and survival percentage of pomegranate (*Punica granatum* L.) cuttings cv. Super Bhagwa under Chhattisgarh plains condition. *International Journal Chemical Studies*, 8(5): 1517-519. DOI:10.22271/chemi.2020.v8.i5u.10514

Olaniyi, A.A., Yakubu, F.B., Nola, M.O., Alaje, V.I., Odewale, M.A., Fadulu, O.O. & Adeniyi, K.K. (2021). Vegetative propagation of *Picralima nitida* (Stapf.) by leafy stem cuttings: Influence of cutting length, hormone concentration and cutting positions on rooting response of cuttings. *Tanzania Journal of Forestry and Nature Conservation*, 90(3): 84-92.

Osman, N.I., Sidik, N.J. & Awal, A. (2015). Pharmacological activities of *Barringtonia racemosa* L. (Putat), a tropical medicinal plant species. *Journal of Pharmaceutical Sciences and Research*, 7(4): 185.

Owusu, S.A., Opuni-Frimpong, E. & Antwi-Boasiako, C. (2014). Improving regeneration of mahogany: techniques for vegetative propagation of four African mahogany species using leafy stem cuttings. *New Forests*, 45: 687-697. DOI:10.1007/s11056-014-9431-y

Pauku, R.L. (2006). Barringtonia procera (cutnut). *Traditional Trees of Pacific Islands: Their Culture, Environment and Use*, 153-170.

Pijut, P.M., Woeste, K.E. & Michler, C.H. (2011). 6 promotion of adventitious root formation of difficult-to-root hardwood tree species. *Horticultural Reviews*, 38: 213.

Piñon, A.A., Carandang, W.M. & de Luna, M.J.O. (2023). Indole-3-Butyric Acid (IBA) and Leaf Trimming Regulate the Adventitious Root Formation of Stem Cuttings Derived from Mature *Aquilaria Cumingiana*. *Journal of Tropical Forest Science*, 35(2): 189-202. DOI:10.26525/jtfs2023.35.2.189

Prance, G.T. (2012). A revision of *Barringtonia* (Lecythidaceae). *Allertonia*, 12:1-164.

Rana, R.S. & Sood, K.K. (2012). Effect of cutting diameter and hormonal application on the propagation of *Ficus roxburghii* Wall. through branch cuttings. *Annals of Forest Research*, 55(1): 69-84.

Rianawati, H. & Siswadi, S. (2020). Effect of donor plants and rooting medium on stem cutting propagation of faloak (*Sterculia quadrifida*). *International Journal of Tropical Drylands*, *4*(2): 31-35. DOI:10.13057/tropdrylands/t040201

Rubasinghe, M.K., Amarasinghe, K.G.K.D. & Krishnarajha, S.A. (2009). Effect of Rooting Media, Nephtheline Acetic Acid and Gibberelic Acid (GA 3) on Growth Performances of *Chirita moonii*. *Ceylon Journal of Science (Biological Sciences)*, 38(1): 17-22. DOI:10.4038/cjsbs.v38i1.1323

Saifuddin, M., Osman, N. & Motior Rahman, M. (2013). Influence of Different Cutting Positions and Rooting Hormones on Root Initiation and Root-soil Matrix of Two Tree Species. *International Journal of Agriculture & Biology*, 15(3): 427–434.

Sedaghathoor, S., Kayghobadi, S. & Tajvar, Y. (2016). Rooting of Mugo pine (Pinus mugo) cuttings as affected by IBA, NAA and planting substrate. *Forest Systems*, 25(2): eSC08.

Selvarajan, M. & Rao, V.N.M. (1982). Studies on rooting of patchouli cuttings under different environments. *South Indian Horticulture*, 30(2): 107-111.

Shah, S.U., Ayub, Q., Hussain, I., Khan, S.K., Ali, S., Khan, M.A., Haq, N., Mehmood, A., Khan, T. & Brahmi, N.C. (2021). Effect of different growing media on survival and growth of Grape (*Vitus vinifera*) cuttings. *Journal Advances of Nutrition Science and Technology*, 1(3): 117-124. DOI:10.15228/ANST.2021.v01.i03.p03

Shokri, S., Zarei, H. & Alizadeh, M. (2014). Effect of rooting media on root production of semi-hardwood stem cuttings in weeping bottlebrush (*Calistemon viminalis*) under greenhouse conditions. *Journal of Soil and Plant Interactions-Isfahan University of Technology*, 5(3): 173-183.

Shrestha, J., Bhandari, N., Baral, S., Marahatta, S.P. & Pun, U. (2023). Effect of rooting hormones and media on vegetative propagation of Bougainvillea. *Ornamental Horticulture*, 29(3): 397-406.

Singh, K.K. (2014). Effect of IBA concentrations on the rooting of pomegranate (*Punica granatum* L.) cv. Ganesh hardwood cuttings under mist house condition. *Plant Archives*, 14(2): 1111-1114.

Singh, K.K., Chauhan, J.S., Rawat, J.M.S. & Rana, D.K. (2015). Effect of different growing conditions and various concentrations of IBA on the rooting and shooting of hardwood cutting of Phalsa (*Grewia asetica* L.) under valley condition of Garhwal Himalayas. *Plant Archives*, 15(1): 131-136.

Soepadmo, E., Saw, L.G., Chung, R.C.K. & Kiew, R. (2002). Tree Flora of Sabah and Sarawak. Volume 4. Sabah Forestry Department. *Forest Research Institute Malaysia, Sarawak Forestry Department, Sabah*, 4: 117-119.

Sorin, C., Bussell, J.D., Camus, I., Ljung, K., Kowalczyk, M., Geiss, G., McKhann, H., Garcion, C., Vaucheret, H., Sandberg, G. & Bellini, C. (2005). Auxin and light control of adventitious rooting in *Arabidopsis* require ARGONAUTE1. *The Plant Cell*, 17(5): 1343-1359. DOI:10.1105/tpc.105.031625

Tschaplinski, T.J. & Blake, T.J. (1995). Growth and carbohydrate status of coppice shoots of hybrid poplar following shoot pruning. *Tree Physiology*, 15(5): 333-338. DOI:10.1093/treephys/15.5.333

Wazir, M.G., Ishtiaq, M., Aziz, A. & Khan, I.A. (2003). Effects of different soil media on the growth of *Dracaena dermensis* var. Janet Craige cuttings. *Sarhad Journal of Agriculture*, 19: 31-40.

Wendling, I., Trueman, S.J. & Xavier, A. (2014). Maturation and related aspects in clonal forestry—Part I: Concepts, regulation and consequences of phase change. *New Forests*, 45: 449-471. DOI:10.1007/s11056-014-9421-0

Zalesny, J., Hall, R.B., Bauer, E.O. & Riemenschneider, D.E. (2003). Shoot position affects root initiation and growth of dormant unrooted cuttings of Populus. *Silvae Genetica*, 52: 273-279.

Borneo Journal of Resource Science and Technology (2025), 15(1): 189-197
DOI: https:doi.org/10.33736/bjrst.7718.2025

Impact of Various Pre-Treatments on the Lignocellulosic Compositions of Sarawak 'Paun' Pineapple Leaf Waste

ALEXANDRA CHERYL ANAK DENNIS, ROSMAWATI SAAT* & DIANA KERTINI MONIR

Faculty of Resource Science and Technology, Universiti Malaysia Sarawak, 94300, Kota Samarahan, Sarawak, Malaysia
*Corresponding author: srosma@unimas.my
Received: 28 August 2024 Accepted: 15 April 2025 Published: 30 June 2025

ABSTRACT

Pre-treatment of lignocellulosic biomass is a crucial step in breaking down the complex structure of the plant`s cell wall to enhance the availability and digestibility of cellulose for bioconversion process of the biomass to value-added products. The overall efficiency of the process designed to convert lignocelluloses also lies on an accurate determination of compositions of the lignocellulosic substrate. In this study, local species of Sarawak 'Paun' pineapple leaves collected from Simunjan, Sarawak, were subjected to various pre-treatment methods including thermal treatment, acidic treatments and alkaline treatments. Compositional analyses of the raw and pre-treated leaves were conducted through a gravimetric method to study the effect of different methods of pre-treatments in altering the lignocellulosic compositions of the pineapple leaf wastes focusing on the hemicellulose, lignin and cellulose content. As the main purpose of a pre-treatment method focuses on its ability and efficiency to disintegrate the biomass complex structure, especially, in reducing lignin content for higher cellulose accessibility of enzymes in enzymatic hydrolyses. This study suggested that pre-treatment with 1.5% (v/v) hydrochloric acid solution displayed the most notable change to the lignocellulose contents of the leaves as highest cellulose content (51.5% w/w) and lowest amount of lignin (10.3% w/w) were recorded, compared to that of other pre-treatment methods. These findings may provide a better understanding for future research in designing a suitable biochemical process with enhanced enzymatic digestibility of cellulose present in the pineapple leaves to yield wealth-added products.

Keywords: Bioconversion, compositional analyses, hydrochloric acid, pineapple leaves, pre-treatments

INTRODUCTION

Lignocellulose or also known as lignocellulosic biomass is the most abundant type of biomass which includes a wide variety of distinct biomass types including grasses, woods, energy crops, agricultural and municipal wastes (Fadeyi *et al*., 2020). The term lignocellulosic is used to describe materials exist in the plant dry matter (biomass) that is mostly composed of three major components which consist of up to 60% of cellulose, 20 to 40% of hemicellulose, and 10 to 25% of lignin from the total dry basis of biomass (Sluiter *et al*., 2010, Maisyarah *et al*., 2019). These major components are bonded together through a covalent bonding, various intermolecular bridges and van der Waals' forces which contributed to their resistance towards enzymatic hydrolysis and their insolubility in water (Fadeyi *et al*., 2020). Cellulose is a glucose polymer linked by ß-1,4 glycosidic bonds with a basic building block of glucose-glucose dimer known as cellobiose (Ayeni *et al*., 2015). The structure of cellulose is organized as micro-fibrils and it possesses alternating regions of crystalline (well-ordered) and amorphous (disordered). On the other hands, hemicellulose, being the second major constituent of cell wall, is made up of short-chain hetero-polysaccharide with a lower degree of polymerization than cellulose (Lobo *et al*., 2021). The heteropolymer consists of different monosaccharide units such as glucose, xylose, mannose, galactose, arabinose, fucose, glucuronic acid, and galacturonic acid in various amounts or traces dependent on the natural source (Hu *et al*., 2020). Lignin, a third major component of lignocellulosic biomass, is a highly cross-linked phenyl propylene polymer and the largest non-carbohydrate fraction of the lignocellulose (Ayeni *et al*., 2015). It acts significantly as the permanent binder in all plants by gluing the cellulose fibers together,

thus, providing mechanical strength, rigidity and permeability of the plant's cell wall (Tumuluru *et al*., 2011; Lobo *et al*., 2021).

Over the years, lignocellulosic biomass has continued to be studied as a source of fermentable sugars for bioconversion of lignocelluloses to value-added products such as biofuels production, enzymes, and bio-based chemicals, due to its high availability in nature and cellulose as the major constituent of the feedstocks (Widihastuty *et al*., 2021; Saini *et al*., 2022). Pineapple leaves generated majorly from pineapple-related industry, are a potential feedstock and can be used as substrates in many biochemical processes such as microbial fermentation and anaerobic digestion due to the presence of fibre (Aili *et al*., 2021). Pineapple leaf wastes have extensively been used as lignocellulosic feedstock for the production of enzymes such as cellulases, by using *Trichoderma reesei* and *Aspergillus* sp. which are known as the most common and efficient producer of cellulases (Saravanan *et al*., 2013; Zhao *et al*., 2018). However, the overall efficiency of processes designed to convert lignocelluloses depends on the compositions of such materials which can be varied greatly due to the complex and heterogeneous nature of biomass (Fadeyi *et al*., 2020). Another fact that should be taken into account is the complex network of cellulose-hemicellulose-lignin present in the biomass. The hydrolysis of cellulose becomes highly difficult due to lignin which is covalently bound to the polysaccharides and the presence of complex lignin-hemicellulose shield, forming a protective covering surrounding the cellulose micro-fibrils and shields them from enzyme attack (Ariffin *et* al., 2020; Pendse *et al*., 2023). Hence, pre-treatment of the biomass is significantly required to deconstruct the lignocellulosic matrix especially in breaking down the lignified structure and degrading hemicellulose, making cellulose more available to enzymatic hydrolysis (Iroba *et al*., 2013; Pendse *et al*., 2023). The effectiveness of lignocellulosic biomass modification to useful fermentable sugars relies on the residues and type of pre-treatment that have been selected (Ariffin *et al*., 2020).

The present study aims to assess the impact of various pre-treatment methods on the compositional change of three major lignocellulosic components present in the local pineapple leaves. Prior to a gravimetric method by Maisyarah *et al.* (2019) adopted for the compositional analysis in this study, the local pineapple leaves were subjected to thermal treatment by autoclave, acidic treatment with dilute hydrochloric acid solutions, and alkaline treatment with sodium hydroxide solutions, separately. Changes in the cellulose, hemicellulose, lignin, and extractives contents of raw and pre-treated leaves evaluated in this present study may elucidate on the efficiency of various pre-treatment methods in breaking down the complex structure of the biomass. Subsequently, this may contribute to a better understanding for future studies in enhancing the enzymatic digestibility of cellulose present in the pineapple leaves as potential agro-based substrates for bioconversion processes in liberating valuable products.

MATERIALS AND METHODS

Collection and Preparation of Local Pineapple Leaves

Pineapple leaves from Sarawak 'Paun' cultivar used in this study were obtained locally from Sebangan, Simunjan, Sarawak, Malaysia. The leaves were rinsed with tap water and distilled water for the preliminary removal of unwanted impurities, followed by oven drying at 60 °C. The leaves were then cut into smaller pieces and ground by using an electrical blender, and sieved into particle size in between 0.5 mm to 1.0 mm. These ground samples were kept in a sterilised glass bottle prior to the pre-treatment process.

Pre-treatments of Pineapple Leaves

In this study, three different methods of pre-treatments were applied in treating the ground pineapple leaves in order to study the effect of different pre-treatments mainly on the lignocellulosic materials in the pineapple leaves.

Thermal Treatment

The method performed for thermal treatment was carried out according to Corbin *et al*. (2015). A ratio of 1:10 of solid to liquid was applied, in which distilled water was added to the lignocellulosic sample to prevent burning of

the sample, followed by autoclaving at 121 °C for 30 minutes. Subsequently, the sample was let to cool down to room temperature prior to filtration. The sample was then dried in a drying oven at 60 °C and then, the dried sample was kept in an airtight container prior to the compositional analysis.

Acidic Treatment

Two different concentrations of hydrochloric acid (HCl) solutions were used in the acidic pre-treatment of pineapple leaves by adopting a method by Bansal *et al*. (2012) with a slight modification. A volume of 200 ml of 1% (v/v) and 1.5% (v/v) of HCl solution was poured separately into each Erlenmeyer flask. Then, an amount of 50 g of ground pineapple leaves was added, and followed with incubation for 2 hours at room temperature in a static condition. Upon completion of incubation, the sample was filtered and rinsed with distilled water for several times to discard any remaining acid residues, followed by drying process at 60 °C in a drying oven. Once dried, the treated leaves were kept in an airtight container prior to the compositional analysis.

Alkaline Treatment

The alkaline pre-treatment process was performed according to Bansal *et al*. (2012), with a slight modification. In this study, concentrations of 1% (w/v) and 1.5% (w/v) of sodium hydroxide (NaOH) solutions were used. An amount of 50 g of the ground leaves was added into an Erlenmeyer flask containing 200 ml of NaOH solution of each concentration, separately. The mixture was incubated for 2 hours at room temperature, statically. The sample was then filtered and thoroughly rinsed for several times with distilled water to remove any traces of base, followed by drying in a drying oven at 60 °C before the pre-treated sample was kept in an airtight container.

Compositional Analysis

A gravimetric method by Maisyarah *et al*. (2019) was performed on the dried raw sample (ground leaves) and dried pre-treated leaves for the compositional analysis in determining the amount of three major lignocellulosic components, namely, hemicellulose, lignin and cellulose.

Amount of Extractives

A mixture of 1 g of the sample (A) and 60 ml of acetone (as a solvent for the extraction) was refluxed at 90 °C for 2 hours on a hot plate. After 2 hours, the sample was dried in a drying oven at 105 – 110 °C until a constant weight (B) was obtained. By using the equation, Eq. (1), stated below, the amount of extractives was determined.

$$\text{Amount of Extractives (g)} = (A - B) \qquad \text{Eq. (1)}$$

Amount of Hemicellulose

A volume of 150 ml of 0.5 M of sodium hydroxide (NaOH) solution was added to 1 g of extractive-free sample (B). Then, the mixture was boiled on a hot plate at 80 °C for 3.5 hours. After boiling, the sample was washed multiple times with deionised water for the removal of excess basic solution. A pH meter was used to confirm complete removal of basic solution when the pH of the solution is closer to 7. The sample was then dried in a drying oven at 105 – 110 °C to a constant weight (C). The amount of hemicellulose was determined by using the following equation, Eq. (2).

$$\text{Amount of Hemicellulose (g)} = (B - C) \quad \text{Eq. (2)}$$

Amount of Lignin

Prior to handling concentrated sulphuric acid and to prevent excessive evaporation of the acid, a reflux apparatus was prepared before hands which basically includes the setting up of heating mantle, round bottom flask (containing the sample mixture with concentrated acid), reflux condenser and rubber tubing as connecting glassware (Ferreira *et al*., 2013). A volume of 30 ml of 98% sulphuric acid (H_2SO_4) was added to 1 g of sample with extractives free (B), in which the mixture was then left at room temperature for 24 hours, prior to boiling at 100 °C for 1 hour. After boiling, the mixture was filtered by using Whatman filter paper no. 1 and the solid residue was washed multiple times by using deionised water until sulphate ion was undetectable. The detection of sulphate ion was performed through a titration with 10% of Barium chloride ($BaCl_2$) solution in which the disappearance of white precipitation indicated that the solid residue was free from acidic solution. The sample was then left to dry in a

drying oven at 105 – 110 °C until a constant weight (D) was achieved. The final weight of the solid residue was recorded as lignin content, Eq. (3).

Amount of Lignin (g) = D Eq. (3)

Amount of Cellulose

The amount of cellulose was determined by calculating the difference between initial weight of the sample with the weight of three other components obtained from the previous steps, assuming that the only components of an entire sample are extractives, hemicellulose, lignin and cellulose. Thus, cellulose content (E) was determined by using the following equation, Eq. (4), in which 1 g refers to the total amount of sample used in the experiment.

(A – B) + (B – C) + D + E = 1 g Eq. (4)

RESULTS AND DISCUSSION

The basic lignocellulosic compositions of raw (ground leaves) and pre-treated 'Paun' pineapple leaves are as shown in Table 1 and Figure 1. Each experimental procedure was conducted in duplicates, thus, reported results below indicates the average values of the replicates.

Based on the results, it is observed that the lowest content of extractives was identified at 8.5% (w/w) when the sample was subjected to acid pre-treatment with 1.5% (v/v) of HCl solution, by which it was reduced by two-fold compared to the extractives observed in raw pineapple leaves. The extractives include non-structural components of biomass such as sucrose, nitrate/nitrite, protein, ash, chlorophyll, waxes, that are required to be removed because they have the potential to interfere with downstream analysis of biomass sample (Ayeni *et al*., 2015). Hemicelluloses, being one of the polysaccharides in the biomass, were identified to be the lowest at 13.1% (w/w) for raw pineapple leaves but recorded the highest hemicellulose content at 31.1% (w/w) of the total biomass dry mass when the Sarawak 'Paun' pineapple leaves were pre-treated with 1% (v/v) HCl solution. On the other hands, amount of lignin of raw and treated pineapple leaf wastes was observed to be in the range 10.3% (w/w) to 15.7% (w/w), with the lowest lignin content recorded when the samples were subjected to acid pre-treatment with hydrochloric solutions of 1% (v/v) and 1.5% (v/v). Cellulose, which is stated to be the main component in most lignocellulosic biomass, was also revealed to be the major constituent of the Sarawak 'Paun' pineapple leaves with 37.0% (w/w) of cellulose content recorded. The cellulose content displayed an increased amount across all the pre-treatments employed, compared to that of raw pineapple leaves (37.0% w/w). The highest content of celluloses recorded was at 51.5% (w/w) of its total dry mass when the local pineapple leaves were pre-treated with 1.5% (v/v) HCl solution. Based on the findings of this present study, different pre-treatment methods gave a notable impact in altering the lignocellulosic compositions present in the Sarawak 'Paun' pineapple leaf wastes. As the main purpose of a pre-treatment method focuses on its ability and efficiency to disintegrate the biomass complex structure, especially, in reducing lignin content for higher cellulose accessibility of enzymes in enzymatic hydrolyses, pre-treatment with 1.5% (v/v) of HCl solution is shown to be the most effective method in treating the pineapple leaves as the lowest lignin content at 10.3% (w/w) and the highest content of cellulose at 51.5% (w/w) were recorded.

Even though a number of researches on the pre-treatment of pineapple leaves have been published, previous findings that reported mainly on the correlation between various pre-treatment methods applied on local pineapple leaf waste particularly from Sarawak pineapple cultivar and their impacts on lignocellulosic compositions are still very limited. Table 2 shows the amounts of major lignocellulosic constituents, mainly the hemicellulose, cellulose, lignin and extractives, in pineapple leaf wastes illustrated in previous literatures. In this study, cellulose contents in the Sarawak 'Paun' pineapple leaves regardless of treatment methods were the major constituent at the range of 37.0 – 51.5% (w/w), followed by hemicellulose and lignin contents at 13.1 – 31.1% (w/w) and 10.3 – 19.7% (w/w), respectively. Hemicellulose contents in Sarawak 'Paun' leaves were comparable with most of the literatures stated in Table 2, but, faintly lower than the hemicellulose value acquired by Maisyarah *et al*. (2019) which was at 37% (w/w). On the other hands, the amounts

of cellulose in the present study were significantly lower than the cellulose contents obtained by Nashiruddin *et al*. (2020) and Reddy and Yang (2005), but, slightly higher than the cellulose amount by Maisyarah *et al*. (2019).

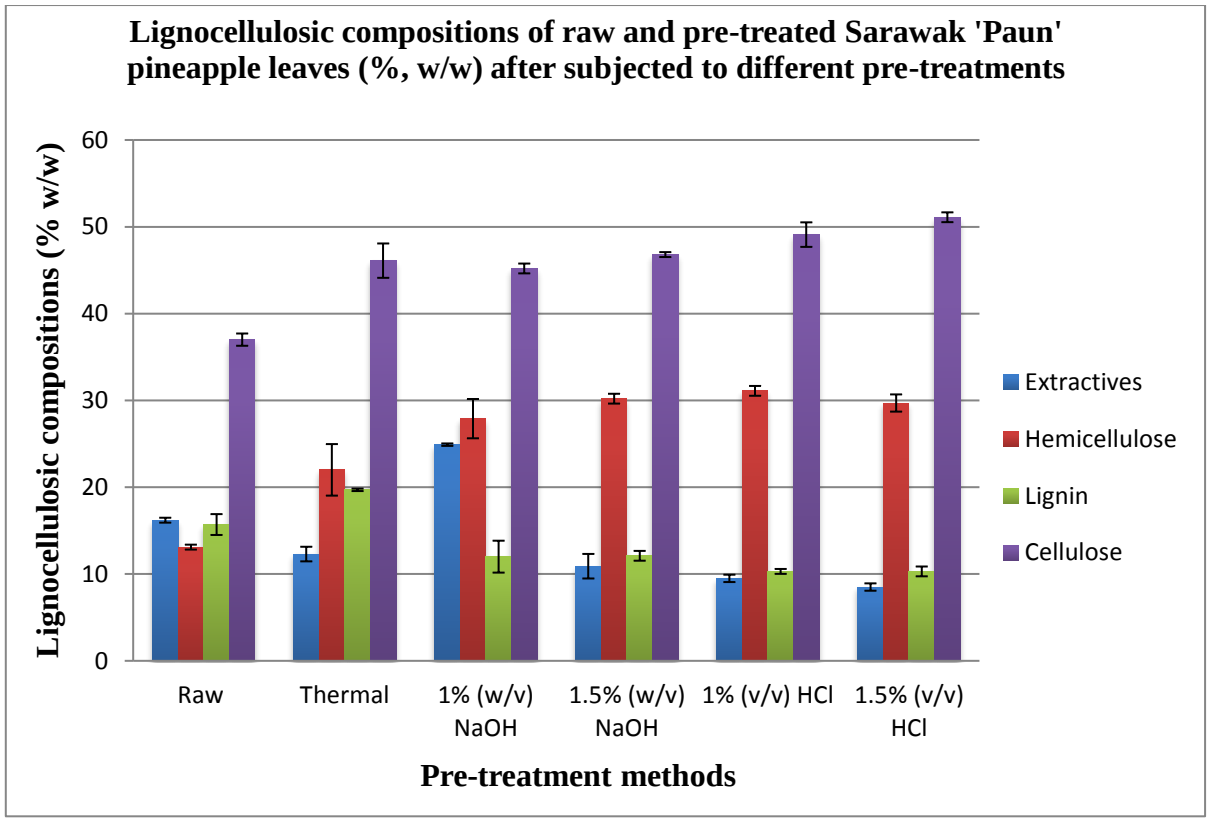

Figure 1. Bar chat interpretation of lignocellulosic compositions of raw and pre-treated Sarawak 'Paun' pineapple leaves (%, w/w)

Table 1. Lignocellulosic compositions of raw and pre-treated Sarawak 'Paun' pineapple leaves (%, w/w) after subjected to different pre-treatments

Lignocellulosic component	Raw PL	Pre-treatment				
		Thermal by autoclave	1% (w/v) NaOH	1.5% (w/v) NaOH	1% (v/v) HCl	1.5% (v/v) HCl
Extractives	16.2±0.3	12.3±0.8	24.9±0.1	10.9±1.4	9.5±0.4	8.5±0.4
Hemicellulose	13.1±0.3	22.0±3.0	27.9±2.3	30.2±0.6	31.1±0.6	29.7±1.0
Lignin	15.7±1.2	19.7±0.1	12.0±1.8	12.1±0.6	10.3±0.3	10.3±0.6
Cellulose	37.0±0.7	46.1±2.0	45.2±0.6	46.8±0.3	49.1±1.4	51.5±0.6

Note: PL indicates pineapple leaves.

Table 2. Lignocellulosic compositions (cellulose, hemicellulose, lignin and exrractives) of pineapple leaves from various studies

Cellulose (% w/w)	Hemicellulose (% w/w)	Lignin (% w/w)	Extractives (% w/w)	References
37.0 - 51.5	13.1 – 31.1	10.3 – 19.7	8.5 – 24.9	This study
72.76	17.15	4.76	-	Nashiruddin *et al*. (2020)
30	37	22	11	Maisyarah *et al*. (2019)
56.0 – 82.0	-	4.4 – 4.7	26.21 – 28.47	Yuliasmi *et al*. (2017)
66.2	19.5	4.28	-	Zawawi *et al*. (2014)
70 – 82	18	5 – 12	3.6 – 7.0	Reddy and Yang (2005)

The ideal cellulose content of the biomass used in biochemical and bioconversion process is typically preferred to be in between 30% to 50% as the range allows efficient enzymatic hydrolysis and sugar extraction while sustaining a balanced composition with other major components, especially, hemicellulose and lignin (Vélez-Mercado *et al*., 2021). In addition, the high cellulose proportion of up to 37.0% (w/w) and low lignin content of 15.7% (w/w) present in the raw Sarawak 'Paun' pineapple leaves (refer Table 1) are comparable with several previous findings in Table 2 that suggested local pineapple leaf wastes from few Malaysian pineapple varieties used in their studies were majorly made up of high cellulose content up to 66.2% (w/w), as well as low lignin content ranging between 4% to 22% (w/w) of their total dry masses (Zawawi et al., 2014; Maisyarah et al., 2019). Cellulose component of the biomass is the most abundant renewable organic source and a high content of this compound contributes to the potential of the lignocellulose of being a valuable use in the production of various high value products through bioconversion process (Fadeyi *et al*., 2020). In most enzymatic hydrolyses occurring in biochemical processes, it is important to identify the cellulose contents of a lignocellulosic biomass used as it acts as a cellulolytic enzymes inducer and that, the production of cellulose is affected by the nature of the substrate (Lodha *et al*., 2020; Singh, 2021). Besides, knowing the lignocellulosic compositions of a biomass is vital prior to its use in biochemical and bioconversion process involving microbes, such as fermentation, as lignocellulosic substrate acts as a source of nutrients and that, a biomass which contains sufficient amount of nutrients to supplement the microbial growth is highly preferable (Yoon *et al*., 2014).

This present study has also shown that pre-treated Sarawak 'Paun' pineapple leaves displayed a substantial change in their major lignocellulosic compositions, compared to that of raw leaves. The changes in the cellulose and lignin contents of the pre-treated local pineapple leaves compared to that of raw leaves used in this study are similar with a previous study by Awoyale and Lokhat (2021). Awoyale and Lokhat (2021) mentioned that the values of the cellulose content in the pre-treated biomasses (corn cobs, rice husks, cassava peels, sugar cane bagasse and white yam peels) used in the study illustrated a significant difference from the amount of cellulose in raw biomass, with values ranging from 33.2 wt% to 43.8 wt% and, that of the lignin content decreasing significantly regardless of the pre-treatment methods. Utilisation of lignocellulosic biomass for the production of wealth-added products such as fuels, fine chemicals and industrially-important enzymes requires an effective pre-treatment method to enhance the available enzymes for enzymatic hydrolysis process by disrupting the hemicellulose-lignin complex structure (Nashiruddin *et al*., 2020).

Besides, lignin is often regarded as the main parameter that limits the biodegradation of lignocellulosic biomass due to its major mechanism involving the covalent cross linking of lignin with other cell wall compounds which imparts the predominant role in the biomass recalcitrance (Rajesh *et al*., 2021). Thus, a pre-treatment method is significantly required to remove lignin for higher cellulose accessibility of enzymes in enzymatic hydrolyses occurring in the bioconversion and biochemical process (Iram *et al*., 2020). Another fact that should be highlighted is the effectiveness of dilute HCl solution in pre-treating local pineapple leaves from this present study, which can be supported with earlier findings that also applied similar method of chemical treatment in pre-treating lignocellulosic agro-substrates as the promising feed stocks in bioconversion and biochemical processes (Cho *et al*., 2019; Ariffin *et al*., 2020; Usino *et al*., 2020). It was suggested that pre-treatment of agro-based substrates with dilute acid solution such as HCl have particularly improved cellulose contents and reduced lignin composition in pre-treated samples, compared to those in raw samples (Cho *et al*., 2019; Ariffin *et al*., 2020; Usino *et al*., 2020). Unlike alkaline pre-treatment that primarily interacts with lignin for lignin removal, acid pre-treatment is more suitable for biomass with low lignin content as its core reaction involves hydrolysis of hemicellulose and solubilisation of small fractions of lignin (Kim *et. al.*, 2016; Oriez *et al.*, 2019). As alkaline pre-treatment is better suited for biomass with high lignin content, the alkaline pre-treatment in the current study might not be effective enough in pre-treating the Sarawak 'Paun' leaves due to the

nature of the leaves of having low lignin content as it might slow down the primary interaction between the alkaline solution and lignin (Kim *et. al.*, 2016; Oriez *et al.*, 2019). In addition, during pre-treatment of biomass with dilute acid solution, the hydrolysis of hemicelluloses might highly occur as acid interrupts the hydrogen bonds that linked hemicelluloses and celluloses, as well degrading the covalent bonds between hemicelluloses and lignin (Amin *et al*., 2017).

Consequently, the chemical reaction caused by acid pre-treatment of the biomass can lead to high solubilisation of hemicellulose, thereby increasing the accessibility to cellulose to be transformed into valuable sugars (Amin *et al*., 2017; Ariffin *et al*., 2020). In fact, the glycosidic bonds present in hemicelluloses are susceptible to acid, leading to the removal of hemicellulose which subsequently increases the pore size of the biomass and enhances the digestibility of cellulose (Shi *et al*., 2020). Thus, this explains the results of this present study by which pre-treatment with dilute HCl solution, especially, 1.5% (v/v) HCl solution, works better and gave more impacts on the lignocellulosic compositions of Sarawak 'Paun' pineapple leaves, compared to the leaves treated with sodium hydroxide solutions. In addition, acid solutions have been used as reagents in enhancing degradation efficiency of the glycosidic bonds in lignocellulose to promote the release of fermentable sugars, but, only diluted acids are recommended to minimize the risk of toxicity, corrosion and handling (Awogbemi & Kallon, 2022).

CONCLUSION

Efficiency of process designed for bioconversion processes lies on the effectiveness of a pre-treatment method in causing compositional changes in the lignocelluloses by breaking down its complex compositional make-up and physicochemical structure. Removal of lignin and solubilisation of hemicellulose are taken as a significant consideration for an efficient method of pre-treatment in enhancing availability of cellulose to enzymatic hydrolysis for higher conversion yields. Compositional analysis of the Sarawak 'Paun' pineapple leaves by gravimetric method in this present study indicated that acid pre-treated leaves with 1.5% (v/v) hydrochloric solution displayed a notable change in its lignocellulose contents with the highest value of cellulose at 51.5% (w/w), hemicelluloses at 29.7% (w/w) and lowest lignin content of 10.3% (w/w), compared to that of raw leaves and other pre-treatment methods applied in this study. These findings may contribute for a better understanding in designing a biochemical process in converting lignocellulosic materials to valuable products, with greater efficiency and effectiveness.

ACKNOWLEDGMENTS

Our gratitude to Tun Zaidi Chair Grant (F07/TZC/2162/2021), UNIMAS for funding this project and the Faculty of Resource Science & Technology, UNIMAS, Malaysia in providing the equipment.

REFERENCES

Aili Hamzah, A.F., Hamzah, M.H., Che Man, H., Jamali, N.S., Siajam, S.I. & Ismail, M.H. (2021). Recent updates on the conversion of pineapple waste (*Ananas comosus*) to value-added products, future prespectives and challenges. *Agronomy*, 11: 2221. DOI: 10.3390/agronomy11112221

Amin, F.R., Khalid, H., Zhang, H., Rahman, S.U., Zhang, R., Liu, G. & Chen, C. (2017). Pre-treatment methods of lignocellulosic biomass for anaerobic digestion. *AMB Express*, 7(72): 1-12. DOI: 10.1186/s13568-017-0375-4

Ariffin, K.K., Masngut, N., Seman, M.N.A., Saufi, S.M., Jamek, S. & Sueb, M.S.M. (2020). Dilute acid hydrolysis pretreatment for sugar and organic acid production from pineapple residues. *IOP Conference Series: Materials Science and Engineering*, 991: 1-9. DOI: 10.1088/1757-899X/991/1/012057

Awogbemi, O. & Kallon, D.V.V. (2022). Pretreatment techniques for agricultural waste. *Case Studies in Chemical and Environmental Engineering*, 6: 1-9. DOI: 10.1016/j.cscee.2022.100229

Awoyale, A.A. & Lokhat, D. (2021). Experimental determination of the effects of pretreatment on selected Nigerian lignocellulosic biomass in bioethanol production. *NatureResearch*, 11(2021): 557. DOI: 10.1038/s41598-020-78105-8

Ayeni, A.O., Adeeyo, O.A., Oresegun, O.M. & Oladimeji, T.E. (2015). Compositional analysis of lignocellulosic materials: evaluation of an economically viable method suitable for woody and non-woody biomass. *American Journal of Engineering Research (AJER)*, 4(4): 14-19.

Bansal, N., Tewari, R., Soni, R. & Soni, S.K. (2012). Production of cellulases from *Aspergillus niger* NS-2 in solid state fermentation on agricultural and kitchen waste residues. *Waste Management*, 32(7): 1341–1346. DOI: 10.1016/j.wasman.2012.03.006

Cho, E.J., Trinh, L.T.P., Song, Y., Lee, G.Y. & Bae, H.J. (2019). Bioconversion of biomass waste into high value chemicals. *Bioresource Technology*, 2019: 1-48. DOI: 10.1016/j.biortech.2019.122386

Corbin, K.R., Hsieh, Y.S.Y., Betts, N.S., Byrt, C.S., Henderson, M., Stork, J., DeBolt, S., Fincher, G.B. & Burton, R.A. (2015). Grape marc as a source of carbohydrates for bioethanol: chemical composition, pre-treatment and saccharification. *Bioresource Technology*, 2015: 1-34. DOI: 10.1016/j.biortech.2015.06.030

Fadeyi, A.E., Akiode, S.O., Emmanuel, S.A. & Falavi, O.E. (2020). Compositional analysis and characterization of lignocellulosic biomass from selected agricultural wastes. *Journal of Science and Mathematics Letters*, 8(1): 48-56. DOI: 10.37134/jsml.vol8.1.6.2020

Ferreira, S.L.C., Silva, L.O.B., de Santana, F.A., Junior, M.M.S., Matos, G.D. & dos Santos, W.N.L. (2013). A review of reflux systems using cold finger for sample preparation in the determination of volatile elements. *Microchemical Journal*, 106(2013): 307-310. DOI: 10.1016/j.microc.2012.08.015

Hu, L.S., Fang, X.Z., Du, M.H., Luo, F. & Guo, S. (2020). Hemicellulose-based polymers processing and application. *American Journal of Plant Sciences*, 11: 2066-2079. DOI: 10.4236/ajps.2020.1112146

Iram, A., Cekmecelioglu, D. & Demirci, A. (2020). Ideal feedstock and fermentation process improvements for the production of lignocellulolytic enzymes. *Process*, 9(38): 1-26. DOI: 10.3390/pr9010038

Iroba, K.L., Tabil, L.G., Dumonceaux, T. & Baik, O. (2013). Effect of alkaline pretreatment on chemical composition of lignocellulosic biomass using radio frequency heating. *Biosystems Engineering*, 116: 385-398. DOI: 10.1016/j.biosystemseng.2013.09.004

Kim, J.S., Lee, Y.Y. & Kim, T.H. (2016). A review on alkaline pretreatment technology for bioconversion of lignocellulosic biomass. *Bioresource Technology*, 2015: 1-7. DOI: 10.1016/j.biortech.2015.08.085

Lobo, F.C.M., Franco, A.R., Fernandes, E.M. & Reis, R.L. (2021). An overview of the antimicrobial properties of lignocellulosic materials. *Molecules*, 26: 1749. DOI: 10.3390/molecules26061749

Lodha, A., Pawar, S. & Rathod V. (2020). Optimised cellulase production from fungal co-culture of *Trichodetma reesei* NCIM 1186 and *Penicillium citrinum* NCIM 768 under solid state fermentation. *Journal of Environmental Chemical and Engineering*, 8(5): 1-6. DOI: 10.1016/j.jece.2020.103958

Maisyarah, A., Lim, J.S., Ani, F.N., Hashim, H. & Ho, W.S. (2019), Characteristics of cellulose, hemi-cellulose and lignin of MD2 pineapple biomass. *Chemical Engineering Transaction*, 72: 79–84. DOI: 10.3303/CET1972014

Nashiruddin, N.I., Mansor, A.F., Rahman, R.A., Ilias, R.M. & Wan Yussof, H. (2020). Process parameter optimization of pretreated pineapple leaves fiber for enhancement of sugar recovery. *Industrial Crops and Products*, 152(112514): 1-8. DOI: 10.1016/j.indcrop.2020.112514

Oriez, V., Peydecastaing, J. & Pontalier, P. (2019). Lignocellulosic biomass fractionation by mineral acids and resulting extract purification processes: conditions, yields, and purities. *Molecules*, 24(2019): 4273. DOI: 10.3390/molecules24234273

Pendse, D.S., Deshmukh, M. & Pande, A. (2023). Different pre-treatments and kinetic models for bioethanol production from lignocellulosic biomass: A review. *Heliyon*, 9: 1-15. DOI: 10.1016/j.heliyon.2023.e16604

Rajesh, B.J., Sugitha, S., Kavitha, S., Yukesh, K.R., Merrylin, J. & Kumar, G. (2021). Lignocellulosic biomass pretreatment for enhanced bioenergy recovery: Effect of lignocelluloses recalcitrance and enhancement strategies. *Frontiers in Energy Research*, 9: 1-17. DOI: 10.3389/fenrg.2021.646057

Reddy, N. & Yang, Y. (2005). Biofibers from agricultural byproducts for industrial applications. *TRENDS in Biotechnology*, 23(1): 22-27. DOI: 10.1016/j.tibtech.2004.11.002

Saini, R., Chen, C., Patel, A.K., Saini, J.K., Dong, C. & Singhania, R.R. (2022). Valorization of pineapple leaves waste for the production of bioethanol. *Bioengineering*, 9(557): 1-9. DOI: 10.3390/bioengineering9100557

Saravanan, P., Muthuvelayudham, R. & Viruthagiri, T. (2013). Enhanced production of cellulase from pineapple waste by response surface methodology. *Journal of Engineering*, 2013: 1-8. DOI: 10.1155/2013/979547

Shi, F., Wang, Y., Davaritouchaee, M., Yao, Y. & Kang, K. (2020). Directional structure modification of poplar biomass- inspired high efficacy of enzymatic hydrolysis by sequential dilute acid-alkali treatment. *ACS Omega*, 5: 24780-24789. DOI: 10.1021/acsomega.0c03419

Singh, A., Bajar, S., Devi, A. & Bishnoi, N.R. (2021). Evaluation of cellulase production of *Aspergillus niger* and *Aspergillus heteromorphus* under submerged and solid-state fermentation. *Environmental Sustainability*, 4: 437-442. DOI: 10.1007/s42398-021-00173-x

Sluiter, J.B., Ruiz, R.O., Scarlata, C.J., Sluiter, A.D. & Templeton, D.W. (2010). Compositional analysis of lignocellulosic feedstocks. 1. Review and description of methods. *Journal of Agricultural Food Chemistry*, 58: 9043-9053. DOI: 10.1021/jf1008023

Tumuluru, J.S., Sokhansanj, S., Wright, C.T. & Boardman, R.D. (2011). A review on biomass torrefaction process and product properties for energy applications. *Industrial Biotechnology*, 7(5): 384-401. DOI: 10.1089/ind.2011.0014

Usino, D.O., Sar, T., Ylitervo, P. & Richards, T. (2023). Effect of acid pretreatment on the primary products of biomass fast pyrolysis. *Energies*, 16: 2377. DOI: doi.org/10.3390/en16052377

Vélez-Mercado, M.I., Talavera-Caro, A.G., Escobedo-Uribe, K.M., Sánchez-Muñoz, S., Luévanos-Escareño, M.P., Hernández-Terán, F., Alvarado, A. & Balagurusamy, N. (2021). Bioconversion of lignocellulosic biomass into value added products under anaerobic conditions: Insight into proteomic studies. *International Journal of Molecular Sciences*, 22(12249): 1-26. DOI: 10.3390/ijms222212249

Widihastuty, Y.R., Sutini & Nur Ramadhani, A. (2021). Optimization of fermentable sugar production from pineapple leaf waste (*Ananas comosus [L.] Merr*) by enzymatic hydrolysis. *Jurnal Presipitasi*, 18(1): 73-80. DOI: 10.14710/presipitasi.v18i1.73-80

Yoon, L.W., Ang, T.N., Ngoh, G.C. & Adeline, S.M.C. (2014). Fungal solid-state fermentation and various methods of enhancement in cellulase production. *Biomass and Bioenergy*, 67: 319-338. DOI: 10.1016/j.biombioe.2014.05.013

Yuliasmi, S., Nerdy & Husnita, A. (2017). Characterization of microcrystalline from pineapple leaf (*Ananas comosus* L. Merr). *IOP Conference Series: Materials Science and Engineering*, 180: 1-7. DOI: 10.1088/1757-899X/180/1/012267

Zawawi, D., Mohd Zainuri, M.H., Angzzas S.M.K., Halizah, A. & Ashuvila, M.A. (2014). Exploring of agro waste (pineapple leaf, corn stalk, and napier grass) by chemical composition and morphological study. *BioResources*, 9(1): 872-880. DOI: 10.15376/biores.9.1.872-880

Zhao, C., Deng, L. & Fang, H. (2018). Mixed culture of recombinant *Trichoderma reesei* and *Aspergillus niger* for cellulase production to increase the cellulose degrading capability. *Biomass and Bioenergy*, 112(2018): 93-98. DOI: 10.1016/j.biombioe.2018.03.001